Faculty of Mathematical, Physical, and Natural Sciences

Department of Chemistry

Doctoral school "Vito Volterra"

FROM WASTE TO SORBENTS: RECYCLING POLYMERS FOR SAMPLE PREPARATION AND WATER REMEDIATION APPLICATIONS

PhD Candidate: Lorenzo Antonelli

PhD Supervisor:

Prof. Alessandra Gentili

PhD Coordinator:

Prof. Paola D'Angelo

PhD Thesis in Chemical Science
Academic Year 2024 - 2025

From waste to sorbents: recycling polymers for sample preparation and water remediation applications

Faculty of Mathematical, Physical, and Natural Sciences

Department of Chemistry

Doctoral school "Vito Volterra"

PhD Candidate: Lorenzo Antonelli

PhD Supervisor:

Prof. Alessandra Gentili

PhD Coordinator:

Prof. Paola D'Angelo

PhD Thesis in Chemical Science
XXXVIII cycle
Academic Year 2024 - 2025

From waste to sorbents: recycling polymers

for sample preparation and water remediation applications

PhD Thesis, Sapienza University of Rome.

Version: December 15, 2025

Author’s e-mail: lo.antonelli@uniroma1.it

Contents

PhD Publications

1. L. Antonelli, M. C. Frondaroli, M. G. De Cesaris, N. Felli, C. Dal Bosco, E. Lucci, A. Gentili (2024). **Nanocomposite microbeads made of recycled polylactic acid for the magnetic solid phase extraction of xenobiotics from human urine.** Microchimica Acta, 191(5), 1-14. https://doi.org/10.1007/s00604-024-06335-y
2. L. Antonelli, S. Grasso, M. G. De Cesaris, N. Felli, C. Dal Bosco, S. Cinti, A. Gentili (2025). **Composite microbeads of cellulose acetate upcycled from waste for water remediation.** Green Analytical Chemistry, 100283. https://doi.org/10.1016/j.greeac.2025.100283
3. L. Antonelli, Á. I. López-Lorente, A. Gentili, R. Lucena, S. Cárdenas (2025). **Microbeads from recycled polystyrene yogurt cups for the in-syringe micro solid-phase extraction of four opioids from environmental and biological samples.** Sustainable Chemistry and Pharmacy, 45, 102036. https://doi.org/10.1016/j.scp.2025.102036
4. L. Antonelli, N. Felli, M. G. De Cesaris, S. Cinti, A. Gentili (2026). **From waste to adsorbent: recycling polymers and natural materials for sample preparation and water remediation.** *Under submission*
5. L. Antonelli, Á. I. López-Lorente, A. Gentili, R. Lucena, S. Cárdenas (2026). **Sulfonated polystyrene nanospheres from waste sources for the extraction of sulfonamide antibiotics from complex matrices.** *Under submission*
6. L. Antonelli, M. Bartocci, N. Felli, M. G. De Cesaris, A. Gentili (2026). **LEGO® brick supporting a thermo-responsive sorptive phase: a modular platform for circular sample preparation.** *Under submission*

Other Publications

1. E. Lucci, C. Dal Bosco, L. Antonelli, C. Fanali, S. Fanali, A. Gentili, B. Chankvetadze (2022). **Enantioselective high-performance liquid chromatographic separations to study occurrence and fate of chiral pesticides in soil, water, and agricultural products.** Journal of Chromatography A,1685463595. https://doi.org/10.1016/J.CHROMA.2022.463595
2. L. Antonelli, C. Dal Bosco, M. G. De Cesaris, N. Felli, E. Lucci, A. Gentili (2023). **Solid-phase extraction combined with dispersive liquid-liquid microextraction for the analysis of glucocorticoids in environmental waters using liquid chromatography-tandem mass spectrometry.** Journal of Chromatography Open 4, 100100. https://doi.org/10.1016/j.jcoa.2023.100100
3. L. Antonelli, E. Lucci, S. Fanali, C. Fanali, A. Gentili, B. Chankvetadze (2023). **An enantioselective high-performance liquid chromatography-mass spectrometry method to study the fate of quizalofop-P-ethyl in soil and selected agricultural products.** Journal of Chromatography A 1707, 464289. https://doi.org/10.1016/j.chroma.2023.464289
4. M. G. De Cesaris, N. Felli, L. Antonelli, E. Lucci, C. Dal Bosco, A. Gentili (2025). **Extraction of organic contaminants from grab and composite water samples.** In Sample Handling and Trace Analysis of Pollutants (pp. 35–63). Elsevier Science. https://doi.org/10.1016/B978-0-323-85601-0.00031-X

5. E. Lucci, L. Antonelli, M. Gherardi, C. Fanali, S. Fanali, A. Scipioni, P. Lupattelli, A. Gentili, B. Chankvetadze (2023). **A liquid chromatography-mass spectrometry method for the enantioselective multiresidue determination of nine chiral agrochemicals in urine using an enrichment procedure based on graphitized carbon black.** Analytical and Bioanalytical Chemistry: 1-11. https://doi.org/10.1007/s00216-023-05098-4
6. M. G. De Cesaris, N. Felli, L. Antonelli, I. Francolini, C. Dal Bosco, A. Gentili (2024). **Recovery of cellulose acetate bioplastic from cigarette butts: realization of a sustainable sorbent for water remediation.** Science of The Total Environment 929 (2024): 172677. https://doi.org/10.1016/j.scitotenv.2024.172677
7. M. G. De Cesaris, L. Antonelli, E. Lucci, N. Felli, C. Dal Bosco, A. Gentili (2024). **Current trends to green food sample preparation.** A review. Journal of Chromatography Open, 100170. https://doi.org/10.1016/j.jcoa.2024.100170
8. M. G. De Cesaris, G. Bertini, C. Dal Bosco, N. Felli, E. Lucci, L. Antonelli, A. Gentili (2025). **One-step extraction for a high throughput multiresidue analysis of chiral and achiral pesticides in milk.** Green Analytical Chemistry, 12, 100229. https://doi.org/10.1016/j.greeac.2025.100229
9. E. Lucci, G. Falcinelli, L. Antonelli, C. Dal Bosco, N. Felli, M. G. De Cesaris, A. Gentili (2025). **Hydrophobic deep eutectic solvent-ferrofluid microextraction followed by liquid chromatography–mass spectrometry for the enantioselective determination of chiral agrochemicals in natural waters.** Analytical and Bioanalytical Chemistry, 417(7), 1341–1357. https://doi.org/10.1007/s00216-024-05619-9
10. N. Felli, D. Filardi, R. Sergi, L. M. Migneco, M. G. De Cesaris, L. Antonelli, A. Gentili (2025). **Exploring the extraction capabilities of natural cyclodextrin-nanosponges: The improvement moving from α- to γ-cyclodextrin-based polymers.** Advances in Sample Preparation, 14. https://doi.org/10.1016/j.sampre.2025.100169
11. C. Dal Bosco, M. G. De Cesaris, L. Antonelli, N. Felli, A. Gentili (2025). **The complex world of eutectic solvents: Guidelines for a correct characterization and use in sample preparation.** Advances in Sample Preparation, 100189. https://doi.org/10.1016/j.sampre.2025.100189
12. R. De Santo, L. Antonelli, A. Gentili, J. González-Sálamo (2025). **Sorption of cortisone on polypropylene, polystyrene, and polyethylene microplastics.** Journal of Chromatography A, 1756, 466082. https://doi.org/10.1016/j.chroma.2025.466082
13. S. Singh, A. Glovi, A. Miglione, W. Cimmino, G. Iula, L. Antonelli, M. G. De Cesaris, N. Felli, C. Martinelli, M. De Laurentiis, A. Giordano, S. Cinti (2025). **Electrochemical (bio)sensors for cancer therapy monitoring.** Electrochimica Acta, 146929. https://doi.org/10.1016/j.electacta.2025.146929
14. C. M. Montone, N. Felli, M. G. De Cesaris, L. Antonelli, T. Gasperi, M. Bianchi, A. Gentili (2025). **An analytical methodology for the quantitative profiling of fat-soluble antioxidants in maternal blood, umbilical cord blood and meconium.** Journal of Chromatography Open, 100253. https://doi.org/10.1016/j.jcoa.2025.100253
15. G. Iula, A. Raucci, L. Antonelli, P. M. Kalligosfyri, M. G. De Cesaris, N. Felli, A. Gentili (2025). **Smart and sustainable 3D-printed electrochemical device for diclofenac remediation and monitoring in water.** Talanta, 128597. https://doi.org/10.1016/j.talanta.2025.128597

16. L. Antonelli, M. G. De Cesaris, N. Felli, C. Dal Bosco, A. Gentili (2025). **Enantioselective Analysis of Chiral Agrochemicals with High-Performance Liquid Chromatography.** In *Chiral Separations: Methods and Protocols* (pp. 159–172). Springer US, New York, NY.

Abstract

Analytical chemistry plays a pivotal role in advancing sustainable development, acting both as a driver and a testing ground for the integration of sustainable practices into laboratory activities. A key aspect of this transition lies in the development of eco-friendly sample preparation strategies that reduce environmental impact without compromising analytical performance. This work presents the design and application of innovative adsorbent materials derived from recycled polymeric waste for use in solid-phase extraction and water remediation. The proposed materials, originating from biopolymer residues, industrial by-products, and post-consumer plastics, offer sustainable and cost-effective alternatives to conventional synthetic sorbents. Representative examples include extractive media fabricated from cellulose acetate (sourced from cigarette filters), polystyrene (from yogurt containers), and polylactic acid (from disposable products). A green and efficient synthetic protocol, combining microemulsion solidification with polymer dissolution–recycling, was developed to produce polymeric microspheres exhibiting excellent extraction capabilities for various classes of contaminants, including opioids, antibiotics, and pesticides in biological samples. Moreover, cellulose acetate microbeads were successfully employed in cartridge format for the remediation of organic pollutants from environmental waters. In a novel approach that merges recycling with modular design, functionalized LEGO® bricks were repurposed as reusable extraction platforms. The use of menthol as a thermo-responsive extraction medium, integrated into the LEGO®-based device, further expanded the versatility of the system, providing a simple, efficient, and solvent-saving procedure. Overall, this work demonstrates the feasibility and potential of integrating end-of-life polymeric materials into analytical workflows, opening new perspectives for customizable and sustainable sample preparation devices. The findings underscore the capability of recycled polymer-based sorbents to meet the rigorous requirements of modern analytical chemistry while advancing the principles of environmental sustainability.

Chapter 1: Recycling in analytical chemistry applications

1. The challenge of waste upcycling

As the scientific community strives to meet the sustainability targets outlined in Agenda 2030, recycling and the circular economy have emerged as key strategies in combating resource depletion and minimizing waste [1]. According to the EU Waste Framework Directive (2008/98/EC) "Recycling is any recovery operation by which waste materials are reprocessed into products, materials or substances whether for the original or other purposes" [2]. Several Sustainable Development Goals (SDGs) established by the United Nations directly support recycling and responsible resource management [1]. These include SDG 11 (Sustainable Cities and Communities), SDG 12 (Responsible Consumption and Production), SDG 13 (Climate Action), and SDG 15 (Life on Land). Together, they promote the use of sustainable materials and the development of innovative waste recovery technologies, fostering a more environmentally responsible society.

In this context, analytical chemists have risen to this global challenge by placing increasing attention on sustainable practices, as evidenced in the 12 principles of Green Analytical Chemistry (GAC) [3]. The aim is to make analytical methodologies greener without compromising process performance. Among the most innovative responses to the sustainability discourse is the development of recycling strategies at the laboratory scale [4]. One of the most promising advancements in this direction is the development of adsorbent materials derived from recycled waste. These materials, recognized as part of the emerging green adsorbents, have gained significant attention as sustainable alternatives for sample preparation techniques, particularly in solid-phase extraction (SPE), dispersive solid-phase extraction (d-SPE) and microextraction methods. This trend aligns closely with the principles of GAC, Green Sample Preparation (GSP) [5], and Circular Analytical Chemistry (CAC) [4], encompassing minimization of waste, use of non-hazardous materials, energy efficiency maximization, improved resource recovery and integration of circular economy practices into laboratory workflows. **Fig. 1** reports the principles of GAC, GSP, and CAC.

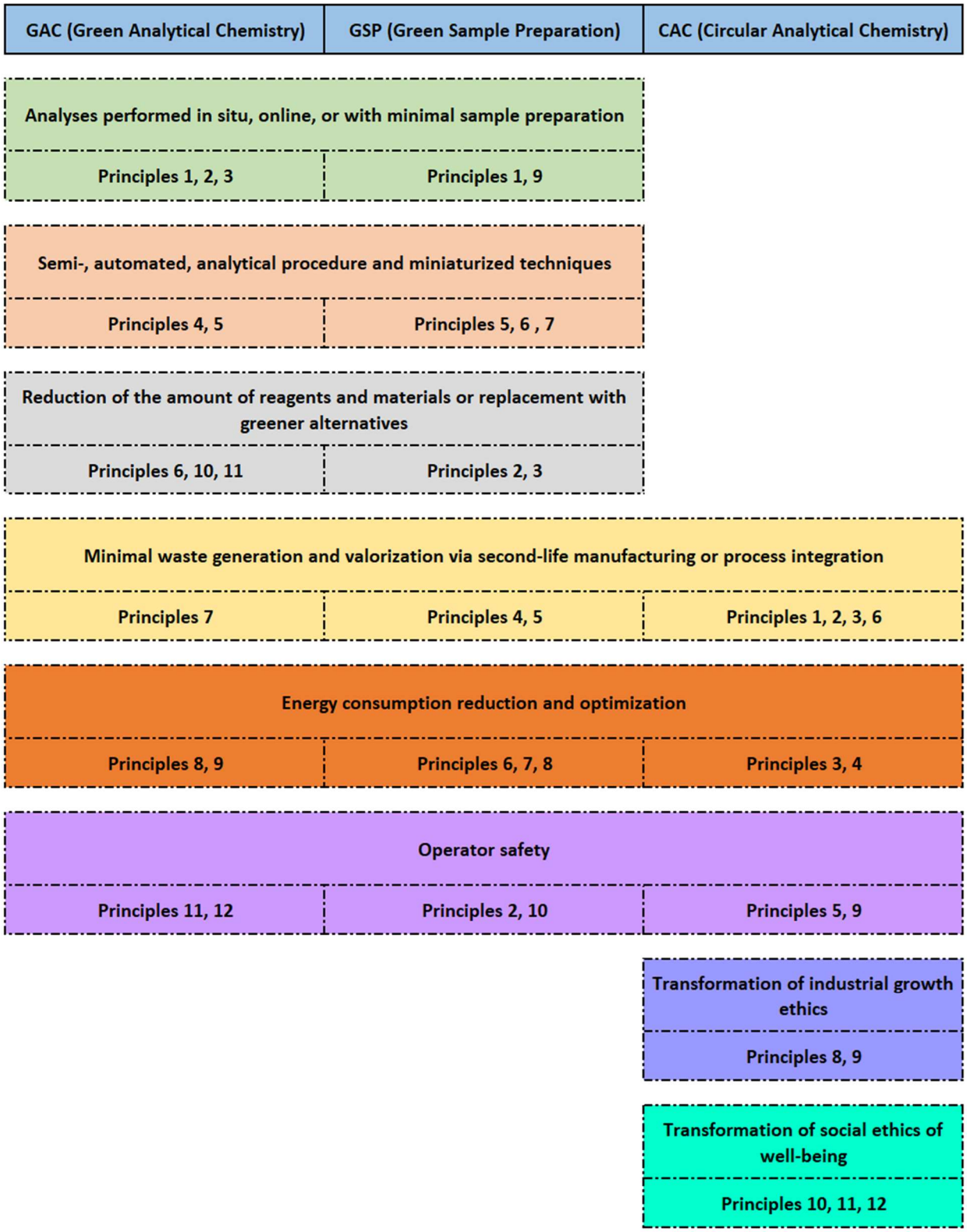

Fig. 1 Comparison between GAC, GSP and CAC principles, underling common perspectives and goals.

Recycled adsorbents can be sourced from various types of waste, including biopolymers, industrial by-products, and post-consumer plastics, and might offer several advantages over conventional

synthetic sorbents [6]. They not only reduce the environmental footprint of analytical procedures but also provide efficient and cost-effective alternatives for the extraction of contaminants from complex matrices. Additionally, functionalizing these recycled materials with selective adsorptive properties enhances their performance in analytical applications, expanding their potential use in both environmental, food and biomedical sample preparation [7].

This review article aims to compile and critically examine recent literature on recycled materials used as adsorbents in sample preparation, with a focus on their composition, performance, and applicability. The overarching goal is to demonstrate how recycling can be effectively integrated into laboratory-scale analytical procedures, thereby aligning with the principles of GAC and contributing to a more sustainable scientific practice. To structure this overview, recycled materials are grouped into three main categories: (i) natural waste resources as precursors for the fabrication of sorbent phases, (ii) end-of-life polymeric materials and (iii) single-use commercial devices and virgin natural sources as extraction supports. According to the previously cited definition of recycled materials, only the first and second category strictly aligns with the formal concept, as they involve directly reprocessing waste materials into new functional products. In contrast, the use of virgin natural resources or commercially available materials that are not at the end of their life cycle does not technically qualify as recycling.

2. Recycling, downcycling and upcycling

From a strictly thermodynamic perspective, the term "recycling" is inaccurate. In fact, the concept of recycling suggests a perfect cycle, but the Second Law of Thermodynamics, in particular, tells us that all real processes involve energy losses and increases in entropy, preventing complete restoration [8, 9]. In practical terms, this means that recycling processes always involve an energy cost in the form of heat dissipation, mechanical work, or chemical transformations, all with an impact on the environment. At best, recycling mitigates this impact by extending the useful life of materials and reducing the demand for virgin resources. For example, regarding the plastic recycling [10],

incineration recovers some energy, but it generates harmful emissions and does not address long-term resource depletion or create economic value. On the other hand, mechanical processes, especially referred to post-consumer plastics, are hindered by poor sorting, contamination, and complex materials [11], often resulting in “downcycling” because the recycled product has reduced quality and functionality [12]. Chemical recycling offers a promising alternative by converting plastics into high-purity monomers for repolymerization. However, with current technologies, only a limited range of commodity plastics can be chemically recycled efficiently and cost-effectively. Both mechanical and chemical recycling face challenges because the resulting products are often more costly or energy-intensive than their petroleum-based counterparts, limiting large-scale adoption. An alternative is to treat plastic waste as a chemical feedstock, placing it at the start of the value chain rather than the end. In this model, post-consumer plastics become a low-cost, abundant resource for producing new materials or molecules. Emerging strategies focus on upcycling, converting plastics into higher-value materials for targeted applications within the circular economy [10].

In conclusion, all forms of material reuse—recycling, upcycling, and downcycling—entail energy use and entropy increase. Recycling restores materials to near-original quality, demanding energy to counteract degradation. Upcycling creates higher-value products, often requiring even more energy. Downcycling, which produces lower-value goods, may use less energy but reduces the material’s long-term usefulness. Each strategy has its pros and cons (as shown in **Fig. 2**); thus, the analytical chemist should be guided by the specific context - balancing environmental impact, energy availability, material type, and the desired end-use - to achieve the most sustainable and efficient outcome.

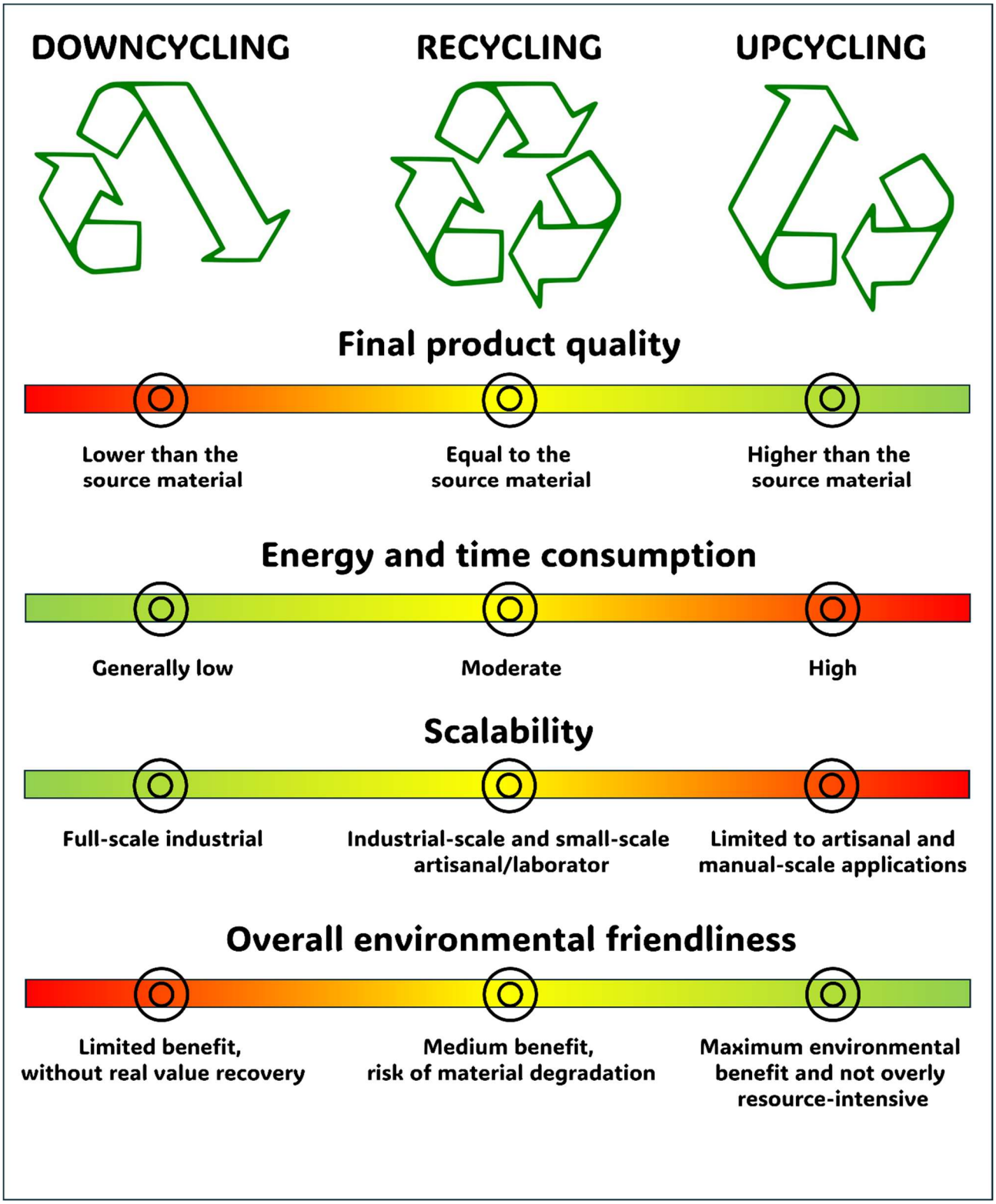

Fig. 2 Advantages and disadvantages of upcycling, recycling and downcycling.

3. Origin, classification and modification strategies of recyclable adsorbents

The materials, object of the review, are grouped into three main categories. The first one includes natural waste materials, such as agricultural by-products, shells, or residues from food and plant processing. These materials are given a second life through minimal processing and are often valued for their inherent porosity, surface functionality, or biodegradability, which make them suitable for adsorption applications [13]. The second category comprises plastic waste-derived materials, which are either used directly in their recycled form or after undergoing chemical or physical modification to enhance their adsorption properties [14]. Among these, polyethylene terephthalate (PET), polystyrene (PS), cellulose acetate, polylactic acid, and polyolefins represent the most investigated plastics due to their spread and surface modifiability. Finally, the third category includes single-use commercial items (such as cotton swabs, wooden toothpicks, and textiles) and natural materials (like plant tissues or vegetal fibres) which, although not currently repurposed from post-consumer waste, are attractive for their sustainability and availability. These three categories and their applications are discussed in detail in **Sections 4.1-4.3**. In addition, to boost their high-performance adsorption processes physical or chemical modifications are required to tailor their physicochemical properties for specific applications [15], as reported in **Table 1**.

Table 1 Physical treatments (**a**) and chemical modifications (**b**) of waste-derived materials.

(a) Physical treatments affect surface area, porosity, subsequent functionalization	
Dissolution	Particularly relevant for polymeric waste, dissolution in suitable solvents allows the reshaping of the material or its blending with other functional components. This step is often a precursor to reprocessing or incorporation into composite adsorbents.
Grinding or comminution	A simple effective method to reduce the particle size of waste materials, increasing their surface area and facilitating subsequent modifications or direct adsorption applications. It also improves material dispersibility in aqueous media.
Hydrogel formation	In some cases, waste polymers can be transformed into hydrogels, either by simple swelling in water or through partial depolymerization (chemical process). Hydrogels provide a highly hydrated, porous matrix ideal for aqueous adsorption processes.
Spin coating and electrospinning	These techniques are commonly employed to produce thin films or nanofibrous layers on waste-derived materials. Spin coating involves depositing a polymer solution onto a substrate to form a uniform, thin coating. Electrospinning uses a high-voltage electric field to generate ultrafine fibres from a polymer solution, creating highly porous, high-surface-area mats.
Annealing	A simple thermal treatment performed below the decomposition temperature of the material. It is used to relax internal stresses, enhance crystallinity, improve mechanical stability, and, in some cases, fine-tune the porosity.
Physical deposition	The surface of the waste material is coated with other substances (such as metal oxides, carbon-based nanostructures, or molecular layers) through simple deposition techniques, introducing active adsorption sites.
Dip coating	A versatile and scalable technique in which the substrate is immersed in a functional solution and withdrawn at a controlled rate, forming a uniform coating. This process enables the deposition of thin layers (e.g., polymers, metal oxides, nanocomposites) that can impart new surface functionalities or enhance mechanical, chemical, or technological performance (e.g., wettability, conductivity, selectivity).
(b) Chemical modifications affect porosity, reactivity, and interaction with target analytes	
Sulfonation	It introduces sulfonic acid groups to the polymer chains, enhancing hydrophilicity and ionic interaction with polar or charged species.
Crosslinking (induced)	It enhances chemical and thermal stability by introducing covalent bonds between polymer chains, often using polyfunctional reagents.
Aminolysis	It involves the reaction of polymers with amine-containing compounds, introducing nitrogen functionalities (e.g., $–NH_2$, –NH–), which can act as binding sites for metal ions or acidic analytes.
Carbonization and pyrolysis	For biomass and agricultural waste (e.g., peels, shells, plant matter). It is a thermal decomposition under inert atmosphere produces porous carbon materials with high surface area and thermal stability.
Biochar production and activation	For biomass and agricultural waste (e.g., peels, shells, plant matter). Biomass waste is converted into biochar - a stable, carbon-rich material- produced via pyrolysis, then activated using physical or chemical agents to optimize pore structure and surface functionality.
Calcination	Applied to inorganic-rich biomass (e.g., eggshells, bones), this process yields oxide- or carbonate-based materials suitable for adsorption
Oxidation	Concentrated nitric acid oxidizes the biomass surface, introducing nitro and carboxyl groups that enhance hydrophilicity and metal-binding capacity
Silanolization	Surface functionalization using silane reagents (e.g., 3-aminopropyltriethoxysilane, APTES) introduces silanol or organosilane groups that can be tailored for selectivity toward polar or metal-containing analytes.

4. Applications of the three classes of recyclable adsorbents

The practical implementation of adsorbents developed from recycled materials spans two main areas: sample preparation for analytical purposes and environmental remediation [16].

In analytical sample preparation, waste-derived materials have been mainly used to prepare sorbents in common formats including d-SPE, in-syringe microextraction, packed-bed extraction systems, bar adsorptive microextraction (BAμE), ultrasound-assisted dispersive micro SPE (USA-DmSPE), vortex-assisted SPE (VA-SPE) and pipette-tip microextraction [17]. It is important to note that using a recycled material within a lengthy, solvent-intensive, and energy-consuming extraction process can undermine the intended goal of reducing environmental impact, potentially resulting in "greenwashing" [18]. Therefore, the use of recycled adsorbents is most effective and coherent when paired with miniaturized techniques that maximize processing yields while minimizing waste and energy input.

In the field of water remediation, adsorbents from waste sources have been applied into two main operational modes [19]: 1) Batch systems, where the adsorbent is in contact with contaminated water for a fixed contact time. 2) Flow-through systems, in which the contaminated stream passes through a column or membrane containing the adsorbent material. From a practical standpoint, batch systems are generally more adaptable to irregular or small-scale waste-derived adsorbents, especially when morphology, particle size, or mechanical resistance is suboptimal [20, 21]. Conversely, flow-through systems require more structurally robust and uniform materials, often demanding additional processing steps (e.g., pelletizing, immobilization), which may complicate the use of raw or lightly modified waste [22].

The following sections (**4.1-4.3**) are aimed at discussing the applications of the three classes of recyclable adsorbents for sample preparation and remediation of waters and soil.

4.1. Adsorbents from Agricultural and Food Waste of Natural Origin

Natural-origin waste, particularly from agricultural and livestock production, represents a rich and diverse source of materials for the development of sustainable adsorbents [23]. Their intrinsic chemical nature is largely governed by the presence of biopolymers such as cellulose, hemicellulose, lignin, pectin, and other polysaccharides and structural proteins [24].

A representative example of recycled agricultural waste is presented in the work by Batool et al. [25], where biochars derived from farmyard and poultry manure were evaluated for their efficiency in removing Cu^{2+} from water. In this study, both types of manure were pyrolyzed in a low-oxygen environment and filtered to obtain low-cost sorbents with a surface area of about 9 m^2 g^{-1}. The maximum Cu^{2+} adsorption was around 44 mg g^{-1} with a pseudo-second order kinetics indicating the chemical interaction between Cu^{2+} and the negative charged surface of biochars.

Among the various carbonaceous materials derived from agricultural waste, bamboo-based adsorbents are particularly noteworthy due to their exceptionally high surface area-to-mass ratio, which enables the efficient adsorption of diverse substances, including organic compounds and heavy metals. Among the different developed adsorbents, bamboo-activated carbon, bamboo biochar, and bamboo aerogels exhibit distinct physicochemical properties suitable for water purification [26]. For instance, Wang et al. verified the excellent adsorption capability of bamboo biochar towards dimethyl sulfide, which is present in industrial discharges or agricultural runoff as a degradation product of sulfur compounds [27]. The high efficiency of the material (up to 70% removal at 10 mg dosage) is attributed to its key characteristics, including small particle size, abundant acidic and alcohol functional groups, and a unique mineral composition rich in Fe (0.4 wt%) and Mn (0.6 wt%).

Among industrial natural by-products, Reinert et al. demonstrated a notable example using spent diatomaceous earth, a silica-rich material from fossilized algae, used in beer filtration to remove yeast, proteins, and other suspended solids due to its porosity and high surface area [28]. To prepare the SPME coating for the determination of polycyclic aromatic hydrocarbons (PAHs) in water samples, the material was submitted to a heat treatment to eliminate organic residues and subsequently sieved to obtain homogeneous particle size (<200 mesh). Then, the particles were adhered on a 1-cm nitinol

wire using epoxy glue and heated at 180 °C for 90 min. The extraction procedure consisted of immersing the SPME fibre directly in 25 mL of water kept under magnetic stirring. After the extraction, the fibre was immediately inserted into the GC injection port at 240 °C for 15 min for the thermal desorption of the analytes. Relative recoveries were greater than 83% with precision ranging between 2 and 17%.

Other industrially derived adsorbents include those from cork industry by-products; a material widely used in manufacturing cork stoppers. Since cork is mainly composed of hydrophobic biopolymers (lignin and suberin) and polysaccharides (cellulose and hemicellulose), it is particularly suitable for the sorption of organic compounds [29]. Studies by Pintor et al. and applications by Celeiro et al., Hinz et al., and Morelli et al. [29-32] have shown that granular cork residues can be used either as-is or after washing, to adsorb pesticides and parabens from environmental waters. It has been verified that the interactions of cork with hydrophobic organic pollutants is favoured by the aromatic rings and carboxyl and hydroxyl groups of suberin and lignin; in particular, the aromatic components of lignin interact with the aromatic moieties of the adsorbed compounds via π-π interactions. However, adsorption is less successful in the case of hydrophilic pesticides with $\log P < 2$. Mallek et al. evaluated the ability of granulated cork to adsorb various phenolic, pharmaceutical, and cosmetic pollutants from water [33]. The adsorption efficiency was influenced by the concentration of the compounds, the amount of cork used, and, particularly for phenolic compounds, the pH of the solution. Results showed that adsorption increased with the electronegativity of the substituent groups on the phenols: for instance, 2,4-dichlorophenol was removed up to 75%, while plain phenol reached only 20%. Pharmaceutical and cosmetic compounds such as naproxen, ketoprofen, carbamazepine, diclofenac, and triclosan also showed high removal rates, in some cases up to 100%, even at low concentrations and with small amounts of cork. Adsorption was almost complete within 30 minutes for all micropollutants.

Besides recovered cork, another excellent example of cost-effective agro-industrial residues is the sugarcane bagasse, the fibrous residue left after sugar extraction or bioethanol production from

sugarcane. Major sugarcane-producing countries such as Brazil, India, China, and Bangladesh generate large volumes of bagasse; in Bangladesh, for example, 15 sugar mills producing 0.15 million tons of sugar annually generate an estimated 0.8 million tons of sugarcane bagasse as a by-product. This abundant biomass offers significant potential for value-added applications in water remediation. For example, Lebre et al. [34] explored its valorisation as an adsorbent of hormonal contaminants of industrial wastewater, following simple physical treatments such as drying, grinding, and sieving. The efficiency was greater than 99%, thanks to the presence of macromolecules (e.g. lignin, cellulose) that contain various functional groups acting as efficient absorption sites.

The last category regards the regeneration and application of food waste, both of plant and animal origin. A significant body of literature has investigated the use of fruit and vegetable waste as adsorbent precursors; examples include the use of orange and pomelo peels [35, 36] (**Fig. 3b**), grapefruit peel [37, 38], mangosteen shell [39], garlic skin [40] (**Fig. 3d**), peanut shells [41], banana peel [42, 43], coconut shells [44-46], jujube pit and shell [47, 48], pineapple peel, pomegranate peel [49], avocado seeds [50] and so forth. These materials can be subjected to carbonization, activation, or biochar formation to enhance their surface area and adsorption capabilities (see **Table 1**). Of particular interest is the study by Abiodun Adenuga et al. [51], in which agricultural biochar derived from various sources (spent seedcake of *Calophyllum inophyllum*, coconut husk (*Cocos nucifera*), and *Moringa oleifera* seeds) was evaluated for the d-SPE clean-up of acetonitrile extracts (see **Fig. 3c**) with excellent performance in terms of recovery rates ($\geq$ 83%) and precision (RSD $\leq$ 20%).

Ramón-Gonçalves et al. and Abdurahman et al. [52, 53] reported the use of spent coffee grounds as precursors for adsorbent synthesis: the former employed them to develop activated carbons for water remediation, while the latter utilized them in the synthesis of a magnetic adsorbent for extracting zinc oxide nanoparticles from water samples. This type of residue is particularly promising due to its highly porous structure and large surface area, especially when subjected to thermal activation, as well as its potential for chemical functionalization with various moieties. Haq et al. [54] extended this concept to industrial coffee husks (CH), demonstrating their transformation into adsorbents through

washing and sequential acid-base treatment (HCl/NaOH), which led to an enhanced adsorption capacity.

Beyond plant-based biomass [55], some researchers have recourse to animal-derived food waste to produce adsorbents due to their abundance as by-products of the food industry and their intrinsic chemical composition. In particular, biogenic mineral matrices such as hydroxyapatite (HAP), predominantly found in bones and fish skeletons, and calcium carbonate, abundant in eggshells, have emerged as highly effective materials for water purification. Their ion-exchange properties make them especially suitable for the removal of heavy metal ions and anionic contaminants from aqueous systems. Recent studies have explored the sustainable synthesis of natural HAP bioceramics from camel bone meal and fish scales (FS) [56, 47], which are rich in calcium phosphate. In particular, in the work of Aziz et al. [56], HAP was successfully obtained through an alkaline heat treatment of these wastes and subsequently employed for the removal of bisphenol A from wastewater. A calcium carbonate-based biosorbent derived from eggshells was investigated by Slimani et al. [58] in dye remediation applications. In their study, the material demonstrated promising adsorption performance for Basic Yellow 28 dye, achieving a maximum biosorption capacity of 28.87 mg g^{-1}. Notably, the eggshells required only minimal pretreatment, restricted to solvent washing, drying, and mechanical grinding, underscoring the potential of such waste-derived materials to serve as low-cost and sustainable sorbents. Hydroxyapatite synthesized from eggshells has also proven effective in metal remediation; for instance, De Angelis et al. [21] reported 91% removal of Ni^{2+} from contaminated water within 80 min of treatment (**Fig. 3a**). Another notable example of animal-derived waste valorisation is the use of recycled unspun wool fibres as adsorbent precursors for oil spill remediation in aqueous environments, as proposed by Rajakovic et al [59]. In their study, the sorption performances of organic loose natural wool fibres (NWF) and a recycled wool-based nonwoven material (RWNM) were evaluated and compared with those of a conventional inorganic sorbent, sepiolite. Under batch tank oil removal conditions, both wool-based sorbents demonstrated significantly superior sorption capacities (5.56 g g^{-1} for NWF and 5.48 g g^{-1} for RWNM) compared

to sepiolite, which exhibited a markedly lower capacity of 0.19 g g^{-1}. These findings highlight the promising potential of wool-derived materials as sustainable alternatives for oil sorption applications. Four significative examples of recycled adsorbents and their applications are schemed in **Fig. 3**.

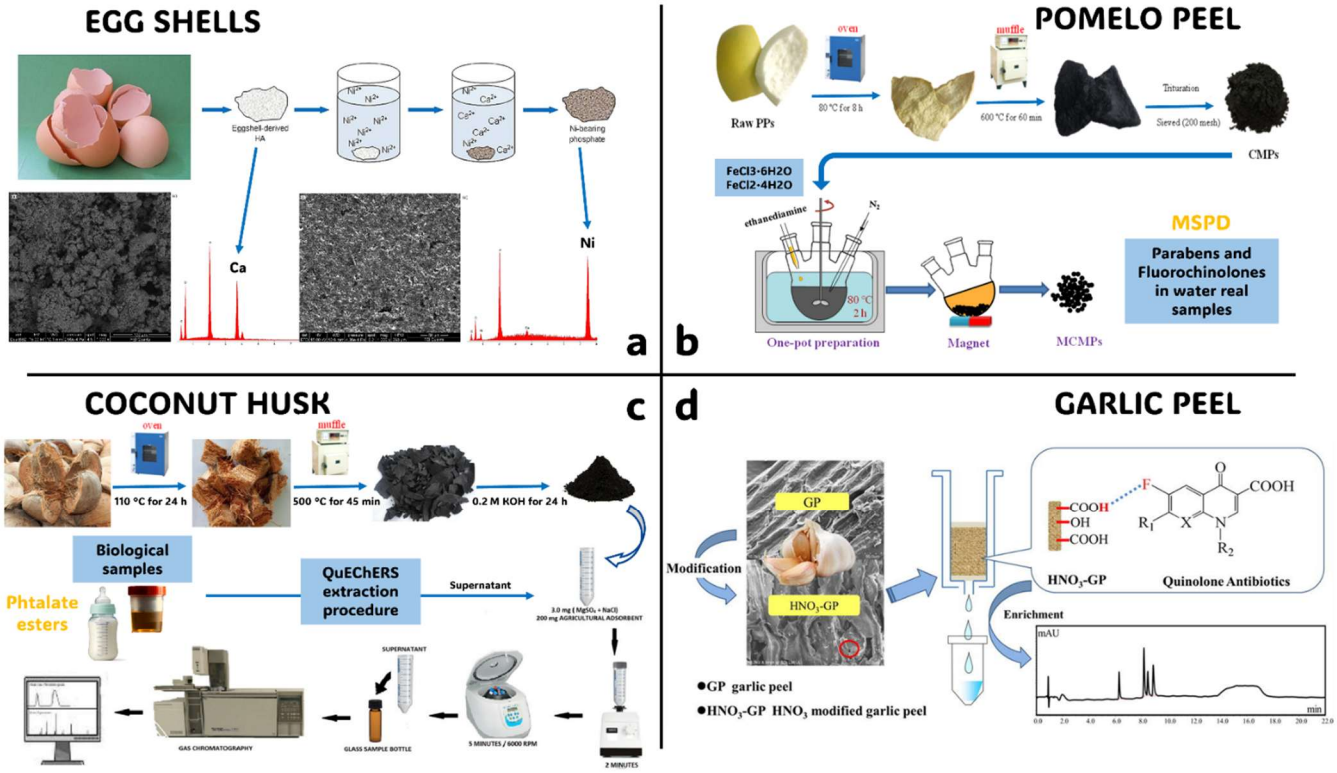

Fig. 3 Significative examples of adsorbents material from different natural, food or agricultural waste sources (**a**: [21]; **b**: [36]; **c**: [51]; **d**:[40]).

4.2. Adsorbent materials from recycled synthetic plastic polymers

A second major category of recycled adsorbents includes those developed from synthetic plastic polymers. These materials have gained increasing attention due to their inherent versatility, resulting from their mechanical robustness, processability, surface modifiability, and chemical tunability [60]. Depending on their structure, polymeric adsorbents can engage in a variety of interactions with target analytes [61-64], representing a highly promising platform for the design of selective, sustainable sorbents.

4.2.1. Polystyrene-Based Adsorbents

Recycling strategies and adsorption-related applications involving PS waste encompass both expanded polystyrene (EPS) and high-impact polystyrene (HIPS). Although chemically similar in their backbone structure, these two PS variants exhibit markedly different behaviours in terms of solvent solubility, thermal resistance, and reactivity toward functionalizing agents [65]. As such, they require tailored processing conditions when being recycled or chemically modified. This is clearly demonstrated by Ruziwa et al. [66], who compared the performance of sulfonated EPS and HIPS as heavy metal adsorbents. Their results showed that sulfonated HIPS had significantly higher adsorption capacities for Zn^{2+} (5.01 mg g^{-1}) and Pb^{2+} (6.80 mg g^{-1}), compared to sulfonated EPS, which retained amounts ten times lower. These differences are attributed to the distinct structural and morphological properties of the two polymers, which influence the efficiency of sulfonation and the accessibility of functional groups on the surface. This process, typically conducted using concentrated sulfuric acid, introduces sulfonic acid groups (–SO_3H) onto the polymer backbone. These groups, with a pKa around 1, remain deprotonated across a wide range of environmental pH values, conferring strong cation-exchange capabilities [67]. An innovative alternative sulfonation method proposed by Sułkowski et al. [68] involves the use of crystalline silica impregnated with sulfuric acid as a heterogeneous sulfonating agent. This approach offers practical advantages, such as easier separation of the final product from the acid medium and reduced solvent consumption. However, it yields a lower degree of sulfonation (~9%) compared to the ~25% achieved by Ruziwa et al. [66]. Regardless the applied method, sulfonated PS has demonstrated good adsorption capabilities for heavy metals such as Zn^{2+}, Cd^{2+}, and Pb^{2+} in aqueous media, even if they are at least an order of magnitude lower than those of other adsorbents, such as pyrolyzed biomass-derived materials.

The sulfonated polymer can be directly used as an adsorbent or serve as a platform for further chemical modifications. For example, Jia et al. [69] employed crosslinking reactions to enhance the structural stability and thermal resistance of the material, achieving adsorption capacities against Cd ions ranging from 68.90 to 80.46 mg g^{-1}. These findings highlight the potential for post-sulfonation functionalization of recycled PS adsorbents to further improve their performance. Another relevant

approach was proposed by Chang et al. [70], who functionalized sulfonated PS with organic chelating ligands. This surface modification strategy proved particularly effective for the selective adsorption of fluoroquinolone antibiotics. The resulting chelator-functionalized sulfonated PS exhibited a maximum adsorption capacity (q_{max}) of 1250 mg g^{-1}, approximately 32 times greater than that of unmodified sulfonated PS (q_{max} = 38.6 mg g^{-1}).

In addition to surface functionalization, another widely explored strategy for PS recycling involves dissolving the polymer waste in suitable solvents. This step not only helps in cleaning the material of dirt and residual additives but also allows reshaping or partial depolymerization. Once dissolved, the polymer can be re-solidified by solvent evaporation, either through vaporization via direct contact with water in tubular evaporators at around 85-88 °C, or during extrusion processes [71]. The resulting polymer solution serves as a precursor for the fabrication of shaped adsorbents, using various techniques that allow fine control over morphology and surface area. Dip-coating onto solid supports has been widely and successfully applied to produce thin polymeric films with controlled thickness and surface morphology [72-74]. In these systems, the adsorptive performance is primarily attributed to the polymer layer formed on the support surface. The dip-coating technique involves immersing the support into an organic polymer solution, followed by solvent evaporation, allowing for the fabrication of composite materials. For instance, Samkampang et al. [74] employed this method to deposit recycled PS onto flower-shaped cellulose paper, yielding an extraction medium with mixed-mode interactions, combining both polar and aromatic/nonpolar affinities, suitable for detecting VOCs in tap water at concentrations in the μg L^{-1} range (see **Fig. 4c**). Alternative strategies for depositing recycled PS onto various supports include film casting [75] and gelation-based methods [76]. In the latter case, PS was deposited onto magnetic Fe_2CoO_4 nanoparticles through a solvent-switching gelation process, whereby transferring the system from chloroform to acetone drastically reduced PS solubility, inducing its gelation around the magnetic core. The resulting composite material was used for d-mSPE of four parabens from water, achieving excellent analytical performance with limits of quantification ranging from 0.15 to 0.5 μg L^{-1}. Collectively, these

approaches demonstrate the versatility of recycled PS. Although all these deposition techniques are relatively low-cost, simple, and analytically effective, the choice of the most appropriate method is largely dictated by the nature of the support and the intended application. Dip-coating is particularly advantageous for porous or high-surface-area supports when the final material is designed as a membrane, filter, or disk. In contrast, gelation and surface chemical modification are better suited for particle-based supports with well-defined nanostructures.

4.2.2. Recycled PET: Activation, Functionalization, and Composite Formation

Among recycled plastic wastes, PET stands out as one of the most extensively investigated and reused polymers, primarily due to its widespread use in food packaging, beverage bottles, and containers. The chemical and mechanical stability of PET, coupled with its surface modifiability, makes it a versatile substrate for the development of adsorbent materials [77]. Although PET is rarely employed in its unaltered form, it is frequently utilized as a support for further chemical functionalization. The intrinsic structure of PET, rich in aromatic rings and ester functionalities, provides an ideal platform for establishing π-π stacking, hydrogen bonding, and dipole-dipole interactions with various environmental pollutants [78]. Numerous studies have demonstrated the reuse of post-consumer PET for fabricating membranes aimed at oil-water separation, a process that has gained significant attention due to increasing concerns about industrial wastewater and oil spills. Among the various approaches, electrospun fibrous membranes have emerged as highly promising materials, offering excellent flexibility and high separation efficiency. For example, in the works by Baggio et al. and Doan et al. [79, 80], post-consumer PET was dissolved in appropriate solvents and processed via electrospinning to produce composite membranes incorporating chitosan and polydimethylsiloxane (PDMS), respectively. These copolymers serve distinct roles in enhancing membrane performance: small amounts of chitosan were added prior to electrospinning to improve fibre uniformity and prevent the formation of polymeric beads, while varying concentrations of PDMS were used to create a superhydrophobic membrane (water contact angle = 149.7°, oil contact angle = 0°), achieving over 98% separation efficiency for oil-water mixtures. A similar strategy has been employed using PET

waste to fabricate membranes for the remediation of cationic dyes. A notable example is the study by Lin et al. [81], in which waste PET was dissolved in a phenol/tetrachloroethane mixture (7:3 w/w) and combined with water bamboo husk particles to form a porous composite membrane via water-vapor-induced phase inversion (see **Fig. 4d**). The synergistic effect of the two waste-derived components resulted in a membrane capable of adsorbing methylene blue and methyl violet 2B with capacities ranging from 307 to 326 mg g^{-1}.

In contrast to membrane fabrication approaches, Semyonov et al. [82] repurposed PET chips without altering their bulk structure, using them as substrates for the in-situ growth of UiO-66 metal-organic frameworks (MOFs). The carboxylic acid groups exposed on the PET surface, originating from terephthalic acid, enable the anchoring of zirconium-based MOF crystals, which in turn allow for the selective adsorption of pesticides from environmental water samples. Although this strategy is more complex, time-consuming, and costly to implement, it offers the significant advantage of selectively modifying the surface of an otherwise non-selective material. Such an approach could prove particularly valuable when applied to the selective extraction of analytes from complex matrices, combining plastic recycling with high-affinity adsorbent systems. More intensive chemical and thermal treatments are applied when PET is used as a carbon source for the synthesis of high-surface-area sorbents, such as activated carbon and graphene-based materials. For instance, Adibfar et al. [83] reviewed several strategies for converting PET waste into activated carbon (AC), noting the prevalence of physical activation methods (typically involving steam or CO_2) alongside the growing interest in chemical activation using agents such as NaOH, KOH, H_2SO_4, and HNO_3. Chemical activation offers the advantage of simultaneous carbonization and pore development at lower temperatures compared to physical approaches, typically followed by washing steps to remove residual activating agents. Both physical and chemical activation strategies have been extensively reported in the literature [83-85], with the resulting materials showing high adsorption capacities, on the order of hundreds of milligrams per gram. Specifically, reported removal capacities include 74 mg g^{-1} for Fe(III), 145.03 mg g^{-1} for Pb(II), 146.93 mg g^{-1} for Cu(II), 142.34 mg g^{-1} for Cr(VI), 147.31

mg g^{-1} for Zn(II), and 71.42 mg g^{-1} for cephalexin, a first-generation cephalosporin antibiotic, demonstrating the effectiveness of PET-derived activated carbons in water purification applications.

El Essawy et al. [86, 87] demonstrated the potential of upcycling PET waste into high-value carbon nanomaterials through two distinct approaches: the synthesis of graphene via high-temperature pyrolysis (800 °C) and the preparation of a magnetic fullerene-based nanocomposite via catalytic thermal decomposition using ferrocene as both carbon source and magnetic precursor (**Fig. 4a**). However, when compared to activated carbon derived from PET, the adsorption efficiencies of these nanomaterials were lower, primarily due to their reduced surface area (721.7 $m^2 g^{-1}$ for the graphene-based material and 336.84 $m^2 g^{-1}$ for the fullerene-based composite, versus 1338 $m^2 g^{-1}$ for KOH-activated carbon) and smaller total pore volume (0.38 $cm^3 g^{-1}$ vs. 0.79 $cm^3 g^{-1}$, respectively). In addition to these limitations, the synthesis of graphene and fullerene composites involves more complex procedures and higher resource consumption, positioning activated carbon as the more practical and efficient alternative for PET-derived sorbents in environmental applications.

Another research line focuses on the partial or complete depolymerization of PET, aiming either to recover monomers such as terephthalic acid or to generate oligomeric intermediates. Farahani et al. [88] utilized terephthalic acid, recovered from depolymerized PET, to synthesize a calcium-terephthalate MOF, which was subsequently evaluated for its ability to remove industrial dyes from aqueous solutions. The material exhibited a maximum adsorption capacity of 979.0 mg g^{-1} for Alizarin Red S, as determined using the Langmuir-Freundlich isotherm model. This performance represents a significant improvement over the composite membranes for dye removal discussed earlier in this section, highlighting the potential of MOF-based systems derived from PET waste for advanced wastewater treatment applications.

In two studies conducted by Chan and Zinchenko [89, 90], PET was partially depolymerized via aminolysis using tri- and tetra-amines to produce either magnetic adsorptive microparticles or hydrogel networks. Both materials were evaluated for their dye adsorption performance. The PET-derived hydrogel exhibited an adsorption capacity of approximately 500 mg g^{-1} for the anionic dye

Congo Red, while the magnetic microparticles achieved a capacity of around 780 mg g^{-1}. A key advantage of both materials lies in their exceptionally rapid adsorption kinetics, reaching saturation within less than one minute of contact with the dye solution, an attribute that significantly enhances their applicability in fast and efficient water treatment processes. A further example of chemical modification involves the functionalization of recycled PET granules with phenolic compounds, a strategy designed to introduce chelating functionalities onto the polymer surface. As reported by Ungureanu et al. [91], hydroxyquinone was employed as a surface modifier, doubling the copper ion retention capacity compared to unmodified PET granules (from 12.80 to 61.73 mg g^{-1}). Nonetheless, this performance remains significantly lower than that of KOH-activated carbon, which, due to its ease of synthesis and high adsorption efficiency, stands out as the most effective option for water remediation applications. However, a different set of criteria applies to sample preparation, where selectivity toward a specific analyte or chemical class often outweighs total adsorption capacity. In such contexts, the surface functionalization of recycled PET may not only be the most suitable approach but also the only practical solution, offering the necessary chemical specificity for targeted extraction.

4.2.3. Polyolefins and Other Plastics

Recycling strategies involving polyolefins, namely low-density polyethylene (LDPE), high-density polyethylene (HDPE), and polypropylene (PP), have been increasingly explored for applications in both water remediation and analytical sample preparation. Owing to their chemical inertness, hydrophobicity, and extensive use in packaging and consumer products, these polymers represent an abundant and cost-effective resource for developing adsorbent materials [63]. A pivotal step toward this goal was demonstrated by Saleem et al. [92], who investigated the selective identification and sorting of plastic waste from mixed refuse streams. This initial separation phase is critical for isolating polyolefin-rich fractions, thereby enabling more controlled and predictable chemical behaviour and adsorption properties in the final materials. Building on this approach, the same study repurposed polyolefin waste (polymeric blends enriched in PE and PP) into functional oil-adsorbent films through

a combination of dissolution, spin coating, and thermal annealing. By tailoring surface morphology and porosity during these processing steps, the authors significantly enhanced the retention of hydrophobic organic pollutants, such as oils, in aqueous environments (see **Fig. 4b**). Notably, the resulting membranes exhibited exceptional performance, achieving oil uptake capacities ranging from 70 to 140 g of oil per gram of membrane. As an example of application in sample preparation, Samkampang et al. [74] utilized LDPE waste derived from garment packaging films, dissolving it to create a polymeric solution suitable for dip-coating cellulose-based substrates. The resulting composite materials were successfully employed for the extraction of organic contaminants from environmental water samples. Owing to the specific geometry of the extraction device and the retention capabilities of the composite material, the method achieved satisfactory analytical performance, with limits of quantification in the range of 9-10 $\mu g\ L^{-1}$.

Beyond polyolefins, other polymeric matrices have also been incorporated into adsorbent systems using similar strategies. Govindappa et al. [93] reported the use of recycled polyvinyl chloride (PVC) to fabricate hybrid membranes functionalized with benzalkonium chloride (BAC) for the selective extraction of arsenate (As(V)) from contaminated water. In their approach, both PVC and BAC were co-dissolved in tetrahydrofuran (THF), and the resulting solution underwent controlled gelation and solvent evaporation in Petri dishes, forming a stable hybrid polymeric membrane featuring both ionic and hydrophobic functionalities. In addition to its extremely low production cost (approximately $0.0016 per square meter), the resulting membrane demonstrated strong remediation potential, removing around 91% of As(V) from spiked water samples. A similar solvent-based approach was adopted by Dahdouh et al. [94], who recycled polymethyl methacrylate (PMMA) waste, sourced from discarded plexiglass sheets, by first subjecting it to cryogenic grinding, followed by sulfonation with concentrated sulfuric acid. The resulting sulfonated PMMA demonstrated high adsorption capacity for synthetic dyes in aqueous solution, highlighting the potential to chemically upgrade even highly inert thermoplastics into functional sorbents. The dye uptake capacities for methylene blue ($97.09\ mg\ g^{-1}$) and Basic Yellow 28 ($222.22\ mg\ g^{-1}$) significantly surpass those of conventional

synthetic cation-exchange resins reported in the literature [95, 96]. These results underscore the promise of PMMA-based materials in water treatment applications, particularly for textile dye removal.

A further example of composite material fabrication from recycled polymers is provided by Lopez-Tellez et al. [73], who developed functional adsorbent filters by repurposing commercial polyurethane foam (PUF) and PS from yogurt containers. In their approach, the foam was dip-coated with a PS solution in tetrahydrofuran (THF), resulting in a robust composite structure designed for the extraction of organic pollutants from urban air. This material not only exhibited strong mechanical stability and ease of handling but also demonstrated enhanced adsorption performance, respect to commercially available glass filters. The PUF served as a durable structural support, while the PS coating significantly increased affinity and retention capacity for PAHs. The recycled composite showed superior adsorption efficiency at lower flow rates compared to conventional approaches, without compromising analytical precision or accuracy. Supporting its strong retention capabilities, the method achieved limits of detection for PAHs in the range of 0.06-0.24 ng m^{-3} of air.

Taken together, these examples highlight several converging strategies in the valorisation of plastic waste into adsorbent systems. A common and effective approach involves the dissolution of the polymer in appropriate organic solvents, which facilitates not only morphological reshaping of the macromolecular chains but also partial purification from plasticizers and additives, and, where applicable, controlled depolymerization. Subsequent solvent evaporation, often performed at room temperature, leads to the re-solidification of the material in a form tailored to the desired application. Nevertheless, the choice of solvent plays a dual role: it determines both the structural features of the final product and the environmental sustainability of the entire process. In several cases, the use of hazardous solvents, combined with limited processing scales and high energy consumption, raises concerns about the overall eco-efficiency of these recycling pathways [97]. Therefore, future research should prioritize the development of greener, solvent-free, or aqueous-compatible methods, as well

as scalable processing techniques that enable industrial translation without compromising the environmental benefits of recycling.

Four significative examples of recycled adsorbents from polymeric waste sources and their applications are displayed in **Fig. 4**.

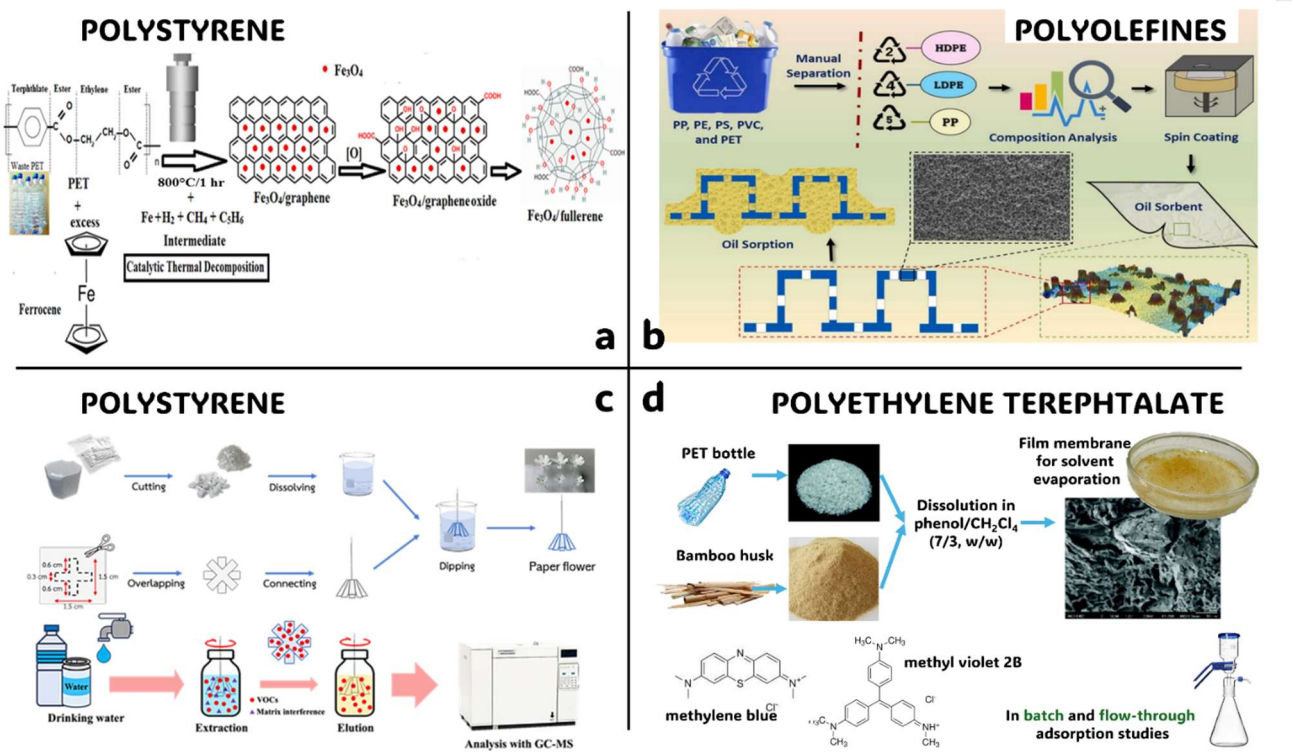

Fig. 4 Significative examples of adsorbents material from different polymeric waste sources (**a**: [87]; **b**: [92]; **c**: [74]; **d**:[81]).

4.3. Beyond recycling: commercial single-use items and natural materials as adsorbents-a strategic outlook

Although the primary focus of this review is on recycled polymers and second-life materials, it is both timely and strategically valuable to dedicate a specific discussion to commercial single-use products and virgin natural materials that are increasingly employed as adsorbents in sample preparation and water remediation. While these substrates are not derived from waste according to the criteria defined in the introduction, their inclusion is justified by the fact that they share several critical characteristics with recycled materials: low cost, broad availability, ease of processing, and

most importantly, high potential for reuse and integration into circular systems. Highlighting such materials broadens the scope of the review and supports the underlying goal of promoting circular analytical chemistry approaches not only by recovering waste but also by rethinking common, often discarded items as valuable sorbents after primary use. Moreover, many of the methodologies described in this section could be directly applied, or easily adapted, to post-consumer or discarded counterparts of these items, thus serving as blueprints for future sustainable reuse practices. A conceptual subdivision is proposed here, distinguishing between (i) commercial single-use products, such as adhesive tape, cellulosic paper, wooden tips, sawdust, and toothpicks, and (ii) non-waste natural materials, like pure cotton or unprocessed plant-derived matrices.

Following examples illustrate how commercially available, low-cost substrates can deliver meaningful analytical performance with minimal intervention, while also serving as ideal starting points for more sophisticated modification strategies. For instance, Calero-Cañuelo et al. [98, 99] demonstrated the use of adhesive tape as a sampling substrate for solid, dust-like matrices, followed by thermal desorption and direct environmental-ESI-MS/MS analysis (see **Fig. 5b**). The workflow was applied to caffeine quantification in various solid coffee samples, achieving a detection limit of 0.18 mg g^{-1} of coffee powder. Although the method does not provide extremely high sensitivity, it offers a rapid, fully integrated, and minimal-processing approach, laying the groundwork for the future application of post-consumer adhesive materials in rapid screening protocols. Cellulose-based materials, such as cellulosic paper, offer several intrinsic advantages as sustainable and cost-effective adsorbents, including a highly porous fibrous microstructure, natural abundance, renewability, low environmental footprint, and excellent chemical modifiability. In this context, González-Bermúdez et al. and Jain et al. [100, 101] employed unmodified or impregnated paper disks for the extraction of a broad spectrum of analytes (see **Fig. 5a**). In particular, Jain et al. introduced a rotating paper disk impregnated with n-octanol, enabling liquid-phase microextraction from complex biological fluids. While the method delivered excellent analytical performance (LOQ = 0.060-0.099 μg mL^{-1}), it does not constitute a technological breakthrough from an application standpoint: prolonged adsorption and

solvent desorption times position it as a conventional technique, albeit integrated with a highly accessible commercial material. In another application, Takagai et al. [102] employed medical-grade cellulose cotton pads as a sorptive medium for the preconcentration of nonylphenol from water samples prior to homogeneous liquid-liquid extraction. In this workflow, the commercial product serves as a critical preconcentration step, enhancing the enrichment factor and enabling highly competitive detection limits (LOD ≈ 0.22 μg L^{-1}). The main drawback of this approach is its multistep nature, which necessitates an additional extraction phase to fully exploit the material's potential. This approach highlights the compatibility of medical or hygiene-derived natural products with environmental analysis protocols. Moving to wood-based commercial items, Millán Santiago et al., González-Galán et al., and Hammadi et al. [103-105] reported the direct use of wooden toothpicks, wooden tips, and sawdust as adsorbents for pharmaceutical compounds from biological fluids. These materials, although virgin in the referenced studies, are inherently biodegradable, mechanically robust, and chemically modifiable, qualities that make them strong candidates for post-use repurposing in analytical workflows. Owing to their lignocellulosic composition, rich in cellulose, hemicellulose, and lignin, wood-based substrates offer a versatile chemical framework capable of interacting with a wide range of analytes through hydrogen bonding, π-π interactions, and hydrophobic forces. Taken together, these studies suggest that simple and accessible materials, often overlooked or disposed of after single use, could play an active role in future circular sorbent technologies.

In addition to recycled materials and single-use commercial consumables, natural raw materials, although not strictly classified as recycled, can be integrated into circular reuse cycles and play a significant role in the design of sustainable adsorbents [106, 107]. Natural fibrous materials such as cotton and kapok fibres have attracted significant attention for three main reasons: (i) they are composed primarily of cellulose, a highly interactive and modifiable biopolymer; (ii) they exhibit a high surface-area-to-volume ratio due to their microstructured morphology; and (iii) they are amenable to rapid and mild chemical treatments to tailor their surface functionalities. Cotton fibre,

for instance, has been employed in its pristine form [108-110] (see **Fig. 5d**), as a substrate for holding organic extracting solvents [111, 112], or chemically modified to enhance surface interactions [113-115]. It has also been incorporated into nanostructured composite adsorbents for solid-phase microextraction and d-SPE [108, 116-118]. Beyond its intrinsic adsorption advantages, owing to its chemical composition, it is worth emphasizing that cellulosic fibre is among the most inexpensive natural materials available (with market prices typically around 1-2 USD kg^{-1}), highly consistent in composition, and extremely abundant worldwide. Other fibrous materials of natural origin, such as kapok fibres, have also demonstrated considerable potential as supports for liquid-phase extractions [119] or as functional components in magnetic SPE materials [120]. These fibres combine intrinsic porosity and hydrophobicity with a high degree of chemical modifiability. Although significantly more expensive than cellulosic fibres (20-25 USD kg^{-1}), kapok offers distinct advantages, including substantially higher porosity and pronounced hydrophobic character, often resulting from a natural wax coating with a high degree of lipophilicity. The primary drawback of kapok fibres lies in their low mechanical strength, which necessitates careful handling and precludes their use in dispersive extraction techniques. Additional examples include lignocellulosic biomass, cork, and pollen-based materials, which have been employed in the design of novel sorbents. In some studies, raw biological matrices such as Spirulina maxima algae, Phragmites australis, and plant bracts have been directly used as adsorbents following minimal physical processing [121-123]. In others, biochar or activated carbon materials derived from biomass pyrolysis have been developed and applied to heavy metal remediation or organic pollutant extraction [124, 125]. Nature also offers unique morphologies suitable for aqueous environments, such as natural sponges. The work of Makkliang et al. [126] proposed the use of Luffa cylindrica sponge as an adsorbent support for VA-SPE, leveraging its high porosity and mechanical robustness to retain analytes from water matrices. A particularly intriguing natural biopolymer is sporopollenin, the main component of the exine layer of pollen grains. Sporopollenin is an extremely rigid and chemically inert polymer, with a complex polyaliphatic and polyaromatic structure that provides both mechanical strength and surface modifiability. In analytical

applications, sporopollenin has been exploited as a stable solid substrate for chemical derivatization, enabling the design of composite nanomaterials for various SPE techniques [127-130] (see **Fig. 5c**). In conclusion, natural materials (whether used in pristine form, chemically activated, or transformed into carbonaceous adsorbents) demonstrate remarkable versatility and efficiency in analytical extraction and environmental remediation. Their intrinsic biopolymeric nature provides a rich landscape of interactive functionalities, while their ease of modification and sustainable origin make them ideal candidates for integration into circular recycling and reuse strategies, especially when coupled with post-consumer biowaste.

Four significative examples of adsorbents from single-use commercial items and natural unprocessed materials are displayed in **Fig. 5**.

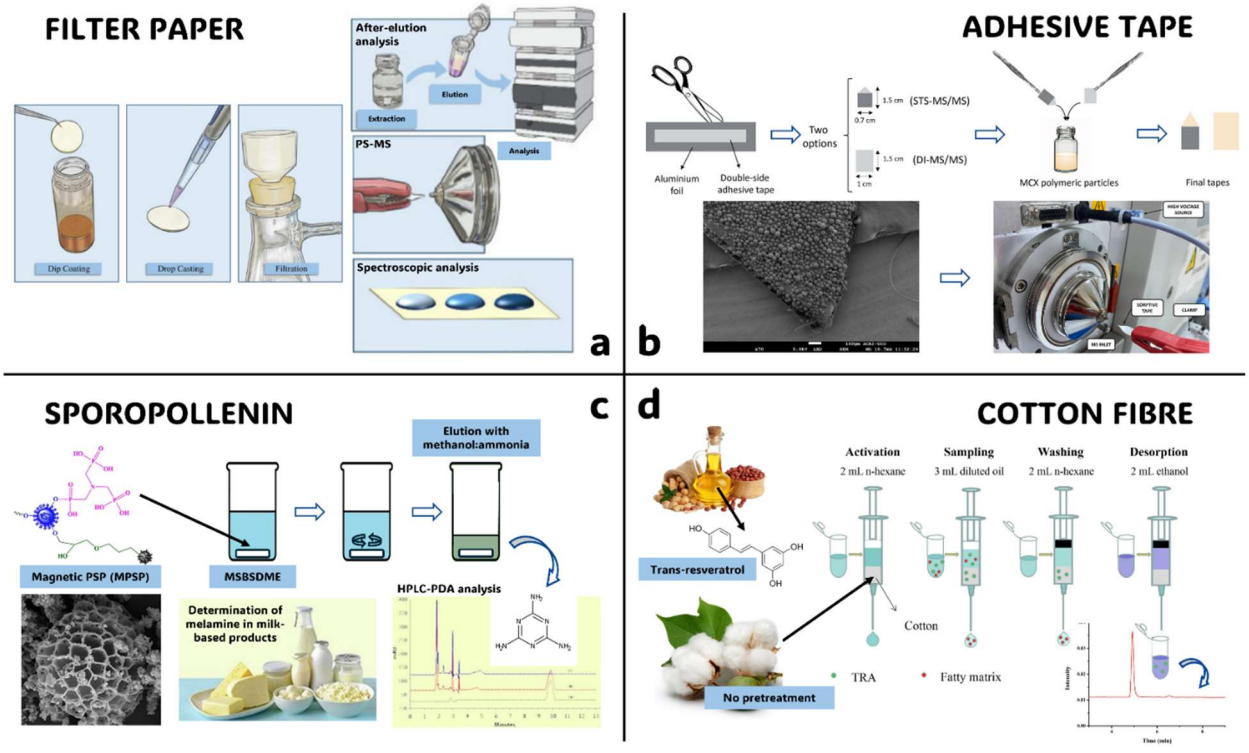

Fig. 5 Significative examples of adsorbents material from single commercial items and natural unprocessed natural sources (**a**: [100]; **b**: [99]; **c**: [128]; **d**:[109]).

References

[1] THE 17 GOALS, Sustainable Development. https://sdgs.un.org/goals, (accessed 03/09/2025).

[2] EU Waste Framework Directive (2008/98/EC). https://eur-lex.europa.eu/eli/dir/2008/98/oj/eng, (accessed 03/09/2025).

[3] Gałuszka, A., Migaszewski, Z., & Namieśnik, J. (2013). The 12 principles of green analytical chemistry and the SIGNIFICANCE mnemonic of green analytical practices. TrAC Trends in Analytical Chemistry, 50, 78-84. https://doi.org/10.1016/j.trac.2013.04.010

[4] Psillakis, E., & Pena-Pereira, F. (2024). The twelve goals of circular analytical chemistry. TrAC Trends in Analytical Chemistry, 175, 117686. https://doi.org/10.1016/j.trac.2024.117686

[5] López-Lorente, Á. I., Pena-Pereira, F., Pedersen-Bjergaard, S., Zuin, V. G., Ozkan, S. A., & Psillakis, E. (2022). The ten principles of green sample preparation. TrAC Trends in Analytical Chemistry, 148, 116530. https://doi.org/10.1016/j.trac.2022.116530

[6] Escamilla-Lara, K. A., Lopez-Tellez, J., & Rodriguez, J. A. (2023). Adsorbents obtained from recycled polymeric materials for retention of different pollutants: A review. Chemosphere, 335, 139159. https://doi.org/10.1016/j.chemosphere.2023.139159

[7] Yantasee, W., Rutledge, R. D., Chouyyok, W., Sukwarotwat, V., Orr, G., Warner, C. L., Marvin, Warner, M. G., Fryxell, G. E., Wiacek, R. J., Timchalk, C., & Addleman, R. S. (2010). Functionalized nanoporous silica for the removal of heavy metals from biological systems: adsorption and application. ACS applied materials & interfaces, 2(10), 2749-2758. https://doi.org/10.1021/am100616b

[8] Stein, R. S. (1998, December). Polymer recycling: Thermodynamics and economics. In Macromolecular Symposia (Vol. 135, No. 1, pp. 295-314). Weinheim, Germany: WILEY-VCH Verlag GmbH & Co. KGaA. https://doi.org/10.1002/masy.19981350131

[9] Gutowski, T. G. (2008, May). Thermodynamics and recycling, a review. In 2008 Ieee International Symposium on Electronics and the Environment (pp. 1-5). IEEE. https://doi.org/10.1109/ISEE.2008.4562912

[10] Jehanno, C., Alty, J. W., Roosen, M., De Meester, S., Dove, A. P., Chen, E. Y. X., Leibfarth, F. A., & Sardon, H. (2022). Critical advances and future opportunities in upcycling commodity polymers. Nature, 603(7903), 803-814. https://doi.org/10.1038/s41586-021-04350-0

[11] Vogt, B. D., Stokes, K. K., & Kumar, S. K. (2021). Why is recycling of postconsumer plastics so challenging? ACS Applied Polymer Materials, 3(9), 4325-4346. https://doi.org/10.1021/acsapm.1c00648

[12] Helbig, C., Huether, J., Joachimsthaler, C., Lehmann, C., Raatz, S., Thorenz, A., Faulstich, M., & Tuma, A. (2022). A terminology for downcycling. Journal of Industrial Ecology, 26(4), 1164-1174. https://doi.org/10.1111/jiec.13289

[13] Sihem, A., Lehocine, M. B., & Miniai, H. A. (2012). Preparation and characterisation of an natural adsorbent used for elimination of pollutants in wastewater. Energy Procedia, 18, 1145-1151. https://doi.org/10.1016/j.egypro.2012.05.129

[14] Formela, K., Kurańska, M., & Barczewski, M. (2022). Recent advances in development of waste-based polymer materials: A review. Polymers, 14(5), 1050. https://doi.org/10.3390/polym14051050

[15] Demirbas, A. (2011). Waste management, waste resource facilities and waste conversion processes. Energy conversion and management, 52(2), 1280-1287. https://doi.org/10.1016/j.enconman.2010.09.025

[16] Chen, Z., Wei, W., Chen, H., & Ni, B. J. (2022). Recent advances in waste-derived functional materials for wastewater remediation. Eco-Environment & Health, 1(2), 86. 10.1016/j.eehl.2022.05.001

[17] Jalili, V., Barkhordari, A., & Ghiasvand, A. (2020). A comprehensive look at solid-phase microextraction technique: A review of reviews. Microchemical Journal, 152, 104319. https://doi.org/10.1016/j.microc.2019.104319

[18] de Freitas Netto, S. V., Sobral, M. F. F., Ribeiro, A. R. B., & Soares, G. R. D. L. (2020). Concepts and forms of greenwashing: A systematic review. Environmental Sciences Europe, 32(1), 19. https://doi.org/10.1186/s12302-020-0300-3

[19] Mukhopadhyay, A., Duttagupta, S., & Mukherjee, A. (2022). Emerging organic contaminants in global community drinking water sources and supply: A review of occurrence, processes and remediation. Journal of Environmental Chemical Engineering, 10(3), 107560. https://doi.org/10.1016/j.jece.2022.107560

[20] Cashin, V. B., Eldridge, D. S., Yu, A., & Zhao, D. (2018). Surface functionalization and manipulation of mesoporous silica adsorbents for improved removal of pollutants: a review. Environmental Science: Water Research & Technology, 4(2), 110-128. https://doi.org/10.1039/C7EW00322F

[21] De Angelis, G., Medeghini, L., Conte, A. M., & Mignardi, S. (2017). Recycling of eggshell waste into low-cost adsorbent for Ni removal from wastewater. Journal of Cleaner Production, 164, 1497-1506. https://doi.org/10.1016/j.jclepro.2017.07.085

[22] Candido, I. C. M., Pires, I. C. B., & de Oliveira, H. P. (2021). Natural and synthetic fiber-based adsorbents for water remediation. CLEAN–Soil, Air, Water, 49(6), 2000189. https://doi.org/10.1002/clen.202000189

[23] Hakeem, K., Sabir, M., Ozturk, M., & Mermut, A. R. (Eds.). (2014). Soil remediation and plants: prospects and challenges. Elsevier, New York, pp 287–312.

[24] Ahsan, S., Kaneco, S., Ohta, K., Mizuno, T., & Kani, K. (2001). Use of some natural and waste materials for waste water treatment. Water research, 35(15), 3738-3742. https://doi.org/10.1016/S0043-1354(01)00047-1

[25] Batool, S., Idrees, M., Hussain, Q., & Kong, J. (2017). Adsorption of copper (II) by using derived-farmyard and poultry manure biochars: Efficiency and mechanism. Chemical Physics Letters, 689, 190-198. https://doi.org/10.1016/j.cplett.2017.10.016

[26] Lamaming, J., Saalah, S., Rajin, M., Ismail, N. M., & Yaser, A. Z. (2022). A review on bamboo as an adsorbent for removal of pollutants for wastewater treatment. International Journal of Chemical Engineering, 2022(1), 7218759. https://doi.org/10.1155/2022/7218759

[27] Wang, M., Huang, Z. H., Liu, G., & Kang, F. (2011). Adsorption of dimethyl sulfide from aqueous solution by a cost-effective bamboo charcoal. Journal of hazardous materials, 190(1-3), 1009-1015. https://doi.org/10.1016/j.jhazmat.2011.04.041

[28] Reinert, N. P., Vieira, C. M., Da Silveira, C. B., Budziak, D., & Carasek, E. (2018). A low-cost approach using diatomaceous earth biosorbent as alternative SPME coating for the determination of PAHs in water samples by GC-MS. Separations, 5(4), 55. https://doi.org/10.3390/separations5040055

[29] Celeiro, M., Vazquez, L., Sergazina, M., Docampo, S., Dagnac, T., Vilar, V. J., & Llompart, M. (2020). Turning cork by-products into smart and green materials for solid-phase extraction-gas chromatography tandem mass spectrometry analysis of fungicides in water. Journal of Chromatography A, 1628, 461437. https://doi.org/10.1016/j.chroma.2020.461437

[30] Pintor, A. M., Ferreira, C. I., Pereira, J. C., Correia, P., Silva, S. P., Vilar, V. J., Botelho, C. M. S., & Boaventura, R. A. (2012). Use of cork powder and granules for the adsorption of pollutants: A review. Water research, 46(10), 3152-3166. https://doi.org/10.1016/j.watres.2012.03.048

[31] Hinz, J. S., Morés, L., & Carasek, E. (2021). Exploring the use of cork pellets in bar adsorptive microextraction for the determination of organochloride pesticides in water samples with gas chromatography/electron capture detection quantification. Journal of Chromatography A, 1645, 462099. https://doi.org/10.1016/j.chroma.2021.462099

[32] Morelli, D. C., Mafra, G., Santos, A. V., Merib, J., & Carasek, E. (2020). Designing a green device to BAμE: recycled cork pellet as extraction phase for the determination of parabens in river water samples. Talanta, 219, 121369. https://doi.org/10.1016/j.talanta.2020.121369

[33] Mallek, M., Chtourou, M., Portillo, M., Monclus, H., Walha, K., ben Salah, A., & Salvado, V. (2018). Granulated cork as biosorbent for the removal of phenol derivatives and emerging contaminants. Journal of environmental management, 223, 576-585. https://doi.org/10.1016/j.jenvman.2018.06.069

[34] Lebre, D. T., Thipe, V. C., Cotrim, M. E., & Bustillos, J. O. V. (2022). Use of sugar cane bagasse as solid extraction phase sorbent to analyze hormones from industrial effluent. ACS omega, 7(12), 10069-10076. https://doi.org/10.1021/acsomega.1c06064

[35] Abid, M., Niazi, N. K., Bibi, I., Farooqi, A., Ok, Y. S., Kunhikrishnan, A., Ali, F., Ali, S., Igalavithana, A. D., & Arshad, M. (2016). Arsenic (V) biosorption by charred orange peel in aqueous environments. International journal of phytoremediation, 18(5), 442-449. https://doi.org/10.1080/15226514.2015.1109604

[36] Huang, Y., Peng, J., & Huang, X. (2018). One-pot preparation of magnetic carbon adsorbent derived from pomelo peel for magnetic solid-phase extraction of pollutants in environmental waters. Journal of Chromatography A, 1546, 28-35. https://doi.org/10.1016/j.chroma.2018.03.001

[37] Fu, Y., Yang, Z., Xia, Y., Xing, Y., & Gui, X. (2021). Adsorption of ciprofloxacin pollutants in aqueous solution using modified waste grapefruit peel. Energy Sources, Part A: Recovery, Utilization, and Environmental Effects, 43(2), 225-234. https://doi.org/10.1080/15567036.2019.1624877

[38] Huang, H. Y., Luo, L. D., Zhang, H., Lu, Y. Q., & Zhang, D. (2014). Adsorption of Congo red from aqueous solutions by the activated carbons prepared from grapefruit peel. Applied Mechanics and Materials, 529, 3-7. https://doi.org/10.4028/www.scientific.net/AMM.529.3

[39] Peng, L. Q., Zhang, Y., Yan, T. C., Gu, Y. X., & Cao, J. (2021). Carbonized biosorbent assisted matrix solid-phase dispersion microextraction for active compounds from functional food. Food Chemistry, 365, 130545. https://doi.org/10.1016/j.foodchem.2021.130545

[40] Zhao, Y., Li, W., Liu, J., Huang, K., Wu, C., Shao, H., Chen, H., & Liu, X. (2017). Modification of garlic peel by nitric acid and its application as a novel adsorbent for solid-phase extraction of quinolone antibiotics. Chemical Engineering Journal, 326, 745-755. https://doi.org/10.1016/j.cej.2017.05.139

[41] Khiaophong, W., Jaroensan, J., Kachangoon, R., Vichapong, J., Burakham, R., Santaladchaiyakit, Y., & Srijaranai, S. (2022). Modified peanut shell as an eco-friendly biosorbent for effective extraction of triazole fungicide residues in surface water and honey samples before their determination by high-performance liquid chromatography. ACS omega, 7(39), 34877-34887. https://doi.org/10.1021/acsomega.2c03410

[42] Ali, S. M. (2018). Fabrication of a nanocomposite from an agricultural waste and its application as a biosorbent for organic pollutants. International Journal of Environmental Science and Technology, 15, 1169-1178. https://doi.org/10.1007/s13762-017-1477-x

[43] Li, M., Jiao, C., Yang, X., Wang, C., Wu, Q., & Wang, Z. (2017). Solid phase extraction of carbamate pesticides with banana peel derived hierarchical porous carbon prior to high performance liquid chromatography. Analytical Methods, 9(4), 593-599. https://doi.org/10.1039/C6AY02678H

[44] Kumrić, K., Vujasin, R., Egerić, M., Petrović, Đ., Devečerski, A., & Matović, L. (2019). Coconut shell activated carbon as solid-phase extraction adsorbent for preconcentration of selected pesticides from water samples. Water, Air, & Soil Pollution, 230, 1-10. https://doi.org/10.1007/s11270-019-4359-7

[45] Acheampong, M. A., Pakshirajan, K., Annachhatre, A. P., & Lens, P. N. (2013). Removal of Cu (II) by biosorption onto coconut shell in fixed-bed column systems. Journal of Industrial and Engineering Chemistry, 19(3), 841-848. https://doi.org/10.1016/j.jiec.2012.10.029

[46] Kachangoon, R., Vichapong, J., & Santaladchaiyakit, Y. (2024). Surfactant modified coconut husk fiber as a green alternative sorbent for micro-solid phase extraction of triazole fungicides at trace level in environmental water, soybean milk, fruit juice and alcoholic beverage samples. RSC advances, 14(11), 7290-7302. https://doi.org/10.21203/rs.3.rs-2759857/v1

[47] Gao, J., Liu, Y., Li, X., Yang, M., Wang, J., & Chen, Y. (2020). A promising and cost-effective biochar adsorbent derived from jujube pit for the removal of Pb (II) from aqueous solution. Scientific reports, 10(1), 7473. https://doi.org/10.1038/s41598-020-64191-1

[48] El Messaoudi, N., El Khomri, M., Lacherai, A., Bentahar, S., Dbik, A., & Bakiz, B. (2017). Valorization and characterization of wood of the jujube shell: application to the removal of cationic dye from aqueous solution. J Eng Sci Technol, 12(2), 421-436.

[49] Turkmen Koc, S. N., Kipcak, A. S., Moroydor Derun, E., & Tugrul, N. (2021). Removal of zinc from wastewater using orange, pineapple and pomegranate peels. International Journal of Environmental Science and Technology, 18, 2781-2792. https://doi.org/10.1007/s13762-020-03025-z

[50] Ago, K. A., Kitte, S. A., & Gure, A. (2024). Determination of organochlorine pesticides from juice samples using magnetic biochar-based dispersive micro-solid phase extraction in combination with dispersive liquid-liquid microextraction. Emerging Contaminants, 10(1), 100283. https://doi.org/10.1016/j.emcon.2023.100283

[51] Adenuga, A. A., Ayinuola, O., Adejuyigbe, E. A., & Ogunfowokan, A. O. (2020). Biomonitoring of phthalate esters in breast-milk and urine samples as biomarkers for neonates' exposure, using

modified quechers method with agricultural biochar as dispersive solid-phase extraction absorbent. Microchemical Journal, 152, 104277. https://doi.org/10.1016/j.microc.2019.104277

[52] Ramón-Gonçalves, M., Alcaraz, L., Pérez-Ferreras, S., León-González, M. E., Rosales-Conrado, N., & López, F. A. (2019). Extraction of polyphenols and synthesis of new activated carbon from spent coffee grounds. Scientific reports, 9(1), 17706. https://doi.org/10.1038/s41598-019-54205-y

[53] Abdurahman, Y., Bekana, D., Temesgen, A., Bussa, N., Aschale, M., Teju, E., & Amde, M. (2023). Magnetic coffee residue biosorbent for selective extraction of zinc oxide nanoparticles in water samples. Bulletin of the Chemical Society of Ethiopia, 37(4), 859-873. https://doi.org/10.4314/bcse.v37i4.5

[54] Haq, N., Iqbal, M., Hussain, A., Shakeel, F., Ahmad, A., Alsarra, I. A., AlAjmi, M. F., Mahfooz, A., & Abouzadeh, M. A. (2023). Utilization of Waste Biomaterial as an Efficient and Eco-Friendly Adsorbent for Solid-Phase Extraction of Pantoprazole Contaminants in Wastewater. Separations, 10(4), 253. https://doi.org/10.3390/separations10040253

[55] Dodson, J. R., Parker, H. L., García, A. M., Hicken, A., Asemave, K., Farmer, T. J., He, H., Clark, J. H., & Hunt, A. J. (2015). Bio-derived materials as a green route for precious & critical metal recovery and re-use. Green Chemistry, 17(4), 1951-1965. https://doi.org/10.1039/C4GC02483D

[56] Aziz, K., Mamouni, R., Azrrar, A., Kjidaa, B., Saffaj, N., & Aziz, F. (2022). Enhanced biosorption of bisphenol A from wastewater using hydroxyapatite elaborated from fish scales and camel bone meal: A RSM@ BBD optimization approach. Ceramics International, 48(11), 15811-15823. https://doi.org/10.1016/j.ceramint.2022.02.119

[57] Pal, D., & Maiti, S. K. (2020). An approach to counter sediment toxicity by immobilization of heavy metals using waste fish scale derived biosorbent. Ecotoxicology and Environmental Safety, 187, 109833. https://doi.org/10.1016/j.ecoenv.2019.109833

[58] Slimani, R., El Ouahabi, I., Abidi, F., El Haddad, M., Regti, A., Laamari, M. R., El Antri, S., & Lazar, S. (2014). Calcined eggshells as a new biosorbent to remove basic dye from aqueous solutions: thermodynamics, kinetics, isotherms and error analysis. Journal of the Taiwan Institute of Chemical Engineers, 45(4), 1578-1587. https://doi.org/10.1016/j.jtice.2013.10.009

[59] Rajakovic, V., Aleksic, G., Radetic, M., & Rajakovic, L. (2007). Efficiency of oil removal from real wastewater with different sorbent materials. Journal of hazardous materials, 143(1-2), 494-499. https://doi.org/10.1016/j.jhazmat.2006.09.060Get rights and content

[60] Monnerie, L. (1990). Mechanical properties of polymeric materials. In Statistical Models for the Fracture of Disordered Media (pp. 66-76). North-Holland. https://doi.org/10.1016/B978-0-444-88551-7.50012-4

[61] Li, W., Xie, Z., Xue, S., Ye, H., Liu, M., Shi, W., & Liu, Y. (2021). Studies on the adsorption of dyes, Methylene blue, Safranin T, and Malachite green onto Polystyrene foam. Separation and purification technology, 276, 119435. https://doi.org/10.1016/j.seppur.2021.119435

[62] Welle, F., Bayer, F., & Franz, R. (2012). Quantification of the sorption behavior of polyethylene terephthalate polymer versus PET/PA polymer blends towards organic compounds. Packaging Technology and Science, 25(6), 341-349. https://doi.org/10.1002/pts.984

[63] Elgharbawy, A. S., & Ali, R. M. (2022). A comprehensive review of the polyolefin composites and their properties. Heliyon, 8(7). 10.1016/j.heliyon.2022.e09932

[64] Nilsson, R., Olsson, M., Westman, G., Matic, A., & Larsson, A. (2022). Screening of hydrogen bonds in modified cellulose acetates with alkyl chain substitutions. Carbohydrate Polymers, 285, 119188. https://doi.org/10.1016/j.carbpol.2022.119188

[65] Singh, A., Chauhan, A., & Gaur, R. (2025). A comprehensive review on the synthesis, properties, environmental impacts, and chemiluminescence applications of polystyrene (PS). Discover Chemistry, 2(1), 47. https://doi.org/10.1007/s44371-025-00125-y

[66] Ruziwa, D., Chaukura, N., Gwenzi, W., & Pumure, I. (2015). Removal of Zn2+ and Pb2+ ions from aqueous solution using sulphonated waste polystyrene. Journal of Environmental Chemical Engineering, 3(4), 2528-2537. https://doi.org/10.1016/j.jece.2015.08.006

[67] Coughlin, J. E., Reisch, A., Markarian, M. Z., & Schlenoff, J. B. (2013). Sulfonation of polystyrene: Toward the "ideal" polyelectrolyte. Journal of Polymer Science Part A: Polymer Chemistry, 51(11), 2416-2424. https://doi.org/10.1002/pola.26627

[68] Sułkowski, W. W., Nowak, K., Sułkowska, A., Mikuła, B., & Wierzba, P. (2013). The conditions of cationic exchange with the use of recycling polystyrene derivative, the product of sulfonation by silica sulfuric acid. Journal of applied polymer science, 128(5), 2611-2617. https://doi.org/10.1002/app.38429

[69] Jia, J., Fu, Z., Wang, L., Huang, Z., & Liu, C. (2019). Conversion of waste polystyrene foam into sulfonated hyper-crosslinked polymeric adsorbents for cadmium removal in a fixed-bed column. Chemical Engineering Research and Design, 142, 346-354. https://doi.org/10.1016/j.cherd.2018.12.025

[70] Chang, S. H., Lu, C. C., Lin, C. W., Wang, K. S., Lee, M. W., & Liu, S. H. (2022). Waste expanded polystyrene modified with H2SO4/biodegradable chelating agent for reuse: As a highly efficient adsorbent to remove fluoroquinolone antibiotic from water. Chemosphere, 288, 132619. https://doi.org/10.1016/j.chemosphere.2021.132619

[71] Cella, R. F., Mumbach, G. D., Andrade, K. L., Oliveira, P., Marangoni, C., Bolzan, A., Bernard, S., & Machado, R. A. F. (2018). Polystyrene recycling processes by dissolution in ethyl acetate. Journal of Applied Polymer Science, 135(18), 46208. https://doi.org/10.1002/app.46208

[72] Mehmandost, N., Soriano, M. L., Lucena, R., Goudarzi, N., Chamjangali, M. A., & Cardenas, S. (2019). Recycled polystyrene-cotton composites, giving a second life to plastic residues for environmental remediation. Journal of Environmental Chemical Engineering, 7(5), 103424. https://doi.org/10.1016/j.jece.2019.103424

[73] Lopez-Tellez, J., Ibarra, I. S., Cruz-Borbolla, J., Vega, M., & Rodriguez, J. A. (2023). Retention and Determination of Polycyclic Aromatic Hydrocarbons from Urban Air Based on Recycled Polyurethane Foam Modified with Expanded Polystyrene. Polycyclic Aromatic Compounds, 43(10), 9347-9359. https://doi.org/10.1080/10406638.2022.2162931

[74] Samkampang, K., Soriano, M. L., Lucena, R., Thammakhet-Buranachai, C., & Cárdenas, S. (2025). A flower-shaped recycled polymeric-coated cellulose paper for the isolation of organic contaminants from waters. Journal of Chromatography A, 1751, 465949. https://doi.org/10.1016/j.chroma.2025.465949

[75] Lopez-Tellez, J., Rodriguez, J. A., Miranda, J. M., Mondragon, A. C., & Ibarra, I. S. (2024). Determination of polycyclic aromatic hydrocarbons in aqueous samples using recycled polystyrene for pipette tip-solid phase extraction followed by HPLC-FLD. International Journal of Environmental Analytical Chemistry, 104(15), 3486-3495. https://doi.org/10.1080/03067319.2022.2086051

[76] Ghambari, H., Reyes-Gallardo, E. M., Lucena, R., Saraji, M., & Cárdenas, S. (2017). Recycling polymer residues to synthesize magnetic nanocomposites for dispersive micro-solid phase extraction. Talanta, 170, 451-456. https://doi.org/10.1016/j.talanta.2017.04.026

[77] Chen, W., & McCarthy, T. J. (1998). Chemical surface modification of poly (ethylene terephthalate). Macromolecules, 31(11), 3648-3655. https://doi.org/10.1021/ma9710601

[78] Pulitika, A., Karamanis, P., Kovačić, M., Božić, A. L., & Kušić, H. (2024). An Atomic-Level Perspective on the interactions between Organic Pollutants and PET particles: A Comprehensive Computational Investigation. ChemPhysChem, 25(5), e202300854. https://doi.org/10.1002/cphc.202300854

[79] Baggio, A., Doan, H. N., Vo, P. P., Kinashi, K., Sakai, W., Tsutsumi, N., Fuse, Y., & Sangermano, M. (2021). Chitosan-functionalized recycled polyethylene terephthalate nanofibrous membrane for sustainable on-demand oil-water separation. Global Challenges, 5(4), 2000107. https://doi.org/10.1002/gch2.202000107

[80] Doan, H. N., Vo, P. P., Hayashi, K., Kinashi, K., Sakai, W., & Tsutsumi, N. (2020). Recycled PET as a PDMS-Functionalized electrospun fibrous membrane for oil-water separation. Journal of Environmental Chemical Engineering, 8(4), 103921. https://doi.org/10.1016/j.jece.2020.103921

[81] Lin, C. H., Gung, C. H., Wu, J. Y., & Suen, S. Y. (2015). Cationic dye adsorption using porous composite membrane prepared from plastic and plant wastes. Journal of the Taiwan Institute of Chemical Engineers, 51, 119-126. https://doi.org/10.1016/j.jtice.2015.01.019

[82] Semyonov, O., Chaemchuen, S., Ivanov, A., Verpoort, F., Kolska, Z., Syrtanov, M., Svorcik, V., Yusubov, M. S., Lyutakov, O., Guselnikova, O., & Postnikov, P. S. (2021). Smart recycling of PET to sorbents for insecticides through in situ MOF growth. Applied Materials Today, 22, 100910. https://doi.org/10.1016/j.apmt.2020.100910

[83] Mendoza-Carrasco, R., Cuerda-Correa, E. M., Alexandre-Franco, M. F., Fernández-González, C., & Gómez-Serrano, V. (2016). Preparation of high-quality activated carbon from polyethyleneterephthalate (PET) bottle waste. Its use in the removal of pollutants in aqueous solution. Journal of environmental management, 181, 522-535. https://doi.org/10.1016/j.jenvman.2016.06.070

[84] Ilyas, M., Khan, H., & Ahmad, W. (2024). Conversion of waste plastics into carbonaceous adsorbents and their application for wastewater treatment. International Journal of Environmental Analytical Chemistry, 104(10), 2432-2450. https://doi.org/10.1080/03067319.2022.2062571

[85] Rai, P., & Singh, K. P. (2018). Valorization of Poly (ethylene) terephthalate (PET) wastes into magnetic carbon for adsorption of antibiotic from water: Characterization and application. Journal of environmental management, 207, 249-261. https://doi.org/10.1016/j.jenvman.2017.11.047

[86] El Essawy, N. A., Ali, S. M., Farag, H. A., Konsowa, A. H., Elnouby, M., & Hamad, H. A. (2017). Green synthesis of graphene from recycled PET bottle wastes for use in the adsorption of dyes in aqueous solution. Ecotoxicology and environmental safety, 145, 57-68. https://doi.org/10.1016/j.ecoenv.2017.07.014

[87] El Essawy, N. A., Elnouby, M., Gouda, M. H., Hamad, H. A., Taha, N. A., Gouda, M., & Eldin, M. S. M. (2020). Ciprofloxacin removal using magnetic fullerene nanocomposite obtained from sustainable PET bottle wastes: Adsorption process optimization, kinetics, isotherm, regeneration and recycling studies. Chemosphere, 239, 124728. https://doi.org/10.1016/j.chemosphere.2019.124728

[88] Farahani, S. D., & Zolgharnein, J. (2022). Removal of Alizarin red S by calcium-terephthalate MOF synthesized from recycled PET-waste using Box-Behnken and Taguchi designs optimization approaches. Journal of Solid State Chemistry, 316, 123560. https://doi.org/10.1016/j.jssc.2022.123560

[89] Chan, K., & Zinchenko, A. (2021). Conversion of waste bottles' PET to a hydrogel adsorbent via PET aminolysis. Journal of Environmental Chemical Engineering, 9(5), 106129. https://doi.org/10.1016/j.jece.2021.106129

[90] Chan, K., & Zinchenko, A. (2022). Conversion of waste bottle PET to magnetic microparticles adsorbent for dye-simulated wastewater treatment. Journal of Environmental Chemical Engineering, 10(3), 108055. https://doi.org/10.1016/j.jece.2022.108055

[91] Ungureanu, O. I., Bulgariu, D., Mocanu, A. M., & Bulgariu, L. (2020). Functionalized PET waste based low-cost adsorbents for adsorptive removal of Cu (II) ions from aqueous media. Water, 12(9), 2624. https://doi.org/10.3390/w12092624

[92] Saleem, J., Moghal, Z. K. B., & McKay, G. (2023). Up-cycling plastic waste into swellable super-sorbents. Journal of Hazardous Materials, 453, 131356. https://doi.org/10.1016/j.jhazmat.2023.131356

[93] Govindappa, H., Bhat, M. P., Uthappa, U. T., Sriram, G., Altalhi, T., Kumar, S. P., & Kurkuri, M. (2022). Fabrication of a novel polymer inclusion membrane from recycled polyvinyl chloride for the real-time extraction of arsenic (V) from water samples in a continuous process. Chemical Engineering Research and Design, 182, 145-156. https://doi.org/10.1016/j.cherd.2022.03.052

[94] Dahdouh, N., Amokrane, S., Murillo, R., Mekatel, E., & Nibou, D. (2020). Removal of methylene blue and basic yellow 28 dyes from aqueous solutions using sulphonated waste poly methyl methacrylate. Journal of Polymers and the Environment, 28, 271-283. https://doi.org/10.1007/s10924-019-01605-w

[95] Wang, Q., Zhang, D., Tian, S., & Ning, P. (2014). Simultaneous adsorptive removal of methylene blue and copper ions from aqueous solution by ferrocene-modified cation exchange resin. Journal of Applied Polymer Science, 131(21). https://doi.org/10.1002/app.41029

[96] Wang, J., Yu, J., Li, M., & Zhang, Y. (2024). Synthesis of sodium polystyrene sulfonate resins for the removal of methylene blue from wastewater. Journal of the Taiwan Institute of Chemical Engineers, 159, 105501. https://doi.org/10.1016/j.jtice.2024.105501

[97] Sheldon, R. A. (2017). The E factor 25 years on: the rise of green chemistry and sustainability. Green Chemistry, 19(1), 18-43. https://doi.org/10.1039/C6GC02157C

[98] Calero-Cañuelo, C., Casado-Carmona, F. A., Lucena, R., & Cárdenas, S. (2024). Sorptive tape-spray tandem mass spectrometry using aluminum foil coated with mixed-mode microparticles. Talanta, 272, 125774. https://doi.org/10.1016/j.talanta.2024.125774

[99] Calero-Cañuelo, C., Lucena, R., & Cárdenas, S. (2025). Adhesive tapes as sampling probes and thermal desorption substrates, in search of direct analysis of particulate solid samples using Soft Ionization by Chemical Reaction In Transfer mass spectrometry. Talanta, 293, 128042. https://doi.org/10.1016/j.talanta.2025.128042

[100] González-Bermúdez, M., López-Lorente, Á. I., Lucena, R., & Cárdenas, S. (2023). Paper-based sorptive phases for a sustainable sample preparation. Advances in Sample Preparation, 5, 00051. https://doi.org/10.1016/j.sampre.2023.100051

[101] Jain, B., Jain, R., Kaur, S., Haque, S. M., Sharma, S., Ghoneim, M. M., & Al-Khateeb, L. A. (2024). Multi-drug extraction using octanol supported rotating cellulose paper disc (RPD) device from complex biological matrices: Fabrication and application in forensic case work. Sustainable Chemistry and Pharmacy, 41, 101724. https://doi.org/10.1016/j.scp.2024.101724

[102] Takagai, Y., Kubota, T., Akiyama, R., Aoyama, E., & Igarashi, S. (2004). Preconcentration technique for nonylphenol using cellulose cotton with homogenous liquid–liquid extraction for liquid chromatographic analysis. Analytical and bioanalytical chemistry, 380, 351-354. https://doi.org/10.1007/s00216-004-2777-9

[103] Millán-Santiago, J., Lucena, R., & Cárdenas, S. (2022). Pre-cleaned bare wooden toothpicks for the determination of drugs in oral fluid by mass spectrometry. Analytical and Bioanalytical Chemistry, 414(18), 5287-5296. https://doi.org/10.1007/s00216-022-03977-w

[104] González-Galán, C., Millán-Santiago, J., Martínez-Pérez-Cejuela, H., Armenta, S., Herrero-Martínez, J. M., Lucena, R., & Cárdenas, S. (2024). Pipette-tip microextraction using carboxymethylated wooden-based sawdust sorbent for the determination of antidepressants in oral fluid by direct infusion mass spectrometry. Microchemical Journal, 207, 112002. https://doi.org/10.1016/j.microc.2024.112002

[105] Hammadi, S., Millán-Santiago, J., El Atarche, L. L., Lucena, R., & Cárdenas, S. (2023). Octanol-supported wooden tips as sustainable devices in microextraction: A closer view of the influence of wood matrix. Microchemical Journal, 186, 108358. https://doi.org/10.1016/j.microc.2022.108358

[106] Allgaier-Díaz, D. W., Trujillo-Rodríguez, M. J., Ayala, J. H., Díaz, D. D., & Pino, V. (2023). Unmodified biopolymers as sustainable microextraction materials for the environmental monitoring of polycyclic aromatic hydrocarbons and personal care products. Microchemical Journal, 191, 108873. https://doi.org/10.1016/j.microc.2023.108873

[107] Xu, X. L., Wang, B., Liu, Y. W., Li, W. X., Wu, J. Y., Yuan, H., Xu, X., & Chen, D. (2023). In-pipette-tip natural-feather-supported liquid microextraction for conveniently extracting hydrophobic compounds in aqueous samples: A proof-of-concept study. Microchemical Journal, 185, 108274. https://doi.org/10.1016/j.microc.2022.108274

[108] Feng, J., Han, S., Ji, X., Li, C., Wang, X., Tian, Y., & Sun, M. (2019). A green extraction material—natural cotton fiber for in-tube solid-phase microextraction. Journal of separation science, 42(5), 1051-1057. https://doi.org/10.1002/jssc.201801233

[109] Han, W. C., Shi, N., Wang, X. Y., Wang, Z. H., Wang, K. L., Gao, M., Yu, L., & Xu, X. (2021). Application of natural cotton fibers as an extraction sorbent for the detection of trans-resveratrol in adulterated peanut oils. Food Chemistry, 339, 127885. https://doi.org/10.1016/j.foodchem.2020.127885

[110] Wang, J., Liu, S., Chen, C., Zou, Y., Hu, H., Cai, Q., & Yao, S. (2014). Natural cotton fibers as adsorbent for solid-phase extraction of polycyclic aromatic hydrocarbons in water samples. Analyst, 139(14), 3593-3599. https://doi.org/10.1039/C4AN00195H

[111] Karimi, M., Dadfarnia, S., & Shabani, A. M. H. (2017). Application of deep eutectic solvent modified cotton as a sorbent for online solid-phase extraction and determination of trace amounts of copper and nickel in water and biological samples. Biological trace element research, 176, 207-215. https://doi.org/10.1007/s12011-016-0814-0

[112] Chen, D., Zhang, M. Y., Bu, X. M., Wang, B., Xu, X. L., Yang, S., Sun, Z., & Xu, X. (2022). In-syringe cotton fiber-supported liquid extraction coupled with gas chromatography-tandem mass spectrometry for the determination of free 3-mono-chloropropane-1, 2-diol in edible oils. Journal of Chromatography A, 1673, 463081. https://doi.org/10.1016/j.chroma.2022.463081

[113] Yu, M., Tian, W., Sun, D., Shen, W., Wang, G., & Xu, N. (2001). Systematic studies on adsorption of 11 trace heavy metals on thiol cotton fiber. Analytica Chimica Acta, 428(2), 209-218. https://doi.org/10.1016/S0003-2670(00)01238-1

[114] Gong, R., Hu, Y., Chen, J., Chen, F., & Liu, Z. (2007). A cellulose-based carboxyl cotton chelator having citric acid as an anchored ligand: preparation and application as solid phase extractant for copper determination by flame atomic absorption spectrometry. Microchimica Acta, 158, 315-320. https://doi.org/10.1007/s00604-006-0722-7

[115] Liu, L., Jin, S., Mei, P., & Zhou, P. (2019). Preparation of cotton wool modified with boric acid functionalized titania for selective enrichment of glycopeptides. Talanta, 203, 58-64. https://doi.org/10.1016/j.talanta.2019.05.050

[116] Sanaei, Y., Zeeb, M., Homami, S. S., Monzavi, A., & Khodadadi, Z. (2021). Fabrication of ZIF-71/Fe 3 O 4/polythionine nanoarray-functionalized carbon cotton cloth for simultaneous extraction and quantitation of febuxostat and diclofenac. RSC advances, 11(48), 30361-30372. https://doi.org/10.1039/D1RA04670E

[117] Sanaei, Y., Zeeb, M., Homami, S. S., Monzavi, A., & Khodadadi, Z. (2022). Magnetic solid-phase extraction based on the Carbonized cotton fabric/zeolite imidazolate framework-71/Fe3O4/polythionine followed by atomic absorption spectrometry for cadmium monitoring in water, tomato and cabbage samples. Analytical Methods in Environmental Chemistry Journal, 5(02), 60-75. https://doi.org/10.24200/amecj.v5.i02.186

[118] Qu, R., Sun, C., Wang, M., Ji, C., Xu, Q., Zhang, Y., Wang, C., Chen, H., & Yin, P. (2009). Adsorption of Au (III) from aqueous solution using cotton fiber/chitosan composite adsorbents. Hydrometallurgy, 100(1-2), 65-71. https://doi.org/10.1016/j.hydromet.2009.10.008

[119] Chen, D., Liu, F., Rong, Y., Qi, M., Li, Y., Shi, X., Xie, Y., & Xu, X. (2023). Coupling in-syringe kapok fiber-supported liquid-phase microextraction with flow injection-mass spectrometry for rapid and green biofluid analysis: Determination of antidepressants as an example. Journal of Pharmaceutical and Biomedical Analysis, 229, 115380. https://doi.org/10.1016/j.jpba.2023.115380

[120] Wang, B., Chen, Y., Li, W., Liu, Y., Xia, X., Xu, X., Yang, Y., & Chen, D. (2024). Magnetic phytic acid-modified kapok fiber biochar as a novel sorbent for magnetic solid-phase extraction of antidepressants in biofluids. Analytica Chimica Acta, 1296, 342295. https://doi.org/10.1016/j.aca.2024.342295

[121] Southichak, B., Nakano, K., Nomura, M., Chiba, N., & Nishimura, O. (2006). Phragmites australis: a novel biosorbent for the removal of heavy metals from aqueous solution. Water Research, 40(12), 2295-2302. https://doi.org/10.1016/j.watres.2006.04.027

[122] Ingrassia, E. B., Fiorentini, E. F., Wuilloud, R. G., da Silva, S. M., & Escudero, L. B. (2023). Novel bionanomaterial based on Spirulina maxima algae and graphene oxide for lead microextraction and determination in water and infant beverages. Analytical and Bioanalytical Chemistry, 415(22), 5475-5486. https://doi.org/10.1007/s00216-023-04821-5

[123] do Carmo, S. N., Merib, J., & Carasek, E. (2019). Bract as a novel extraction phase in thin-film SPME combined with 96-well plate system for the high-throughput determination of estrogens in

human urine by liquid chromatography coupled to fluorescence detection. Journal of Chromatography B, 1118, 17-24. https://doi.org/10.1016/j.jchromb.2019.04.037

[124] Sujitha, R., & Ravindhranath, K. (2017). Extraction of phosphate from polluted waters using calcium alginate beads doped with active carbon derived from A. aspera plant as adsorbent. Journal of Analytical Methods in Chemistry, 2017(1), 3610878. https://doi.org/10.1155/2017/3610878

[125] Teng, D., Zhang, B., Xu, G., Wang, B., Mao, K., Wang, J., Sun, J., Feng, X., Yang, Z., & Zhang, H. (2020). Efficient removal of Cd (II) from aqueous solution by pinecone biochar: Sorption performance and governing mechanisms. Environmental Pollution, 265, 115001. https://doi.org/10.1016/j.envpol.2020.115001

[126] Makkliang, F., Pianjing, P., Kanatharana, P., Thavarungkul, P., & Thammakhet-Buranachai, C. (2023). Natural Luffa cylindrica sponge sorbent for the solid phase extraction of estrone, 17-β-estradiol, and testosterone in aquaculture water. Microchemical Journal, 191, 108892. https://doi.org/10.1016/j.microc.2023.108892

[127] Syed Yaacob, S. F. F., Kamboh, M. A., Wan Ibrahim, W. A., & Mohamad, S. (2018). New sporopollenin-based β-cyclodextrin functionalized magnetic hybrid adsorbent for magnetic solid-phase extraction of nonsteroidal anti-inflammatory drugs from water samples. Royal Society Open Science, 5(7), 171311. https://doi.org/10.1098/rsos.171311

[128] Shirani, M., Kamboh, M. A., Akbari-Adergani, B., Akbari, A., Arain, S. S., & Nodeh, H. R. (2021). Sonodecoration of magnetic phosphonated-functionalized sporopollenin as a novel green nanocomposite for stir bar sorptive dispersive microextraction of melamine in milk and milk-based food products. Food Chemistry, 341, 128460. https://doi.org/10.1016/j.foodchem.2020.128460

[129] Sereshti, H., Toloutehrani, A., & Nodeh, H. R. (2020). Determination of cholecalciferol (vitamin D3) in bovine milk by dispersive micro-solid phase extraction based on the magnetic three-dimensional graphene-sporopollenin sorbent. Journal of Chromatography B, 1136, 121907. https://doi.org/10.1016/j.jchromb.2019.121907

[130] Zhou, Y. L., Yue, S. W., Cheng, B. W., & Zhao, Q. (2022). Determination of fipronil and its metabolites in edible oil by pollen based solid-phase extraction combined with gas chromatography-electron capture detection. Food Chemistry, 377, 132021. https://doi.org/10.1016/j.foodchem.2021.132021

Aim of the thesis

The aim of this research project is to propose an alternative approach to conventional analytical practices. In response to the increasing demand for sustainable and operator-friendly methodologies, this work embraces a radical shift in perspective, in which the availability of resources, material reuse, and life-cycle considerations become primary objectives, on par with analytical performance. Within this framework, the study seeks to identify practical strategies for integrating material recycling into analytical workflows. This concept encompasses all consumables used in analytical chemistry, including plasticware, adsorbent materials for sample preparation, and solvents employed in analytical or pre-treatment procedures. The main goal of this research is to develop recycling procedures for plastic materials to generate adsorbent phases suitable for sample preparation and water remediation. Specifically, the work aims to design a versatile process applicable to a wide variety of waste materials, enabling their reshaping and optimization for enhanced adsorptive performance. This strategy would make it possible to transform virtually any polymeric matrix into an extractive phase for sample preparation or a retention medium for water remediation applications. Furthermore, the advent of 3D printing technologies for the fabrication of laboratory devices and small-scale instruments has highlighted the growing interest of the analytical community in modular, customizable, and performance-optimized materials and tools. However, this trend introduces new synthetic polymers into laboratory practice, potentially conflicting with sustainability principles. To address this issue, the present study proposes a strategy for designing analytical extraction devices that are both modular and derived from recycled sources, combining sustainability with analytical functionality. The solutions envisioned by this research work would represent a significant step forward in the field of material chemistry applied to sample preparation, paving the way for new sustainable paradigms that may redefine the focus of future research.

Chapter 2: Recycling in Sample preparation techniques

Overview

In line with the principles of Circular Analytical Chemistry [1] and Green Sample Preparation [2], the reuse of polymeric waste as a raw material for the synthesis of functional materials represents a sustainable strategy to reduce the environmental impact of analytical chemistry. Within this framework, the development of adsorbent materials for sample preparation from recycled polymers offers a valuable alternative to conventional synthetic sorbents, combining waste valorization with analytical performance.

A microemulsion solidification technique was optimized as a versatile and sustainable approach for the reshaping of waste-derived polymers into microspherical materials. This process exploits the immiscibility of an organic polymer solution and an aqueous phase to induce controlled polymer precipitation, leading to the formation of uniform microspheres with tunable physicochemical properties. The technology draws inspiration from a reshaping process originally proposed in the 1990s by Ibrahim et al. [3, 4] to produce regular, dispersible polymer powders from pre-existing polymers.

As a proof of concept, the methodology was applied to two different recycled polymers: polylactic acid (PLA) recovered from cigarette residues, and polystyrene obtained from yogurt containers. PLA-based microspheres were engineered as magnetic nanocomposites for the dispersive solid-phase extraction of xenobiotics from human urine. Polystyrene microspheres were tested both in their native form and after post-functionalization with sulfonic groups, for the extraction of opioids and sulfonamide antibiotics from complex matrices, respectively.

The obtained materials exhibited good structural reproducibility, adsorption efficiency, and analytical performance, confirming the feasibility of integrating polymer recycling strategies into sample preparation workflows. This studies therefore highlights the potential of microemulsion solidification as a circular and sustainable platform for the development of new analytical sorbents from polymeric

waste. All three applications presented here are discussed in detail in the manuscripts reported in the following sections.

References

[1] Psillakis, E., & Pena-Pereira, F. (2024). The twelve goals of circular analytical chemistry. *TrAC Trends in Analytical Chemistry*, *175*, 117686. https://doi.org/10.1016/j.trac.2024.117686

[2] López-Lorente, Á. I., Pena-Pereira, F., Pedersen-Bjergaard, S., Zuin, V. G., Ozkan, S. A., & Psillakis, E. (2022). The ten principles of green sample preparation. TrAC Trends in Analytical Chemistry, 148, 116530. https://doi.org/10.1016/j.trac.2022.116530

[3] Ibrahim, H., Bindschaedler, C., Doelker, E., Buri, P., & Gurny, R. (1992). Aqueous nanodispersions prepared by a salting-out process. International journal of pharmaceutics, 87(1-3), 239-246. https://doi.org/10.1016/0378-5173(92)90248-Z

[4] Allémann, E., Gurny, R., & Doelker, E. (1992). Preparation of aqueous polymeric nanodispersions by a reversible salting-out process: influence of process parameters on particle size. International journal of pharmaceutics, 87(1-3), 247-253. https://doi.org/10.1016/0378-5173(92)90249-2

Paper I: Polylactic acid from cigarette residues

Microchimica Acta (2024) 191:251
https://doi.org/10.1007/s00604-024-06335-y

ORIGINAL PAPER

Check for updates

Nanocomposite microbeads made of recycled polylactic acid for the magnetic solid phase extraction of xenobiotics from human urine

Lorenzo Antonelli[1] · Maria Chiara Frondaroli[1] · Massimo Giuseppe De Cesaris[1] · Nina Felli[1] · Chiara Dal Bosco[1] · Elena Lucci[1] · Alessandra Gentili[1]

Received: 24 January 2024 / Accepted: 26 March 2024 / Published online: 9 April 2024

Graphical abstract

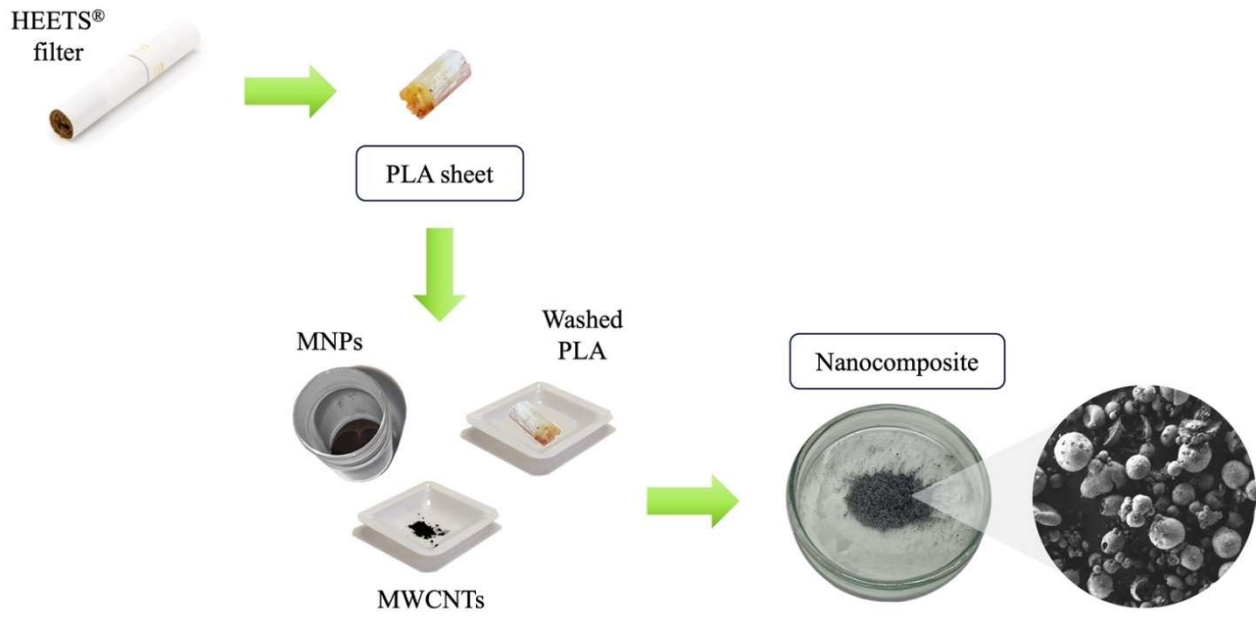

Abstract

In this work, nanocomposite microbeads (average diameter = 10-100 μm) were prepared by a microemulsion-solidification method and applied for the magnetic solid-phase extraction (m-SPE) of fourteen analytes, among pesticides, drugs, and hormones, from human urine samples. The microbeads, perfectly spherical in shape to maximize the surface contact with the analytes, were composed of magnetic nanoparticles dispersed in a polylactic acid (PLA) solid bulk, decorated with multi-walled carbon nanotubes (mPLA@MWCNTs). In particular, PLA was recovered from filters of smoked electronic cigarettes after an adequate cleaning protocol. A complete morphological characterization of the microbeads was performed via Fourier-transform infrared (FTIR) spectroscopy, UV-Vis spectroscopy, thermogravimetric and differential scanning calorimetry analysis (TGA and DSC), scanning electron microscopy (SEM) and X-Ray diffraction analysis (XRD). The recovery study of the m-SPE procedure showed yields ≥ 64%, with the exception of 4-chloro-2-methylphenol (57%) at the lowest spike level (3 μg L^{-1}). The method was validated according to the main FDA guidelines for the validation of bioanalytical methods. Using liquid chromatography-tandem mass spectrometry, precision and accuracy were below 11% and 15%, respectively, and the detection limits were 0.1-1.8 μg L^{-1}. Linearity was studied in the range of interest 1-15 μg L^{-1} with determination coefficients greater than 0.99. In light of the obtained results, the nanocomposite microbeads have proved to be a valid and sustainable alternative to traditional sorbents, offering good analytical standards and being synthetized from recycled plastic material. One of the main objectives of the current work is to provide an innovative and optimized procedure for the recycling of a plastic waste, to obtain a regular and reliable microstructure, whose application is here presented in the field of analytical chemistry. The simplicity and greenness of the method endows the procedure with a versatile applicability in different research and industrial fields.

Keywords

Solid phase extraction; microbeads; green analytical chemistry; carbon nanomaterials; recycled plastic; polylactic acid

1. Introduction

Within Green Analytical Chemistry, one of the main objectives of today's research is the quest for sorbent materials that, according to the 3rd principle of Green Sample Preparation (GSP), have characteristics of sustainability, reusability and renewability [1]. This tendency goes together with the miniaturization and automation of existing extraction techniques [2, 3] to reduce waste (4th principle), minimize sample, chemicals and materials (5th principle), and cut down energy consumption (8th principle) [1]. To have an idea of the current trends of microextraction innovative technique, framework that acts as a background of the presented research, a quite detailed table is reported in the Appendix A (**Table A1**). The use of new technologies to make such materials smaller can lead to significant operating advantages. Compared to conventional micro-sized sorbents, the nano-scaled ones exhibit wider specific surface area, improved sorption capacity, greater surface energy, higher diffusivity, and a more rapid achievement of adsorption equilibrium [4]. Nanostructured or nanocomposite materials are of special interest in sample preparation [5]. Two different approaches can be used to realize a nanocomposite [6]. The first one is a bottom-up approach, which involves the realization of a material starting from the single monomer up to a microstructure. The alternative is the top-down method, which begins with a pre-synthesized polymer and allows for reshaping it into a microscopic structure. The aspiration to recycle polymeric material from consumer sources is best served by a top-down approach [7].

Between 2016 and 2017, the World Economic Forum and the Ellen MacArthur Foundation launched the "New Plastic Economy" initiative [8] with the aim to promote a change in the use of plastics around three mainstays: redesign, reuse, and recycling. In 2018, the European Union declared in their new plastics strategy that 100 % of plastics should either be reusable or recyclable by 2030 [9]. In

this context, Analytical Chemistry may play its role, recycling plastics to prepare new materials for analytical applications. If within the sample preparation sector, it is common to use microparticle polymeric sorbents for solid phase extraction (SPE), there have been not many papers dealing with the preparation of sorbents from recycled plastic so far [10, 11]. In 2016, Psillakis et al. reported for the first time the use of low-density polyethylene plastic pellets as a low-cost and effective sorbent for extracting polycyclic aromatic hydrocarbons from environmental waters [10]. In 2017, Cárdenas et al. recycled polystyrene, whose degradation rate in the environment is very low, to synthesize magnetic nanocomposites for the dispersive micro-SPE of parabens from water samples [7].

The present article fits into this context by proposing the recycling of polylactic acid (PLA) into nanocomposite microbeads to extend the usable life of this plastic and to reduce the pollution generated by its littering [11]. The PLA used in this work was recovered from the filters of heated tobacco electronic cigarettes (HEETS®), which have skyrocketed in popularity especially among young people becoming one of the most diffuse solid wastes. PLA, which in HEETS® filters acts as a cooling agent for the aerosol created by heating tobacco [12], is a plastic-biopolymer that, in recent years, has attracted considerable attention thanks to its excellent properties of good workability and mechanical resistance [13]. The synthesis of the magnetic nanocomposite microbeads is based on a microemulsion-solidification method after a careful cleaning of the PLA-based filters. The technical advantage of the use of magnetic responsive materials in sample preparation applications is already well defined and reported in literature, both for solid and liquid phase extraction techniques [14, 15]. On this purpose, the use of magnetic nanoparticles (MNPs) is the recommended solution to guarantee a homogeneous distribution of the magnetic properties [16]. PLA itself did not show high affinity with the studied xenobiotics. To enhance the adsorption ability of the material, different active carbon materials were tested as coadjutants of the adsorption and components of the nanocomposite. As already reported, multi walled carbon nanotubes (MWCNTs) and graphene oxide (GO) have excellent properties for analytical applications but some drawbacks from the applicability point of view [17-19]. The strong interaction between different nanotubes or GO sheets is responsible for the

aggregation of the material and a loose in terms of superficial area and extraction yields. The presented material aim is to use the bulk polymer (PLA) as a solid dispersant agent for carbonaceous active adsorbent, to avoid aggregation and to let MWCNTs and GO exploit their adsorption ability at full power, against the target analytes. The efficiency of the filter washing procedure as well as the synthesized nanocomposite microbeads were characterized via Fourier-transform infrared (FTIR) spectroscopy, UV-Vis spectroscopy, thermogravimetric and differential scanning calorimetry analysis (TGA and DSC), scanning electron microscopy (SEM) and X-Ray diffraction analysis. Finally, the magnetic microbeads were evaluated for the magnetic-SPE (m-SPE) of fourteen model compounds (among pesticides, non-steroidal anti-inflammatory drugs, and hormones) from urine samples. The chosen xenobiotics are commonly found in urine of workers employed in the agricultural sector and selected as reference analytes for the evaluation of the adsorption performances of the synthetized material.

2. Experimental section

2.1. Materials and reagents

PLA was recovered from filters of HEETS® cigarettes produced by one of the largest tobacco companies in the world. MWCNTs (length 6-13 nm, diameter 2.5–20 μm) and graphene oxide (GO; 15–20 sheets) were purchased from Merck Life Science S.r.l. (Milan, Italy).

A neodymium magnet from Atechmagnet (Beijing, China) was used as a magnetic lure.

Tetrahydrofuran (THF), isopropyl alcohol (≥ 99.5%), isopropyl acetate (≥ 99.6%), acetonitrile (≥ 99.9%), and sodium hydroxide (≥ 98%) were purchased from Merck Life Science S.r.l. (Milan, Italy). Absolute ethanol (≥ 99.5%) and hydrochloric acid (37.0%) were bought from VWR International (Radnor, USA). Formic acid (≥ 98%) was from Acros Organics B.V.B.A. (Waltham, USA). Milli-Q water was generated by the "Direct-Q® 3 UV System", Merck KGaA (Darmstadt, Germany).

Iron (III) chloride (≥ 97.0%) and iron (II) sulphate (≥ 99.0%), the salts used to prepare MNPs, were bought from Merck Life Science S.r.l. (Milan, Italy).

The standard used for the analytical procedure were: 4-chloro-2-methylphenol (≥ 98.0%), bensulfuron-methyl (≥ 98.0%), carprofen (≥ 98.0%), diclofenac (≥ 98.5%), diuron (≥ 98.0%), flamprop (≥ 95.0%), ibuprofen (≥ 98.0%), linuron (≥ 98.0%), malathion (≥ 98.0%), 4-(4-Chloro-2-methylphenoxy)butanoic acid (MCPB) (≥ 98.0%), methyl-testosterone (≥ 98.0%), 2-(±)-(4-chloro-2-methyl)phenoxypropanoic acid (mecoprop; ≥ 98.0%), nimesulide (≥ 98.0%), progesterone (≥ 99.0%), creatinine (≥ 99.0%). All analytical standards were purchased from Merck Life Science S.r.l. (Milan, Italy), except for flamprop, purchased from Lab. Instruments S.R.L. (Bari, Italy), and MCPB and nimesulide, purchased from VWR International (Radnor, USA). The chemical structure, exact mass, IUPAC name, chemical classification, and agrochemical/pharmaceutical action of each analyte is reported in **Table A2** in the Appendix A. The individual standards were weighed using a precision analytical balance (Ohaus DV215CD Discovery semi-micro and analytical balance, 81/210 g capacity, 0.01/0.1 mg readability) and diluted in 1 mL of methanol (VWR International, Radnor, USA) to prepare stock solutions (1 mg mL^{-1}). A stock composite standard solution of the 14 analytes was prepared at 100 µg L^{-1}. Other working solutions and calibrators at different concentrations were prepared by diluting the stock composite standard solution with methanol. All solutions were stored at 4 °C.

2.2. Urine samples

Urine samples, used as analyte-free matrices, were taken daily from healthy male volunteers, aged between 25 and 30 years, within our lab. A pool of urine from the different donors (~ 50 mL) was then subsampled to be used for the method optimization and validation. All urine samples were iced and stored at -18 °C till their analysis.

2.3. Synthesis of magnetic nanoparticles

Between different methodologies for magnetic nanoparticles synthesis [20], the Avram et al. [21] procedure was used, having proven effective for controlling size and magnetic properties. For the detailed procedure, please refer to Appendix A (**Section A.1**).

2.4. Synthesis of nanocomposite microbeads

Used-PLA filters (50 filters) were shredded and washed with 100 mL of hot ethanol at 50°C for 30 min. After being used, ethanol was distilled and reused for a subsequent washing cycle. The cleaned PLA sheets were dried at room temperature for the next synthetic procedure, consisting in a microemulsion-solidification process. To this end, 57 mg of PLA was solubilized in 2 mL of THF to obtain a saturated solution. 2.8 mg of MWCNTs and 18 mg of MNPs was added to this organic solution, which was then transferred into a 10 mL glass vial (diameter: 2 cm) containing a magnetic bar on the bottom. The effect of alternating a stirring cycle (10 min at 600 rpm) with gentle heating (about 50°C for 2 min) resulted in the production of a homogeneous dispersion of components. Five minutes in an ultrasonic bath favored the dispersion of MWCNTs, avoiding the formation of aggregates in solution.

Saturated NaCl aqueous solution and 2% w/v n-dodecylamine aqueous solution were prepared and mixed in a ratio 1:1 v/v. The resulting aqueous solution was mixed 1:1 v/v with the previous organic dispersion in another glass vial. The formation of a biphasic system was the result of the salting-out effect. The two-phases system was shaken (600 rpm) on a magnetic stirrer to form a microemulsion with microdroplets of the organic phase dispersed into the aqueous phase. To break down the emulsion and solidify PLA in the shape of microbeads, 4 mL pure water was added drop by drop. After removing the supernatant, the obtained nanocomposite was manually shaked three times with 5 mL of Milli-Q water to remove the salt and surfactant excess. After each washing the supernatant was separated by magnetic capture of the microbeads. Finally, the composite was dried under nitrogen flow. The whole procedure takes less than 10 min, and the synthesis yield of the final material

(mPLA@MWCNTs(5); see **Section 3.2** for the acronym explanation) is higher than 90% (in terms of final weight of microbeads with respect to the total weight of components). **Fig. 1** shows the cross-section of a magnetic microbead and provides a detailed scheme of the microbeads preparation procedure.

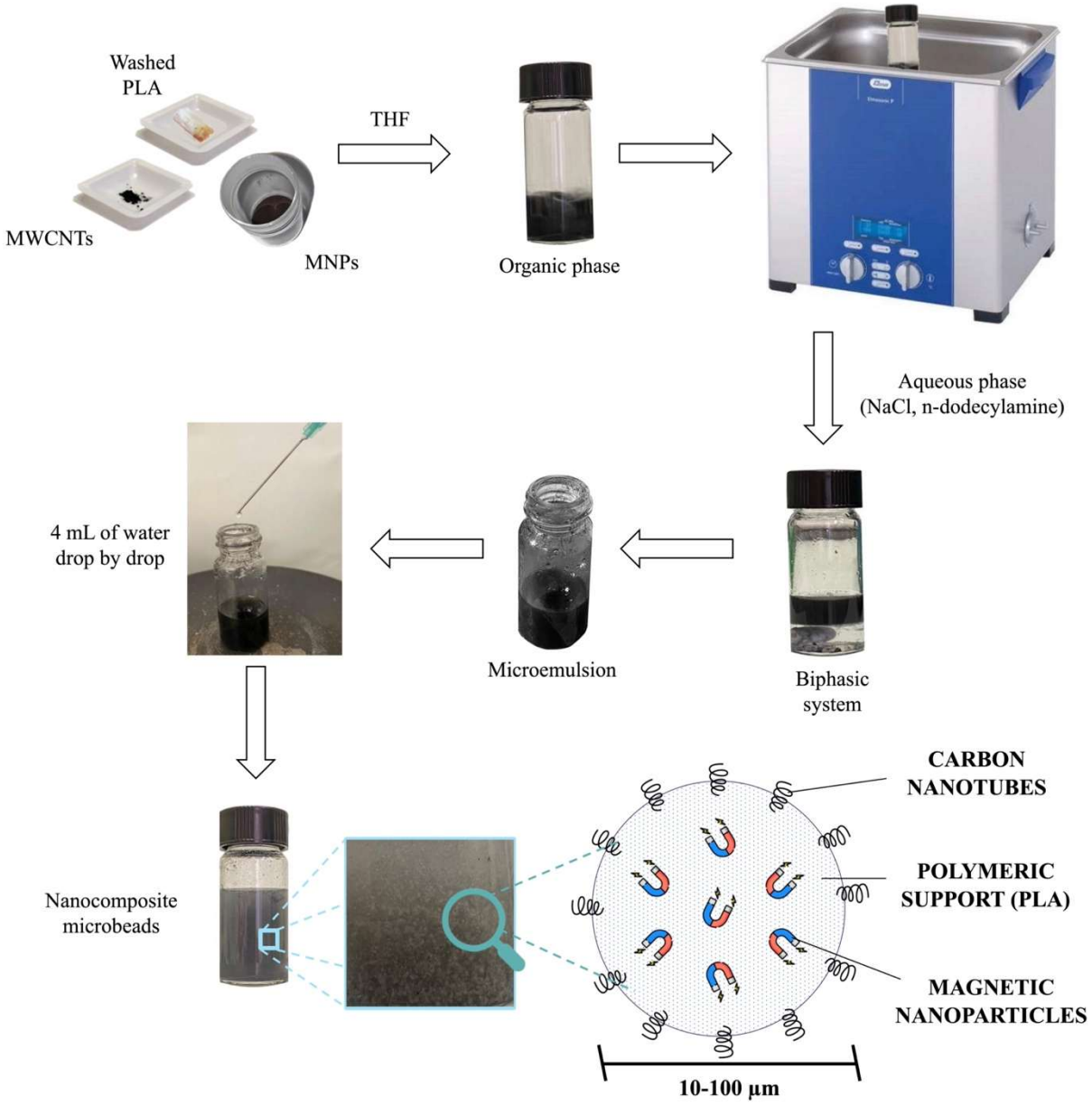

Fig. 1 Representation of the synthetic strategy for the realization of mPLA@MWCNTs(5) nanocomposites and schematic image of the final material structure

2.5. Characterization of the magnetic nanocomposite microbeads

Several instrumental techniques were applied to check the efficiency of the filter cleaning procedure (ATR-FTIR and UV-Vis spectroscopy), the morphology of magnetic microbeads (SEM and XRD) and their stability (TGA and DSC).

The ATR-FTIR spectra were collected by using a Nicolet 6700 (Thermo Fisher Scientific, Waltham, USA) equipped with a Golden Gate single-reflection diamond with a resolution of 2 cm^{-1} and co-addition of 200 scans.

The UV-Vis analysis was conducted with a Model 760 spectrophotometer from PG Instrument Limited (Leicester, UK).

The TGA analysis was carried out with a Mettler TG 50 thermobalance (Mettler Toledo, Columbus, USA). 5 mg of a sample (PLA; microbeads) was placed in the platinum crucible and the analysis was performed under nitrogen flow, in the temperature range between 25°C and 500°C, with a heating rate of 10 °C min^{-1}.

Differential Scanning Calorimetry (DSC) analysis of the composite device was performed by a Mettler TA-3000DSC apparatus. Thermograms were acquired at 10°C min-^{1} in the +25 to +250°C temperature range, under N_2 flux.

The microbeads were also analyzed with an AURIGA model SEM (Carl Zeiss, Oberkochen, Germany, 0.5–30 keV, 10 –10 mbar) to investigate their sizes and morphology.

X-ray diffraction (XRD) measurements were performed by a Malvern Panalytical X'Pert PRO apparatus (Cu Kα radiation, λ = 1.54184 Å) in an angle scan range (2θ) between 10-90 for a structural characterization of the composite. The peaks were identified through the instrumental spectral library.

2.6. Extraction procedure

A 0.6-mL aliquot of urine was diluted with 0.4 mL of Milli-Q water (V_T=1 mL) and poured into a glass vial containing 15 mg of mPLA@MWCNTs(5). The analyte adsorption on the microbeads was assisted by mixing on a vortex-stirrer for 5 min. Then, the magnetic microbeads were recovered with

a magnetic lure, and the analytes were desorbed three times with 500 µL of methanol. The pooled extract (1.5 mL) was transferred to an Eppendorf tube and dried under nitrogen flow. The residue was reconstituted in 100 µL of mobile phase, consisting of a 1:1 (v/v) solution of acetonitrile and water; finally, 10 µL was injected into the chromatographic system. The entire analytical procedure is displayed in **Fig. 2**.

Analyte concentrations were normalized towards creatinine concentration as follows (**Equation 1**):

$$C_{normalized} = \frac{C_{analyte}\ in\ \mu g\ L^{-1}}{C_{creatinine}\ in\ g\ L^{-1}} \quad (1)$$

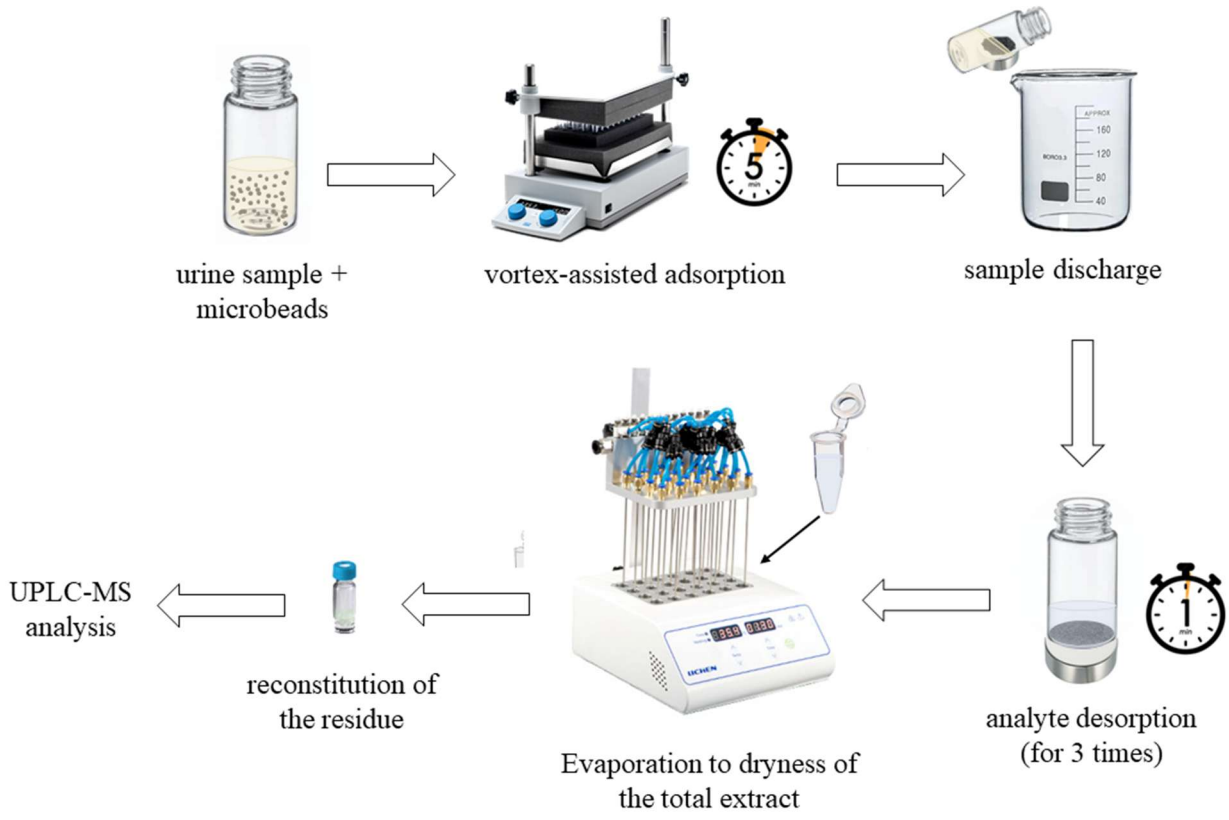

Fig. 2 Schematic representation of the extraction procedure

2.7. Creatinine determination

Creatinine concentration in urine reaches up to 0.4-3.0 g L^{-1} [22]. Owing to these high concentrations, 20 µL of urine was diluted with Milli-Q water in a 20-mL volumetric flask; then, a 2-µL volume was directly injected for the UPLC-MS analysis. Being the matrix effect negligible due to the high dilution

ratio (1:1000), the concentration of creatinine in real samples was calculated by means of external calibration, building a calibration curve in solvent [23, 24].

2.8. UPLC-MS/MS conditions

The analyte separation was performed using an ACQUITY UPLC H-Class PLUS® instrumentation from Waters Corporation (Milford, MA, USA). The column was an ACQUITY UPLC® BEH C_{18} (2.1×100 mm, 1.7 μm), purchased from Waters Corporation (Milford, MA, USA). The column was protected by a VanGuard Pre-Column® with the same stationary phase, 2.1 × 5 mm sized. The separation was carried out by using purified water (A) and acetonitrile (B), both acidified with 0.1% of formic acid, at a flow rate of 0.3 mL min^{-1}. The elution was as follows: t_0-t_{10} in isocratic mode at 50% B; t_{10} -t_{30} in linear gradient from 50% to 100% of B.

The mobile phase was entirely directed towards the Turbo V source, equipped with the electrospray probe, of a triple quadrupole mass spectrometer (API 4000 Qtrap from AB SCIEX, Foster City, CA, USA). The detection was performed in dual polarity mode (capillary voltage: + 5000V in positive mode and -4500 V in negative mode) by acquiring in Multiple Reaction Monitoring (MRM) and selecting two MRM transitions per analyte. Nitrogen in its purest state was supplied by a generator (Parker-Balston model 75A74, Haverhill, MA, USA) (nitrogen collision gas: 4 mTorr; nitrogen curtain gas: 5 L min^{-1}) connected to a compressor (Jun-Air 4000-40M, Bromsgrove, UK) (air nebulizer gas 2 L min^{-1}; air drying gas at 450°C and 20 L min^{-1}).

To operate with a unit resolution, the full width at half maximum (FWHM) was set at 0.7 ± 0.1 m/z in each mass-resolving quadrupole.

The LC-MS parameters for each of the 14 analytes, selected in this study, are reported in **Table 1**. **Fig. 3** shows the UPLC-MRM chromatogram resulting from the injection of 5 μL of the working composite solution (0.5 ng injected).

The software used to acquire and process the LC-MS data was Analyst 1.5.1.

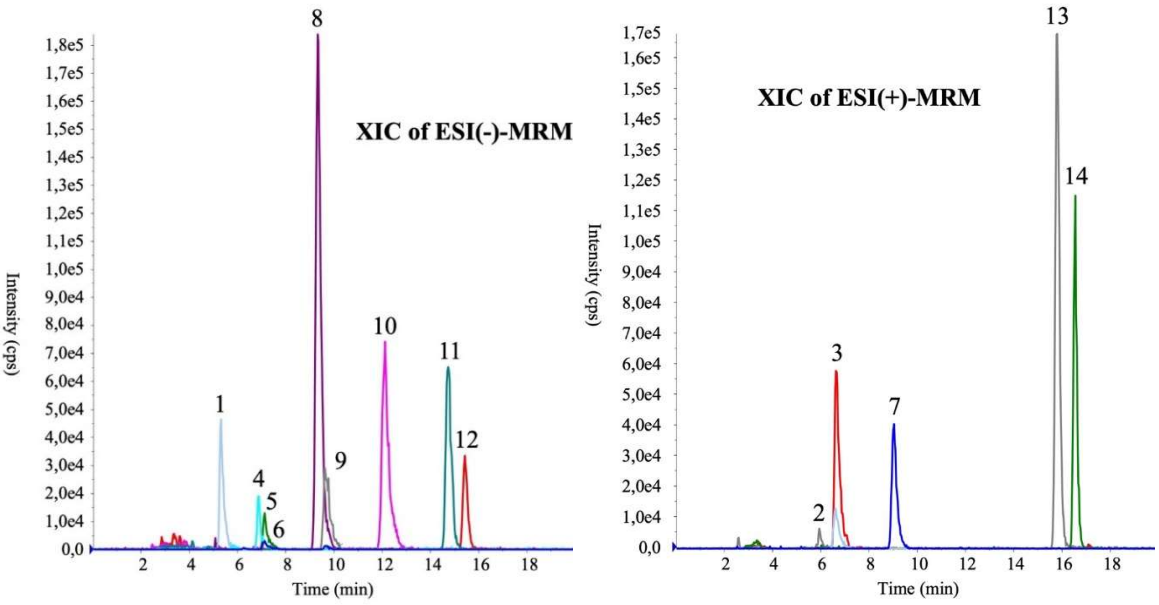

Fig. 3 UPLC-MRM chromatograms in positive and negative polarity, under the optimized chromatographic conditions. The 14 analytes are separated in less than 18 min.

Table 1 LC-MS parameters for the identification of the fourteen analytes under optimized conditions.

Elution order	Compound	Retention time (min)	1st Transition (m/z)[a]	2nd Transition (m/z)[a]	Detection polarity (+)/(-)
1	**Diuron**	5.31	230.9/149.7	230.9/185.8	-
2	**Bensulfuron-methyl**	6.60	411.1/149.1	411.1/182.1	+
3	**Methyl-testosterone**	6.64	303.2/109.2	303.2/97.1	+
4	**Flamprop**	6.87	320.0/121.0	320.0/248.0	-
5	**4-chloro-2-methylphenol**	7.12	141.0/104.9	141.0/76.8	-
6	**Mecoprop**	7.12	213.0/140.8	213.0/71.0	-
7	**Linuron**	9.03	249.0/182.1	249.0/159.9	+
8	**Nimesulide**	9.33	307.0/228.9	307.0/198.0	-
9	**MCPB**	9.62	227.1/140.9	227.1/104.9	-
10	**Carprofen**	12.11	272.0/228.0	272.0/212.8	-
11	**Diclofenac**	14.73	294.1/249.9	294.1/213.8	-
12	**Ibuprofen**	15.43	205.2/160.9	205.2/188.9	-
13	**Malathion**	15.79	331.0/127.1	331.0/285.0	+
14	**Progesterone**	16.55	315.2/109.1	315.2/97.1	+

[a] The first MRM transition is the most intense one (quantifier), while the other is the second most intense (qualifier)

Urinary creatinine, which is a chemical metabolism by-product whose excretion is not affected by urine flow [25], was determined to correct the analyte concentration in urine. The determination of creatinine was achieved in a separate run by using the same column and mobile phases in isocratic conditions, maintaining 65% of phase A for 5 min at the flow of 0.300 mL min^{-1}. Retention time was 1.4 min and the monitored MRM transitions were 114.0/44.2 (qualifier) and 144.0/86.0 (quantifier).

2.9 The method validation

The method was validated in matrix according to the FDA guidelines for the validation of bioanalytical methods [26]. Recovery, within-run and between-run precision and accuracy, limit of detention (LOD), lower limit of quantification (LLOQ), sensitivity, and linearity were the parameters evaluated. All calculations were performed by using with Microsoft Excel 2010 (Microsoft Corporation, Redmond, WA, USA).

3. Results and discussion

3.1. Optimization of the washing procedure to clean HEETS® filters

The nanocomposite microbeads were prepared by recycling thin sheets of PLA from HEETS® filters. The individual components of a HEETS® filter are shown in **Fig. A1** of the Appendix A. The filter that comes into direct contact with the lips of the user is made up of cellulose acetate. To lower the vapor temperature, a cooling plug made of PLA is required. A ventilation chamber, in contact with the tobacco, consists of a cellulose acetate cylinder, with a hole in the middle. After the tobacco stick's usage, the PLA film shows a change in color and consistency due to the high temperature of the steam and the deposition of low boiling products caught. Therefore, a preliminary washing procedure was introduce to return a polymer as similar as possible to the pristine PLA sheet. To this end, low toxic and low volatile solvents such as water, ethanol, isopropyl alcohol, and isopropyl acetate were tested to clean the material, keeping the properties of the polymer unchanged.

About 12.50 g of dirty PLA, were immersed in 100 mL of a washing solvent, and magnetically stirred to promote optimal contact between the solvent and the polymer. The removal capability of a solvent system was evaluated by ATR-FTIR (**Fig. 4a**) and UV-Vis (**Fig. 4b**) spectroscopic analyses, comparing the spectra of PLA sheets treated under different conditions with the one from unused tobacco sticks.

A treated-PLA portion was put on the zinc selenide crystal of the ATR-FTIR instrument (**Fig. A2a**). The results indicates that hot ethanol and isopropyl acetate guarantee the highest degree of cleanliness preserving at the same the polymeric materials. Hot ethanol was thus selected thanks its lower toxicity, cost, and ease of recycling.

Before the UV-Vis analysis, the PLA sheets washed with the selected solvents were solubilized in 2 mL of tetrahydrofuran (**Fig. A2b**). The spectra in **Fig. 4b**, acquired for both the cleaned PLA sheets and the pristine one, show how the different solvents affected the polymer.

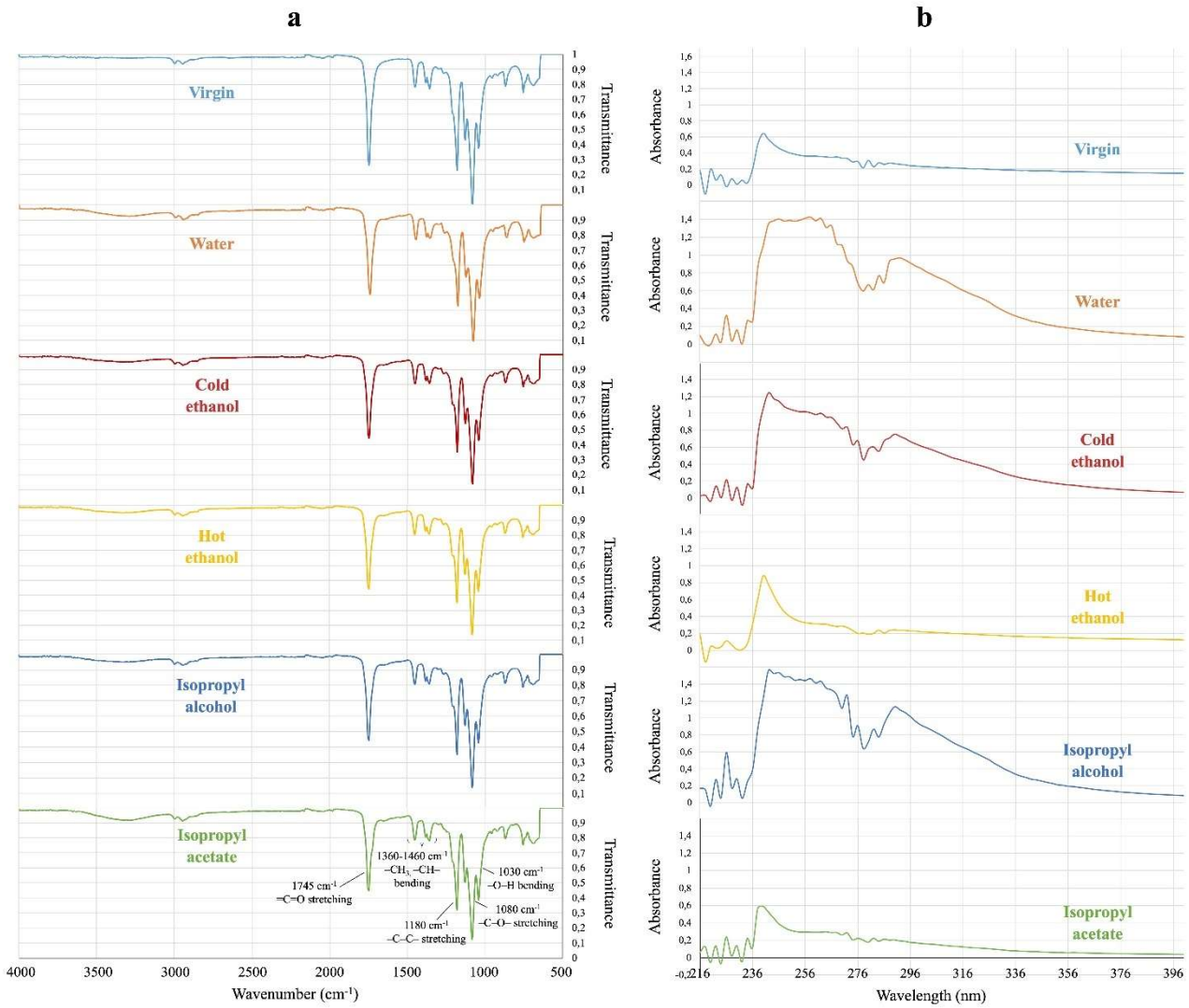

Fig. 4 ATR-FTIR (**a**) and UV-Vis (**b**) spectra of the used-PLA filters: comparison among the spectral profiles obtained with different solvents as cleaning agents

3.2. Selection and characterization of the most performant nanocomposite microbeads

A characterization study on the synthesized microbeads was performed by ATR-FTIR, TGA, DSC, XRD and SEM analyses.

Six types of microbeads differing for carbon nanomaterials (MWCNTs, GO) and their quantity (5%, 10%, 20% of the polymeric weight) were synthesized. In what follows, we will refer to these materials using a common strategy of abbreviation. The bulk polymer is reported before the symbol "@", the carbon nanomaterial is mentioned after the same symbol, and in round brackets there is its percentage with respect to the total weight of the polymer. The capital M at the beginning revers to the magnetic

properties of the obtain materials (e.g. mPLA@GO(15) is the PLA-based material containing 15% w/w of GO).

Among the six types of microbeads, mPLA@GO(15) and mPLA@MWCNTs(5) provided the best performance when tested (15 mg of sorbent per test) to recover the 14 analytes from urine samples spiked at 1 μg L^{-1} (see **Fig. A3a**). Based on the observed trend, other nanocomposites were prepared: one with the 1.8 % of MWCNTs (w/w) and another one with the 20 % of GO (w/w). In the first case, a dramatic reduction in extraction yield was obtained, whilst in the second one, a structural failure of the nanocomposite material was observed, with the collapse of the spherical shape as an effect of the high quantity of GO. However, it was observed that the two materials show an opposite tendency to adsorption: for GO adsorption rates tend to increase as the percentage of active sorbent increases; on the other hand, for MWCNTs, an increase of the adsorption performances is registered with decreasing quantity of carbonaceous sorbent. This result can be explained in light of the better dispersion of MWCNTs in the PLA bulk at lower concentrations, that influences most the absolute recovery than the total quantity and availability of the carbonaceous active adsorbent. As already stated, the risk of the aggregation of CNTs is enhanced at higher concentrations and when an adequate dispersion in the polymeric support is not provided. On the other hand, since aggregation tendency is less significant for GO, greater extraction yields are provided by the devices that can guarantee an improved availability of active carbonaceous adsorption surface, namely the ones with higher concentrations of GO.

Both mPLA@GO(15) and mPLA@MWCNTs(5) were submitted to characterization. To confirm the preservation of the polymeric structure, clean PLA sheets were also analyzed.

The comparison of the ATR-FTIR spectra of carbonaceous nanocomposites with the one of the pure PLA is shown in **Fig. A4a**. A wide and weak band around 3000 cm^{-1} is due to the –OH stretching (free) of the PLA chain. Sharp bands, between 2940-3000 cm^{-1} are caused by the symmetric and asymmetric stretching of –CH– bonds. The carbonyl stretching (=C=O) is responsible for a sharp and intense band at 1760 cm^{-1}. Two signals between 1360-1460 cm^{-1} are the result of the bending of –

CH_3 groups. Signals below 1300 cm^{-1} are much less informative and arise from the stretching of the –C-O– and C—O—C bond and bendings of the carbonyl and hydroxyl groups. Similar results and spectral evidence are reported in different previous works, here cited for comparison purposes [27, 28]. Spectroscopic profiles for the tested materials were almost completely superimposable and the major bands were similar for all the types of tested nanocomposites. The synthetic protocol does not result in an alteration of the bulk polymeric structure.

The **Fig. A4b** shows the TGA curves of mPLA@GO(15), mPLA@MWCNTs(5), and pristine PLA sheet. The thermogravimetric profiles are similar for all materials, which exhibit a single thermal transition, corresponding to a mass loss of 75%, in the same temperature range of PLA degradation, as reported in the literature [29]. Such results confirm the preservation of the polymer bulk composition in the nanocomposite microbeads.

The DSC analyses on the composite device (**Fig. A5**) shows an endothermic double peak between 150-162.5 °C associated with the temperature melting point I of PLA [30].

The characteristic double peak may be related to the complex structure of PLA where several crystalline domains coexist, as a result of the organization of different lengths polymer chains. The first peak would be relatable to the melting of smaller crystals or shorter polymer chains, while greater thermal energy is required for larger crystals melting [31, 32].

The XRD diffractogram, shown in **Fig. A6** confirms the synthesis procedure is effective in the incorporation of magnetite and PLA into the composite. The most intense peak located at 14.8°, 16.4°, 19.2°, and 22.5° can be associated with the semicrystalline structure of PLA [33, 34] while the ones at 30.4°, 35.6°, and 43.2° can be related to iron oxide nanoparticles [35].

Both nanocomposites were studied by means of SEM at different magnifications: a) 100 X, to have an overlook of the obtained material; b) 1.00K X, to verify the spherical shape of the nanocomposite; c) 10.00K X, to observe the porous surface; d) 100.00K X, to observe the MWCNT nanostructure and the arrangement of the PLA filaments. From the images it is possible to assess that the microbead diameters are dispersed in a narrow range of sizes, between 10 and 100 μm. From a comparison

between both types of microbeads, mPLA@MWCNTs(5) seems to be more regular in shape and in the surface conformation. **Fig. 5a-5d** show the images of mPLA@MWCNTs(5).

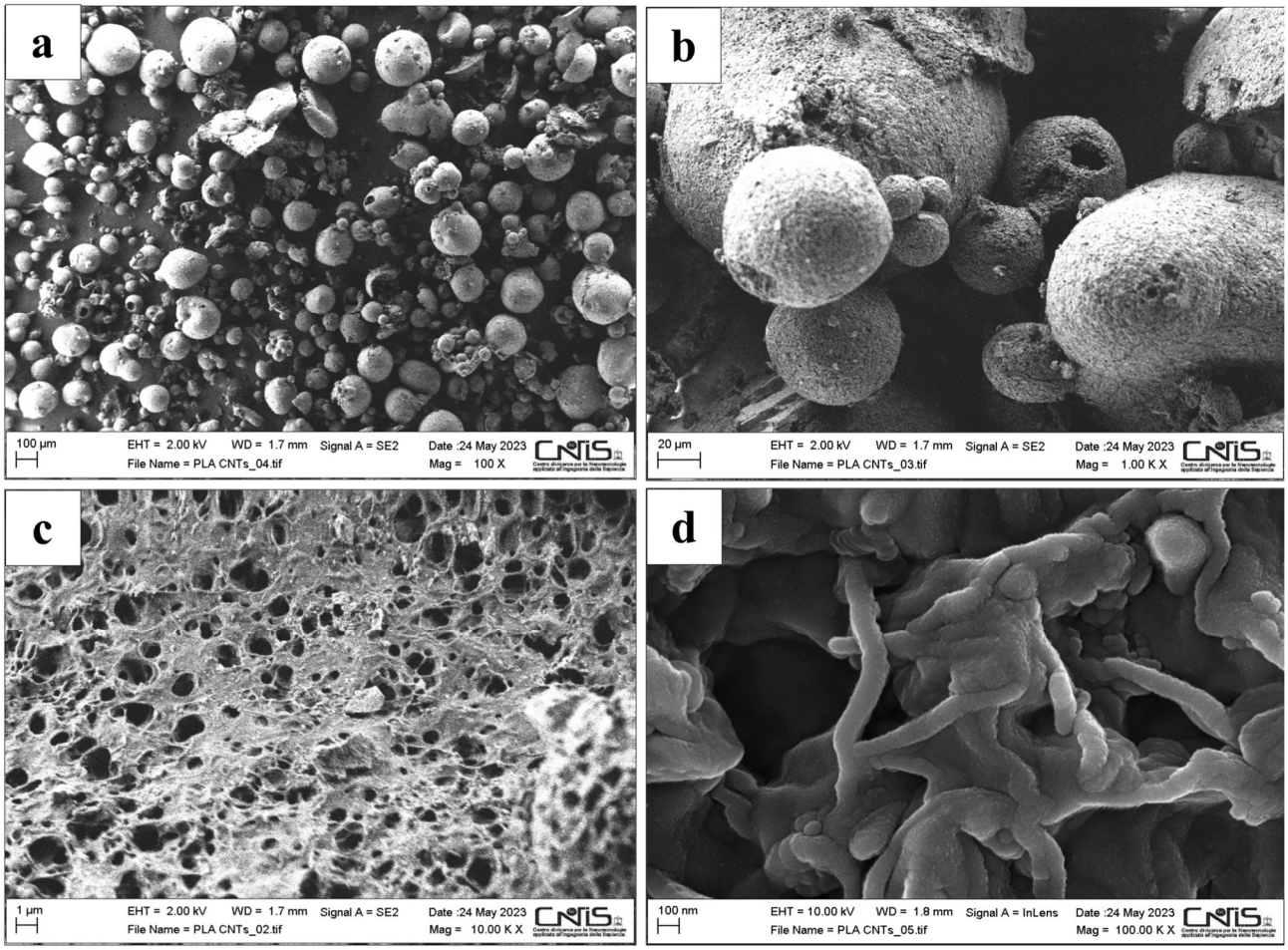

Fig. 5 SEM images of mPLA@MWCNTs(5) at the following magnifications: 100X (**a**), 1.00K X (**b**), 10.00K X (**c**) and 100.00 K X (**d**)

mPLA@MWCNTs(5) microbeads were thus selected for further steps of optimization considering it the best compromise between the synthesis greenness and the analytical performance.

3.3. Optimization of the extraction procedure

The experiments to optimize the m-SPE procedure with mPLA@MWCNTs(5) were performed using 1-mL aliquots of diluted urine (spike level of urine before dilution with water was 1 µg L^{-1}). To this end, a One-Variable-At-a-Time (OVAT) optimization approach (three replicates for each condition tested) was adopted.

The first parameter to be optimized was the amount of the sorbent: 10 mg, 15 mg, and 20 mg. Adsorption time and desorption time were kept at 30 min; for the analyte desorption was used a 2-mL volume of methanol. Recoveries obtained with 15 and 20 mg of microbeads were substantially unvaried (~77%), while 10 mg of mPLA@MWCNTs(5) were not sufficient to provide a complete extraction of the analytes from urine (61%) (see **Fig. A3b)**. Although the dispersion of 15 mg and 20 mg leads to similar results, it was chosen to disperse the smaller amount in a greener perspective.

The following experiments, performed using 15 mg of mPLA@MWCNTs(5), were aimed at optimizing the adsorption time. To this end, a kinetic study was performed by evaluating the chromatographic area, averaged on all the analytes, at the following contact times: 5 min, 15 min, 1 h, 3 h and 6 h. The desorption step was carried out in a fixed contact time (30 min). Plotting the average chromatographic area against the adsorption time (see **Fig. A7a)**, an asymptotic value is reached for all the analytes in less than 10 min. The results show that the adsorption rate of the analytes on the microbead surface is very fast. After the first 5 min of contact, no further significant adsorption was observed, due to the complete saturation of the available sites on the microbead surface. For this reason, it was decided to select a contact adsorption time of 5 min, as a compromise between processing time and extraction efficiency.

Once the adsorption time was selected, the desorption kinetic was investigated. The pretreatment procedure was repeated performing the desorption step with methanol (2 mL) at different contact times: 1 min, 2.5 min, 5 min and 10 min. The desorption curves are shown in **Fig. A7b**. The results prove that, even in this case, the kinetics are fast, and the plateau is easily reached within 1 min. Therefore, this time was selected to obtain the analyte desorption from the active sites of microbeads. Finally, keeping unvaried the optimized parameters, it was evaluated type and volume of the desorption solvent (methanol, acetonitrile, and ethyl acetate). To this end, for each desorption solvent tested, four 0.5-mL fractions were collected and analyzed. The recovery yields showed that three 0.5 mL fractions of methanol allowed one to maximize the average recovery of the analytes (76%).

3.4. Results of the method validation

Tables 2 and **A3** summarize the figures of merit of the validated method (LOD, LLOQ, recovery precision and accuracy), while **Tables A4** and **A5** list the calculated linear regression parameters (slope, related to the method sensitivity, and intercept).

Matrix-matched calibration curves were prepared by analyzing 7 calibrators, spiked pre-extraction with the analytes in a dynamic linear range of interest from 1 μg L^{-1} to 15 μg L^{-1}. Slope and intercept were estimated by means of the least-square method using the linear model y = a + b C; the error associated to a and b was estimated too. The determination coefficients R^2 were found to be higher than 0.99, showing a good linear correlation.

LOD was calculated as the analyte concentration capable of providing a signal 3 times higher than the background noise (S = 3N). Therefore, 0.6-mL aliquots of urine were spiked with decreasing concentrations of the analytes, diluted with 0.4 mL of Milli-Q water (1 mL of diluted urine), and analyzed until a signal to noise ratio of about 3 was reached for each analyte. Likewise, LLOQ was calculated as the concentration generating a signal 5 times higher than the background noise (S = 5N) provided that precision and accuracy values were within 20%. Once established, LODs and LLOQs were confirmed by means of five independent replicates.

Recovery, precision and accuracy were estimated at the three different levels of fortification: 1 μg L^{-1} for all the analytes with the exception of 4-chloro-2-methylphenol and mecoprop, for which the spike level was set at 3 μg L^{-1} (i.e., within three times the analyte LLOQ; see **Table 2**); 6 μg L^{-1} (i.e. around 50% of the linear dynamic range; see **Table A3**); 15 μg L^{-1} (i.e. close to the upper limit of the calibration curve; see **Table A3**). Five replicates were performed at each level. Precision and accuracy provided *within-run* figures of merit when calculated on the same analytical session and *between-run* figures of merit when calculated on three different analytical sessions.

For each analyte, the recovery rates were calculated as (**Equation 2**)

$$R\% = \frac{C_{measured} - C^*}{C^*} x100 \quad (2)$$

where C^* is the spike level applied and $C_{measured}$ is the average concentration measured at a specific spike level. To calculate $C_{measured}$, the average of the chromatographic areas obtained at each spike level (5 replicates) was interpolated in the post-extraction calibration curve (**Table A5** shows the linear regression parameters; the linear dynamic range is the same as for the pre-extraction spiked curves). Recoveries, calculated at the different spike levels (see **Table 2** for the lowest spike level and **Table A3** for the other two ones), were greater than 64% with the exception of 4-chloro-2-methylphenol that shows a yield of 57% at the lowest spike level.

The precision was expressed in terms of relative standard deviation (RSD%). According to the FDA criteria, the RSD% should be ≤ 15%, with the only exception of the lowest fortification level (within 3 times LLOQ), for which an RSD ≤ 20% is also allowed. **Tables 2** and **A3** show that all RSD were lower than 15%.

The relative accuracy was evaluated as follows (**Equation 3**)

$$Accuracy\% = \frac{C_{spiked} - C_{measured}}{C_{spiked}} x100 \quad (3)$$

In this case, $C_{measured}$ was calculated by interpolating the average of the chromatographic areas, obtained at each spike level, in the pre-extraction calibration line. As for precision, the accepted deviation for the accuracy evaluation is a maximum of 20% for the lowest level of fortification and 15% for all the others. Even in this case, the accuracy values are all lower than 15%, as it is shown in **Tables 2** and **A3**.

Finally, the enrichment factors (EF) were calculated according to the following equation:

$$EF = \frac{C_{analyte\ in\ the\ final\ extract}}{C_{analyte\ in\ the\ urine\ sample}} \quad (4)$$

The results were spanned between 3.42 to 6.00 depending on the analyte recovery.

Table 2 Figures of merit of the 14 analytes analyzed with the m-SPE-UPLC-MS/MS method proposed in this work. Recovery, precision and accuracy are reported for the lowest level of fortification (within three times the analyte LLOQ).

Compound	LOD (µg L^{-1})	LLOQ (µg L^{-1})	Recovery (%)	Precision (%)		Accuracy (%)	
				Within-run	Between-run	Within-run	Between-run
Diuron	0.4	0.8	64	5.0	5.8	13.5	14.0
Bensulfuron-methyl	0.6	0.9	76	7.2	9.0	8.5	9.2
Methyl-testosterone	0.5	0.9	68	7.6	7.9	10.0	10.6
Flamprop	0.6	1.0	72	6.8	7.4	10.2	10.8
4-Chloro-2-methylphenol	1.8	3.0	57	5.6	6.2	5.1	5.7
Mecoprop	1.3	2.2	86	9.0	10.6	9.9	10.5
Linuron	0.4	0.7	75	5.8	8.8	5.2	5.5
Nimesulide	0.1	0.3	69	9.0	10.7	5.4	6.0
MCPB	0.5	0.8	70	4.7	5.2	5.0	5.5
Carprofen	0.6	1.0	89	6.4	7.0	9.2	9.9
Diclofenac	0.2	0.4	100	5.5	6.3	5.4	6.0
Ibuprofen	0.5	0.8	70	5.5	5.8	5.1	5.5
Malathion	0.2	0.3	94	5.9	6.5	5.0	5.5
Progesterone	0.7	0.4	79	4.7	5.5	13.3	13.8

3.5. Selectivity of the method and adsorption mechanism conclusions

From a mechanistic point of view, the extraction performances of the synthetized material can be explained by the interactions MWCNTs are responsible for. The parts of a MWCNT that are available for the adsorption of analytes are the external surface and the groove areas. The internal part of the nanotube is mostly inaccessible, for the presence of coaxial graphene sheets, round-folded, to give rise to smaller diameter tubes. For this reason, molecular volume and geometrical characteristics of the analytes are not a discriminant parameter for the definition of the recovery yields [36]. Otherwise, carbon nanotubes are responsible for non-covalent interactions, in particular Van der Wals, π-stacking and electron-donor-acceptor interactions; chemical moieties and specific electron distribution on the analyte surface are discriminant parameters responsible for the distinct affinity of xenobiotics on MWCNTs. The highest the hydrophobicity of the analyte is, the highest the possibility of the molecule to participate in weak non-polar interactions with MWCNTs, resulting in an increasing of the

adsorption on the material surface [37]. This theoretical tendence is confirmed from the experimental point of view for our 14 analytes: the evidence of a linear correlation between logP of the analytes and extraction yields of the material is displayed in **Fig. A8** of the Appendix A. Despite the clear linear dependence, the analytes in the current study were chosen in a quite narrow range of polarity, with logP varying between 1.6 and 4.4. In light of a parallel study conducted on a higher number of contaminants on spiked water samples, it was possible to recognize the same strong dependence between analytes logP and recovery efficiency of the prepared material. Analytes with higher logP values result in higher affinities with mPLA@MWCNTs(5), showing enhanced recovery values. The same tendency was already reported in literature in a comprehensive study, by Zhao et al. [38], relatively to the single MWCNTs. From this evidence, we concluded that the PLA support does not play a relevant role in the adsorption mechanism of the composite material. As a confirmation, experimental analysis were performed with magnetic microspheres, obtained following the same showed procedure, but delating the addition of the active carbonaceous adsorbent (MWCNTs). The recovery yields, as expected, decreased to values below 5%, giving an experimental confirmation of the spectator's role of PLA in the adsorption dynamics. As already stated, the polymeric bulk is otherwise fundamental to disperse MWCNTs and avoid the aggregations of the structures, providing, at the same time, a micrometric-sized material, easy to collect and to manipulate [39]. These conclusions, along with the extremely wide applicability of the device as it was presented, makes the present material a good extraction device for organic xenobiotics, in particular for the low-polarity ones, with logP higher than 3.

3.6. Comparison with previous methods

Table A6 reports the main figures of merit (recovery, precision, LLOQ, EF, and analysis time) of the described procedure as well as those of previous methods developed to extract the same analytes from human, animal and synthetic urine samples [40-46]. As far as method limits are concerned, our method has comparable or lower (normalized) values like some of the chromatographic methods

relying on MS detection [43-46]. All methods show low EFs with the exception of the procedures based on stir bar sorptive extraction (SBSE) [44] and cloud point extraction (CPE) [43]. Regarding recovery and precision, our method exhibits comparable performance than the others, with the difference that we evaluated these parameters applying lower spike levels (from 10 up to 5000 times), except the SBSE-GC-MS method for the determination of ibuprofen [44] whose evaluation was performed at 0.5 μg L^{-1} due to the dilution of the extract before the injection (see **Table A6**). Regarding extraction time, our procedure is rapid even if three out of the eight compared procedures (dispersive liquid-liquid microextraction (DLLME) [40], CPE [43], disposable pipette extraction (DPE) [45]) show time shorter than 10 min. Besides being more sensitive, our method is more sustainable due to the use of recycled PLA. At the best of our knowledge, the present method is the first one reporting a quantification method for flamprop in urine.

4. Conclusion

The PLA-based nanocomposite described in this work is a sustainable product due to the intrinsic nature of PLA, a biodegradable polymer derived from a renewable natural resource such as corn. The nanocomposite is simple to prepare and exhibits a perfect compatibility between PLA and the other components (MWCNTs/GO and magnetic nanoparticles). The micrometric size and reactivity to magnetic fields greatly simplify the extraction procedure, avoiding the use a of a centrifuge and reducing analysis time. The properties of the composite and the ease of application allowed us to obtain good analytical performance in terms of recoveries, precision and accuracy. The nanocomposite could also be applied to extract pollutants from environmental waters as well as for water remediation purposes.

Although PLA is biodegraded in the environment by enzymes and bacteria into CO_2, water and humus, its high production to replace part of petroleum-based plastics is leading to a large amount of waste PLA accumulation due to its slow degradation rate [47]. Thus, the extension of PLA's lifetime through recycling is a convenient solution with environmental and economic benefits because PLA

is also an expensive polymer, more than conventional plastics such as polyethylene. Under this point of view, this work offers a contribute proposing a strategy of PLA recycling and a new use of such a polymer.

References

[1] Á.I. López-Lorente, F. Pena-Pereira, S. Pedersen-Bjergaard, V.G. Zuin, S.A. Ozkan, E. Psillakis (2022). The ten principles of green sample preparation, Trends Anal. Chem. 148. https://doi.org/10.1016/J.TRAC.2022.116530.

[2] J. Płotka-Wasylka, N. Szczepańska, K. Owczarek, J. Namieśnik (2017). Miniaturized Solid Phase Extraction. In Green Extraction Techniques: Principles, Advances and Applications; Ibañez, E., Cifuentes, A., Eds.; Comprehensive Analytical Chemistry; Elsevier: Amsterdam, The Netherlands, 2; Volume 76, pp. 279–318.

[3] M. Alexovič, B. Horstkotte, P. Solich, J. Sabo (2016). Automation of static and dynamic non-dispersive liquid phase microextraction. Part 1: approaches based on extractant drop-, plug-, film-and microflow-formation. Analytica Chimica Acta, 906, 22-40. https://doi.org/10.1016/j.aca.2015.11.038

[4] M. L. Soriano, M. Zougagh, M. Valcárcel, Á. Ríos, (2018). Analytical Nanoscience and Nanotechnology: Where we are and where we are heading. Talanta, 177, 104-121. https://doi.org/10.1016/j.talanta.2017.09.012

[5] E. Omanović-Mikličanin, A. Badnjević, A. Kazlagić, M. Hajlovac (2020). Nanocomposites: A brief review. Health Technol. (Berl), 10, 51-59. https://doi.org/10.1007/s12553-019-00380-x

[6] A. B. Cook, T. D. Clemons (2022). Bottom-up versus top-down strategies for morphology control in polymer-based biomedical materials. Adv. Nanobiomed. Res., 2(1), 2100087. https://doi.org/10.1002/anbr.202100087

[7] H. Ghambari, E. M. Reyes-Gallardo, R. Lucena, M. Saraji, S. Cárdenas (2017). Recycling polymer residues to synthesize magnetic nanocomposites for dispersive micro-solid phase extraction. Talanta, 170, 451-456. https://doi.org/10.1016/j.talanta.2017.04.026

[8] B. Mrowiec (2018). Plastics in the circular economy (CE). Environ. Nat. Resour. J., 29(4), 16-19. https://doi.org/10.2478/oszn-2018-0017

[9] E. Foschi, A. Bonoli (2019). The Commitment of Packaging Industry in the Framework of the European Strategy for Plastics in a Circular Economy, Adm. Sci. 2019, Vol. 9, Page 18 9 18. https://doi.org/10.3390/ADMSCI9010018

[10] C. E. Nika, E. Yiantzi, E. Psillakis (2016). Plastic pellets sorptive extraction: Low-cost, rapid and efficient extraction of polycyclic aromatic hydrocarbons from environmental waters, Anal. Chim. Acta 922 30–36. https://doi.org/10.1016/J.ACA.2016.03.037

[11] EUR-Lex - 32019L0904 - EN - EUR-Lex, (n.d.). https://eur-lex.europa.eu/eli/dir/2019/904/oj (accessed January 7, 2024).

[12] V. O. Topuzyan, S. G. Grigoryan, On the release of a toxicant from PLA film filter on iQOS heat stick. http://oldstcopc.sci.am/sources/Article_iQOS.pdf

[13] K. Hamad, M. Kaseem, M. Ayyoob, J. Joo, F. Deri (2018). Polylactic acid blends: The future of green, light and tough, Prog. Polym. Sci. 85 83–127. https://doi.org/10.1016/j.progpolymsci.2018.07.001

[14] M. Á. Aguirre, A. Canals (2022). Magnetic deep eutectic solvents in microextraction techniques. TrAC Trends in Analytical Chemistry, 146, 116500. https://doi.org/10.1016/j.trac.2021.116500

[15] N. Heidari, A. Ghiasvand (2020). A review on magnetic field-assisted solid-phase microextraction techniques. Journal of Liquid Chromatography & Related Technologies, 43(3-4), 75-82. https://doi.org/10.1080/10826076.2019.1668804

[16] H. N. Abdelhamid, Y. C. Lin, H. F. Wu (2017). Magnetic nanoparticle modified chitosan for surface enhanced laser desorption/ionization mass spectrometry of surfactants. RSC advances, 7(66), 41585-41592. https://doi.org/10.1039/C7RA05982E

[17] Y. Yuan, M. Wang, N. Jia, C. Zhai, Y. Han, H. Yan (2019). Graphene/multi-walled carbon nanotubes as an adsorbent for pipette-tip solid-phase extraction for the determination of 17β-estradiol in milk products. Journal of Chromatography A, 1600, 73-79. https://doi.org/10.1016/j.chroma.2019.04.055

[18] S. Zhang, T. Shao, S. S. K. Bekaroglu, T. Karanfil (2009). The impacts of aggregation and surface chemistry of carbon nanotubes on the adsorption of synthetic organic compounds. Environmental science & technology, 43(15), 5719-5725. https://doi.org/10.1021/es900453e

[19] C. D. Bosco, M. G. De Cesaris, N. Felli, E. Lucci, S. Fanali, A. Gentili (2023). Carbon nanomaterial-based membranes in solid-phase extraction. Microchimica Acta, 190(5), 175. https://doi.org/10.1007/s00604-023-05741-y

[20] S. Majidi, F. Zeinali Sehrig, S. M. Farkhani, M. Soleymani Goloujeh, A. Akbarzadeh (2016). Current methods for synthesis of magnetic nanoparticles. Artificial cells, nanomedicine, and biotechnology, 44(2), 722-734. https://doi.org/10.3109/21691401.2014.982802

[21] A. Avram, A. Radoi, V. Schiopu, M. Avram, H. Gavrila (2011). Synthesis and characterization of γ-Fe2O3 nanoparticles for applications in magnetic hyperthermia. Synthesis, 10(P151), 1.

[22] W. R. de Araújo, M. O. Salles, T. R. Paixão (2012). Development of an enzymeless electroanalytical method for the indirect detection of creatinine in urine samples. Sensors and Actuators B: Chemical, 173, 847-851. https://doi.org/10.1016/j.snb.2012.07.114

[23] V. Gallo, P. Tomai, M. Gherardi, C. Fanali, L. De Gara, G. D'orazio, A. Gentili (2021). Dispersive liquid-liquid microextraction using a low transition temperature mixture and liquid chromatography-mass spectrometry analysis of pesticides in urine samples, J. Chromatogr. A 1642 462036. https://doi.org/10.1016/j.chroma.2021.462036

[24] V. Gallo, P. Tomai, V. Di Lisio, C. Dal Bosco, P. D'angelo, C. Fanali, G. D'orazio, I. Silvestro, Y. Picó, A. Gentili (2021). Application of a low transition temperature mixture for the dispersive liquid–liquid microextraction of illicit drugs from urine samples, Mol. 26. https://doi.org/10.3390/molecules26175222

[25] M. A. Pearson, C. Lu, B.J. Schmotzer, L.A. Waller, A.M. Riederer (2008). Evaluation of physiological measures for correcting variation in urinary output: Implications for assessing environmental chemical exposure in children, J. Expo. Sci. Environ. Epidemiol. 2009 19:3 19 336–342. https://doi.org/10.1038/jes.2008.48

[26] Fda, Cder (2018). Bioanalytical Method Validation Guidance for Industry Biopharmaceutics Bioanalytical Method Validation Guidance for Industry Biopharmaceutics Contains Nonbinding Recommendations.
http://www.fda.gov/Drugs/GuidanceComplianceRegulatoryInformation/Guidances/default.htmand/orhttp://www.fda.gov/AnimalVeterinary/GuidanceComplianceEnforcement/GuidanceforIndustry/default.htm (accessed January 7, 2024).

[27] Y. Cai, J. Lv, J. Feng (2013). Spectral characterization of four kinds of biodegradable plastics: poly (lactic acid), poly (butylenes adipate-co-terephthalate), poly (hydroxybutyrate-co-hydroxyvalerate) and poly (butylenes succinate) with FTIR and raman spectroscopy. Journal of Polymers and the Environment, 21, 108-114. https://doi.org/10.1007/s10924-012-0534-2

[28] W. A. Herrera-Kao, M. I. Loría-Bastarrachea, Y. Pérez-Padilla, J. V. Cauich-Rodríguez, H. Vázquez-Torres, J. M. Cervantes-Uc (2018). Thermal degradation of poly (caprolactone), poly (lactic acid), and poly (hydroxybutyrate) studied by TGA/FTIR and other analytical techniques. Polymer Bulletin, 75, 4191-4205. https://doi.org/10.1007/s00289-017-2260-3

[29] F. Carrasco, O. S. Pérez, M. L. Maspoch (2021). Kinetics of the thermal degradation of poly(Lactic acid) and polyamide bioblends, Polym. (Basel) 13. https://doi.org/10.3390/polym13223996

[30] M. Ayyoob, Y. J. Kim (2018). Effect of chemical composition variant and oxygen plasma treatments on the wettability of PLGA thin films, synthesized by direct copolycondensation. Polymers, 10(10), 1132. https://doi.org/10.3390/polym10101132.

[31] Y. T. Shieh, G. L. Liu (2007). Temperature-modulated differential scanning calorimetry studies on the origin of double melting peaks in isothermally melt-crystallized poly (L-lactic acid). Journal of Polymer Science Part B: Polymer Physics, 45(4), 466-474. https://doi.org/10.1002/polb.21056

[32] M. Yasuniwa, S. Tsubakihara, K. Iura, Y. Ono, Y. Dan, K. Takahashi (2006). Crystallization behavior of poly (l-lactic acid). Polymer, 47(21), 7554-7563. https://doi.org/10.1016/j.polymer.2006.08.054

[33] E. Y. Gómez-Pachón, R. Vera-Graziano, R. M. Campos (2014). Structure of poly (lactic-acid) PLA nanofibers scaffolds prepared by electrospinning. In IOP conference series: materials science and engineering (Vol. 59, No. 1, p. 012003). IOP Publishing. https://doi.org/10.1088/1757-899X/59/1/012003

[34] J. Gu, J. M. Catchmark (2013). Polylactic acid composites incorporating casein functionalized cellulose nanowhiskers. Journal of biological engineering, 7, 1-10. https://doi.org/10.1186/1754-1611-7-31

[35] K. C. Kim, E. K. Kim, J. W. Lee, S. L. Maeng, Y. S. Kim (2008). Synthesis and characterization of magnetite nanopowders. Current Applied Physics, 8(6), 758-760. https://doi.org/10.1016/j.cap.2007.04.021

[36] M. W. Maddox, K. E. Gubbins (1995). Molecular simulation of fluid adsorption in buckytubes. Langmuir, 11(10), 3988-3996. https://doi.org/10.1021/la00010a059

[37] D. H. Carrales-Alvarado, R. Leyva-Ramos, I. Rodríguez-Ramos, E. Mendoza-Mendoza, A. E. Moral-Rodríguez (2020). Adsorption capacity of different types of carbon nanotubes towards metronidazole and dimetridazole antibiotics from aqueous solutions: effect of morphology and surface chemistry. Environmental Science and Pollution Research, 27, 17123-17137. https://doi.org/10.1007/s11356-020-08110-x

[38] H. Zhao, X. Liu, Z. Cao, Y. Zhan, X. Shi, Y. Yang, J. Zhou, J. Xu (2016). Adsorption behavior and mechanism of chloramphenicols, sulfonamides, and non-antibiotic pharmaceuticals on multi-walled carbon nanotubes. Journal of hazardous materials, 2016, 310: 235-245. https://doi.org/10.1016/j.jhazmat.2016.02.045

[39] J. Zhao, A. Buldum, J. Han, J. P. Lu (2002). Gas molecule adsorption in carbon nanotubes and nanotube bundles. Nanotechnology, 2002, 13(2): 195. https://doi.org/10.1088/0957-4484/13/2/312

[40] C. Will, E. Omena, G. Corazza, G. Bernardi, J. Merib, E. Carasek (2020). Expanding the applicability of magnetic ionic liquids for multiclass determination in biological matrices based on dispersive liquid–liquid microextraction and HPLC with diode array detector analysis. J. Sep. Sci., 43(13), 2657-2665. https://doi.org/10.1002/jssc.202000143

[41] N. Rosales-Conrado, M. E. León-González, L. V. Pérez-Arribas, L. M. Polo-Díez (2008). Multiresidue determination of chlorophenoxy acid herbicides in human urine samples by use of solid-phase extraction and capillary LC–UV detection. Anal. Bioanal. Chem., 390, 759-768. https://doi.org/10.1007/s00216-007-1701-5

[42] C. Sweeney, Y. Park, J. S. Kim (2019). Comparison of sample preparation approaches and validation of an extraction method for nitrosatable pesticides and metabolites in human serum and urine analyzed by liquid chromatography-Orbital ion trap mass spectrometry, J. Chromatogr. A 1603 83–91. https://doi.org/10.1016/j.chroma.2019.06.065

[43] O. G. Makukha, L. A. Ivashchenko, O. A. Zaporozhets, Volodymyr O. Doroschuk (2019). Cloud point extraction combined with HPLC-MS for the determination of nimesulide in biological samples, Chem. Zvesti. 73, 693–699. https://doi.org/10.1007/s11696-018-0618-0

[44] P. Mohammadi, M. Masrournia, Z. Es'haghi, M. Pordel (2021). Hollow fiber coated Fe3O4@Maleamic acid-functionalized graphene oxide as a sorbent for stir bar sorptive extraction of ibuprofen, aspirin, and venlafaxine in human urine samples before determining by gas chromatography-mass spectrometry, J. Iran. Chem. Soc. 18 2249–2259. https://doi.org/10.1007/s13738-021-02185-0

[45] A. Luiz Oenning, J. Merib, E. Carasek (2018). An effective and high-throughput analytical methodology for pesticide screening in human urine by disposable pipette extraction and gas chromatography-mass spectrometry. J. Chromatogr. B, 1092, 459-465. https://doi.org/10.1016/j.jchromb.2018.06.047

[46] Y. Zhou, Z. Cai (2020). Determination of hormones in human urine by ultra-high-performance liquid chromatography/triple-quadrupole mass spectrometry, Rapid Communications in Mass Spectrom. 34 e8583. https://doi.org/10.1002/RCM.8583

[47] D. Maga, M. Hiebel, N. Thonemann (2019). Life cycle assessment of recycling options for polylactic acid. Resour. Conserv. Recycl., 149, 86-96. https://doi.org/10.1016/j.resconrec.2019.05.018

Paper II: Polystyrene microbeads from yogurt containers

Sustainable Chemistry and Pharmacy 45 (2025) 102036

Contents lists available at ScienceDirect

Sustainable Chemistry and Pharmacy

journal homepage: www.elsevier.com/locate/scp

Microbeads from recycled polystyrene yogurt cups for the in-syringe micro solid-phase extraction of four opioids from environmental and biological samples

Lorenzo Antonelli [a,b], Ángela Inmaculada López-Lorente [a,*], Alessandra Gentili [b], Rafael Lucena [a], Soledad Cárdenas [a,**]

Graphical abstract

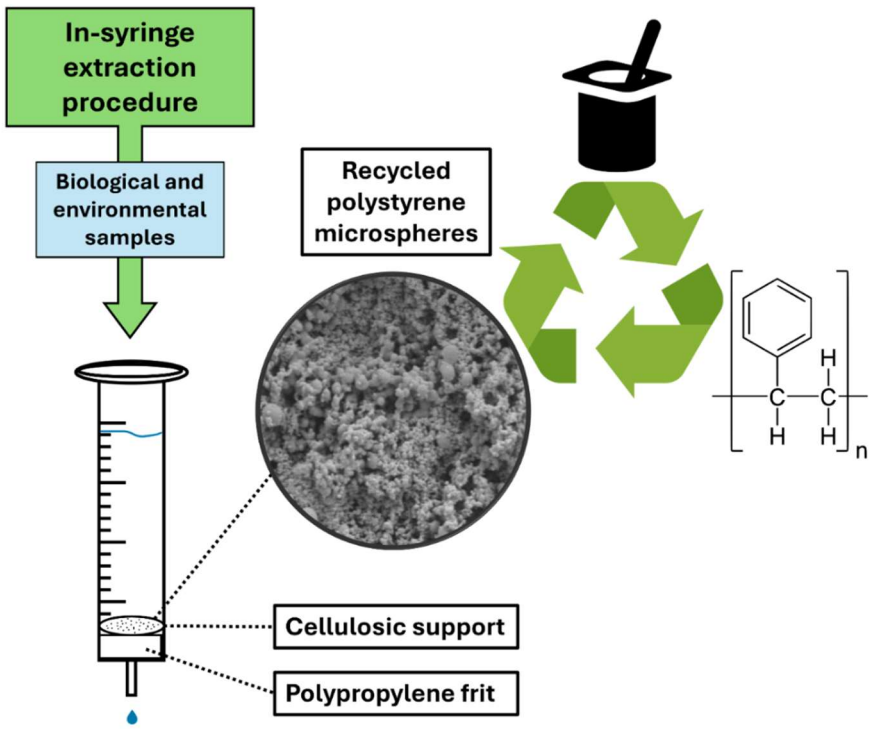

Abstract

A novel procedure for the extraction and determination of four opioids from environmental and biological fluids is presented. The main goal of this study is to introduce an innovative method for recycling plastic waste (i.e., polystyrene), aiming to achieve a consistent and dependable microstructure. Polystyrene microbeads, deposited on a rounded piece of paper, have been used as a sorbent material in an in-syringe extraction device. For the preparation of the polymeric sorbent, an emulsion solidification technique was optimized, achieving a regular micro material, obtained from second-hand regenerated polystyrene polymer from yogurt cups. This work presents, for the first time, the use of recycled polystyrene as micro-sorbent integrated into a paper-based support, combining waste valorization with effective analyte extraction. Under the optimum conditions, methadone, tramadol, codeine, and morphine were determined by direct injection mass spectrometry in environmental water as well as biofluids as saliva and urine. Limits of detection lower than 8 μg L^{-1} and precision better than 14.9 % have been obtained for all the analytes in saliva and environmental water samples. The interference of the endogenous compounds of urine prevents the determination of morphine and codeine in this matrix. The trueness, expressed as relative recovery (RR), ranged from 85 % to 114 %. The extraction device has proved to be a valid and sustainable alternative to traditional sorbents, offering good analytical standards and being transversal for the application to different matrices. The simplicity and environmental friendliness of this approach make it highly adaptable across various research and industrial domains.

1. Introduction

Polystyrene (PS) is an incredibly versatile polymer, finding nowadays applications in different fields, from packaging to electronic industry, consumer goods and construction [1]. Its widespread use due to its unique characteristics, such as low density, durability, low cost and easy processability, render it very attractive and easily applicable to a variety of industry processes [2]. Despite the growing

demand of materials with such characteristics, plastic solid waste is becoming a global issue, limiting the production of newly synthetized polymers, and empowering the research for new recycling strategies of them. Polystyrene is used in solid (i.e., coffee cups, trays) and expanded forms, both of which can be recycled. Most common strategies for PS recycling are the dissolution technique [3, 4], chemical recycling [5, 6], and thermochemical processes [7, 8], involving or not energy recovery. All these processes are well established for huge quantities of waste polymeric materials at an industrial scale. Otherwise, new procedures for polystyrene recycling, eventually returning applications of reconstituted materials in a lab scale dimension are demanded. Catalytical depolymerization [9] and solvent dissolution represent the most common strategies, allowing to obtain different results, depending on the required final material. In the first case, the catalytic process returns styrene monomers and other aromatic hydrocarbons (as side products), to be reused in other industrial processes [6]. The second approach deals with the dissolution of the polymer itself, without touching the chemical structure of the waste material and giving back restored polystyrene [10]. Plastic waste managing with solvents involves several stages [11]. Initially, the polymeric materials are dissolved, establishing a procedure for the restoration of the polymeric material and for a proper solvent management. Filtration can effectively remove any insoluble contaminants, leaving the polymer clean for further processing. This dissolution process also enables the separation of plastics from other waste types and insoluble polymers based on their chemical properties, a method known as selective dissolution in recycling [12, 13]. Recently, a wide variety of green solvents have been proposed for the dissolution of polystyrene, among them terpenoids, ethyl acetate and supercritical CO_2 [4, 12, 14-17]. All the reported experimental works and presented procedures offer recycling strategies involving foam polystyrene. Starting from an already reported micro-emulsion solidification method [18, 19], the first strategy for the preparation of micro and nano polystyrene spheres from solid polystyrene is here presented. This material is less soluble in classical solvents than the respective foam, and a lab made recycling strategy in dissolution mode has not been proposed yet. Microextraction techniques have emerged in recent years as powerful tools in analytical chemistry,

offering high efficiency with minimal solvent and sample consumption. Their ability to isolate target analytes from complex matrices while maintaining high selectivity and sensitivity makes them particularly suitable for trace-level analysis. These techniques, including solid-phase microextraction (SPME) [20], dispersive solid-phase extraction (dSPE) [21, 22], and pipette-tip SPME [23], are widely adopted in environmental, food, and biomedical analyses. The development of innovative sorbent materials has further enhanced their applicability, allowing for improved analyte recovery across a broad range of chemical polarities. In this context, integrating recycled materials into microextraction strategies represents a sustainable and cost-effective approach to sample preparation. Polystyrene microbeads have been reported as sorbent material for the extraction of contaminants from environmental, food and biological samples [24-40]. In other cases, the application of polystyrene in other micro-formats for the extraction or remediation of contaminants from real complex matrices are disclosed, while polystyrene nanofibers have been described for adsorption purposes [5, 34, 41]. A noteworthy study by Shin et al. [42] presented a method for producing nanofibers from waste expanded polystyrene, involving its dissolution in D-limonene, a green solvent. Paper supported PS has been reported [31, 5, 33, 35] where the combined action of cellulose and polystyrene chains is underlined, in favour of an enhanced extraction ability against a broad polarity spectrum of analytes. The production and usage of recycled PS magnetic nanoparticles was recently presented by Ghambari et al. [43] as an alternative device for microextraction in dispersive mode. In this article, at the best of our knowledge, the first in-syringe device, using recycled polymeric material, for the extraction of analytes from real complex matrices is presented. The advantage of the in-syringe extraction, coupled with a one-time synthetic preparation of polystyrene microbeads from waste material, is the simplicity and reproducibility of the procedure. The synthetic process was scaled down to obtain the precise optimized quantity of polystyrene to be charged in a syringe device. Deposition of PS on paper, washing protocol of the synthetized material, adsorption, and desorption of analytes are all performed in the syringe body, sequentially. The extraction of four opioids was used as a control model to define the best operational parameters to maximize the figures

of merit for the extraction of analytes. Polarity of the selected analytes are representative for the extraction of organic contaminants in a typical occurring range of logP values.

2. Experimental section

2.1. Materials and reagents

All reagents were of analytical grade or better. Methadone, codeine, morphine, tramadol, related internal standards (i.e., d3- methadone, d6-morphine, d3-codeine), sodium chloride and ammonium fluoride were supplied by Sigma-Aldrich (Madrid, Spain). Stock standard solutions were prepared in methanol (MeOH, Panreac, Barcelona, Spain) at a concentration of 1 mg mL^{-1} and stored at 4 °C in the dark. Working solutions were prepared by dilution of the stock in methanol or Milli-Q water (Millipore Corp., Madrid, Spain), as required. The whole optimization study was conducted with microspheres synthetized departing from commercially available PS in beads (average molecular mass 192,000 u.m.a., Sigma-Aldrich, Madrid, Spain). The final material, used for the validation study and for the analysis of real samples, was prepared with PS from commercial yogurt cups, pooled. Ethyl acetate, acetonitrile, ethanol, ammonia and formic acid were purchased from Panreac.

2.2. Real samples

Saliva samples were collected by passive drooling from healthy volunteers, aged between 22 and 28 years, within our laboratory. A pool of blank saliva from the different donors (~ 50 mL) was then subsampled to be used for the method optimization and validation within the same day. The samples were centrifuged, and the solid residue eliminated. For analysis, saliva was diluted 1:4 (v/v) in MilliQ water. Similarly, blank urine samples were obtained from the same volunteers. They were pooled, subsampled (50 mL fractions) and stored in freezer until use. The samples were 1:1 (v/v) diluted in pure water before spiking with the analytes. Environmental water was sampled via a 1-liter amber

glass bottle, by filling it completely. The matrix spiking and analysis was performed within 1 week from the sampling and the water was stored at room temperature.

2.3. Preparation of PS microbeads modified paper (PS–P)

A 2.5 % (w/v) solution of PS (commercial or from waste material) in ethyl acetate was prepared, assisting the dissolution with a gentle magnetic stirring. 250 µL of this solution was transferred into a 10 mL glass vial (diameter: 2 cm) containing a magnetic bar. For the emulsion-solidification procedure two aqueous solutions, one saturated in NaCl and another containing 1 % (w/v) sodium dodecyl sulphate, were prepared and mixed (2:5, v/v), resulting in a homogeneous phase. This aqueous solution was added to the vial, according to a 7:1 volumetric ratio (1.75 mL). The formation of a biphasic system was the result of the salting-out effect. The two-phases system was magnetically stirred (1600 rpm) to form a microemulsion of organic polymeric droplets into the aqueous phase. To break down the emulsion and let PS precipitate in the shape of microbeads, 1.2 mL of absolute ethanol was added all at once, while the system is stirring. The PS microbeads dispersion was charged in a 5 mL syringe, equipped with a frit in polypropylene and a circular piece of paper that perfectly fits the internal diameter of the syringe. The syringe was then installed on a vacuum pump equipment, to let the supernatant gently flow through the paper and the frit, leaving the dispersed microspheres on the top of the paper. Two aliquots of 2.5 mL of ethanol were used to ensure the complete transference of the microparticles and eliminate the residual salt and surfactant. Finally, the PS-P was left to dry at room temperature under vacuum. A thermal curing of the PS-P is performed by heating the whole syringe system in an oven for 30 min, at 110 °C. This temperature was chosen since it is slightly over the glass transition temperature of PS. This treatment ensures a low-level merging of the PS microspheres, which provides higher mechanical stability to the material without missing out the high surface area of the thin PS layer. The synthetic procedure for one device takes less than 3 min, considering emulsion solidification technique, filtration and washing step. The thermal curing step, lasting 30 min, can be performed simultaneously for a high number of devices, significantly

increasing the throughput of the procedure. For this reason, more than 30 devices can be prepared in 1 h. The synthesis yield of the final material is higher than 90 % (in terms of weight of microbeads with respect to the weight of employed PS). **Fig. 1a** displays a scheme of the whole procedure.

2.4. Characterization of the PS modified paper device

PS microbeads were analysed after the synthesis and deposition on the paper by attenuated total reflection Fourier transformed infrared spectroscopy (ATR-FTIR) and scanning electron microscopy (SEM). Thermogravimetric analysis (TGA) was carried out with a Mettler TG 50 thermobalance (Mettler Toledo, Columbus, USA). A weighted amount of sample was placed in the platinum crucible and the analysis was performed under nitrogen flow (20 mL min^{-1}), in the temperature range between 50 °C and 500 °C, with a heating rate of 10 °C min^{-1}. ATR-FTIR spectra were collected by using a Bruker LUMOS II FTIR micro-spectrometer (Bruker, Ettlingen, Germany), equipped with a germanium diamond ATR cell. Spectra were collected with a spectral window of 4000–550 cm^{-1}, coadding 2048 scans for each sample. Data collection and processing were made using the OPUS software package (Bruker, Ettlingen, Germany). The extraction devices were also analysed with a JEOL JSM 6300 model SEM (Central Service for Research Support (SCAI) at the University of Cordoba) ´ to investigate their sizes and morphology.

2.5. Optimization of the synthetic and extraction processes

The variables related with the synthesis of the polymeric microparticles as well as those affecting to the extraction procedure were investigated. Detailed information can be found in the Appendix B, see text and **Table B1**.

2.6. Analytical procedure

For the extraction, 5 mL of sample (i.e., saliva, urine, water with the appropriate dilution) containing the analyte at a concentration within the linear range were transferred to the syringe system. Pressure was applied with a syringe plunger, so that the sample flows through the paper supported microbeads. After the sample loading, the PS bed was left to dry for 2–3 min at room temperature. Analytes were then desorbed by adding 500 µL of methanol to the body of the syringe, which is left in contact for 1 min after which pressure is applied with the plunger and the eluate is collected in a MS vial. The entire extraction procedure takes less than 5 min, with the possibility of performing more than one extraction at the same time. The average throughput of the method amounts to 20–25 extractions in 1 h. The analytical procedure is displayed in **Fig. 1b**. Analyses were performed by direct infusion-mass spectrometry (DI-MS/MS) on an Agilent 1260 Infinity HPLC system (Agilent, Palo Alto, CA, USA) equipped with a binary high-pressure pump for mobile phase delivery and an autosampler. The carrier consisted of an aqueous phase (water with 0.1 % ammonium fluoride) and acetonitrile in a 50:50 v/v ratio. The target analytes were quantified on an Agilent 6420 Triple Quadrupole MS with an electrospray source. The mass spectrometer settings were fixed to improve the multiple reaction monitoring (MRM) signals (**Table B2**). The flow rate and the temperature of the drying gas (N2, 99 % purity) were 10 L min^{-1} and 300 °C, respectively. The nebulizer pressure was 18 psi and the capillary voltage was kept to 2000 V in positive mode for all the analytes. Agilent MassHunter Software (Version B.06.00) was used for qualitative and quantitative analyses.

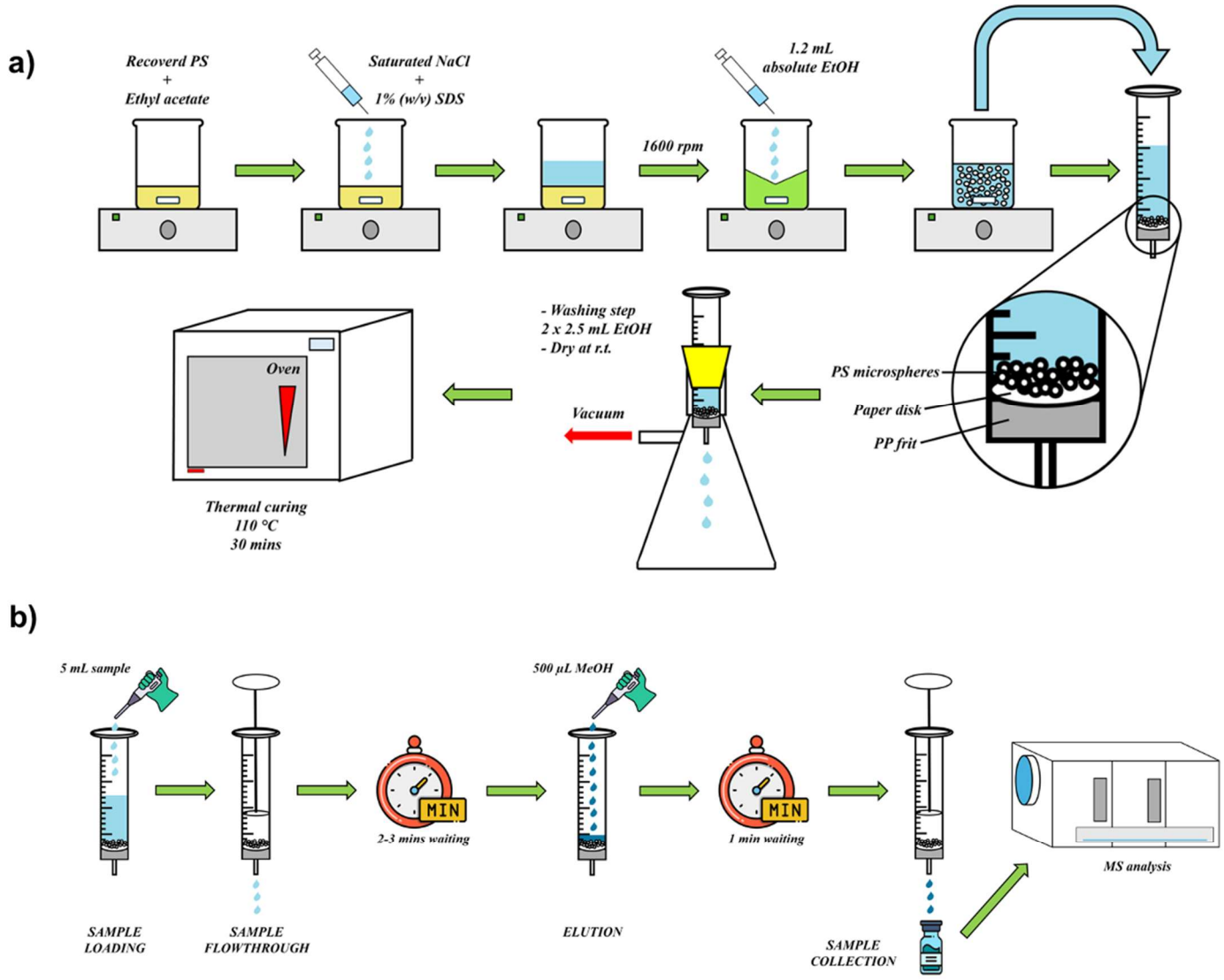

Fig. 1 Schematic representation of a) the synthetic route of the PS-P and b) the analytical procedure for the microextraction and MS analysis of the opioids.

3. Results and discussion

3.1. Optimization of synthetic parameters

The effect of four different procedural parameters, namely volume of the polymeric phase (mL), concentration of the PS in the organic phase (w/v %), ratio of the organic and aqueous phase (o:w) and ratio of the saturated NaCl and sodium dodecyl sulphate solutions in the aqueous phase (NaCl:SDS), influencing the synthesis of PS microbeads, have been studied together, selecting a

reasonable range and relevant values for each of the considered variables. The detailed procedure is included in the Appendix B. Three values were selected for each of these parameters (see **Table B1**), to monitor their influence in defining the final material. Qualitative evaluation of the final PS dispersion (yield of synthesis and visual assessment of the regularity of the obtained dispersed solid) was taken as the desirability parameter to discriminate between different experimental procedures. Best results were achieved with higher ratios of aqueous phase against organic polymeric phase and with low volumes and concentrations of the polymeric solution. At the end, the selected procedure comprises 0.25 mL of organic polymeric phase at a 2.5 % (w/v) concentration, keeping a 1:7 ratio o:w phases and 2:5 ratio of NaCl:SDS in the aqueous phase, which is the lowest consuming alternative that guarantees high throughput and desirable structured material.

3.2. Characterization of the PS-P

SEM analysis was performed on the final optimized PS-P prepared via in syringe physical deposition. The micrographs shown in **Fig. 2** highlight the effect of the thermal curing on the final material. In **Fig. 2a**, the material has not been submitted to the curing step; microbeads of PS appear well separated and the surface area is at its highest. In **Fig. 2b**, the thermal curing is responsible for a partial merging of the micrometric structures, with a slight decreasing of the surface development. Anyway, the curing represents a technological advance, being accountable for the mechanical stability and durable deposition of the PS structures on the paper disk. The cured device maintains unchanged wettability levels, resisting the sample/eluent flowthrough. In **Fig. 2c**, a micrograph of the material obtained with the commercial recycled PS is displayed, where an almost complete correspondence with **Fig. 2a** is observed. In **Fig. 2d**, **e**, and **f**, micrographs at different magnifications of the thermal cured optimized PS-P are shown. Microparticles are regular in shape, but the diameters are dispersed in a quite wide range of sizes. Occurring microbeads can be grouped in fine particles with a diameter ranging from 0.1 to 2.5 μm as well as coarse particles with diameters within 2.5 and 10 μm.

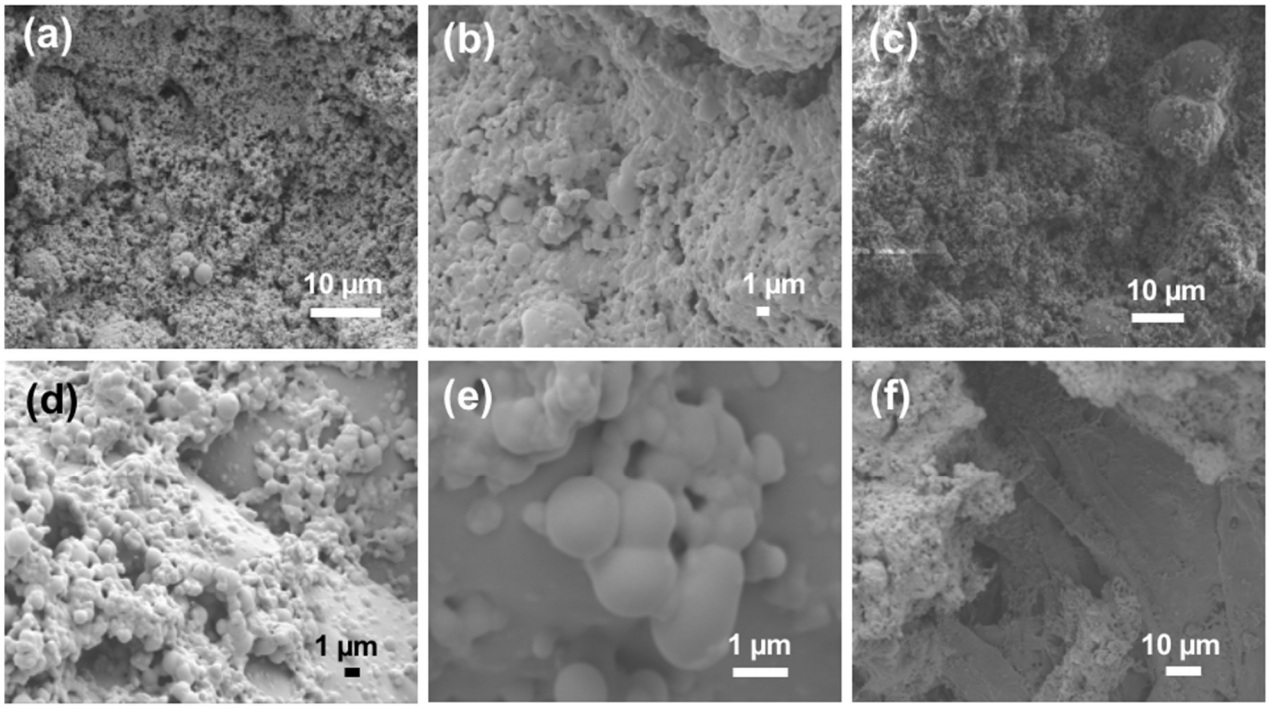

Fig. 2 SEM images of the optimized polystyrene on-paper adsorbent material. The reported images are related to different materials; (a): non cured polystyrene microsphere from reference polymer; (b, d, e, f): cured polystyrene microsphere after thermal curing, from reference polymer; (c): non cured polystyrene microspheres from commercial recycled polymer. The micrograms are collected at the following magnifications: 2000 X (**a**), 3000 X (**b**), 1500 X (**c**) 4000 X (**d**), 16000 X (**e**) and 1000 X (**f**).

TGA analysis was carried out on the analytical standard PS beads (3–5 mm, purchased from Goodfellow Cambridge Ltd., Huntingdon, UK), on powdered yogurt container material, and on the synthesized PS microspheres. Results are displayed in **Fig. B1**. In all three analyses conducted, a single degradation process was observed at 400–420 °C, aligning with the thermal degradation temperature of polystyrene reported in the literature [44]. The slight temperature shift between standard and commercial polystyrene can be attributed to differences in the degree of polymerization and the average molecular weight of the polymer. Curve for PS from yogurt containers is completely overlapping with the one obtained for the PS microspheres, obtained with the optimized microemulsion solidification technique, confirming the stability of the polymeric support. The solid residue, thermally stable up to 500 °C, confirms the presence of plasticizers and other additives in the commercial PS. ATR-FTIR was used also to confirm the actual conservation of the polymeric material after the synthetic process. For comparative purposes, PS-P as well as raw cellulose paper, PS microspheres and the original waste polymeric material have been analysed. Spectra are shown in

Fig. B2 and bands are assigned and described in detail in Appendix B. The spectra of the final PS-P display all the absorption bands of polystyrene, with the expected relative intensities. On the other hand, none of the absorption bands of cellulose are detectable in the spectrum of the extraction device. This can be explained with a complete and successful coverage of the cellulosic disk surface with the synthetized microspheres.

3.3. Optimization of extraction methodology

The variables affecting the extraction procedure were also submitted to an optimization study, i.e., volume and concentration of the sample solution loaded, quantity of deposited PS on the paper, pH, ionic strength, and chemistry of the desorption phase. First of all, the effect of the PS functionalization on paper was studied, to confirm and test the actual benefit of using PS microspheres as an additive of cellulosic paper for extraction purposes. For this reason, the performances of the raw paper disk as well as PSP have been studied and compared by carrying out the extraction procedure inside the syringe device at the same conditions. For this purpose, 5 mL of aqueous spiked solution, at a concentration of 500 μg L^{-1} of each analyte adjusted to pH 9 have been loaded, the elution being carried out with 300 μL of MeOH. The final extract has been analysed in triplicate at the optimized instrumental conditions and the results are displayed in **Fig. B3** of the Appendix B. As shown, functionalization with PS significantly enhances recoveries compared to raw paper, with a minimum increase of approximately 14-fold for methadone and a maximum boost of around 74-fold for morphine. This clearly highlights the crucial role of PS in the extraction of the target analytes. As described in literature [45], the presence of hydrophobic benzene rings in PS may promote π-π interactions between the polymeric microbeads and the aromatic moieties of analytes, in addition to van der Waals interactions between them. Response Surface Methodology (RSM) was utilized to evaluate the correlation between variables directly involved in the extraction procedure of analytes and contributing to the definition of the extraction yields of the protocol. As explain in detail in the Appendix B, a Box–Behnken design methodology was employed. For all the analytes the loading

volume is a crucial parameter for the definition of performances. High volumes are responsible for the saturation of the material, even with high loading amounts of PS. For the same reason, desirability becomes worse for higher values of concentration of the initial loading phase. By plotting the surface responses of the design for different fixed volume values, it is possible to estimate a maximum load quantity for each analyte before the saturation (coinciding with a decrease in the desirability). In **Fig. 3**, surface responses for each analyte at two different loading volume values (i.e., 1 and 5 mL) are plotted. At a volume of 1 mL, recovery increases while improving the amount of PS on the paper, while by increasing the volume up to 5 mL, the influence is less marked, or even it worsens in some cases. In addition, from a visual point of view, it can be observed that the thermal curing is not effective for higher quantities of PS, observing in the case of 2 and 3 loadings of the synthetized microbeads a partial leaching of the material during the desorption step. Thus, one loading of PS microbeads was selected for further studies, since it is also simpler, faster and requires less reagents and material. Regarding concentration, whether in the case of 1 mL no saturation of the adsorption capacity of the sorbent phase is observed for any of the analytes, thus an increase in the recovery values is observed upon increasing the concentration, by increasing the volume to 5 mL, especially for methadone and tramadol, a decrease in recovery is observed, which is related to saturation of the sorption sites. Therefore, a volume of 5 mL of sample, which is the maximum sample allowed to be simultaneously loaded by the capacity of the syringe, was selected for further studies, so that improved recoveries are obtained. Taking into account the saturation observed for certain analytes at concentrations above 100 μg L^{-1}, a concentration of 50 μg L^{-1} was selected for the studies of the influence of the next variables.

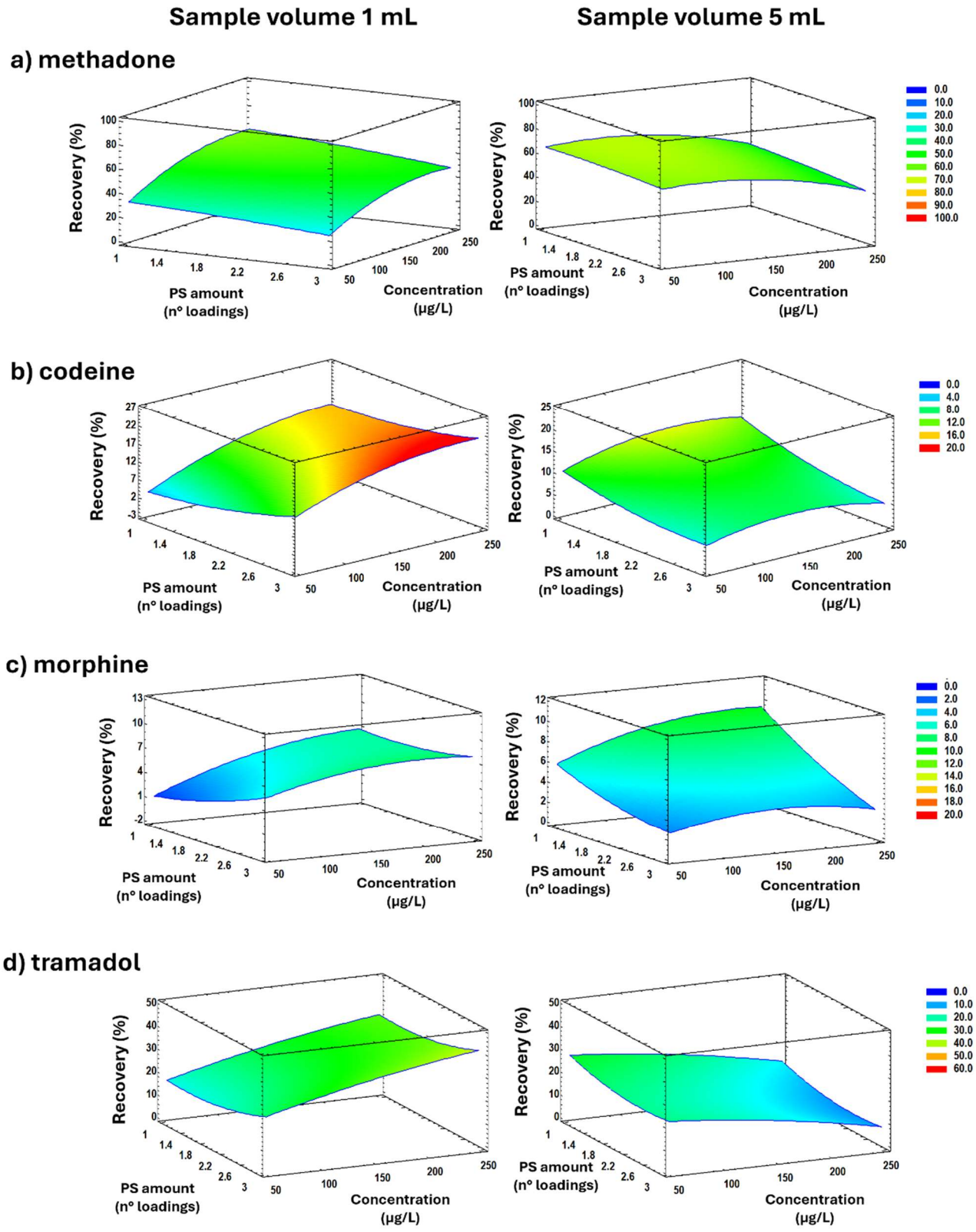

Fig. 3 Response surface plots of the recoveries obtained for the four analytes, i.e., (a) methadone, (b) codeine, (c) morphine and (d) tramadol, showing the interaction of analyte concentration and PS amount at a fixed sample volume (1 and 5 mL).

Once defined the conditions for further studies, the extraction procedure was optimized in terms of pH and ionic strength of the loaded sample by using aqueous standards. The pH of the sample defines the ionization form of the analytes, which are basic substances (pKa in the range from 8.2 to 9.2), cationic at physiological and environmental conditions. As shown in **Fig. 4a**, the extraction of the analytes is favoured at intermediate pH values. The pH of the sample without pH adjustment is around 8.3, and the use of internal standard within the samples would compensate possible fluctuations in the pH of the sample, thus, no pH adjustment of the sample was selected for further studies. On the other hand, ionic strength has not a relevant influence on the extraction yields of the selected analytes. The analyses were conducted without correcting the solution with acidic or basic additives, operating at uncontrolled pH (~ 8.7). The results (**Fig. 4b**) show a decrease of the extraction performances for conductance values higher than 40 mMHO (corresponding to NaCl concentrations higher than 0.25 %). This evidence may be ascribed to an increase of viscosity of the loaded sample, that has an adverse effect on the wettability and permeability of the adsorbent. For simplicity, the ionic strength of the sample was not adjusted before extraction, as already commented in the case of pH, the use of an internal standard minimizes and corrects the effect of ionic strength, avoiding the strict control of this parameter.

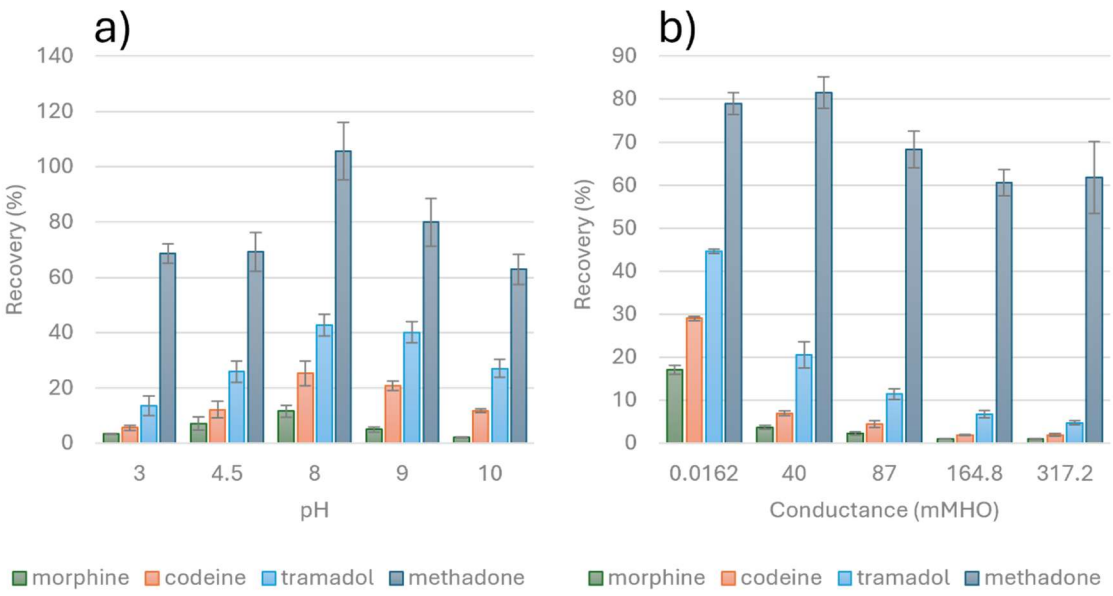

Fig. 4 Effect of pH and ionic strength expressed as conductance of aqueous solutions containing different amounts of NaCl on the recovery (%) obtained for the target analytes. Studies performed on MilliQ water spiked at a fixed concentration of 50 µg L^{-1} for each analyte. For ionic strength evaluation no pH adjustment was carried out.

Last investigated parameters were those related to the elution conditions, i.e., both the nature and volume of the eluent phase. First of all, three different eluents have been tested, namely pure methanol and with the addition of acidic (1 % v/v of formic acid) or basic (1 % v/v of ammonia) modifiers. As it can be seen in **Fig. 5a**, analytes recoveries are only slightly influenced by the addition of pH modifiers. For this reason, pure methanol was chosen as the eluent phase. Eluent phase volume was studied in the range 200–500 µL (**Fig. 5b**). At higher volume there is an increase in the recovery, allowing a better contact of the eluent with the sorbent and a more effective elution of the analytes, while an improvement in precision was also observed. Higher volumes were not evaluated, since the improvement as regards 400 µL was not high and to prevent further dilution of the extract. Thus, 500 µL was selected as the eluent volume for the subsequent validation protocol.

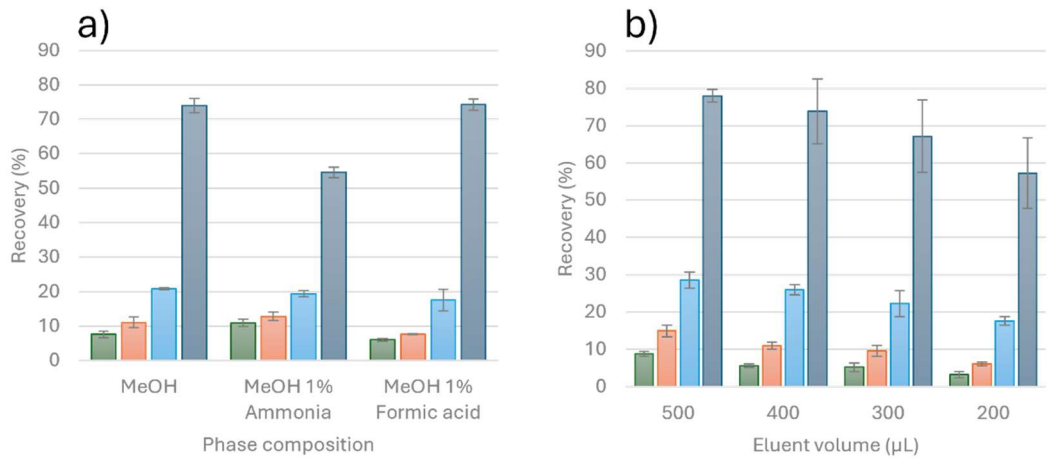

Fig. 5 Results for the optimization of (a) the composition and (b) volume of the eluent phase (solvent pure methanol). Experiments were conducted on MilliQ water spiked at a fixed concentration of 50 µg L^{-1} for each analyte and performing the entire adsorption step at the previous optimized conditions.

3.4. Analytical features of the method

The analytical figures of merit of the method were evaluated. **Table 1** summarizes the values obtained in the validation. Matrix matched calibration curves were prepared for all the analytes in three different real matrices, i.e., pooled saliva and urine samples and environmental water. To control the whole procedure, from the extraction to the direct injection, internal standards (i.e., d3-methadone, d6-morphine, d3-codeine) have been used. For tramadol, d3-methadone proved to be a good internal standard and for this reason it was used to normalize its analytical signal. Sample solutions were spiked prior extraction with the analytes at six different concentration levels and a fixed concentration of IS of 20 µg L^{-1} and were submitted to the entire analytical procedure. Calibration curves were built by plotting the peak area of each analyte divided by the area of the internal standard versus the concentration (**Fig. B4**). The determination coefficients R^2 were found to be higher than 0.99, showing a good linear correlation in the dynamic range from the limit of quantification (LOQ) to 100 µg L^{-1}. In **Fig. B4**, linear models obtained with saliva, urine and water matrices are shown along with the ones obtained in ultrapure water. Limit of detection (LOD) was calculated as the analyte concentration capable of providing a signal 3 times higher than the background noise (S = 3·N). Likewise, LOQ was calculated as the concentration generating a signal 10 times higher than the background noise (S = 10·N), responsible for precision and accuracy values below 20 %. LODs were

below 2.7 μg L^{-1} for saliva matrix and 1.9 μg L^{-1} in environmental water, with LOQs below 9.1 and 6.5 μg L^{-1}, respectively. Precision and accuracy were estimated at the three different levels of fortification, performing five replicates at each level. The precision was expressed in terms of relative standard deviation (RSD %). As can be seen in **Table 1**, all RSD values were lower than 15 %, which is in agreement with the FDA criteria [46]. The accuracy was evaluated via the relative recovery, calculated as follows:

$$R\% = \frac{C_{measured} - C_{spiked}}{C_{spiked}} x100$$

in this case, $C_{measured}$ was calculated by interpolating the average of the chromatographic areas, obtained at each spike level, in the matrix-matched calibration line. C_{spiked} is the known level of fortification of the specific spiking level. The accuracies obtained were in the range 85.2-118.2 %. In the case of urine matrix, detection sensitivity of codeine and morphine did not allow to build linear model for these two analytes in the concentration range below 100 μg L^{-1}. Matrix match calibration curves are provided for tramadol and methadone (**Fig. B4**). LOD and LOQ in this matrix were calculated in the same way, leading to higher values with respect to the saliva and aqueous samples. Urine is a complex matrix due to the occurrence of a vast number of small weight molecules (more than 3000 compounds), which are responsible for suppression of the ESI ionization of analytes [47], leading to a decline of the analyte's sensibility. To evaluate the extent of interference signal suppression on the studied analytes, a matrix effect study was conducted across all matrices by comparing the slopes of standard models with those of matrix-matched curves. A high matrix effect was observed for tramadol in urine, highlighting the complexity of this sample. In contrast, all other cases showed acceptable values ranging between 74 % and 116 %. The sensitivity ratio, expressed as a percentage, is detailed in **Table 1**. Selected fortification levels for the evaluation of accuracy and precision are chosen to cover the designated concentration range: 20, 50 and 100 μg L^{-1}.

Table 1 Figures of merit of the 4 opioids analysed in spiked samples of saliva, environmental water and urine. Precision and accuracy are reported at all tested concentration levels (i.e., 10 µg L^{-1}, 50 µg L^{-1} and 100 µg L^{-1}).

Analyte	LOD (µg L^{-1})	LOQ (µg L^{-1})	R^2	Matrix effect (%)	Linear range (µg L^{-1})	RSD intra-day, n=5 (%)			Accuracy (% relative recovery, n=5)		
						10 µg L^{-1} [(a)]	50 µg L^{-1}	100 µg L^{-1}	10 µg L^{-1} [(a)]	50 µg L^{-1}	100 µg L^{-1}
Saliva											
Methadone	0.0064	0.021	0.997	93	LOQ-100	4.6	2.5	4.2	89.9	97.1	101.4
Morphine	2.7	9.1	0.991	97		13.6	12.4	10.2	108.3	93.8	95.1
Codeine	1.8	5.9	0.996	94		12.3	2.8	11.3	99.7	105.9	104.7
Tramadol	0.92	3.1	0.989	116		14.7	14.9	4.7	108.6	90.9	105.7
Environmental water											
Methadone	0.012	0.04	0.999	97	LOQ-100	3.5	1.7	2.9	100.7	102.7	99.6
Morphine	1.7	5.6	0.998	102		11.0	8.2	10.6	104.2	96.5	94.2
Codeine	1.9	6.5	0.999	93		11.8	8.7	4.0	95.4	103.2	101.1
Tramadol	0.03	0.1	0.994	74		9.4	8.3	9.0	85.2	95.1	114.3
Urine											
Methadone	0.7	2.4	0.999	98	LOQ-100	3.53	1.20	4.64	103.4	96.1	101.5
Tramadol	4.3	14.5	0.998	33		11.9	12.5	14.9	118.2	108.2	104.7

[(a)] For urine matrix, the lower concentration value to assess the precision and accuracy of the method was 20 µg L^{-1}

3.5. Comparison with previously reported methods

Table B3 provides a comparative overview of the performance of the proposed method against various other approaches commonly used for analysing opioids in biological fluids. The analytical figures of merit achieved with our method align closely with those reported in the literature, with LOQs for individual analytes ranging from 0.02 to 14.5 μg L^{-1}. Our method presents two significant advantages. First, it offers a notably rapid extraction and analysis process, as it bypasses the need for chromatographic separation, substantially reducing total processing time. Second, it incorporates an environmentally conscious approach by utilizing a sorbent material sourced from recycled waste, eliminating the need for newly produced extraction materials. These benefits make the method both time-efficient and sustainable, providing a practical and eco-friendly alternative for opioid detection in biological samples. On the other hand, a more exhaustive sample pretreatment would be needed in the case of urine matrix in order to be able to determine the four analytes with similar sensitivity as in saliva or water. In recent years, growing awareness of environmental sustainability has underscored the need for precise and reliable metrics to assess the "greenness" of chemical processes. In this context, two prominent methodologies are Sample Preparation Metric of Sustainability (SPMS) [48] and Analytical Greenness Metric for Sample Preparation (AGREEprep) [49]. The sustainability of the in-syringe-PS-P microextraction was assessed using both these green metrics. SPMS is highly specifical to the evaluation of sample preparation. The final graphic output is a clock-like diagram, as shown in **Fig. B5a**, which illustrates the greenness scores for key sample preparation parameters, along with an overall score. For the presented microextraction method, the total SPMS score was 7.26 out of 10. Additionally, the AGREEprep tool was applied in this study. AGREEprep uses a similar color-coding scheme as SPMS but evaluates both sample preparation and the broader analytical process. The diagram resulting from the application of this green metric is displayed in **Fig. B5b** of the Appendix B. For the microextraction at issue, the AGREEprep total score was 0.56 out of 1. The score obtained with such a metric is generally lower compared to SPMS, since it takes into account

all the analytical procedure, from the synthetic to the final analysis step. The off-line extraction procedure, the energy-intensive instrumental technique and the lack of integrated and automated steps strongly penalised the final score. Otherwise, both metrics do not account for the origin of the synthetized device, which has been prepare from waste sources, being part of a recycling cycle, potentially endless. To assess the sustainability of the entire analytical process (from material synthesis to instrumental analysis, including the applied extraction strategy) a greenness evaluation tool that comprehensively considers all methodological steps was applied. For this purpose, advanced metrics such as ComplexGAPI [50] and the more recent ComplexMoGAPI [51] provide an assessment system that evaluates all features and characteristics of the analytical method, ultimately yielding a score representative of the process's overall sustainability. Considering the reagents used, the energy demand of the synthesis process, the recycling potential, and the complete environmental and operator safety of the method, the analytical workflow presented here achieved a score of 84 according to the ComplexMoGAPI principles (**Fig. B5c**). This result confirms the development of a procedure that successfully combines analytical efficiency, plastic waste recycling, and sustainability.

3.6. Synthetic procedure greenness assessment

The emulsion solidification technique, as developed, utilizes green solvents, environmentally friendly processes, and minimizes energy and material waste. To assess the sustainability and recycling benefits of this approach, the procedure was analysed using various evaluation tools and compared with other techniques employing commercial materials. For polystyrene recycling, this study proposes dissolving shredded yogurt container fragments in ethyl acetate. Previous research has explored different solvent compositions for PS recycling, including green and low-environmental-impact options such as D-limonene, p-cymene, terpinene, phellandrene, and ethyl acetate [4, 13, 14]. Ethyl acetate was selected due to its high greenness score (6.7) according to GSK's solvent sustainability guide [52] and its ability to form a microemulsion with water under salting-out conditions. Other proposed green solvents were unsuitable due to excessive viscosity or immiscibility

with water under standard conditions. In terms of energy efficiency, the synthesis process requires only brief stirring (less than 1 min per batch) with an energy demand of under 500 J. The deposition step onto the paper disk is performed using a hydraulic vacuum pump, which operates without additional energy consumption. The primary energy-intensive step is thermal curing, requiring approximately 900 kJ; however, this process can be conducted on multiple devices simultaneously, significantly reducing the energy demand per unit. From a health and safety perspective, all reagents involved in the material synthesis process (ethyl acetate, sodium chloride, and water) have a National Fire Protection Association (NFPA) flammability and health hazard rating of ≤ 1, with the exception of sodium dodecyl sulphate and ethanol, which have respective ratings of 2 and 3 according to the same classification system. These reagents are essential for the successful implementation of the emulsion solidification technique. Ongoing studies within our research group are actively exploring safer alternatives to further enhance the environmental sustainability of the synthetic procedure. The total waste generated per synthetic procedure is less than 10 mL, while the preparation of the extraction device (paper-supported polystyrene microspheres) results in an Environmental (E) factor of approximately 10. All the aforementioned aspects contribute to the overall greenness assessment of the synthetic and extraction procedure, as evaluated by the ComplexMoGAPI scoring system [51]. This software, developed in 2024, integrates the sustainability assessment of the extraction process with an evaluation of the impact of pre-extraction procedures (in this case, the preparation of the extraction device) on both the operator and the environment. The final rating (84 for the current method), which reflects the entire analytical workflow, confirms the environmental benefits of the proposed method, albeit without accounting for the recycled origin of the device itself. For comparative purposes, the solid-phase extraction (SPE)-based and dispersive liquid-liquid microextraction (DLLME) methods proposed by Clivillé-Cabré et al. [53] have been considered as reference techniques for the extraction of opioids from urine. Regarding the extraction procedure, both methods require a significant use of reagents and solvents, leading to a greater generation of procedural waste. Specifically, the SPE-based method necessitates over 28 mL of solvents per

extraction. Although the DLLME method is less solvent-intensive, it still requires additional extraction steps, such as vortex shaking and solvent evaporation. Furthermore, the method presented in this study introduces the reuse of end-of-life materials as an extraction support, aligning with a circular approach to production and consumption.

4. Conclusion

A polystyrene modified paper device from a recycled waste source has been developed in this work for the microextraction of opioids. Recycling plays a pivotal role in contemporary research, where efforts are focused on creating innovative applications for end-of-life materials and integrating them into a positive, sustainable cycle of reuse. Thus, a main advantage of this analytical method lies in the use of recycled polystyrene as a sorbent material, allowing for the valorization of common plastic waste. The recycling process yielded a final material with an extensive surface area, optimizing the retention capabilities of the polymer and making it ideal for efficient analyte capture. However, a key limitation is the challenging industrial scalability of the polystyrene microbead synthesis and the manual assembly of the extraction device, which currently restrict its application to the laboratory scale. The extraction process employs an in-syringe methodology that is not only straightforward to execute but also promotes a rapid and effective workflow. In order to reduce analyte loss and limit sample handling, the design incorporates a linear and consecutive operational sequence that allows all procedural steps to take place within the syringe body itself. This setup not only ensures high reproducibility but also simplifies the user handling. The entire extraction process is completed in less than 5 min, making it a highly time-efficient approach. The retention performance achieved by combining the cellulosic substrate with polystyrene microspheres ensures a broad-spectrum extraction capability across a diverse range of analytes, varying in chemical moieties and polarities (with logP from 0.8 to 3.9). The extraction procedure and analytical method is cost-effective and user friendly, suitable for employment in an in-situ analysis. The performance of the device, characterized by high recoveries, precision, and accuracy, demonstrates its reliability and robustness. Furthermore,

its environmental sustainability was evaluated using established green metrics, specifically SPMS and AGREEprep, both of which highlighted the method's alignment with green chemistry principles. The results confirm this approach as a viable, environmentally sustainable alternative to more traditional extraction techniques, providing comparable analytical performance with a significantly reduced ecological impact.

References

[1] Maharana, T., Negi, Y. S., Mohanty, B. (2007). Recycling of polystyrene. Polym.-Plast. Technol. Mater., 46(7), 729–736. https://doi.org/10.1080/03602550701273963

[2] Thakur, S., Verma, A., Sharma, B., Chaudhary, J., Tamulevicius, S., Thakur, V. K. (2018). Recent developments in recycling of polystyrene based plastics. Curr. Opin. Green Sustain. Chem., 13, 32–38. https://doi.org/10.1016/j.cogsc.2018.03.011

[3] Achilias, D. S., Giannoulis, A., Papageorgiou, G. Z. (2009). Recycling of polymers from plastic packaging materials using the dissolution–reprecipitation technique. Polym. Bull., 63, 449–465. https://doi.org/10.1007/s00289-009-0104-5

[4] Cella, R. F., Mumbach, G. D., Andrade, K. L., Oliveira, P., Marangoni, C., Bolzan, A., Machado, R. A. F. (2018). Polystyrene recycling processes by dissolution in ethyl acetate. J. Appl. Polym. Sci., 135(18), 46208. https://doi.org/10.1002/app.46208

[5] Huang, Z., Shanmugam, M., Liu, Z., Brookfield, A., Bennett, E. L., Guan, R., Xiao, J. (2022). Chemical recycling of polystyrene to valuable chemicals via selective acid-catalyzed aerobic oxidation under visible light. J. Am. Chem. Soc., 144(14), 6532–6542. https://doi.org/10.1021/jacs.2c01410

[6] Zhang, Z., Hirose, T., Nishio, S., Morioka, Y., Azuma, N., Ueno, A., Okada, M. (1995). Chemical recycling of waste polystyrene into styrene over solid acids and bases. Ind. Eng. Chem. Res., 34(12), 4514–4519. https://doi.org/10.1021/ie00039a044

[7] Abdel-Raouf, M. E. S., Abdel-Raheim, A. R. M., El-Saeed, S. M. (2013). Thermo-catalytic versus thermo-chemical recycling of polystyrene waste. Waste Biomass Valoriz., 4, 37–46. https://doi.org/10.1007/s12649-012-9136-4

[8] Lettieri, P., Al-Salem, S. M. (2011). Thermochemical treatment of plastic solid waste. In Waste (pp. 233–242). Academic Press. https://doi.org/10.1016/B978-0-12-381475-3.10017-8

[9] Marquez, C., Martin, C., Linares, N., De Vos, D. (2023). Catalytic routes towards polystyrene recycling. Mater. Horiz., 10(5), 1625–1640. https://doi.org/10.1039/D2MH01215D

[10] Mumbach, G. D., Bolzan, A., Machado, R. A. F. (2020). A closed-loop process design for recycling expanded polystyrene waste by dissolution and polymerization. Polymer, 209, 122940. https://doi.org/10.1016/j.polymer.2020.122940

[11] Chaudhary, A., Dave, M., Upadhyay, D. S. (2022). Value-added products from waste plastics using dissolution technique. Mater. Today, 57, 1730–1737. https://doi.org/10.1016/j.matpr.2021.12.363

[12] García, M. T., De Lucas, A., Gracia, I., Rodríguez, J. F. (2008). Expanded polystyrene wastes recycling by using natural solvents and supercritical CO_2 for solvent recovery. In Proc. REWAS 2008, 1821–1827.

[13] García, M. T., Gracia, I., Duque, G., De Lucas, A., Rodríguez, J. F. (2009). Study of the solubility and stability of polystyrene wastes in a dissolution recycling process. Waste Manag., 29(6), 1814–1818. https://doi.org/10.1016/j.wasman.2009.01.001

[14] García, M. T., Duque, G., Gracia, I., De Lucas, A., Rodríguez, J. F. (2009). Recycling extruded polystyrene by dissolution with suitable solvents. J. Mater. Cycles Waste Manag., 11, 2–5. https://doi.org/10.1007/s10163-008-0210-8

[15] Hattori, K., Naito, S., Yamauchi, K., Nakatani, H., Yoshida, T., Saito, S., Miyakoshi, T. (2008). Solubilization of polystyrene into monoterpenes. Adv. Polym. Technol., 27(1), 35–39. https://doi.org/10.1002/adv.20115

[16] Noguchi, T., Miyashita, M., Inagaki, Y., Watanabe, H. (1998). A new recycling system for expanded polystyrene using a natural solvent. Part 1. Packag. Technol. Sci., 11(1), 19–27.

[17] Noguchi, T., Inagaki, Y., Miyashita, M., Watanabe, H. (1998). A new recycling system for expanded polystyrene using a natural solvent. Part 2. Packag. Technol. Sci., 11(1), 29–37.

[18] Antonelli, L., Frondaroli, M. C., De Cesaris, M. G., Felli, N., Dal Bosco, C., Lucci, E., Gentili, A. (2024). Nanocomposite microbeads made of recycled polylactic acid for the magnetic solid phase extraction of xenobiotics from human urine. Microchim. Acta, 191(5), 1–14. https://doi.org/10.1007/s00604-024-06335-y

[19] De Cesaris, M. G., Felli, N., Antonelli, L., Francolini, I., D'Orazio, G., Dal Bosco, C., Gentili, A. (2024). Recovery of cellulose acetate bioplastic from cigarette butts: realization of a sustainable sorbent for water remediation. Sci. Total Environ., 929, 172677. https://doi.org/10.1016/j.scitotenv.2024.172677

[20] Amini, S., Ebrahimzadeh, H., Seidi, S., Jalilian, N. (2021). Preparation of polyacrylonitrile/Ni-MOF electrospun nanofiber as an efficient fiber coating material for headspace solid-phase microextraction. Food Chem., 350, 129242. https://doi.org/10.1016/j.foodchem.2021.129242

[21] Zarabi, S., Heydari, R., Mohammadi, S. Z. (2021). Dispersive micro-solid phase extraction in micro-channel. Microchem. J., 170, 106676. https://doi.org/10.1016/j.microc.2021.106676

[22] Khiltash, S., Heydari, R., Ramezani, M. (2023). Graphene oxide/polydopamine–polyacrylamide nanocomposite as a sorbent for dispersive micro-solid phase extraction. J. Environ. Anal. Chem., 103(19), 7431–7446. https://doi.org/10.1080/03067319.2021.1971211

[23] Millán-Santiago, J., Lucena, R., Cárdenas, S. (2024). Pipette tip-electrospray mass spectrometry for determining opioids in urine. Adv. Sample Prep., 11, 100118. https://doi.org/10.1016/j.sampre.2024.100118

[24] Abdel-Rehim, M., Skansen, P., Vita, M., Hassan, Z., Blomberg, L., Hassan, M. (2005). Microextraction in packed syringe coupled to LC–ESI–MS/MS. Anal. Chim. Acta, 539, 35–39. https://doi.org/10.1016/j.aca.2005.02.061

[25] Abdel-Rehim, M., Andersson, A., Breitholtz-Emanuelsson, A., Sandberg-Ställ, M., Brunfelter, K., Pettersson, K. J., Norsten-Höög, C., 2008. MEPS as a rapid sample preparation method to handle unstable compounds in a complex matrix: determination of AZD3409 in plasma samples utilizing MEPS-LC-MS-MS. J. Chromatogr. Sci., 46(6), 518-523. https://doi.org/10.1093/chromsci/46.6.518

[26] Abdel-Rehim, M., Hassan, Z., Skansem, P., Hassan, M., 2007. Simultaneous determination of busulphan in plasma samples by liquid chromatography-electrospray ionization mass spectrometry utilizing microextraction in packed syringe (MEPS) as on-line sample preparation method. J. Liq. Chromatogr. Relat. Technol., 30(20), 3029-3041. https://doi.org/10.1080/10826070701632337

[27] Altun, Z., Blomberg, L. G., Jagerdeo, E., Abdel-Rehim, M. (2006). Drug screening using microextraction in a packed syringe. J. Liq. Chromatogr. Relat. Technol., 29(6), 829–839. https://doi.org/10.1080/10826070500530526

[28] Bekri-Abbes, I., Bayoudh, S., Baklouti, M. (2006). Converting waste polystyrene into adsorbent. J. Environ. Polym. Degrad., 14(3), 249–256. https://doi.org/10.1007/s10924-006-0018-3

[29] El-Beqqali, A., Kussak, A., Blomberg, L., Abdel-Rehim, M. (2007). Microextraction in packed syringe for beta-blockers. J. Liq. Chromatogr. Relat. Technol., 30(4), 575–586. https://doi.org/10.1080/10826070601093895

[30] Ali, J., Tuzen, M., Kazi, T. G., Hazer, B. (2016). Inorganic arsenic speciation using syringe-based microextraction. Talanta, 161, 450–458. https://doi.org/10.1016/j.talanta.2016.08.075

[31] Benedé, J. L., Chisvert, A., Lucena, R., Cárdenas, S. (2021). Paper-based polystyrene/nylon Janus platform for microextraction. Microchim. Acta, 188, 1–12. https://doi.org/10.1007/s00604-021-05047-x

[32] Hamdona, S. K., Tadros, H. R., Mabrouk, D. M., Refaat, H. M. (2022). Removal of pollutants using waste polystyrene. Int. J. Sci. Res., 12, 67–75.

[33] Li, J., Zheng, Y., Mi, W., Muyizere, T., Zhang, Z. (2018). Polystyrene-impregnated paper substrates for direct mass spectrometric analysis. Anal. Methods, 10(24), 2803–2811. https://doi.org/10.1039/C8AY01081A

[34] Liu, Y., Hou, S., Chen, T., Li, Y., Zhang, M., Zhou, D., Xu, H. (2023). Micro-matrix cartridge extraction using polystyrene nanofibers. Microchim. Acta, 190, 138. https://doi.org/10.1007/s00604-023-05714-1

[35] Matin, P., Ayazi, Z., Jamshidi-Ghaleh, K. (2022). Montmorillonite reinforced polystyrene nanocomposite supported on cellulose. J. Environ. Anal. Chem., 102(17), 5150–5165. https://doi.org/10.1080/03067319.2020.1791333

[36] Pautova, A. K., Sobolev, P. D., Revelsky, A. I. (2020). Microextraction of aromatic microbial metabolites by hypercrosslinked polystyrene. J. Pharm. Biomed. Anal., 177, 112883. https://doi.org/10.1016/j.jpba.2019.112883

[37] Shevchenko, N., Pankova, G., Iakobson, O., Abiev, R., Svetlov, S., Ilin, N. (2020). Microfluidic synthesis of porous polystyrene microspheres. J. Microencapsul., 37(6), 457–465. https://doi.org/10.1080/02652048.2020.1785027

[38] Ullah, N., Hazer, B., Tuzen, M., Saleh, T. A. (2024). Syringe-based microextraction using functionalized polystyrene. J. Mol. Liq., 394, 123703. https://doi.org/10.1016/j.molliq.2023.123703

[39] Vita, M., Skansen, P., Hassan, M., Abdel-Rehim, M. (2005). LC–MS/MS determination using on-line sample preparation. J. Chromatogr. B, 817(2), 303–307. https://doi.org/10.1016/j.jchromb.2004.12.022

[40] Wilton, N., Lyon-Marion, B. A., Kamath, R., McVey, K., Pennell, K. D., Robbat Jr., A. (2018). Remediation of hydrocarbon impacted soil using polystyrene foam beads. J. Hazard. Mater., 349, 153–159. https://doi.org/10.1016/j.jhazmat.2018.01.041

[41] Martins, T. R., Costa, P. S., Bertuol, D. A., Aguiar, M. L., Tanabe, E. H. (2022). Recycled expanded polystyrene nanofibers for metal removal. Metals, 12(8), 1334. https://doi.org/10.3390/met12081334

[42] Shin, C., Chase, G. G. (2005). Nanofibers from recycled expanded polystyrene using natural solvent. Polym. Bull., 55, 209–215. https://doi.org/10.1007/s00289-005-0421-2

[43] Ghambari, H., Reyes-Gallardo, E. M., Lucena, R., Saraji, M., Cárdenas, S. (2017). Recycling polymer residues to synthesize magnetic nanocomposites for dispersive micro-solid phase extraction. Talanta, 170, 451–456. https://doi.org/10.1016/j.talanta.2017.04.026

[44] Faravelli, T., Pinciroli, M., Pisano, F., Bozzano, G., Dente, M., Ranzi, E., 2001. Thermal degradation of polystyrene. J. Anal. Appl. Pyrolysis., 60(1), 103-121. https://doi.org/10.1016/S0165-2370(00)00159-5

[45] Cortés-Arriagada, D., Miranda-Rojas, S., Camarada, M. B., Ortega, D. E., & Alarcón-Palacio, V. B. (2023). The interaction mechanism of polystyrene microplastics with pharmaceuticals and personal care products. Science of the Total Environment, 861, 160632. https://doi.org/10.1016/j.scitotenv.2022.160632

[46] Fda, U. S. 2018. Bioanalytical method validation guidance for industry. US Department of Health and Human Services Food and Drug Administration Center for Drug Evaluation and Research and Center for Veterinary Medicine. https://www.fda.gov/regulatory-information/search-fda-guidance-documents/bioanalytical-method-validation-guidance-industry. Accessed 7 Jan 2024.

[47] Gosetti, F., Mazzucco, E., Zampieri, D., Gennaro, M. C., 2010. Signal suppression/enhancement in high-performance liquid chromatography tandem mass spectrometry. J. Chromatogr. A, 1217(25), 3929-3937. https://doi.org/10.1016/j.chroma.2009.11.060

[48] González-Martín, R., Gutiérrez-Serpa, A., Pino, V., Sajid, M., 2023. A tool to assess analytical sample preparation procedures: Sample preparation metric of sustainability. J. Chromatogr A, 1707, 464291. https://doi.org/10.1016/j.chroma.2023.464291

[49] Wojnowski, W., Tobiszewski, M., Pena-Pereira, F., Psillakis, E. 2022. AGREEprep–analytical greenness metric for sample preparation. TrAC, Trends Anal. Chem., 149, 116553. https://doi.org/10.1016/j.trac.2022.116553

[50] Płotka-Wasylka, J., Wojnowski, W., 2021. Complementary green analytical procedure index (ComplexGAPI) and software. Green Chem., 23(21), 8657-8665. https://doi.org/10.1039/D1GC02318G

[51] Mansour, F. R., Omer, K. M., Płotka-Wasylka, J., 2024. A total scoring system and software for complex modified GAPI (ComplexMoGAPI) application in the assessment of method greenness. Green Anal. Chem., 10, 100126. https://doi.org/10.1016/j.greeac.2024.100126

[52] Alder, C. M., Hayler, J. D., Henderson, R. K., Redman, A. M., Shukla, L., Shuster, L. E., Sneddon, H. F., 2016. Updating and further expanding GSK's solvent sustainability guide. Green Chem., 18(13), 3879-3890. https://doi.org/10.1039/C6GC00611F

[53] Clivillé-Cabré, P., Rosendo, L. M., Borrull, F., Aguilar, C., Calull, M., 2025. A comparative study of SPE- and DLLME-based methods for the determination of opioids and benzodiazepines in urine samples using LC–MS/MS. Microchem. J., 208, 112354. https://doi.org/10.1016/j.microc.2024.112354

Paper III: Polystyrene post-synthesis functionalization

L. Antonelli, Á. I. López-Lorente, A. Gentili, R. Lucena, S. Cárdenas (2026). **Sulfonated polystyrene nanospheres from waste sources for the extraction of sulfonamide antibiotics from complex matrices.** *Under submission*

Graphical abstract

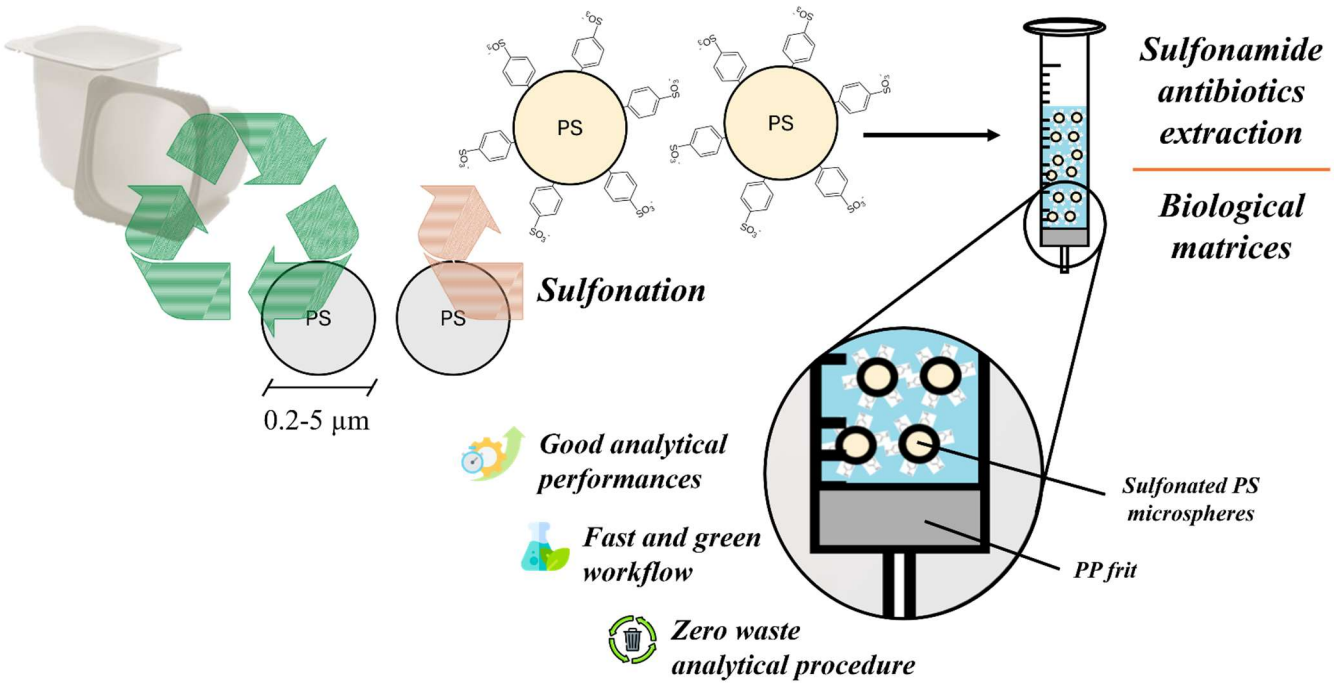

Abstract

Sulfonamides are synthetic antimicrobial agents whose intensive use has raised significant environmental concerns related to their persistence, bioaccumulation, and potential endocrine-disrupting effects, entering ecosystems through agricultural runoff and municipal wastewater. This study introduces a next-generation sorbent phase based on recycled polystyrene microspheres sulfonated with sulfuric acid, thereby imparting both hydrophobic and cation-exchange functionalities, successfully applied to the extraction of four representative sulfonamides (i.e., sulfanilamide, sulfaguanidine, sulfadiazine, and sulfamerazine) in biological matrices. The variables related to the sulfonation process and those affecting the extraction process have been evaluated. The in-syringe dispersive micro solid-phase extraction method coupled to liquid chromatography-tandem mass spectrometry provided limit of detections of 0.8 μg L^{-1} for sulfaguanidine in urine to 32 μg L^{-1} for sulfanilamide in saliva. The precision, expressed as relative standard deviation has been evaluated at four concentration levels both intra-day and inter-day, being lower than 18.3 and 14.3% at the lower limit of detection (LLOQ), respectively. The accuracy, calculated with spiked urine and saliva samples and expressed as relative recovery, ranged from 86.4 to 108.5%. This strategy integrates sustainable waste recovery with the development of a high-performance, low-impact adsorbent, employing recycled materials (such as syringes and frits) to create a nearly zero-waste extraction system. This combination of recycling, analytical performance, and sustainability supports the evolution of environmental analysis toward a “white circular” model, seamlessly merging Green Science with robust analytical standards.

Keywords: Plastic waste upcycling, Sulfonamides antibiotics, Polystyrene sulfonated microspheres, Zero waste extraction, In-syringe dispersive-SPE

1. Introduction

Sulfonamide antibiotics are a class of synthetic antimicrobial agents characterized by the presence of a sulfonamide functional group. These compounds act as competitive inhibitors of dihydropteroate synthase, an enzyme responsible for a key step in folic acid biosynthesis [1]. Folic acid is an essential precursor for DNA and RNA synthesis and plays a crucial role in several biochemical pathways associated with cellular proliferation [2]. By disrupting folic acid production, sulfonamides exert a bacteriostatic effect against a broad spectrum of Gram-positive and Gram-negative bacteria.

The affordability of their synthetic routes and the well-established understanding of their pharmacokinetics have contributed to the widespread use of sulfonamides in both human and veterinary medicine [3]. According to the 2022 ESVAC report published by the European Medicines Agency, sulfonamides rank as the third most widely traded class of veterinary medicinal products [4]. However, their extensive application has raised significant concerns due to their persistence, bioaccumulation potential, and capacity to act as endocrine disruptors [5]. Agricultural runoff and municipal wastewater effluents serve as major pathways for their introduction into aquatic and terrestrial ecosystems. Excreted primarily in their native form or as acetylated derivatives, sulfonamides undergo microbial deacetylation, restoring them to their active parent compounds [6]. While a few degradation pathways for sulfonamide derivatives have been reported [7], a comprehensive overview of their transformation products remains lacking.

Given the environmental and health risks associated with sulfonamide contamination, the development of innovative analytical methods and next-generation materials capable of extracting these compounds from complex matrices is of paramount importance. In particular, sustainable and cost-effective analytical approaches are increasingly sought after. From a chemical perspective, sulfonamides exhibit low pKa values (see **Table C1** of the Appendix C), existing predominantly in their protonated form under physiological and environmental pH conditions [8, 9].

Solid-phase extraction (SPE) remains a well-established technique for the preconcentration of sulfonamide antibiotics, as demonstrated by the on-site extraction of seven target compounds using a 3D-printed device functionalized with Oasis MCX resin, followed by high-performance liquid chromatography with diode array detection (HPLC-DAD) analysis. This approach confirmed the persistence of sulfonamides such as sulfanilamide in environmental waters, with detection ranges between 0.6 and 6 $\mu g\ L^{-1}$ [10]. Dispersive techniques, such as liquid–liquid–liquid microextraction (LLLME), have also been applied for sulfonamide determination in water samples before and after wastewater treatment, achieving quantification limits as low as 0.22 $\mu g\ L^{-1}$ and highlighting the partial removal of these compounds during treatment processes [11]. Building on these traditional methods, several innovations have recently emerged, focusing on miniaturization, portability, and enhanced environmental sustainability. Notably, graphene nanoplatelet-packed pipette-tip micro-solid phase extraction (PT-μSPE) has been integrated with smartphone-based fluorescence detection for rapid screening of four sulfonamides, offering a low-cost, eco-friendly analytical platform with recoveries between 94% and 102% and detection limits below 3.1 $\mu g\ L^{-1}$ [12]. Electrochemical sensing has also gained attention: nitrogen-doped Cu-based metal–organic frameworks have shown excellent surface properties (~1184 m^2/g) and detection limits as low as 0.003 μM for sulfanilamide, supporting their application in fast, highly sensitive pollutant monitoring [13]. Polymeric adsorbents continue to offer competitive extraction performance, with magnetic polystyrene sulfonate sodium material developed for the selective removal of sulfonamides such as sulfamerazine and sulfafurazole, demonstrating high adsorption capacity and ease of magnetic recovery [14].

In this context, the present study explores, for the first time, the use of recycled waste polystyrene (PS) as a cost-effective and sustainable sorbent for the extraction of sulfonamide antibiotics from biological matrices. Waste-derived PS was solubilized in an organic solvent and subjected to an emulsion solidification process, yielding uniformly shaped microspheres [15]. The sulfonation of PS using concentrated sulfuric acid introduced sulfonate functional groups, imparting cation-exchange

properties to the material. Several sulfonation strategies for polystyrene have been reported in the literature, aiming to introduce sulfonate functionalities for enhanced adsorption and extraction capabilities. Traditional sulfonation protocols often employ concentrated sulfuric acid [16], but also acetyl sulfate [17, 18], sulfur trioxide [19] and silica sulfuric acid [20] have been reported as sulfonating agents. Due to the versatility of sulfonated PS derivatives in adsorption and analytical extraction, this material has been integrated into advanced microextraction platforms. For example, magnetic Fe_3O_4@PS microspheres prepared via suspension polymerization have shown efficient magnetic solid-phase extraction (MSPE) performance for food safety contaminants [21]. Composite materials incorporating sulfonated PS with carbon nanotubes have also been designed for PT-μSPE with effervescence-driven dispersion, targeting alkaloids and flavonoids in herbal matrices [22]. These examples support further exploration using recycled polystyrene waste; the present work presents the first synthetic approach that simultaneously achieves effective waste PS recycling and the development of a high-performance sorbent for sulfonamide extraction from real-world matrices.

A key innovation of this methodology is its commitment to a fully circular [23], waste-minimizing approach. The entire extraction system, ranging from the adsorbent material to the support components, relies exclusively on recycled materials. The polystyrene source, the syringe used for extraction, and the frit serving as the physical filter for the sulfonated PS microspheres are all derived from repurposed waste. This strategy represents one of the first extraction techniques to propose an integrated recycling model, achieving near-zero waste generation while maintaining high analytical performance.

2. Experimental section

2.1. Materials and reagents

All reagents were of analytical grade or better. Sulfadiazine, sulfamerazine, sulfanilamide, sulfaguanidine, sodium chloride and sodium dodecyl sulfate (SDS) were supplied by Sigma-Aldrich

(Madrid, Spain). Stock standard solutions were prepared in methanol (MeOH, Panreac, Barcelona, Spain) at a concentration of 1 mg mL^{-1} and stored at 4 °C in the dark. Working solutions were prepared by dilution of the stock in MeOH or Milli-Q water (Millipore Corp., Madrid, Spain), as required. Both the optimization study and the validation workflow have been performed with microspheres synthetized departing from waste polystyrene, coming from different commercial yogurt cups, pooled. Ethyl acetate, ethanol, sulfuric acid (95-98 %) ammonia (30 %) and formic acid (≥ 98 %) were purchased from Panreac.

2.2. Real samples

Saliva samples were collected by passive drooling from healthy volunteers, aged between 23 and 27 years, within our laboratory. All the collected blank samples have been pooled together and stored at 4 °C until analysis (within 3 days from the collection). Aliquots of the pooled saliva sample have been centrifuged, after pH regulation to 4.5 with formic acid (to ensure the entire elimination of precipitating proteins). The supernatant is withdrawn, eliminating the solid residue. The sample is diluted 1:1 (v/v) with MilliQ water to ensure a reproducible and complete dispersion of the sulfonated polystyrene (sPS) microspheres in the extraction media. The pH is checked once again to ensure that the extraction will be conducted at pH 4.5.

Similarly, blank urine samples were obtained from the same volunteers. They were pooled, subsampled (50 mL fractions) and stored in fridge (used within 3 days form the collection). The samples were 1:1 (v/v) diluted in MilliQ water and the pH adjusted at 4.5 with formic acid.

2.3. Preparation of PS microbeads and sulfonation procedure

This synthesis involves scaling up the procedure previously proposed by our group in an earlier publication [24]. A 2.5% (w/v) solution of grinded PS (sourced from pooled waste yogurt containers) in ethyl acetate was prepared, with dissolution facilitated by gentle magnetic stirring.

A 10 mL portion of this solution was transferred into a 200 mL glass bottle containing a magnetic stir bar. For the emulsion-solidification process, two aqueous solutions were separately prepared: one saturated with NaCl and another containing 1% (w/v) sodium dodecyl sulfate. These solutions were sequentially added to the glass bottle (20 mL of the NaCl solution followed by 50 mL of the SDS solution), forming a biphasic system, which was maintained as a microemulsion by magnetic stirring at 900 rpm.

To destabilize the emulsion and precipitate PS in the form of microbeads, 50 mL of absolute ethanol was rapidly added while the system was stirring. The resulting PS microbeads were collected by filtration using a circular glass fiber filter mounted on a vacuum pump, allowing the supernatant to gently flow through while retaining the dispersed microspheres on the filter surface. The microparticles were then sequentially washed with water and ethanol until the washing solvent appeared clear and free of foam. Finally, the PS microspheres were dried overnight at 45 °C.

Once dried, the material underwent a sulfonation process. Specifically, 500 mg of PS microspheres were weighed directly into a 50 mL conical flask, followed by the addition of 30 mL of concentrated sulfuric acid (95-98 %). The reaction was allowed to proceed under gentle magnetic stirring for a duration ranging from 1 to 16 hours, an interval optimized to balance performance and process time. This reaction, already documented in the literature [25], is illustrated in **Fig. C1**. Following sulfonation, the sPS microspheres were filtered using a glass fiber filter mounted on a vacuum pump to remove the reaction medium. The material was then sequentially washed with 10 mL of Milli-Q water, 10 mL of ethanol, and 10 mL of MeOH containing 1% ammonia (same composition of the eluent solution) to eliminate reaction by-products and equilibrate the sPS microspheres in its deprotonated form. Finally, the material was dried overnight in an oven at 45 °C, rendering it ready for application. The whole synthesis yield of the final material is almost 100 % (in terms of final weight of microbeads with respect to the weight of employed PS). **Fig. 1a** displays a scheme of the whole procedure.

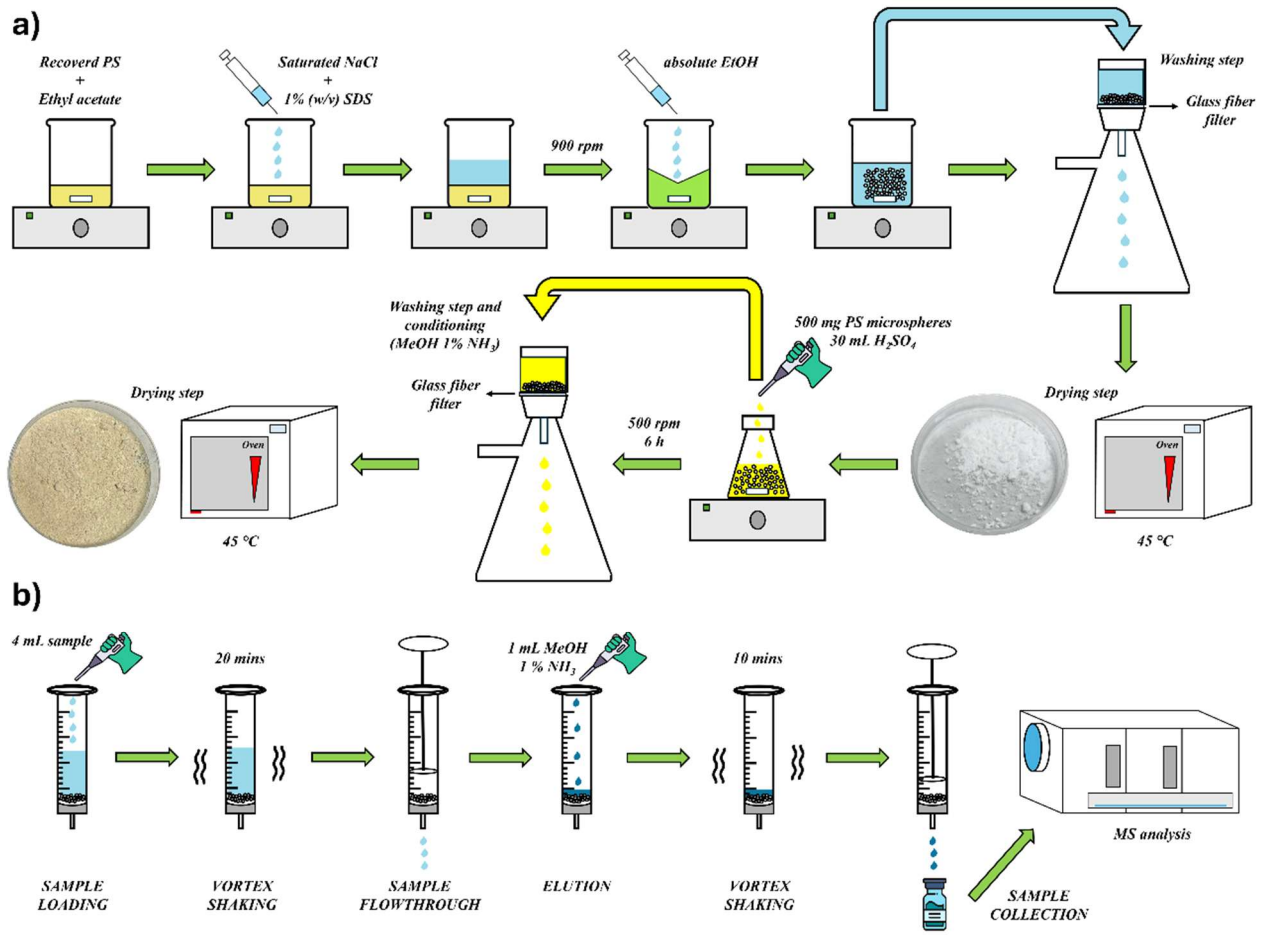

Fig. 1 Schematic representation of the synthetic route of the PS-P (**a**) and the analytical procedure for the microextraction and MS determination of the opioids (**b**).

2.4. Characterization of the sPS microspheres

sPS microbeads were studied after the synthesis by attenuated total reflection Fourier transformed infrared spectroscopy (ATR-FTIR), scanning electron microscopy (SEM) and energy-dispersive X-ray spectroscopy (EDX).

Microbeads, both before and after sulfonation process, were characterized in terms of dimensional and morphological properties via SEM using a JEOL JSM 7800F microscope (Akishima, Tokyo, Japan) available at the Central Service for Research Support of the University of Córdoba. Prior to scanning, all samples were coated with gold to make their surfaces conductive. Micrographs were collected at a magnification of 10000x. With the same instrumentation, via a specific detector for EDX, the material was analyzed in terms of chemical composition and elemental distribution.

ATR-FTIR spectra were collected by using a Thermo Fisher Nicolet Apex FT-IR (Thermo Fisher, Milano, Italy), equipped with a synthetic diamond ATR cell. Spectra were collected with a spectral window of 4000–550 cm^{-1}, coadding 150 scans for each sample. Data collection and processing were made using the OMNIC software package (Thermo Fisher, Milano, Italy). By the comparison of the spectroscopic profiles of the material before and after the sulfonation process, it was possible to assess the efficiency of the chemical modification of the polymeric substrate.

2.5. Analytical procedure

The extraction procedure was developed and optimized inspiring to an in-syringe dispersive micro solid-phase extraction IS-DμSPE 20 mg of the sPS microspheres were transferred to a syringe system, where all the extraction process is driven. The syringe is equipped with a polypropylene frit, used as a physical filter for sPS. Both the syringe and the frit are reusable, allowing a 100 % recyclable extraction process, from the adsorption material to the support devices. For the extraction, 4 mL of sample (i.e., saliva, urine, both 1:1 diluted with MilliQ water) containing the analytes at concentrations within the linear range were transferred to the syringe system. The sPS was allowed to disperse inside the sample for 20 min, maximizing the mass transfer to the sorbent, by the vortex agitation. Next, pressure was applied with a syringe plunger, so that the sample flows through the frit. After the sample loading, sPS microbeads were washed with 1 mL of MilliQ water, to ensure the elimination of matrix interferences, not physically retained on the sorbent. Analytes were then eluted by adding 1 mL of MeOH 1 % in ammonia to the body of the syringe, assisting the process with 10 minutes of vortex agitation. A manual pressure is finally applied, and the eluent was collected in a vial, ready for the subsequent instrumental analysis. The entire analytical procedure is displayed in **Fig. 1b**.

Analyses were conducted using high performance liquid chromatography separation coupled with a mass spectrometry (MS)/MS triple quadrupole system (Agilent 1260 Infinity HPLC system, Agilent, Palo Alto, CA, USA). The system was equipped with a binary high-pressure pump for mobile phase

delivery and an autosampler. C18 stationary phase was selected, in the form of an Eclipse Plus C18 (3.5 µm, 4.6 x 100 mm, from Agilent, Palo Alto, CA, USA). Chromatographic separation was performed in isocratic mode, using a mobile phase consisting of 90% H_2O with 0.1% (v/v) ammonia and 10% MeOH. The mobile phase flow rate was maintained at 0.3 mL min^{-1}, with a total analysis time of 6.5 minutes.

Target analytes were quantified in multiple reaction monitoring (MRM) mode using an Agilent 6420 Triple Quadrupole MS (Agilent, Palo Alto, CA, USA) with an electrospray ionization (ESI) source. The optimized ion transitions, chromatographic retention times and physicochemical descriptors for each analyte are listed in **Table C1**. The drying gas (N_2, 99% purity) was set at a flow rate of 10 L min^{-1} and a temperature of 300 °C. The nebulizer pressure was 18 psi, and the capillary voltage was maintained at 2000 V in positive ionization mode for all analytes. Data acquisition and processing were performed using Agilent MassHunter Software (Version B.06.00).

3. Results and discussion

3.1. Optimization of synthetic parameters

The procedure for preparing PS-based microbeads from recycled material was adapted from a previously published methodology [24]. A scale-up of the synthesis was undertaken to enhance productivity while preserving the reproducibility and morphological consistency of the resulting microbeads. The outcomes of the scaled-up process yielded a material morphologically comparable to the original.

Sulfonation of the PS substrate was carried out via batch reaction with concentrated sulfuric acid, a widely established method in the literature [25-29]. In this study, the protocol was applied to a polymeric substrate derived from waste materials, with the aim of improving its affinity for cationic species.

A critical factor in the sulfonation process is the contact time between the PS microparticles and sulfuric acid. The impact of sulfonation was assessed by evaluating the retention capacity of the material as a function of reaction time. Adsorption experiments were conducted by putting in contact the adsorption phase with a synthetic water sample spiked with four sulfonamide compounds at a concentration of 100 µg L^{-1}. For these preliminary tests, the pH was adjusted to 5 by adding formic acid to Milli-Q water. This pH, being below the pKa of the sulfonamides, ensures that the analytes remain in their fully protonated forms during the sorption process. The sorption was performed in-syringe, following the initial steps of the extraction protocol. After contact with the sorbent phase, the water sample was directly analyzed to quantify the fraction of analytes not retained by the material.

As shown in **Fig. 2**, all analytes exhibited a consistent trend: the concentration of unretained compounds decreased with increasing sulfonation time. Beyond six hours of sulfonation, no statistically significant improvement in retention was observed, indicating that the material had reached a saturation point, likely corresponding to its maximum surface sulfonation. These findings demonstrate that the raw material exhibited negligible affinity for the selected sulfonamides, while sulfonation markedly enhanced adsorption performance. A reaction time of six hours was therefore selected as the optimal condition to achieve full sulfonation and maximize the material's retention capacity.

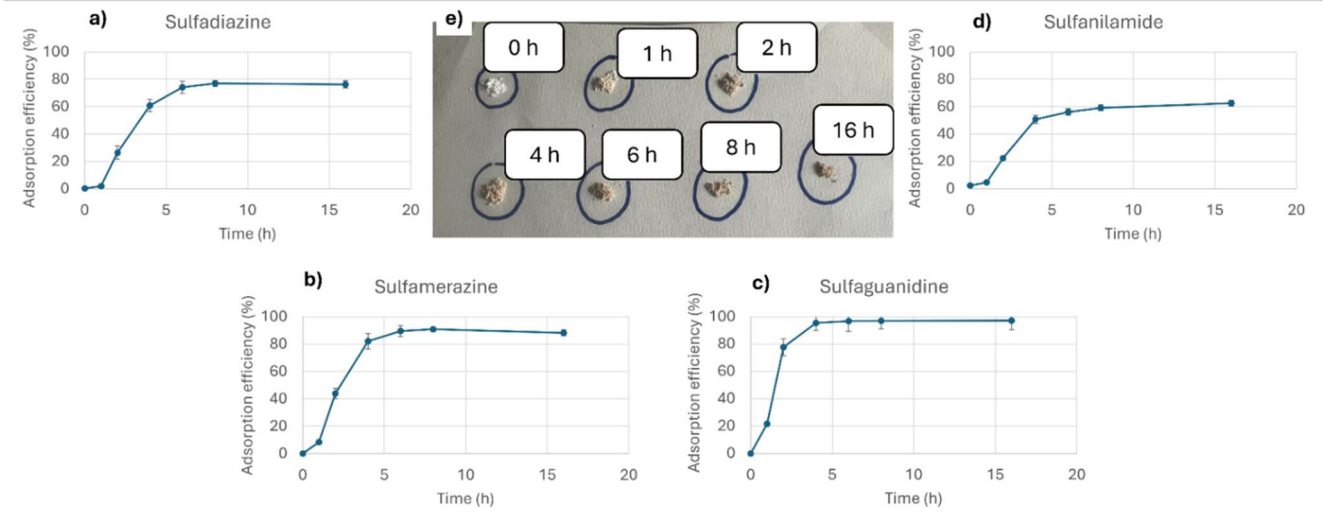

Fig. 2. Effect of sulfonation time on the adsorption efficiency (%) for each analyte: (**a**) sulfadiazine, (**b**) sulfamerazine, (**c**) sulfaguanidine and (**d**) sulfanilamide. The image inset (**e**) illustrates the visual change in microsphere color resulting from sulfuric acid treatment.

3.2. Characterization of the sPS

SEM analysis was conducted to verify the shape and size uniformity of the synthesized material, while EDX analysis was also performed to analyze the elemental composition. For comparison, both the non-sulfonated material and the material subjected to a 6-hour sulfonation process were analyzed. The microbeads obtained with the scaled-up synthesis are, similarly to those previously described, polydisperse in size, observing fine particles with a diameter ranging from 0.1 to 1 μm as well as coarse particles with diameters > 1 μm (**Fig. 3a**). The sulfonation procedure modified neither the shape nor size distribution of the PS microbeads (**Fig. 3b**), while EDX analysis evidenced the presence of S within the surface of the material, although with a low atomic %, the material being composed primarily by C (**Fig. 3c**). It should be noted that the presence of Au within the EDX spectra arises from the gold layer deposited prior SEM analysis to improve the conductivity of the sample and, thus, the acquisition of SEM images.

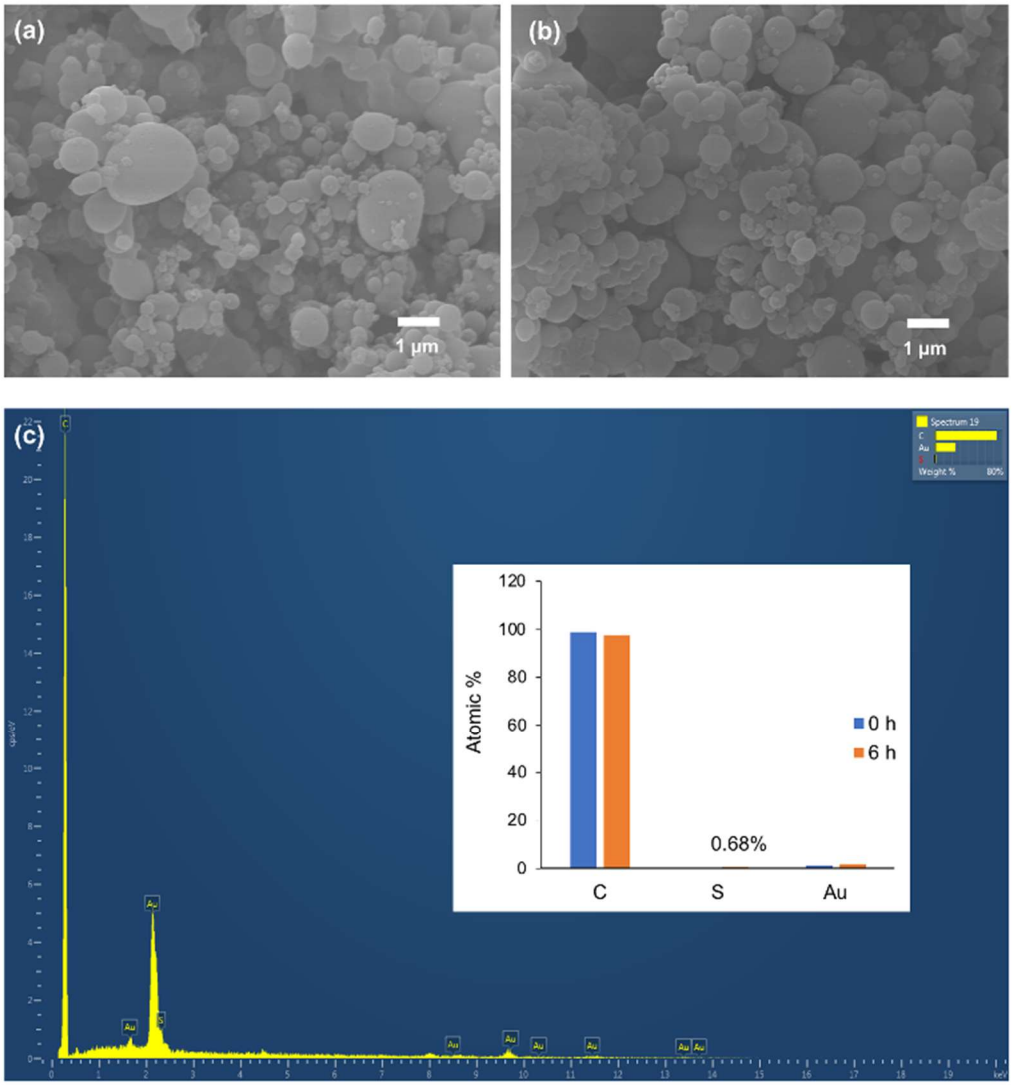

Fig. 3. SEM images of PS microbeads obtained through the emulsion solidification process (**a**) raw PS microbeads without sulfonation, (**b**) PS microbeads treated with sulfuric acid for 6 h. Micrographs were acquired with a magnification of 10000x. (**c**) EDX analysis of the materials. The inset depicts the atomic percentage of the materials (samples were covered with Au prior SEM-EDX analysis to improve sample conductivity).

ATR-FTIR analysis was carried out to rule out degradation of the bulk polymer and to confirm the surface sulfonation induced by sulfuric acid. For comparison, three materials were analyzed: polystyrene waste, pristine polystyrene microbeads prior to sulfonation, and the final sPS microbeads. Their spectra are presented in **Fig. C2**, with band assignments and detailed descriptions available in the Supporting Information. The spectrum of the final material shows complete preservation of the polymeric backbone, with only minimal changes in the spectroscopic profile before and after emulsion solidification and sulfonation. Neither solvent dissolution nor acid treatment appears to alter the chemical composition of the polymeric support. As a second key observation, typical bands

corresponding to sulfonate groups are not clearly detectable (expected at ~1030–1080 cm^{-1} and ~1120–1170 cm^{-1} for symmetric and asymmetric S=O stretching vibrations, and ~1350 cm^{-1} for additional S=O modes). This can be explained by the superficial nature of the functionalization and the preserved predominance of the bulk polymer's characteristic functional groups, which tend to overshadow the spectroscopic evidence of the newly introduced sulfonate groups.

3.3. Optimization of extraction methodology

The variables influencing the extraction procedure were subjected to an optimization study, including the sample solution volume, the amount of sPS in the syringe, pH, ionic strength, and the composition and volume of the desorption phase. All optimization experiments were performed using spiked Milli-Q water samples, with each analyte at a concentration of 100 $\mu g\ L^{-1}$.

Before specific optimizations, the general conditions were as follows: pH = 5, ionic strength = 0.15 µS/cm (no sodium chloride added), eluent phase = MeOH 0.1% aqueous ammonia, and eluent volume = 1 mL. Initially, extraction trials were conducted without adding sPS in the syringe to evaluate the background extraction efficiency of the device. The results of this preliminary test, reported in **Fig. C3** of the Appendix C, indicate that analyte retention on the syringe walls and within the polypropylene frit porosity was negligible, resulting in an extraction yield below 2% of the LLOQ extract. Response Surface Methodology (RSM) was applied to assess the relationship between variables influencing the adsorption step of the extraction procedure and their impact on extraction yields, i.e. sorbent amount, sample volume and vortex time. A 3^3 Box–Behnken design was employed for the optimization. Among all parameters, vortex time was identified as a critical factor affecting extraction performance. As shown in the main effect plot (**Fig. 4**), adsorption reaches completion within 20 minutes, achieving the maximum extraction yield. Therefore, for the 3D response surface analysis, which evaluates the relationship between sample volume, material amount, and process desirability (in terms of recovery percentage), vortex time was fixed at 20 minutes. The response surface plot in **Fig. 4** demonstrates a strong correlation between average recovery and material

amount, with optimal extraction yields observed between 20 and 30 mg of sPS, depending on the specific sulfonamide. To ensure consistent performance across all analytes, a compromise amount of 20 mg was selected. In contrast, sample volume had a minimal effect on extraction yield, as it did not influence process desirability but played a role in determining the enrichment factor. Consequently, the highest tested sample volume was chosen as the optimal condition for the final extraction workflow and maximization of the method sensitivity. In summary, optimal adsorption parameters were set as follows: vortex time = 20 min, material amount = 20 mg, sample volume = 4 mL.

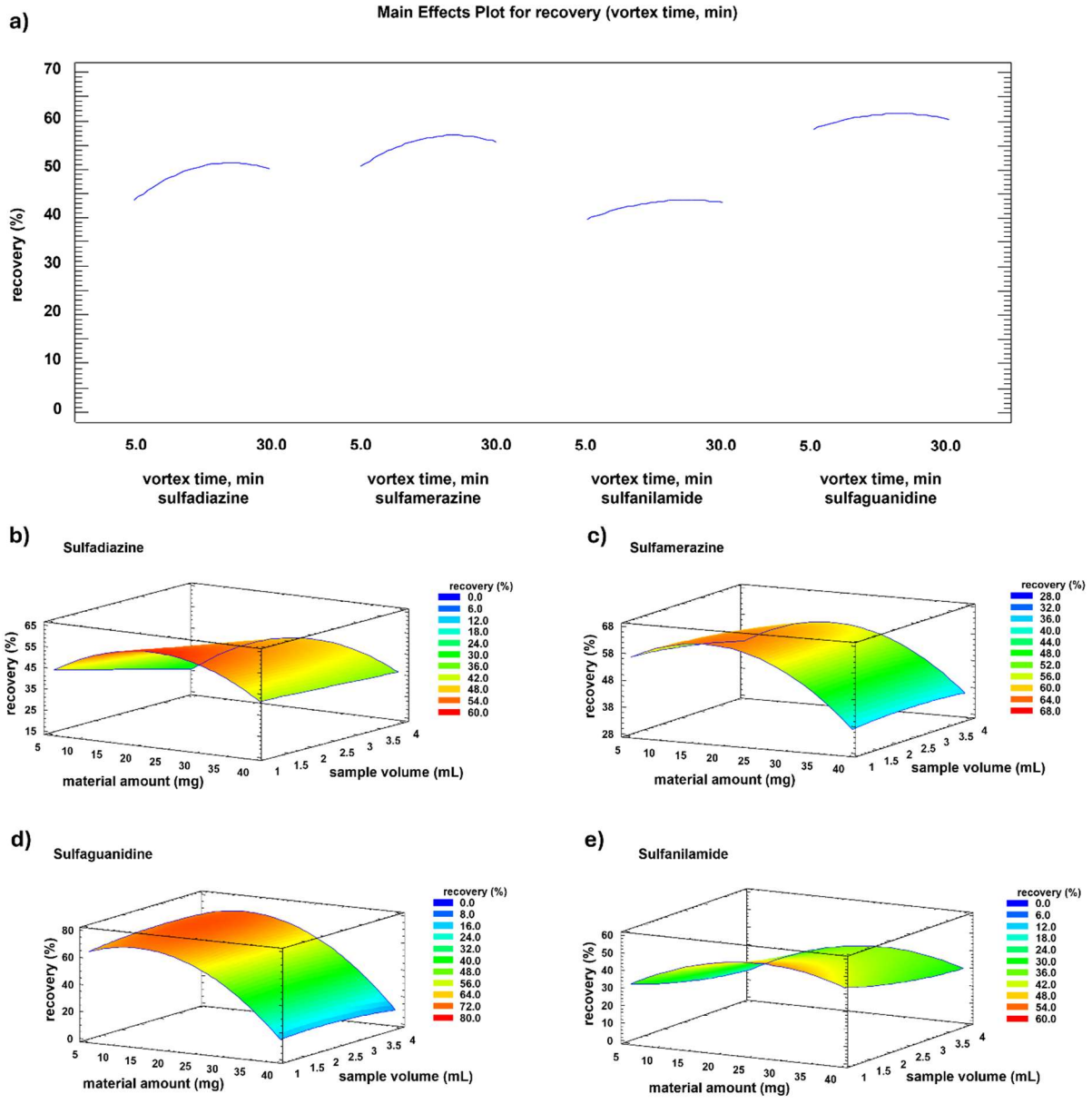

Fig. 4. Main effects plot (**a**) for vortex time and response surface plots showing the influence of sorbent amount and sample volume on extraction recoveries for each analyte. For the response surface analyses (**b** for sulfadiazine, **c** for sulfamerazine, **d** for sulfaguanidine and **e** for sulfanilamide), vortex time was fixed at the optimized value of 20 minutes.

Once the conditions for the adsorption step were established, the extraction procedure was further optimized by investigating the influence of pH and ionic strength on extraction yields from aqueous standards. The pH was adjusted using formic acid or ammonia and measured with a Horiba F-51 pH meter (Kyoto, Japan). Since the pH determines the ionization state of the analytes, it directly influences their interaction with the sorbent material. Extraction performance was evaluated at five different pH values (2.5, 3.5, 4.5, 7.0, and 10.0), with each condition tested in triplicate. As shown in **Fig. 5a**, the extraction efficiency was highest at pH values ≤ 6, where all analytes exist predominantly in their deprotonated form (pKa between 6.5 and 11.3). A pH of 3.5 was selected as optimal, yielding the highest average absolute recoveries.

The effect of ionic strength was assessed by analyzing spiked aqueous samples (100 µg L^{-1}) at pH 3.5 but with varying conductivity levels. Different amounts of NaCl have been added to different spiked water samples (i.e., 0, 0.1, 0.25, 0.5 and 1 %), obtaining solutions with different measured conductance (0.00015, 1.99, 4.62, 8.71, 16.37 mS cm^{-1}, respectively). Each condition was tested in triplicate. As shown in **Fig. 5b**, extraction efficiency decreased with increasing conductivity, suggesting that competing cations interfere with analyte binding. Therefore, no salts were added to adjust the ionic strength before extraction, to maximize interactions between analytes and the active sites of the sorbent.

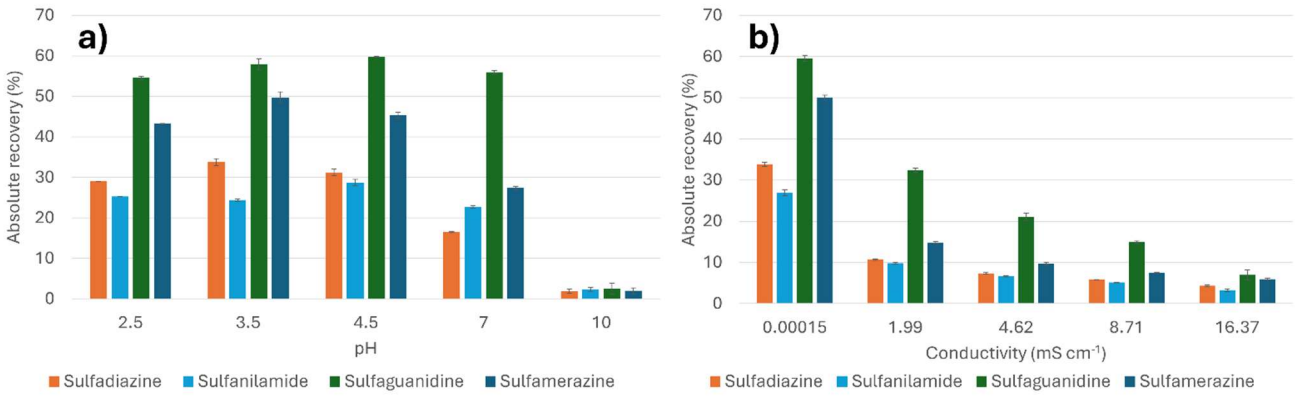

Fig. 5 Effect of (a) pH and (b) ionic strength (expressed as conductivity) on the recovery (%) of target analytes. Experiments were performed using Milli-Q water spiked at 100 µg L^{-1} for each analyte. For the assessment of ionic strength, the pH was fixed at 3.5.

The final set of parameters investigated concerned the elution conditions, specifically the nature and volume of the elution solvent. Preliminary experiments indicated that pure MeOH, either alone or supplemented with varying concentrations of aqueous ammonia, provided the best chromatographic separation. The inclusion of water in the elution mixture was found to reduce peak resolution. The addition of ammonia facilitates the deprotonation of the analytes, promoting their complete desorption from the sorbent and enhancing recovery. Consequently, three eluent compositions were evaluated: MeOH containing 0.1%, 0.5%, and 1% aqueous ammonia. As shown in **Fig. 6a**, only slight differences in recovery were observed among the tested conditions, with MeOH containing 1% aqueous ammonia yielding the highest overall recovery.

The influence of eluent volume on extraction efficiency was assessed in the range of 0.1–1 mL (**Fig. 6b**). Higher elution volumes improved analyte recovery by enhancing contact between the eluent and the sorbent, thus promoting more efficient desorption. An increase in precision was also noted with higher volumes. Volumes beyond 1 mL were not tested to avoid excessive dilution of the extract. Based on these findings, a volume of 1 mL MeOH containing 1% aqueous ammonia was selected for the subsequent validation protocol.

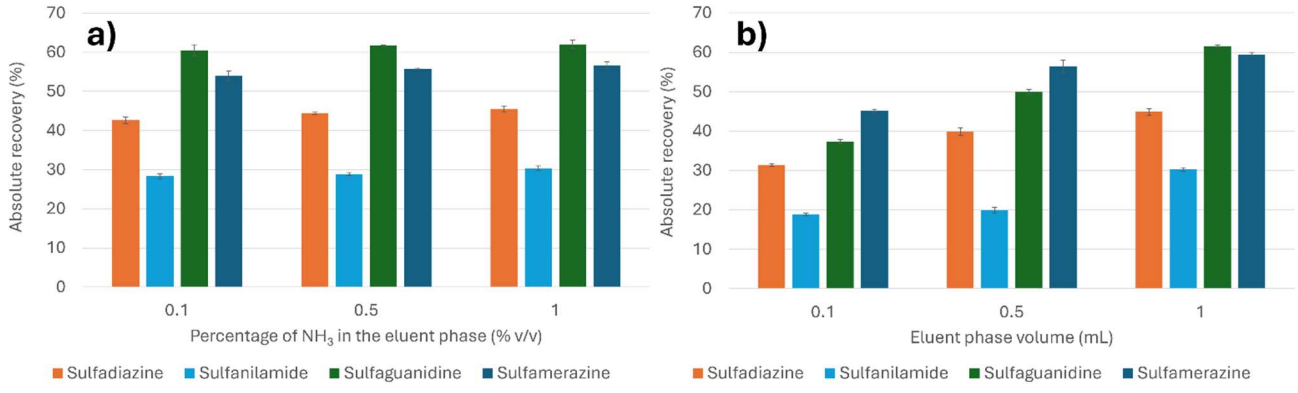

Fig. 6 Results for the optimization of (**a**) the composition and (**b**) volume of the eluent phase (MeOH 1 % NH_3). Experiments were conducted on MilliQ water spiked at a fixed concentration of 100 µg L^{-1} for each analyte and performing the entire adsorption step at the previous optimized conditions.

3.4. Analytical features of the method

The analytical performance of the method was assessed through validation experiments, designed following ICH guideline M10 for bioanalytical method [30]. **Table 1** presents the key figures of merit. Matrix-matched calibration curves were established for all analytes in two real biological matrices, i.e., pooled saliva and urine, using triplicate measurements. Blank samples were spiked at six to eight concentration levels (depending on the analyte-specific quantification limits) prior to extraction and subjected to the complete analytical workflow. Calibration curves were generated by plotting the mean peak area from triplicate analyses against the corresponding analyte concentrations (see **Fig. C4**). All analytes exhibited excellent linearity, with determination coefficients (R^2) exceeding 0.99, across a dynamic range from the lower limit of quantification (LLOQ) up to 800 µg L^{-1}. This wide linear range ensures reliable quantification over a broad concentration spectrum, supporting the method's applicability in diverse clinical and biological sample contexts. **Fig. C4** displays the calibration models for both saliva and urine. Limit of detection (LOD) was determined as the concentration yielding a signal-to-noise ratio of 3 (S/N = 3), while the LLOQ was defined as the lowest analyte concentration ensuring precision and accuracy within 20%. As can be observed in **Table 1**, LODs were in the range 0.8 and 32 µg L^{-1} for urine and saliva samples, while LLOQs ranged from 2 and 50 µg L^{-1}.

Precision and accuracy were assessed in accordance with ICH guidelines. For these studies a different pool of saliva and urine samples were employed, in which no presence of the analytes was found, so they were spiked at four fortification levels. The selected levels included: LLOQ, a low-quality control (L-QC) level (i.e., 2–3 times the LLOQ), a medium QC level (M-QC, approximately 30–50% of the calibration range), and a high QC level (H-QC, at least 75% of the upper calibration range). Precision was expressed as the relative standard deviation (RSD, %), while accuracy was evaluated through relative recovery. Both intra-run (within-run) and inter-run (between-run) precision and accuracy were evaluated. For intra-run analysis, five replicates were analyzed within a single

analytical batch. For inter-run assessment, three independent analytical batches, each consisting of five replicates, were performed on three separate days. As summarized in **Table 1**, all RSD values were below 15 % for all the analytes in the QCs levels and lower than 20 % in the LLOQ concentration, meeting the acceptance criteria established by ICH guidelines. Relative recovery values ranged from 86.4 % to 117.9%, demonstrating acceptable accuracy across all tested concentration levels.

3.5. Comparison with other analytical methods

The most significant innovation introduced by this study lies in the full recyclability of all consumables used throughout the analytical workflow, combined with the implementation of an extraction sorbent derived entirely from recycled polystyrene. The approach yielded satisfactory analytical performance while drastically minimizing material waste. The use of recycled materials as sorbents in analytical chemistry is gaining increasing attention, with several studies confirming comparable performance to conventional synthetic sorbents. This work represents one of the few examples where these concepts have been applied in full, effectively aligning with the principles of "circular analytical chemistry" as theorized by Psillakis et al. [23], and translating them into a genuinely zero-waste and fully recyclable protocol. To confirm the complete reusability of all consumables, including the sorbent and plasticware, a series of reuse tests were carried out, as shown in **Fig. C3** (Appendix C). Procedural blanks after washing routines using both water and acetone, or water alone, were analyzed. For all four sulfonamide antibiotics investigated, residual signals were below 3% of the signal obtained at the LLOQ, confirming that re-use does not compromise analytical integrity.

A comparison with previously reported methods for sulfonamide determination in complex matrices is presented in **Table C2**. Notably, while other approaches (e.g., QuEChERS, SPE, Molecularly Imprinted Polymer Solid-Phase Extraction (MISPE), and LLLME) often rely on single-use materials and generate significant waste, the current IS-DμSPE method uniquely combines low detection limits

(i.e., 4–5 μg L^{-1} for sulfadiazine and sulfamerazine, 50 μg L^{-1} for sulfanilamide, and 2–4.8 μg L^{-1} for sulfaguanidine) with short extraction time (~35 minutes) and full reusability of materials. This positions the method as a promising and sustainable alternative for sulfonamide quantification in biological matrices, bridging the gap between green chemistry and analytical reliability.

Table 1 Figures of merit of the 4 sulfonamide antibiotics analyzed in spiked samples of urine and saliva. Precision and accuracy are reported at all tested concentration levels.

Analyte	LOD (µg L^{-1})	LLOQ (µg L^{-1})	R^2	Linear range (µg L^{-1})	RSD intra-day, n=5 (%)				Accuracy, intra-day (% relative recovery, n=5)				RSD inter-day, n=15 (%)			
					LLOQ	L-QC	M-QC	H-QC	LLOQ	L-QC	M-QC	H-QC	LLOQ	L-QC	M-QC	H-QC
Urine																
SD	1.4	4	0.998	LLOQ-800	13.9	6.0	2.5	4.0	95.8	89.0	98.7	100.7	11.1	11.1	3.4	3.2
SM	1.9	4	0.996		11.4	5.6	4.9	4.2	102.3	91.7	100.5	98.7	8.8	12.1	4.5	3.6
SG	0.8	2	0.998		18.3	4.9	5.8	4.0	105.8	108.5	108.5	107.0	14.3	7.0	6.0	4.3
SA	30	50	0.999		11.3	9.6	8.0	10.3	97.4	101.7	94.8	96.4	9.8	8.6	6.6	10.2
Saliva																
SD	3	5	0.991	LLOQ-800	15.6	6.3	8.0	4.4	117.9	102.5	102.6	102.4	10.3	3.8	3.5	4.8
SM	4	5	0.991		10.1	9.0	8.0	3.1	115.8	101.6	99.4	101.0	5.6	3.7	2.3	3.4
SG	1.3	4.8	0.996		9.2	6.9	10.5	2.9	86.4	101.7	111.8	98.2	6.6	5.3	4.9	3.1
SA	32	50	0.994		7.8	5.6	8.1	7.8	105.0	95.9	106.3	104.1	8.4	4.3	4.2	8.3

SD: sulfadiazine, SM: sulfamerazine, SG: sulfaguanidine, SA: sulfanilamide

4. Conclusion

This study underscores the transformative potential of integrating sustainability into the core of analytical method development. By designing a fully recycled extraction system (from the sorbent material to the structural components such as syringes and filters) this work introduces a truly circular, near-zero-waste analytical approach. The successful reuse and functionalization of waste-derived polystyrene, through sulfonation, demonstrates that post-consumer plastic materials can be upgraded into efficient and selective sorbents for the extraction of priority environmental contaminants such as sulfonamide antibiotics. Crucially, this strategy does not compromise analytical feasibility or performance. On the contrary, the method shows excellent efficiency and reproducibility in extracting multiple sulfonamides from biological matrices. This confirms that sustainability and analytical robustness can go hand in hand, even when relying exclusively on recycled inputs. Furthermore, the functionalization of recycled materials adds a valuable dimension to waste management, shifting the paradigm from simple material reuse to the creation of tailor-made tools for specific analytical purposes. This aligns not only with green chemistry principles but also with broader goals of economic viability and social progress, offering low-cost, accessible solutions that can be adapted to various contexts, including resource-limited settings. Ultimately, this work provides a compelling model for the development of next-generation analytical methods, not only scientifically and cost-effective, but also deeply rooted in environmental responsibility and social relevance.

References

[1] Capasso, C., Supuran, C. T. (2014). Sulfa and trimethoprim-like drugs–antimetabolites acting as carbonic anhydrase, dihydropteroate synthase and dihydrofolate reductase inhibitors. J. Enzyme Inhib. Med. Chem., 29(3), 379-387. https://doi.org/10.1016/j.trac.2024.117686

[2] Shulpekova, Y., Nechaev, V., Kardasheva, S., Sedova, A., Kurbatova, A., Bueverova, E., Kopylov, A., Malsagova K., Dlamini, J. C., Ivashkin V. (2021). The concept of folic acid in health and disease. Mol., 26(12), 3731. https://doi.org/10.3390/molecules26123731

[3] Christensen, S. B. (2021). Drugs that changed society: History and current status of the early antibiotics: Salvarsan, sulfonamides, and β-lactams. Mol., 26(19), 6057. https://doi.org/10.3390/molecules26196057

[4] European Medicines Agency. European Surveillance of Veterinary Antimicrobial Consumption (ESVAC): 2009–2023. EMA; first published November 2023 [cited 2025 Jul 26]. Available from: https://www.ema.europa.eu/en/veterinary-regulatory-overview/antimicrobial-resistance-veterinary-medicine/european-surveillance-veterinary-antimicrobial-consumption-esvac-2009-2023

[5] Geissen, V., Mol, H., Klumpp, E., Umlauf, G., Nadal, M., Van Der Ploeg, M., Van de Zee, S. E. A. T. M., Ritsema, C. J. (2015). Emerging pollutants in the environment: a challenge for water resource management. Int. Soil Water Conserv. Res., 3(1), 57-65. https://doi.org/10.1016/j.iswcr.2015.03.002

[6] Grote, M., Vockel, A., Schwarze, D., Mehlich, A., Freitag, M. (2004). Fate of antibiotics in food chain and environment originating from pigfattening (Part 1). Fresenius Environ. Bull., 13(11), 1216-1224.

[7] Chen, J., Xie, S. (2018). Overview of sulfonamide biodegradation and the relevant pathways and microorganisms. Sci. Total Environ., 640, 1465-1477. https://doi.org/10.1016/j.scitotenv.2018.06.016

[8] Geiser, L., Henchoz, Y., Galland, A., Carrupt, P. A., Veuthey, J. L. (2005). Determination of pKa values by capillary zone electrophoresis with a dynamic coating procedure. J. Sep. Sci., 28(17), 2374-2380. https://doi.org/10.1002/jssc.200500213

[9] Uhlemann, T., Berden, G., Oomens, J. (2021). Preferred protonation site of a series of sulfa drugs in the gas phase revealed by IR spectroscopy. Eur. Phys. J. D., 75(1), 23. https://doi.org/10.1140/epjd/s10053-020-00027-x

[10] Barzallo, D., Palacio, E., March, J., Ferrer, L. (2023). 3D printed device coated with solid-phase extraction resin for the on-site extraction of seven sulfonamides from environmental water samples preceding HPLC-DAD analysis. Microchem. J., 190, 108609. https://doi.org/10.1016/j.microc.2023.108609

[11] Schlüsener, M. P., Bester, K. (2005). Determination of steroid hormones, hormone conjugates and macrolide antibiotics in influents and effluents of sewage treatment plants utilising high-performance liquid chromatography/tandem mass spectrometry with electrospray and atmospheric pressure chemical ionisation. Rapid Commun. Mass Spectrom., 19(22), 3269-3278. https://doi.org/10.1002/rcm.2189

[12] Barzallo, D., Ferrer, L., Palacio, E. (2024). Eco-friendly screening method for sulfonamides using a 3D handheld smartphone-based fluorescence detection device and graphene nanoplatelet-packed pipette tip microextraction. J. Environ. Chem. Eng., 12(2), 111888. https://doi.org/10.1016/j.jece.2024.111888

[13] Chen, S., Wang, C., Zhang, M., Zhang, W., Qi, J., Sun, X., Wang, L., Li, J. (2020). N-doped Cu-MOFs for efficient electrochemical determination of dopamine and sulfanilamide. J. Hazard. Mater., 390, 122157. https://doi.org/10.1016/j.jhazmat.2020.122157

[14] Liu, H., Gong, B., Zhou, Y., Sun, Z., Wang, X., Zhao, S. (2020). Preparation of high-capacity magnetic polystyrene sulfonate sodium material based on SI-ATRP method and its adsorption property research for sulfonamide antibiotics. BMC Chem., 14(1), 3. https://doi.org/10.1186/s13065-019-0658-8

[15] Antonelli, L., Frondaroli, M. C., De Cesaris, M. G., Felli, N., Dal Bosco, C., Lucci, E., Gentili, A. (2024). Nanocomposite microbeads made of recycled polylactic acid for the magnetic solid phase extraction of xenobiotics from human urine. Microchim. Acta., 191(5), 251. https://doi.org/10.1007/s00604-024-06335-y

[16] Wang, J., Yu, J., Li, M., Zhang, Y. (2024). Synthesis of sodium polystyrene sulfonate resins for the removal of methylene blue from wastewater. J. Taiwan Inst. Chem. Eng., 159, 105501. https://doi.org/10.1016/j.jtice.2024.105501

[17] Al-Sabagh, A. M., Moustafa, Y. M., Hamdy, A., Killa, H. M., Ghanem, R. T. M., Morsi, R. E. (2018). Preparation and characterization of sulfonated polystyrene/magnetite nanocomposites for organic dye adsorption. Egypt. J. Petrol., 27(3), 403-413. https://doi.org/10.1016/j.ejpe.2017.07.004

[18] Martins, C. R., Ruggeri, G., De Paoli, M. A. (2003). Synthesis in pilot plant scale and physical properties of sulfonated polystyrene. J. Braz. Chem. Soc., 14, 797-802. https://doi.org/10.1590/S0103-50532003000500015

[19] Kucera, F., Jancar, J. (2009). Sulfonation of solid polystyrene using gaseous sulfur trioxide. Polym. Eng. Sci., 49(9), 1839-1845. https://doi.org/10.1002/pen.21398

[20] Sułkowski, W. W., Nowak, K., Sułkowska, A., Wolińska, A., Bajdur, W. M., Pentak, D., Mikuła, B. (2010). Chemical recycling of polystyrene. Sulfonation with different sulfonation agents. Mol. Cryst. Liq. Cryst., 523(1), 218-790. https://doi.org/10.1080/15421401003720140

[21] Teng, X., Ding, X., She, Z., Li, Y., Xiong, X. (2022). Preparation of functionalized magnetic polystyrene microspheres and their application in food safety detection. Polym., 15(1), 77. https://doi.org/10.3390/polym15010077

[22] Wang, N., Xin, H., Zhang, Q., Jiang, Y., Wang, X., Shou, D., Qin, L. (2017). Carbon nanotube-polymer composite for effervescent pipette tip solid phase microextraction of alkaloids and flavonoids from Epimedii herba in biological samples. Talanta, 162, 10-18. https://doi.org/10.1016/j.talanta.2016.09.059

[23] Psillakis, E., Pena-Pereira, F. (2024). The twelve goals of circular analytical chemistry. TrAC - Trends Anal. Chem., 175, 117686. https://doi.org/10.1016/j.trac.2024.117686

[24] Antonelli, L., López-Lorente, Á. I., Gentili, A., Lucena, R., Cárdenas, S. (2025). Microbeads from recycled polystyrene yogurt cups for the in-syringe micro solid-phase extraction of four opioids from environmental and biological samples. Sustain. Chem. Pharm., 45, 102036. https://doi.org/10.1016/j.scp.2025.102036

[25] Coughlin, J. E., Reisch, A., Markarian, M. Z., Schlenoff, J. B. (2013). Sulfonation of polystyrene: Toward the “ideal” polyelectrolyte. J. Polym. Sci. Part A: Polym. Chem., 51(11), 2416-2424. https://doi.org/10.1002/pola.26627

[26] Ngadiwiyana, Ismiyarto, Gunawan, Purbowatiningrum, R. S., Prasetya, N. B. A., Kusworo, T. D., Susanto, H. (2018, May). Sulfonated polystyrene and its characterization as a material of electrolyte polymer. J. Phys. Conf. Ser. (Vol. 1025, p. 012133). IOP Publishing. doi :10.1088/1742-6596/1025/1/012133

[27] Tran, A. T., Pham, T. T., Nguyen, Q. H., Hoang, N. T., Bui, D. T., Nguyen, M. T., Nguyen, M. K., Van der Bruggen, B. (2020). From waste disposal to valuable material: Sulfonating polystyrene waste for heavy metal removal. J. Environ. Chem. Eng., 8(5), 104302. https://doi.org/10.1016/j.jece.2020.104302

[28] Teo, J. Y., Zheng, X. T., Seng, D. H. L., Hui, H. K., Chee, P. L., Su, X., Loh, X. J., Lim, J. Y. (2022). Waste Polystyrene-derived Sulfonated Fluorescent Carbon Nanoparticles for Cation Sensing. ChemistrySelect, 7(36), e202202720. https://doi.org/10.1002/slct.202202720

[29] Wang, J., Yu, J., Li, M., Zhang, Y. (2024). Synthesis of sodium polystyrene sulfonate resins for the removal of methylene blue from wastewater. J. Taiwan Inst. Chem. Eng., 159, 105501. https://doi.org/10.1016/j.jtice.2024.105501

[30] Guideline, I. H. (2022). Bioanalytical method validation and study sample analysis M10. ICH Harmonised Guideline: Geneva, Switzerland.

Chapter 3: Recycling in Water remediation procedures

Overview

In the field of water remediation, recycling is an already well-established and predominant concept, with numerous studies reporting the reuse of waste-derived materials as adsorbents for pollutant removal [1]. Water treatment is, in fact, an inherently industrial process, which facilitates the large-scale implementation of recycling strategies, making such procedures both economically and operationally viable [2]. As discussed in the general introduction, a wide range of agricultural and food wastes have been successfully employed as adsorbent materials, either in their native form or after chemical or physical modification, in order to enhance their retention capacity toward selected classes of contaminants [3-5]. In this context, applications involving recycled plastics as adsorbent precursors remain comparatively rare, mainly due to concerns related to the potential environmental release and persistence of plastic particles [6]. To address this challenge, the work presented in this chapter explores the use of cellulose acetate, a polymer characterized by slow environmental degradation and the lack of well-defined recycling strategies [7], as a sustainable feedstock for the synthesis of new adsorbent materials. The main objective was to develop a synthetic procedure capable of producing microspherical structures from recycled cellulose acetate, with dimensions sufficiently large (approximately 200 μm in diameter) to prevent the risk of environmental dispersion. To this end, the microemulsion solidification technique was adapted and optimized to generate larger microspheres featuring surface nanostructures with significant adsorptive properties. The versatility of this method allowed precise control over particle size and enabled the functionalization of the regenerated polymer with activated carbon, thereby maximizing the adsorption efficiency of the final product.

References

[1] Dong, X., Akram, A., Comesaña-Gándara, B., Dong, X., Ge, Q., Wang, K., ... & Lau, C. H. (2020). Recycling plastic waste for environmental remediation in water purification and CO2 capture. *ACS Applied Polymer Materials*, *2*(7), 2586-2593. https://doi.org/10.1021/acsapm.0c00224

[2] Musarurwa, H., & Tavengwa, N. T. (2022). Recyclable polysaccharide/stimuli-responsive polymer composites and their applications in water remediation. *Carbohydrate Polymers*, *298*, 120083. https://doi.org/10.1016/j.carbpol.2022.120083

[3] Ramón-Gonçalves, M., Alcaraz, L., Pérez-Ferreras, S., León-González, M. E., Rosales-Conrado, N., & López, F. A. (2019). Extraction of polyphenols and synthesis of new activated carbon from spent coffee grounds. Scientific reports, 9(1), 17706. https://doi.org/10.1038/s41598-019-54205-y

[4] Rai, P., & Singh, K. P. (2018). Valorization of Poly (ethylene) terephthalate (PET) wastes into magnetic carbon for adsorption of antibiotic from water: Characterization and application. Journal of environmental management, 207, 249-261. https://doi.org/10.1016/j.jenvman.2017.11.047

[5] Chan, K., & Zinchenko, A. (2021). Conversion of waste bottles' PET to a hydrogel adsorbent via PET aminolysis. Journal of Environmental Chemical Engineering, 9(5), 106129. https://doi.org/10.1016/j.jece.2021.106129

[6] Moteallemi, A., Taherkhani, S., Ahmadfazeli, A., & Dehghani, M. H. (2025). A systematic review of plastic wastes as new adsorbents for dye removal in aqueous environments. Environmental Sciences Europe, 37(1), 115. https://doi.org/10.1186/s12302-025-01172-z

[7] Puls, J., Wilson, S. A., & Hölter, D. (2011). Degradation of cellulose acetate-based materials: a review. Journal of Polymers and the Environment, 19(1), 152-165. https://doi.org/10.1007/s10924-010-0258-0

Paper IV: Cellulose acetate recycling for water remediation applications

Green Analytical Chemistry 13 (2025) 100283

Contents lists available at ScienceDirect

Green Analytical Chemistry

journal homepage: www.elsevier.com/locate/greeac

Composite microbeads of cellulose acetate upcycled from waste for water remediation

Lorenzo Antonelli [a], Susanna Grasso [a], Massimo Giuseppe De Cesaris [a], Nina Felli [a], Chiara Dal Bosco [a], Stefano Cinti [b,*], Alessandra Gentili [a,*]

Graphical abstract

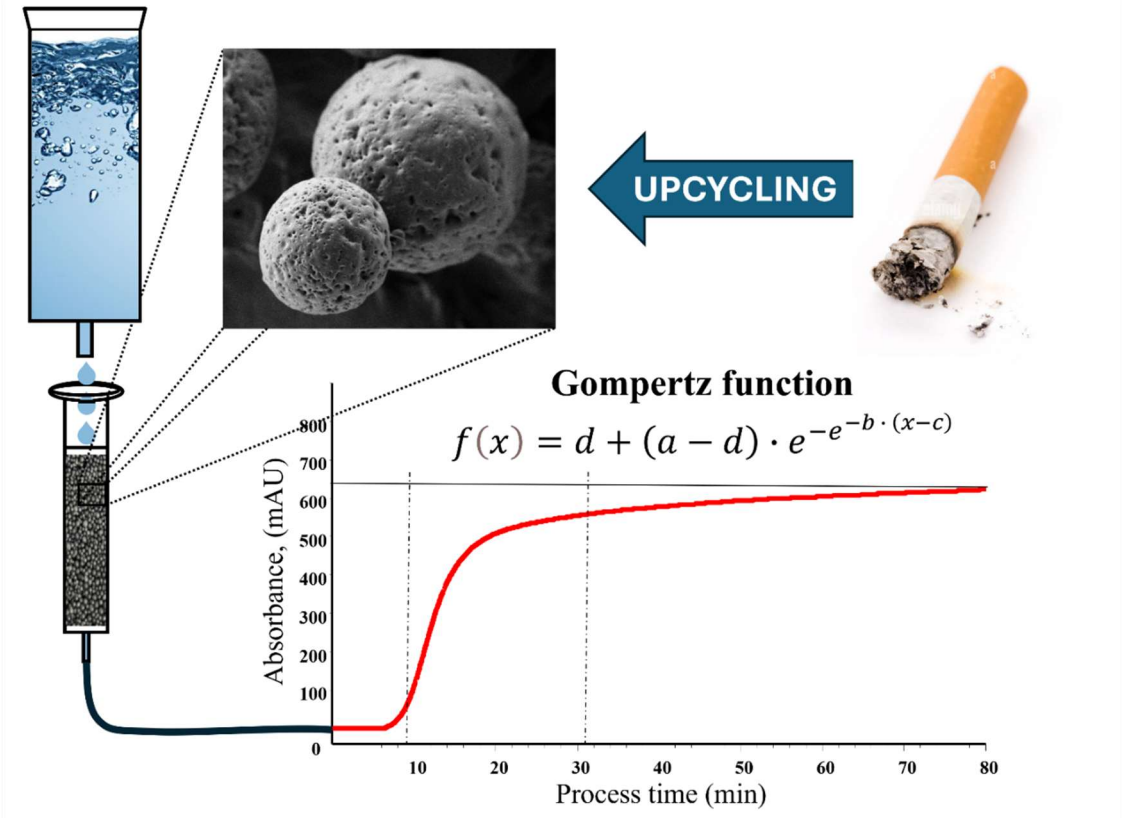

Abstract

The rising level of contaminants in the environment is urgent need for the development of effective sorbents that can be applied to remediate contaminated water. Additionally, if sorbents can be prepared by recycling waste, this is a further added value. This study has aimed to develop a sustainable nanocomposite sorbent of cellulose acetate (CA), a bioplastic that can be recycled from different types of waste, including filters from cigarette butts. After an efficient cleaning protocol, the recovered CA was used to prepare microspheres via an emulsion precipitation technique, in combination with activated carbon as adsorption filler (20 % w/w). The sorption performance of this material was evaluated in flow-through systems, i.e. glass cartridges packed with the microspheres, by simulating a filter for water remediation at the laboratory scale. An experimental 2^3 factorial design was performed to define the best operational conditions of the instrumental setup, defining the flow rate, amount and chemical nature of the packed microbeads. The adsorption performance was tested towards 40 common contaminants chosen as model compounds. To investigate the retention behaviour of the individual analytes, the Gompertz mathematical model was chosen, as it is useful for fitting the sigmoidal release pattern of contaminants from the packed cartridge. Competitive removal studies revealed differential retention based on analyte polarity, with retention capacities spanning from 2.2−4.2 µg of each contaminant per gram of sorbent, with a total loading capacity on the order of 125 $\mu g/g_{sorbent}$. The adsorption studies demonstrated the composite potential for water remediation operations, coupled with advantages in terms of recyclability and sustainability of the material.

Keywords: plastic waste; recycling; green chemistry; composite sorbents; water remediation; breakthrough curves

1. Introduction

Although 71 % of the Earth's surface is covered by water, only 1 % is freshwater suitable for human consumption [1, 2]. The problem of water scarcity is further compounded by pollution caused by anthropic activities, such as the use of fertilizers and pesticides in agriculture, veterinary drugs in livestock farming, and other contaminants from the industrial sector [3]. This pollution has significant consequences not only for the ecosystems, but also for human health as exposure to contaminated water can cause a range of illnesses.

In response to these problems, the scientific community is working hard to develop solutions for water purification to remove physical, chemical, and biological contaminants. Among the most used purification techniques there are oxidation, phytoremediation, bioremediation, membrane filtration, adsorption, reverse osmosis, ion exchange, electro-dialysis, etc. These techniques differ in terms of treatment time, costs, industrial scalability, and release of secondary chemical residues [4]. Among them, adsorption stands out for its low cost (5-200 USD for m^3 of treated water against 10-450 USD of other techniques), efficiency (up to 99.9% mainly depending on the sorbent nature), versatility, low cost, and ease of operation. Sorbent materials like activated carbon, zeolites, silica, and (bio)polymer-based materials are widely used due to their high surface area and porosity, which allows them to trap pollutants effectively [5]. These materials must be non-toxic, readily available, and ideally derived from natural or waste sources to minimize their environmental impact [6, 7]. Additionally, they should be easy to dispose of at the end of their lifecycle [8]. Among them, activated carbon is an excellent sorbent, particularly of nonpolar and medium-polar substances, due to its imperfect graphite-like structure, the presence of heteroatoms, and its high surface area, often greater than 1000 m^2/g [9, 10]. This material can be obtained from natural or waste sources, such as fruit peels, and nutshells [11, 12]. For example, a study by Bansode et al. demonstrated that activated carbons, made from almond and pecan shells, were effective at removing volatile organic compounds from water, performing similarly to conventional activated carbons derived from fossil fuels [13].

Plastic waste can also be repurposed to produce activated carbon. For example, You et al. synthesized activated carbon fibres from industrial polyacrylonitrile waste. The resulting material had a surface area of 2400 m^2/g and a porous volume of 1.15 cm^3/g, making it highly effective for adsorbing dyes from wastewater [14]. Such studies highlight the potential for using waste products to create new materials for water treatment, reducing the waste disposal burden at the same time. Other polymers, from natural or waste sources, have already been applied in water remediation procedures: Qu et al. developed a cotton-based material impregnated with chitosan for removing gold from water, demonstrating a strong interaction between the material and the metal [15, 16]. Similarly, Rajakovic et al. created a sorbent from recycled wool for treating water contaminated by heavy oils, showing excellent adsorption properties comparable to commercial products [17]. Cigarette butts, which are one of the most widely produced and improperly disposed waste items, present a significant environmental challenge [18]. It is estimated that cigarette butts account for around 30 % of global waste, with roughly 6 billion cigarettes smoked worldwide every year [19]. Improper disposal of cigarette butts leads to the release of over 7,000 harmful chemicals into the environment, including heavy metals like chromium, and lead as well as carcinogens such as polycyclic aromatic hydrocarbons [20]. Another issue stemming from improper cigarette butt disposal arises from the fact that cigarettes, in addition to being made of paper and tobacco, also contain polymeric/plastic materials, such as adhesive glues and the filter (primarily composed of cellulose acetate (CA)), which exhibit poor biodegradability in natural environments [21, 22] with degradation times exceeding thirty years [20]. The problem of CA pollution has led to different recycling strategies to prepare sustainable materials of interest in several relevant sectors, such as construction (bricks, concrete, asphalt), acoustics (sound-absorbing materials), electronics (conductive materials, batteries), and chemistry (sorbent materials) [23]. Exploring recycling strategies in the literature, several studies describe procedures that transform cigarette butts into sorbent materials for water treatment [24]. Specifically, considering that the primary polymer, CA, has a high carbon atom content, cigarette butts are often used to synthesize carbon-based materials with strong sorbent capabilities, especially

towards metal ions and inorganic pollutants [25, 26]. However, the literature reveals that applications for removing water contaminants are limited to a narrow range of substances, such as heavy oils, metal ions, and dyes and not explored in depth [27-30]. Considering that water contamination also involves organic substances (emerging organic contaminants, EOCs), studies in this specific field are of pivotal importance to ensure high water protection [31]. In light of these considerations, this study proposes the synthesis of a new sustainable sorbent from CA recovered from cigarette butts and its application in water remediation application via flow through adsorption mode [32] toward common organic contaminants encountered in environmental water. The work is structured into three main phases: the recovery of the polymer, its transformation into a new composite sorbent material, and its application in water decontamination from EOCs [33]. The preparation process involves an accurate washing procedure of CA recovered from cigarette filters and the preparation of a composite sorbent material via an emulsion solidification technique, using activated carbon as a filler to improve the adsorption capability. The composite microbeads were characterized using scanning electron microscopy (SEM) and attenuated total reflectance Fourier-transform infrared spectroscopy (ATR-FTIR) to assess morphology and surface properties. The material applicability in removing a wide range of contaminants (pharmaceuticals, hormones, herbicides, pesticides, and fungicides) from natural waters was tested by designing an experimental setup (a glass cartridge packed with the sorbent microbeads and working in flow-through-mode) to simulate the water treatment operation. The adsorption dynamics of forty model compounds, characterized by different molecular weights, logP, and pKa, was evaluated using the model of the breakthrough curves, by fitting the experimental data with the Gompertz function [34, 35]. A quantitative evaluation was also performed to estimate the overall retained quantity of each contaminant, having being defined a saturation limit, a key parameter for defining the sorbent performance and benchmark for commercially available materials. It's our opinion this work can compensate for a large gap in the scientific literature and contribute to valorizing the harmful waste of cigarette butts in a valuable sorbent for water remediation. To our knowledge this is the first work of recovered CA-based sorbent material, produced from discarded

cigarette butts, applied in flow through adsorption mode for the removal of such a number of organic contaminants.

2. Experimental section

2.1 Reagents and chemicals

Most of the standards for the target analytes (butoxycarboxim, methomyl, sulfaguanidine, sulfamerazine, pirimicarb, sulfamonomethoxine, sulfachloropyridazine, dimethoate, picloram, sulfathiazole, sulfamethoxazole, butocarboxim, prednisolone, thifensulfuron-me, propoxur, dexamethasone, cinosulfuron, metsulfuron-me, chlorsulfuron, carbaryl, atrazine, isoproturon, metobromuron, 2,4-dichlorophenol, 2,4-dichlorophenoxyacid, naproxen, testosterone, flamprop, me-testosterone, linuron, desmedipham, phenmedipham, nimesulide, ibuprofen, procymidone, phenylbutazone, progesterone and iprodion) were purchased from Merk Life Science S.r.l. (Milan, Italy). Malathion, and acephate were obtained from Dr. S. Ehrenstorfer Promochem (Wesel, Germany). **Table D1** of the Appendix C presents the main chemical characteristics and structures of the forty target analytes. Methanol (MeOH, purity > 99 %) and absolute ethanol (EtOH, purity > 99 %) were obtained from VWR International (Radnor, PA, USA); tetrahydrofuran (THF) and acetonitrile (RS-PLUS grade, purity 99.95 %) were purchased from Merk Life Science S.r.l. (Milan, Italy); water was generated by the MilliQ "Direct-Q® 3 UV System" manufactured by Merck KGaA (Darmstadt, Germany); formic acid (HCOOH, purity > 98 %) was acquired from Acros Organics B.V.B.A. (Waltham, MA, USA). Activated carbon was purchased from Special Ingredient Europe (Utrecht, Netherlands); sodium chloride (≥ 99 %) and n-dodecyl amine (≥ 99 %) were acquired from Merck KgaA (Darmstadt, Germany).

2.2 Preparation of the working solutions

The standard solutions of the target analytes were prepared from individual commercial standards, with a purity grade greater than 99 %. The powders were weighed using a precision analytical balance

(Ohaus DV215CD Discovery semi-micro and analytical balance, capacity 81/210 g, resolution 0.01/0.1 mg), transferred into volumetric flasks, and individually solubilized in MeOH. This process yielded stock solutions at 1 mg mL^{-1}, which were placed in amber vials and stored in a freezer at -18 °C. The working standard solution for testing water remediation performance was prepared by diluting the stock solutions in MilliQ water to a concentration of 0.5 mg L^{-1}.

2.3 Regeneration and characterization of cellulose acetate from cigarette stubs

Cigarette butts were collected from designated receptacles located in common spaces of Sapienza University of Rome. Once taken in laboratory, CA filters were recovered after removing paper, tobacco, and ash residues. Afterwards, approximately 3 g of cigarette filters were weighed, placed into a beaker, and submitted to a washing procedure to remove combustion by-products. Under magnetic stirring, two washing steps were performed first with 10 mL of hot MilliQ water (90-100 °C) and then with 10 mL of EtOH. Finally, the clean filters were dried at 48 °C for approximately 40 minutes. For comparative analysis, cellulose acetate (CA) solutions (0.5% w/v in acetone) were prepared from pristine, clean, and unwashed cigarette filters and characterized using UV-VIS spectrophotometry, ATR-FTIR and thermogravimetric analysis. For instrumental conditions, refer to **Section 2.5** and **Section D1**. The results, presented in **Fig. D1**, **D2** and **D3**, demonstrate that the washing procedure effectively preserves the polymeric matrix, with the recovered material exhibiting fully comparable physicochemical and thermal properties to the pristine CA [24].

2.4 Preparation of cellulose acetate microbeads

The synthesis of the recycled sorbent material was conducted via microemulsion solidification of an organic solution of the polymer with a saturated aqueous solution of NaCl and dodecyl amine. The organic solution (dispersed phase) was prepared by dissolving 560 mg of washed filters in 10 mL of THF (5.6 % w/v) under gentle stirring for 2 minutes. Separately, a saturated solution of NaCl in MilliQ water and a 2 % n-dodecylamine solution were prepared and mixed in a 1:1 (v/v) volumetric ratio to create the dispersing solution. Then, 10 mL of this dispersing solution was added, under

magnetic stirring (200 rpm), to 10 mL of the polymer organic solution to induce salting-out and form an emulsion. To break the microemulsion and propitiate the solidification of CA as microspheres, 11 mL of MilliQ water was added dropwise. At the end of the process, the system and the precipitation was stabilized by the addition of 10 mL of EtOH. The precipitate was then filtered using a vacuum pump, washed three times with 5 mL of MilliQ water and once with EtOH (5 mL per washing step) to remove unreacted materials and residual organic solvent. The synthetic procedure is displayed in **Fig. 1**.

A similar procedure was followed for synthesizing composite materials, in which a known quantity of activated carbons was dispersed in the organic phase after dissolving the polymer. As regards the final optimized material, 112.20 mg of activated carbon were added to produce a 20 % w/w composite (CA@AC-20%). Other composites were synthesized by varying the percentage of activated carbon to study the performance trend: 5 % (CA@AC-5%) and 10 % (CA@AC-10%).

2.5 Characterization of the composite microbeads

The composite microbeads were characterized in terms of dimensional and morphological properties using SEM (model AURIGA; Carl Zeiss, Oberkochen, Germany). Prior to scanning, all samples were dried and coated with chromium to make their surfaces conductive. Micrographs were collected at various magnifications (100–1000 X), using a working distance of 14 mm, an electron accelerating voltage of 15 kV, and DISS for digital image acquisition.

A characterization study via ATR-FTIR was carried out using a Nicolet 6700 instrument (Thermo Fisher Scientific, Waltham, PA, USA), equipped with a Golden Gate single-reflection diamond accessory, with a resolution of 2 cm^{-1} over a spectral range of 400-4000 cm^{-1}, and co-addition of 200 scans.

2.6 Instrumental setup and optimization of the process conditions

To test the adsorption capability of the synthesized material, an instrumental setup was assembled to to purify environmental water on a laboratory scale. A total of 40 common environmental

contaminants were used as model compounds and their multi-standard solution (see **Section 2.2**) was used to spike 500-mL of MilliQ water at 0.5 mg L^{-1}. The aqueous sample was flowed through a glass cartridge filled with a known amount of synthesized composite microspheres (CA@AC-20%), packed between two polypropylene frits. Specific constant flow rates were controlled by an HPLC pump (1260 Infinity II, Agilent Technologies, Inc., Milano, Italia). The instrumental setup is represented in **Fig. 1**.

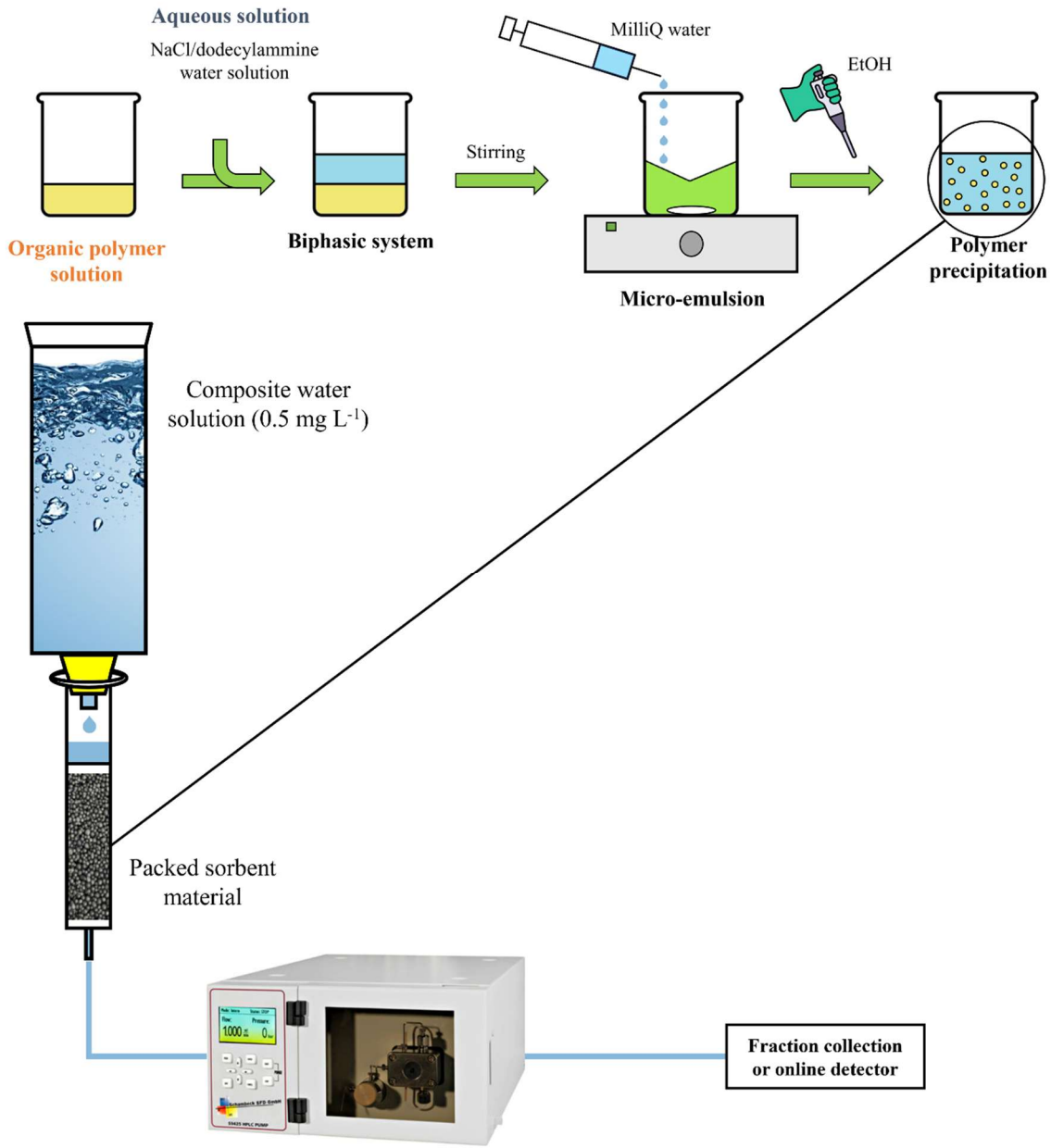

Fig. 1 Synthetic strategy of the new sorbent material and instrumental setup: a chromatographic pump sustains a dynamic flow of a water solution, spiked with all the 40 contaminants at 0.5 mg L^{-1}, inside the cartridge packed with the microbeads.

To define optimal process parameters (flow rate, amount of sorbent, percentage of the activate carbon in the composite material), an experimental design was conducted by processing data with Satgraphic Centurion XV software (StatPoint, Inc., Warrenton, VA, USA). Through a relatively limited number of experiments designed to represent the process parameter variability (9 different experiments, each one made in triplicate for a total of 27 trials), response surfaces could be generated to model the performance of the contaminant removal process as a function of the considered variables. After selecting the process variables crucial in affecting the process performance, other preliminary steps in constructing the experimental design were: *i*) determination of reasonable experimental ranges for the identified variables, and *ii*) definition of desirability parameters to quantitatively define the process efficiency.

As above-mentioned, the process variables selected were: flow rate (X1), amount of sorbent material (X2), and the percentage of activated carbon within the composite (X3). The chosen experimental ranges for these variables were 0.25 – 1 mL min^{-1} for X1, 100–500 mg for X2, and 5–20% for X3. As indicators of the purification level, spectrophotometric responses were recorded for two 500 µL aliquots of the cartridge eluting solution, collected after 10 minutes (Y1) and 60 minutes of processing (Y2). These aliquots were directly injected (100 µL) into an HPLC-UV (1260 Infinity II, Agilent Technologies, Inc., Milano, Italia), working in flow injection analysis under isocratic mode (100 % MilliQ water) at a flow rate of 1 mL min^{-1}; the signal was recorded at a wavelength of 230 nm (a good compromise for all the analytes). The analytical output was the area of the chromatographic peak of all analytes (an integrated signal), coeluting after some seconds from the injection due to the absence of a chromatographic column. This signal facilitates the monitoring of the overall removal process, offering comprehensive insights into the ongoing adsorption dynamics.

Among the various experimental designs reported in the literature, a face-centred experimental design was adopted. This involved eight independent experiments, conducted by setting the process variables to the extremes of the chosen experimental ranges, and one experiment with the process variables set at the central value within the range. By representing each variable as a Cartesian axis, the

experiments conducted appear as points in space, distributed at the vertices and centre of a cube that circumscribes the space of possible variable value combinations.

The results obtained in terms of recorded observables were used to establish the optimal functional relationship between the process variables and the observables themselves, fitting the data with the following equation:

$$y = b_0 + b_1X_1 + b_2X_2 + b_3X_3 + b_{12}X_1X_2 + b_{13}X_1X_3 + b_{23}X_2X_3 + b_{11}X_1^2 + b_{22}X_2^2 + b_{33}X_3^2$$

Upon defining the process variables, their ranges, and the observables, the experimental matrix was generated using the aforementioned software. All experiments were performed in triplicate to develop a robust and reliable model, resulting in a total of 27 experiments. Final conditions for the considered parameters were established as follows: $X1 = 0.25$ mL min^{-1}, $X2 = 500$ mg, $X3 = 20$ %.

2.7 Breakthrough curves

After optimizing the process parameters for the definition of the best operative conditions, the above-described instrumental setup was directly coupled with an online UV detection system (λ = 230 nm) so to monitor in real-time the concentration changes in the solution eluting from the cartridge as a function of flushing time. Signal acquisition occurred from $t_0 = 0$ min, corresponding to the initial contact of the sorbent material in the cartridge with the contaminant solution, up to $t_{fin} = 30$ min. The trend of the spectroscopic signal (proportional to the overall concentration of contaminants in the solution), as a function of time, is referred to as the breakthrough curve. Specifically, this function reflects the integrated retention behaviour of all analytes in the cartridge.

To extract information on the individual analytes, breakthrough curves were obtained under the same treatment conditions by coupling the packed cartridge with a selective detection system such as a mass spectrometer. To monitor the concentration trend of a specific analyte over time, the cartridge effluent was analysed using a UPLC-MS/MS instrumentation (AQUITY UPLC H-Class PLUS system, Waters Corporation, Milford, MA, USA), targeting specific ion transitions. The resulting breakthrough sigmoid reveals the retention behaviour of the individual analyte with the sorbent.

In this case, it was not feasible to directly couple the packed cartridge with the UPLC-MS/MS detection system online. Therefore, effluent fractions were collected at two-minute intervals, transferred into vials, and analysed via UPLC-MS/MS, over a total analysis time of 30 minutes. The tracked signal was the chromatographic peak area associated with the ion transition of each analyte. Instrumental responses were plotted against flushing time, and the data points in the chromatographic area/time space were fitted to the Gompertz sigmoid function, defined as:

$$f(x) = d + (a - d) \cdot e^{-e^{-b \cdot (x-c)}}$$

From the Gompertz function providing the best fit for the experimental data, it was possible to extrapolate relevant information on the adsorption dynamics for each analyte. In fact, the Gompertz function, used to model the variation in recorded signals as a function of process time, is parameterized by four coefficients, each with a specific mathematical significance. The factors **d** and **a** represent the ordinate values to which the function asymptotically converges, at 0 and +∞, respectively. The constant $\boldsymbol{c}$ corresponds to the abscissa of the inflection point, while the coefficient **b** indicates the slope of the curve in the region of rapid growth. Each of these parameters takes on different values for each analyte, defining distinct adsorption dynamics in terms of saturation time, magnitude, and speed at which the asymptotic value is reached. This variability can be attributed to differential retention behaviour on the material due to the different the analyte properties. To provide a physicochemical interpretation of the results, logP, molecular weight, and pKa were plotted against Gompertz's coefficients and saturation times at 10% and 90% of the active sites (see **Section 3.5**).

2.8. Ultra-Performance Liquid Chromatography Coupled with Tandem Mass Spectrometry (UPLC-MS/MS)

To analyse the collected fractions using UPLC-MS/MS instrumentation, it was essential to optimize a separation procedure ensuring the simultaneous quantification of all the analytes. Chromatographic separation was performed using an ACQUITY UPLC H-Class PLUS® system (Waters Corporation, Milan, Italy). Analyte separation was conducted in reverse-phase mode on an XTerra C18 column

(2.1 x 150 mm, 3.5 μm) at a flow rate of 0.2 mL/min. Elution was carried out in a gradient mode with Milli-Q water containing 5 mM HCOOH (phase A) and acetonitrile containing 5 mM HCOOH (phase B) as the mobile phases. At t_0 phase B was 20% and it was increased to 80% in 20 min; this percentage was kept for 10 min, for a total run time of 30 min. The detection was carried out by an API 4000 tandem mass spectrometer (AB-Sciex, Foster City, CA, USA), equipped with a Turbo V source featuring an electrospray ionization (ESI) probe; detection was performed in dual polarity. The tandem mass spectrometry (MS/MS) settings were: capillary voltage +5000 V for positive polarity, and -4500 V for negative polarity, air nebulizer gas at 2 L/min, air drying gas at 450 °C and 20 L/min, nitrogen curtain gas at 5 L/min, and nitrogen collision gas at 4 mTorr. The full width at half maximum (FWHM) was set at 0.7 ± 0.1 m/z in each mass-resolving quadrupole to maintain unit resolution. Analyst® Software version 1.5 was used for data acquisition and processing. For each analyte, **Table D2** shows the mass spectrometric and chromatographic parameters: precursor ion (Q1), product ions (Q3), declustering potential (DP), entrance potential (EP), collision energy (CE), collision cell exit potential (CXP) and retention time.

3. Results and discussion

3.1. Characterization of regenerated material

The washing procedure, described in **Section 2.3**, allowed one to clean cigarette filters and to restore a material similar to the pristine CA. The effectiveness of the washing protocol and the final characteristics of the clean material were verified by the characterization carried out by UV-Vis spectroscopy, ATR-FTIR, and thermogravimetric analysis (TGA). A detailed discussion on the results, displayed in **Fig. D1**-**D3**, is reported in **Section D1** of the Appendix D.

3.2. Optimization of the synthetic strategy

Once the efficiency of the washing procedure was confirmed, a synthetic strategy was developed to produce a new sorbent material. The process variables chosen to optimize the synthetic procedure

were: amount of polymer in solution, percentage of activated carbon in the final material, magnetic stirring speed, quantity of Milli-Q water added during microemulsion breakage. The factors taken into account to evaluate the suitability of the final product included the distribution of microbead size, stability, and yield. Dimensionality and shape uniformity are among the most critical parameters for water remediation applications in flow-through mode, as they directly influence packing quality and, consequently, the efficiency of the purification process itself. Non-uniform material or particles that are excessively large or small can result in undesirable outcomes, such as: *i*) formation of multiple or preferential flow paths, leading to poor interaction between analytes and the material, and therefore, suboptimal water purification; *ii*) excessive back pressure, making the process energetically costly to facilitate water flow through the device.

To optimize the synthetic procedure, process variables were selected within a reasonable range. Three distinct levels were chosen for each parameter, resulting in an experimental matrix of 81 trials. Each synthetic trial was given a score to determine the best operating conditions and finalize the synthetic workflow. The values selected for each parameter are displayed in **Table D3**. The final optimized conditions are those detailed in the synthetic procedure described in **Section 2.4**.

3.3. Characterization of microbeads

3.3.1. SEM micrographs

SEM analyses were performed to investigate the morphology and size of the materials synthesized in form of microbeads (CA, CA@-20%). The two panels **a** and **b** in **Fig. 2** respectively show polymeric microspheres with a homogeneous composition of pure CA and its composite with activated carbons, which enhance adsorption yields. The images were captured at magnifications of 100X and 189X, respectively. In both cases, the CA-based microbeads appear to be reasonably monodispersed, with average diameters of approximately 200 μm.

3.3.2. ATR-FTIR spectra collection

ATR-FTIR analyses revealed that the spectra of commercial and recovered CA are almost superimposable (**Fig. D2**). These results reveal the recovery procedure is not responsible for a relevant degradation of the polymeric material. On the other hand, the activated carbons do not cause significant changes in the FTIR transmittance spectrum of the synthesized material (CA@AC-20%) compared to pristine CA (**Fig. 2**), demonstrating the capability of the synthetic strategy to deeply incorporate the additive within the sorbent. For an accurate identification of IR bands refer to **Section D1** of the Appendix D.

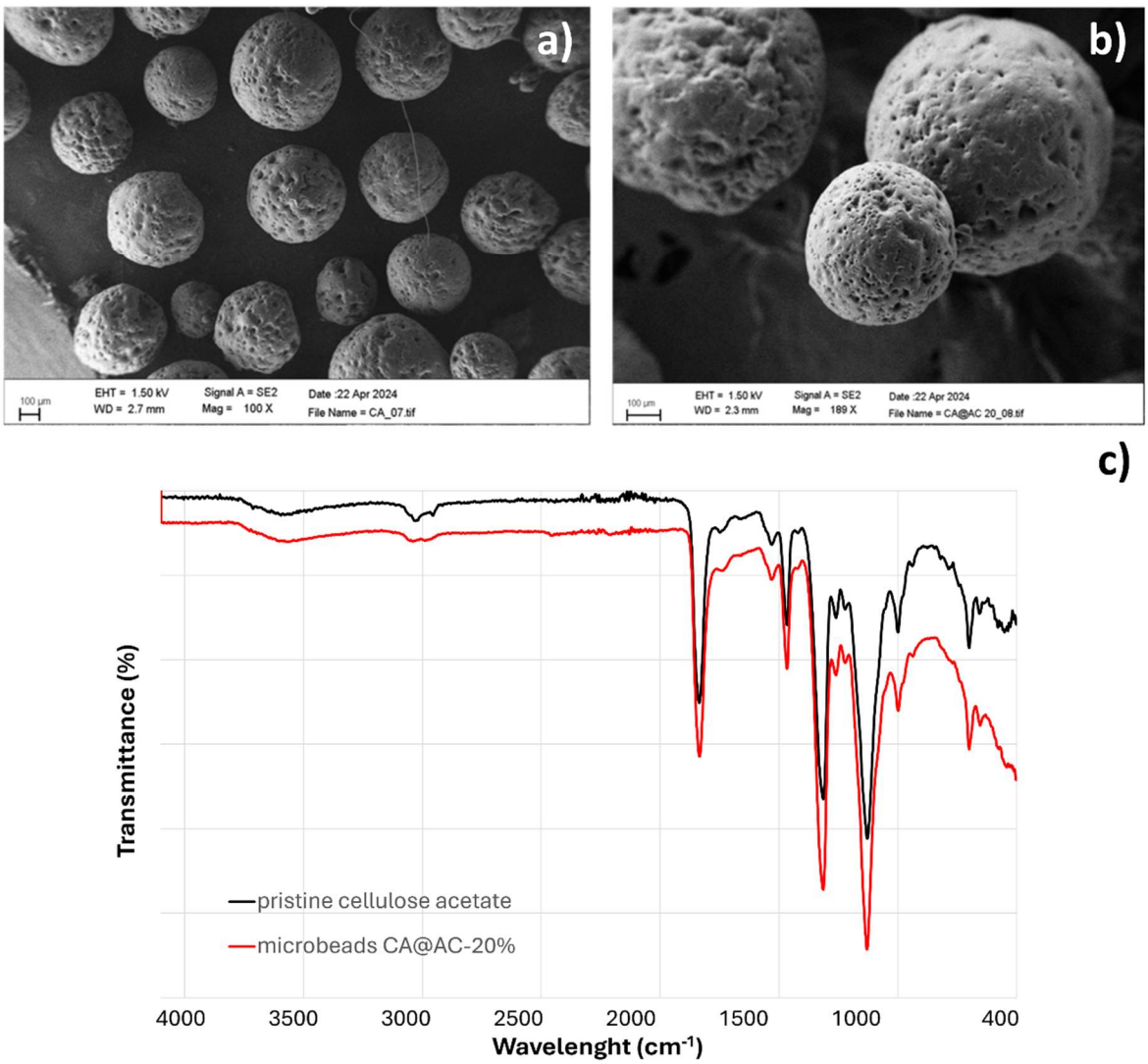

Fig. 2 SEM images and FTIR spectra of both microspheres composed solely of cellulose acetate (CA) (panel **a** and black spectrum) and composite microspheres (CA@-20%) (panel **b** and red spectrum).

3.4. Optimization of the instrumental workflow

Having confirmed that the material meets all the required criteria in terms of shape, size distribution, and stability, its applicability was evaluated. To assess the retention behaviour of the 40 selected contaminants under dynamic conditions, a glass cartridge was packed with a known quantity of the microbeads CA@AC-20%. A composite solution at a known concentration (0.5 mg L^{-1} of each analyte) was used as the test solution to evaluate the material adsorption abilities, in competitive mode. To optimize the critical parameters of the planned instrumental setup, an experimental design approach was employed. Details on the model type and parameters selected are provided in **Section 2.6**. **Table 1** reports the experimental matrix generated by the software. Each experiment, represented by a row in the table with its corresponding process conditions, was conducted in triplicate. For each experiment, mean values of the observables Y_1 and Y_2 were tabulated. From the mathematical fit of the experimental data, the response surface was obtained (**Fig. 3**).

Table 1 Experimental matrix for the optimization of setup parameters (X1 = flow rate, X2 = active carbons amount, X3 = microspheres amount).

X1 (mL min^{-1})	X2 (mg)	X3 (% w/w)
0.625	300	12.5
0.25	500	5
1	100	20
0.25	500	20
1	500	5
1	100	5
0.25	100	20
0.25	100	5
1	500	20

It was observed that, fixing X_1 at 0.25 mL/min, desirability increased upon rising values of the process variables X_2 and X_3. Optimal water treatment conditions were achieved at 0.25 mL/min using 500

mg of sorbent material doped with 20% activated carbon, resulting in a maximum desirability value of 0.707. Higher flow rates led to a faster leakage of the analytes, which can be explained by insufficient interaction time with the active sites of the sorbent.

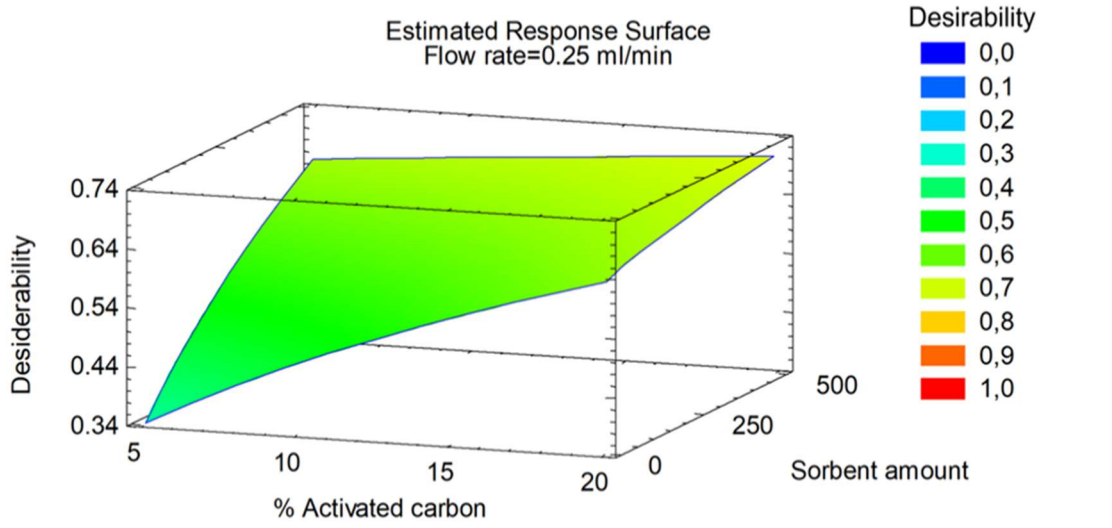

Fig. 3 Surface response of the experimental design obtained by fixing the experimental variable X1 (flow rate) to the fixed value of 0.25 mL min^{-1}.

3.5. Breakthrough curves

Once the optimal process conditions for the instrumental setup were established, the study of the sorbent retention capabilities was conducted. To this end, breakthrough curves related to the adsorption process of analytes were built. Depending on the experimental requirements, the integrated content of both all the analytes and the individual species at the cartridge outlet was monitored.

Following the overall concentration of the contaminants in the effluent solution, the breakthrough curve presented in **Fig. 4** was built. The sigmoid trend is typical of breakthrough curves for homogeneous solid sorbent materials. From the experimental trend, it was possible to drawn time values for the saturation of 10 and 90 % of the total available adsorption sites of the packed material. As an average on five replicates, the saturation times for the 10 and 90 % of saturation are 9.12 ± 0.03 min and 30.96 ± 0.08 min, respectively.

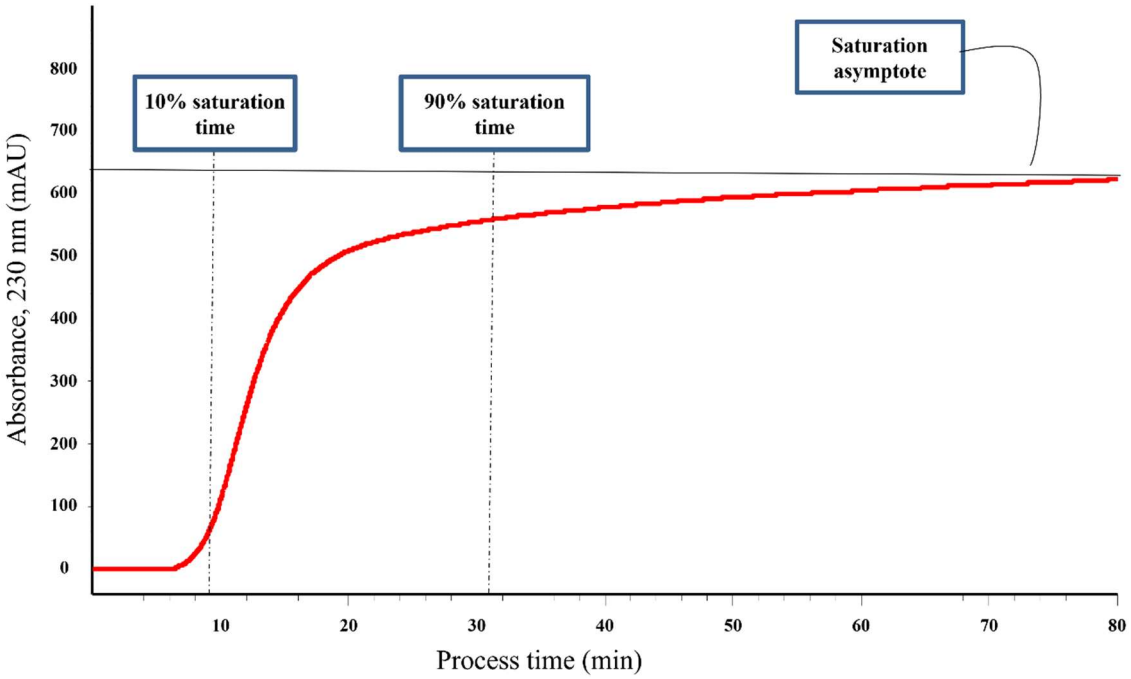

Fig. 4 The breakthrough curve integrated across all the analytes; saturation times corresponding to 10% and 90% saturation of the active sites within the packed cartridge are highlighted.

As described in **Section 2.7**, the breakthrough curves for each analyte were recorded under the same process conditions using an offline connection between the cartridge and a mass spectrometer detector. Based on the developed method, the limits of detection (LODs) for the analytes were calculated. These LODs serve as threshold values, meaning the material's removal effectiveness could only be assessed for concentrations at or above these limits. The LODs range from 0.2 to 14.2 µg/L, enabling the detection of analytes at environmentally relevant concentrations and allowing for the assessment of their removal even at low contamination levels. Instrumental features and performances of the detection method for each analyte are reported in **Table D4** of the Appendix D. Gompertz function is used to fit the experimental data for single analyte, returning a sigmoid trend parameterized by the coefficients defined in **Section 2.7**. **Fig. 5** presents the breakthrough curves for the adsorption process on the composite microspheres, along with the 10% and 90% saturation times of active sites for three representative analytes from each of the five contaminant classes.

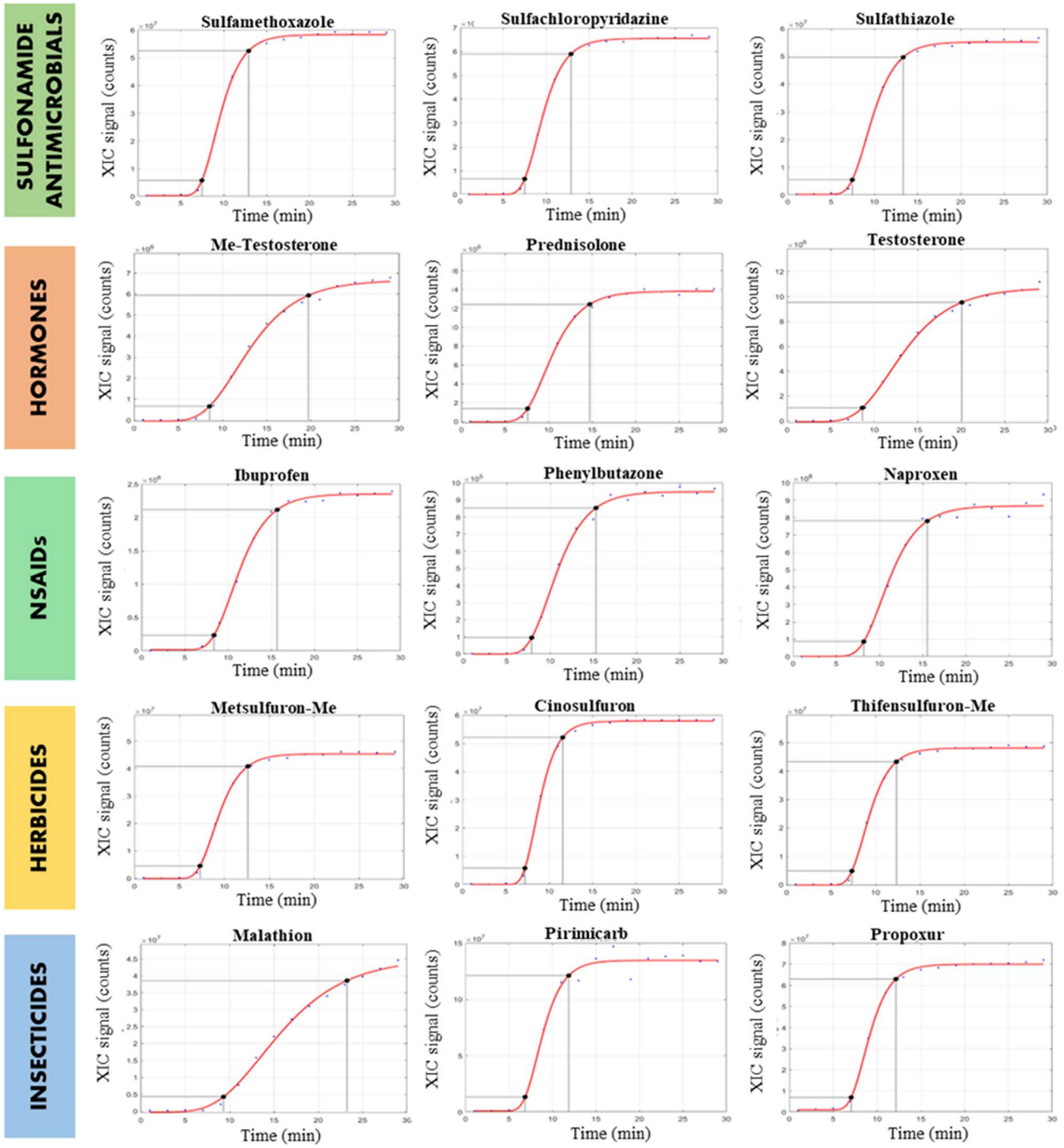

Fig. 5 Breakthrough curves corresponding of three individual analytes from each of the five classes of contaminants: sulfonamide antimicrobials, hormones, NSAIDs, herbicides and insecticides.

Saturation times are directly proportional to the availability of the sorbent active sites per analyte. Lipophilic analytes tend to interact more effectively with the material compared to polar analytes, although the contribution of functional groups on a molecule and their spatial arrangement within the chemical structure must also be considered. Another key parameter in defining the retention capabilities of the material with respect to the analytes is represented by the coefficients c and a of

the Gompertz function, which provides the best fit to the experimental data. All the coefficients of the Gompertz functions that best fit the experimental breakthrough trends of the analytes are reported in **Table 2**. As a measure of goodness of fit, the coefficient of determination (R^2) is reported for the trends provided for each of the analytes. To establish a correlation between these experimental parameters and the physicochemical properties of the analytes, they were plotted against the logP, pKa and molecular weights of the analytes. The best correlation is provided by following the trend of the coefficient c of the Gompertz function against the logP value of the analytes (see **Fig. 6**). The coefficient c of the Gompertz function varies proportionally as the logP values increase, following an approximately exponential trend. A sudden rise in the inflection points of the breakthrough curve is observed for logP values greater than 3.

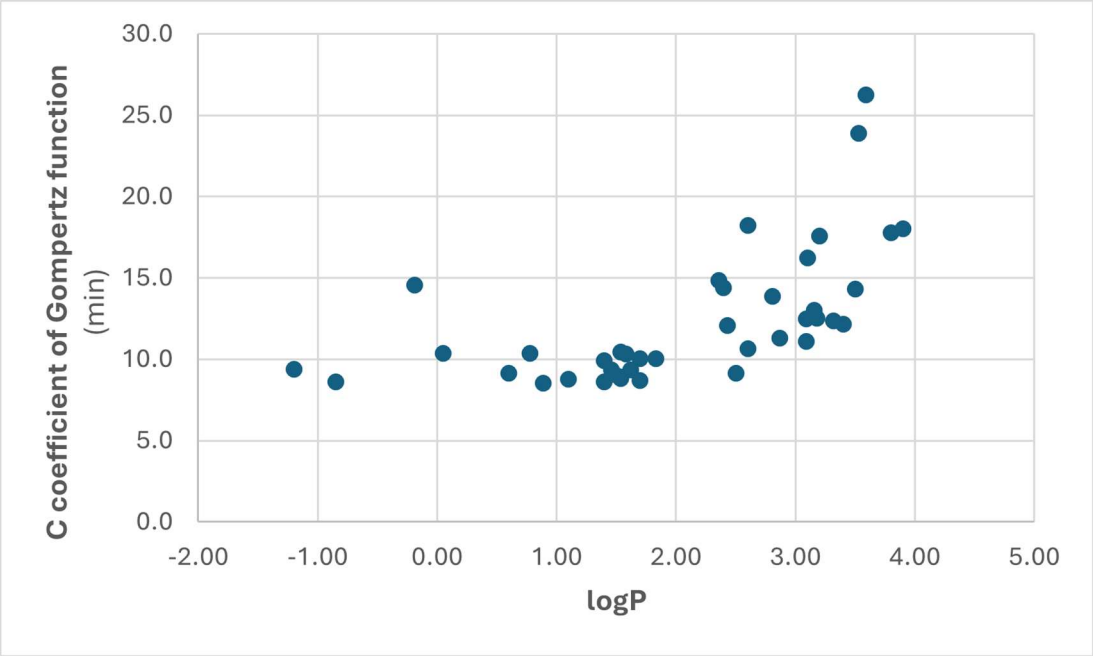

Fig. 6 Correlation of the c coefficient of the Gompertz function against the logP of the analytes.

To provide quantitative data on the material retention capacity, the amount of each analyte retained by the sorbent under saturation conditions was estimated. This information was extrapolated from the breakthrough curves of the individual analytes through geometric considerations. The area under the breakthrough sigmoid represents the amount of analyte that was not retained by the cartridge but instead passed through the material and was detected by the spectrophotometer. A 30-min interval was chosen as a secure temporal threshold, within which the sorbent active sites can be considered

saturated for all analytes, with their respective breakthrough curves reaching a *plateau*. Integrating the sigmoid from 0 to 30 minutes, an estimate of the total amount of analyte not retained by the cartridge during this time is provided. By subtracting this area from the integral of the saturation asymptote over the same interval, the resulting area reflects the amount of analyte retained by the material under competitive saturation conditions. This area value can then be converted into the quantity of analyte, expressed in nanograms, using a multiplicative constant **k**. This constant represents the relationship between the area unit and the analyte quantity and is calculated as the ratio of the area between the asymptotes over a time interval Δt to the amount of analyte passed through the cartridge in the same time interval. The multiplicative factor **k** transforms an area into an estimate of the amount of analyte retained in the cartridge. The analyte amount retained by the cartridge under saturation conditions (30 min) are reported in **Table 2**. As a result of these quantitative considerations, the material is able to adsorb a total amount of contaminants on the order of 125 µg per gram, in competitive mode, by using a dynamic retention strategy.

Table 2 Gompertz coefficients and saturation times of 10 and 90 % of the active sites related to the best model that fits the retention behaviour of each analyte.

	Analytes	Coefficient a of the Gompertz function	Coefficient b of the Gompertz function	Coefficient c of the Gompertz function	Coefficient d of the Gompertz function	10 % saturation time	90 % saturation time	Retained amount (µg)	R^2
1	**Acephate**	$2.71 \cdot 10^7$	0.6	8.6	$3.51 \cdot 10^5$	7.0	12.6	1.19	0.991
2	**Butoxycarboxim**	$1.01 \cdot 10^7$	0.6	8.8	$1.69 \cdot 10^5$	7.2	12.6	1.20	0.998
3	**Methomyl**	$7.66 \cdot 10^7$	0.4	9.2	$-2.11 \cdot 10^5$	7.1	14.7	1.32	0.998
4	**Sulfaguanidine**	$1.62 \cdot 10^7$	0.4	9.4	$2.24 \cdot 10^4$	7.5	14.4	1.33	0.995
5	**Sulfamerazine**	$3.05 \cdot 10^7$	0.4	8.5	$1.62 \cdot 10^5$	6.6	13.6	1.22	0.997
6	**Pirimicarb**	$1.44 \cdot 10^8$	0.6	8.7	$1.75 \cdot 10^6$	7.2	12.4	1.19	0.986
7	**Sulfamonomethoxine**	$9.95 \cdot 10^6$	0.3	10.0	$-3.79 \cdot 10^4$	7.5	16.9	1.47	0.997
8	**Sulfachloropyridazine**	$4.85 \cdot 10^7$	0.3	10.4	$-1.77 \cdot 10^5$	7.9	17.2	1.52	0.999
9	**Dimethoate**	$3.92 \cdot 10^6$	0.3	10.4	$-1.14 \cdot 10^4$	8.0	16.8	1.50	0.998
10	**Picloram**	$5.07 \cdot 10^6$	0.4	13.9	$-1.21 \cdot 10^3$	11.9	19.2	0.08	0.995
11	**Sulfathiazole**	$3.65 \cdot 10^7$	0.3	10.3	$-1.24 \cdot 10^5$	7.9	17.0	1.51	0.999
12	**Sulfamethoxazole**	$4.09 \cdot 10^7$	0.3	10.3	$-1.11 \cdot 10^5$	7.9	16.9	1.50	0.999
13	**Butocarboxim**	$2.16 \cdot 10^6$	0.5	9.4	$5.71 \cdot 10^3$	7.6	14.1	1.32	0.996
14	**Prednisolone**	$1.10 \cdot 10^7$	0.5	9.4	$7.32 \cdot 10^4$	7.7	13.6	1.30	0.999
15	**Thifensulfuron-Me**	$3.88 \cdot 10^7$	0.5	9.1	$2.65 \cdot 10^5$	7.5	13.4	1.90	0.998
16	**Propoxur**	$6.34 \cdot 10^7$	0.6	8.9	$5.82 \cdot 10^5$	7.5	12.6	1.48	0.999
17	**Dexametasone**	$5.59 \cdot 10^6$	0.3	10.0	$-5.81 \cdot 10^4$	7.6	16.9	1.24	0.992
18	**Cinosulfuron**	$5.26 \cdot 10^7$	0.6	8.6	$4.24 \cdot 10^5$	7.2	12.3	1.27	0.999
19	**Metsulfuron-Me**	$3.88 \cdot 10^7$	0.6	8.8	$2.93 \cdot 10^5$	7.3	12.9	1.23	0.999
20	**Chlorsulfuron**	$2.63 \cdot 10^5$	0.4	9.9	$2.15 \cdot 10^3$	7.8	15.5	1.19	0.952

21	**Carbaryl**	$1.18 \cdot 10^{7}$	0.2	14.8	$-1.02 \cdot 10^{5}$	9.6	24.6	1.65	0.995
22	**Atrazine**	$1.22 \cdot 10^{5}$	1.4	10.6	$3.63 \cdot 10^{3}$	10.0	12.2	1.41	0.991
23	**Isoproturon**	$1.67 \cdot 10^{7}$	0.3	11.3	$-9.09 \cdot 10^{4}$	8.3	19.4	1.23	0.995
24	**Metobromuron**	$2.44 \cdot 10^{6}$	0.2	14.5	$-2.07 \cdot 10^{3}$	10.1	23.8	1.89	0.992
25	**2,4-Dichlorophenol**	$9.75 \cdot 10^{5}$	0.2	12.5	$-9.49 \cdot 10^{3}$	8.7	21.8	1.80	0.998
26	**2,4-Dichlorophenoxyacetic Acid**	$2.27 \cdot 10^{7}$	0.2	12.1	$-1.86 \cdot 10^{5}$	8.7	20.9	1.58	0.999
27	**Naproxen**	$2.13 \cdot 10^{6}$	0.2	12.5	$-1.94 \cdot 10^{4}$	9.1	21.3	2.05	0.994
28	**Testosterone**	$8.20 \cdot 10^{6}$	0.2	12.4	$-5.44 \cdot 10^{4}$	9.0	21.0	1.35	0.997
29	**Flamprop**	$2.55 \cdot 10^{7}$	0.4	11.1	$-6.55 \cdot 10^{4}$	8.8	17.1	1.90	0.999
30	**Me-Testosterone**	$4.93 \cdot 10^{6}$	0.2	12.2	$-4.13 \cdot 10^{4}$	8.8	20.9	1.78	0.997
31	**Linuron**	$5.44 \cdot 10^{5}$	0.1	17.6	$-2.00 \cdot 10^{3}$	11.0	26.0	1.23	0.996
32	**Desmedipham**	$5.52 \cdot 10^{5}$	0.1	23.9	$3.77 \cdot 10^{3}$	13.6	27.4	1.76	0.956
33	**Phenmedipham**	$6.48 \cdot 10^{5}$	0.1	26.3	$2.47 \cdot 10^{3}$	13.8	27.6	1.94	0.968
34	**Nimesulide**	$3.44 \cdot 10^{6}$	0.1	18.2	$3.36 \cdot 10^{3}$	11.6	26.2	1.75	0.996
35	**Ibuprofen**	$9.01 \cdot 10^{5}$	0.2	14.3	$-4.34 \cdot 10^{1}$	10.2	23.4	1.79	0.999
36	**Procimidone**	$2.99 \cdot 10^{5}$	0.1	17.8	$-7.59 \cdot 10^{2}$	10.7	26.1	1.47	0.994
37	**Malathion**	$2.76 \cdot 10^{7}$	0.2	14.4	$-2.07 \cdot 10^{5}$	9.6	24.1	1.88	0.997
38	**Phenylbutazone**	$4.07 \cdot 10^{5}$	0.2	13.0	$-4.10 \cdot 10^{3}$	9.3	22.2	1.89	0.997
39	**Progesterone**	$2.33 \cdot 10^{6}$	0.2	18.0	$1.34 \cdot 10^{4}$	12.7	25.9	1.82	0.999
40	**Iprodion**	$3.48 \cdot 10^{4}$	0.2	16.2	$1.29 \cdot 10^{2}$	10.6	25.3	1.94	0.957

3.6 Stability and reuse of composite microbeads

The shelf life of a product is crucial for its possible industrial uses. The possibility of using the material long after its preparation is a characteristic that increases its appeal in industrial processes and expands its potential applications. This study explores the stability of the material after some months from the synthetic process and the performance of it in the adsorption process. For this reason, breakthrough curves have been collected in the same conditions after 6 months from the preparation, by storing the material at room temperature, protecting it from thermal and physical stress. To give an idea of the stability and reproducibility of the result, the comparison of the integrated breakthrough collected after six months, with material from the same synthesis batch, is shown in **Fig. D4** of the Appendix D. The deviation observed between the collected curves was less than 15%, without showing a significant decrease in the material's performance.

Activated carbons are widely used as adsorption additives in techniques and materials for water remediation. One of the main challenges associated with their application is the possibility of reuse. Two primary regeneration strategies for activated carbons have been reported in the literature. By either desorbing or decomposing the adsorbed chemical species, the material can be recovered in its original form, with varying effectiveness depending on the specific technology used [36]. In general, desorption is the most widely adopted method, as it does not require hazardous reagents that could pose environmental concerns [37]. However, solvent desorption, to the best of our knowledge, presents several drawbacks, including the aggressiveness of the solvents used, the poor reversibility of the adsorption process on activated carbon, and the relatively low recovery yields, often below 70%. For these reasons, thermal desorption is more commonly employed. While its efficiency depends on the specific type of activated carbon used, it generally provides higher desorption yields and reduces the need for additional chemical reagents. Thermal desorption is typically conducted at elevated temperatures ranging from 700°C to 1000°C, using either inert gases or controlled amounts of oxidizing gases, such as steam or flue gas. Treating cellulose acetate microspheres under these

conditions results in the desorption of retained organic compounds and, simultaneously, the carbonization of the cellulose acetate support [38]. This process yields activated carbon through regeneration and recycling. The resulting material can be integrated into a new production process for composite microspheres, paving the way for a circular utilization approach with minimal waste generation.

4. Conclusion

Addressing water scarcity and pollution requires a multifaceted approach that includes better resource management, pollution prevention, and the development of new materials for water purification. The innovative use of natural and recycled materials in water remediation represents a crucial step toward a more sustainable future. In the current work new sorbent materials were synthesized from the bioplastic cellulose acetate, recovered from cigarette butts. The sorbents exhibited excellent qualities in terms of both performance and applicability, as well as environmental sustainability. They were found to be non-toxic, eco-friendly, and low-cost materials. Stability of the produced microbeads was tested, showing reproducible performances after six months from the preparation. A reusability workflow was displayed based on the already reported conditions of contaminants desorption and cellulose acetate carbonization, projecting the material into a virtuous economic cycle. Based on the obtained results, it was confirmed that these materials have good retention capacity for a wide range of contaminants, positioning them as a potential alternative to traditional and common sorbents used in water remediation applications. Based on these considerations, the prospects for the use and applicability of the newly synthesized sorbent materials appear particularly promising. Future objectives include exploitation of the reusability of the sorbent as described in **Section 3.3** and the application of this approach to other polymers, the implementation of such materials to sample preparation methodologies and the possibility of a scale up of the process at an industrial level.

References

[1] R. K. Mishra, Fresh water availability and its global challenge, Br. J. multidiscip. Adv. Stud., (2023) 4(3), 1-78. https://doi.org/10.37745/bjmas.2022.0208

[2] N. B. Singh, G. Nagpal, S. Agrawal, Water purification by using sorbents: a review, Environ. Technol. Innov., (2018) 11, 187-240. https://doi.org/10.1016/j.eti.2018.05.006

[3] N. Akhtar, M. I. Syakir Ishak S. A. Bhawani, K. Umar, Various natural and anthropogenic factors responsible for water quality degradation: A review, Water, (2021) 13(19), 2660. https://doi.org/10.3390/w13192660

[4] S. Somma, E. Reverchon, L. Baldino, Water purification of classical and emerging organic pollutants: An extensive review, ChemEngineering, (2021) 5(3), 47. https://doi.org/10.3390/chemengineering5030047

[5] H. H. Ngo, W. Guo, J. Zhang, S. Liang, C. Ton-That, X. Zhang, Typical low cost biosorbents for adsorptive removal of specific organic pollutants from water, Bioresour. Technol., (2015) 182, 353-363. https://doi.org/10.1016/j.biortech.2015.02.003

[6] Á. I. López-Lorente, F. Pena-Pereira, S. Pedersen-Bjergaard, V. G. Zuin, S. A. Ozkan, E. Psillakis, The ten principles of green sample preparation. TrAC, Trends Anal. Chem., (2022) 148, 116530. https://doi.org/10.1016/j.trac.2022.116530

[7] S. Armenta, S. Garrigues, M. de la Guardia, Green analytical chemistry. TrAC, Trends Anal. Chem., (2008) 27(6), 497-511. https://doi.org/10.1016/j.trac.2008.05.003

[8] I. Ali, New generation sorbents for water treatment. Chem. Rev., (2012) 112(10), 5073-5091. https://doi.org/10.1021/cr300133d

[9] J. Li, X. Dong, X. Liu, X. Xu, W. Duan, J. Park, L. Gao, Y. Lu, Comparative study on the adsorption characteristics of heavy metal ions by activated carbon and selected natural adsorbents, Sustainability, (2022) 14(23), 15579. https://doi.org/10.3390/su142315579

[10] M. M. Sabzehmeidani, S. Mahnaee, M. Ghaedi, H. Heidari, V. A. Roy, Carbon based materials: a review of sorbents for inorganic and organic compounds, Mater. Adv., (2021) 2(2), 598-627. https://doi.org/10.1039/D0MA00087F

[11] M. S. Soffian, F. Z. A. Halim, F. Aziz, M. A. Rahman, M. A. M. Amin, D. N. A. Chee, Carbon-based material derived from biomass waste for wastewater treatment, Environ. Adv., (2022) 9, 100259. https://doi.org/10.1016/j.envadv.2022.100259

[12] J. M. Dias, M. C. Alvim-Ferraz, M. F. Almeida, J. Rivera-Utrilla, M. Sánchez-Polo, Waste materials for activated carbon preparation and its use in aqueous-phase treatment: a review, J. Environ. Manag., (2007) 85(4), 833-846. https://doi.org/10.1016/j.jenvman.2007.07.031

[13] R. R. Bansode, J. N. Losso, W. E. Marshall, R. M. Rao, R. J. Portier, Adsorption of volatile organic compounds by pecan shell-and almond shell-based granular activated carbons, Bioresour. Technol., (2003) 90(2), 175-184. https://doi.org/10.1016/S0960-8524(03)00117-2

[14] S. Y. You, Y. H. Park, C. R. Park, Preparation and properties of activated carbon fabric from acrylic fabric waste, Carbon, (2000) 38(10), 1453-1460. https://doi.org/10.1016/S0008-6223(99)00278-X

[15] D. Gomez-Maldonado, I. B. Vega Erramuspe, M. S. Peresin, Natural Polymers as Alternative Sorbents and Treatment Agents for Water Remediation, Bioresour., (2019) 14(4). https://doi.org/10.15376/biores.14.4.gomez-maldonado

[16] R. Qu, C. Sun, M. Wang, C. Ji, Q. Xu, Y. Zhang, C. Wang, H. Chen, P. Yin, Adsorption of Au (III) from aqueous solution using cotton fiber/chitosan composite sorbents, Hydrometallurgy, (2009) 100(1-2), 65-71. https://doi.org/10.1016/j.hydromet.2009.10.008

[17] V. Rajakovic, G. Aleksic, M. Radetic, L. Rajakovic, Efficiency of oil removal from real wastewater with different sorbent materials, J. Hazard. Mater., (2007) 143(1-2), 494-499. https://doi.org/10.1016/j.jhazmat.2006.09.060

[18] P. Stigler Granados, L. Fulton, E. Nunez Patlan, M. Terzyk, T. E. Novotny, Global health perspectives on cigarette butts and the environment, Int. J. Environ. Res. Public Health, (2019) 16(10), 1858. https://doi.org/10.3390/ijerph16101858

[19] T. E. Novotny, K. Lum, E. Smith, V. Wang, R. Barnes, Cigarettes butts and the case for an environmental policy on hazardous cigarette waste, Int. J. Environ. Res. Public Health, (2009) 6(5), 1691-1705. https://doi.org/10.3390/ijerph6051691

[20] E. Slaughter, R. M. Gersberg, K. Watanabe, J. Rudolph, C. Stransky, T. E. Novotny, Toxicity of cigarette butts, and their chemical components, to marine and freshwater fish, Tob. Control, (2011) 20(Suppl 1), i25-i29. https://doi.org/10.1136/tc.2010.040170

[21] J. Torkashvand, M. Farzadkia, H. R. Sobhi, A. Esrafili, Littered cigarette butt as a well-known hazardous waste: a comprehensive systematic review, J. Hazard. Mater., (2020) 383, 121242. https://doi.org/10.1016/j.jhazmat.2019.121242

[22] T. E. Novotny, S. N. Hardin, L. R. Hovda, D. J. Novotny, M. K. McLean, S. Khan, Tobacco and cigarette butt consumption in humans and animals, Tob. Control, (2011) 20(Suppl 1), i17-i20. https://doi.org/10.1136/tc.2011.043489

[23] H. Kurmus, A. Mohajerani, The toxicity and valorization options of cigarette butts, J. Waste Manag., (2020) 104, 104-118. https://doi.org/10.1016/j.wasman.2020.01.011

[24] M. G. De Cesaris, N. Felli, L. Antonelli, I. Francolini, G. D'Orazio, C. Dal Bosco, A. Gentili, Recovery of cellulose acetate bioplastic from cigarette butts: realization of a sustainable sorbent for water remediation, Sci. Total Environ., (2024) 929, 172677. https://doi.org/10.1016/j.scitotenv.2024.172677

[25] J. Ganster, H. P. Fink, Cellulose and cellulose acetate, in Bio-Based Plastics: Materials and Applications (2013) 35-62. https://doi.org/10.1002/9781118676646.ch3

[26] M. Oprea, S. I. Voicu, Cellulose acetate-based materials for water treatment in the context of circular economy, Water, (2023) 15(10), 1860. https://doi.org/10.3390/w15101860

[27] X. Zhang, M. Yu, Y. Li, F. Cheng, Y. Liu, M. Gao, G. Liu, L. Hu, Y. Liang, Effectiveness of discarded cigarette butts derived carbonaceous sorbent for heavy metals removal from water, Microchem. J., (2021) 168, 106474. https://doi.org/10.1016/j.microc.2021.106474

[28] M. Oprea, S. I. Voicu, Cellulose acetate-based membranes for the removal of heavy metals from water in the context of circular economy. Ind. Crop. Prod., (2023) 206, 117716. https://doi.org/10.1016/j.indcrop.2023.117716

[29] J. Uebe, T. Paulauskiene, K. Boikovych, Cost-effective and recyclable aerogels from cellulose acetate for oil spills clean-up. ESPR., (2021) 28, 36551-36558. https://doi.org/10.1007/s11356-021-13369-9

[30] P. Ananthi, K. Hemkumar, S. Manikandan, Cellulose acetate based-membrane supported by metal-organic frameworks for the removal of diclofenac and ciprofloxacin from polluted water. Groundw. Sustain. Dev., (2024) 26, 101308. https://doi.org/10.1016/j.gsd.2024.101308

[31] W. M. Shackelford, D. M. Cline, Organic compounds in water, Environ. Sci. Technol., (1986) 20(7), 652-657. https://pubs.acs.org/doi/pdf/10.1021/es00149a002

[32] H. Patel, Fixed-bed column adsorption study: a comprehensive review, Appl. Water Sci., (2019) 9(3), 45. https://doi.org/10.1007/s13201-019-0927-7

[33] L. Antonelli, M. C. Frondaroli, M. G. De Cesaris, N. Felli, C. Dal Bosco, E. Lucci, A. Gentili, Nanocomposite microbeads made of recycled polylactic acid for the magnetic solid phase extraction of xenobiotics from human urine, Microchim. Acta, (2024) 191(5), 1-14. https://doi.org/10.1007/s00604-024-06335-y

[34] M. A. E. de Franco, C. B. de Carvalho, M. M. Bonetto, R. de Pelegrini Soares, L. A. Féris, Removal of amoxicillin from water by adsorption onto activated carbon in batch process and fixed bed column: kinetics, isotherms, experimental design and breakthrough curves modelling, J. Clean. Prod., (2017) 161, 947-956

[35] K. H. Chu, Fitting the Gompertz equation to asymmetric breakthrough curves, J. Environ. Chem. Eng., (2020) 8, 103713. https://doi.org/10.1016/j.jclepro.2017.05.197

[36] O. Zanella, I. C. Tessaro, L. A. Féris, Desorption-and decomposition-based techniques for the regeneration of activated carbon, Chem. Eng. Technol., (2014) 37(9), 1447-1459. https://doi.org/10.1002/ceat.201300808

[37] F. Huang, W. Liu, S. Chen, Z. Tian, J. Wei, Thermal desorption characteristics of the adsorbate in activated carbon based on a two-dimensional heat and mass transfer model, Appl. Therm. Eng., (2022) 214, 118775. https://doi.org/10.1016/j.applthermaleng.2022.118775

[38] J. Fischer, K. Thummler, S. Fischer, I. G. Gonzalez Martinez, S. Oswald, D. Mikhailova, Activated carbon derived from cellulose and cellulose acetate microspheres as electrode materials for symmetric supercapacitors in aqueous electrolytes, Energy Fuels, (2021) 35(15), 12653-12665. https://doi.org/10.1021/acs.energyfuels.1c01449

Chapter 4: Polymeric blend recycling for sample preparation applications

Overview

As the final development of this project, the principles of circularity and greenness, already extensively discussed, were integrated with one of the most recent trends in analytical chemistry and method development: the use of 3D printing technique for devices preparation [1]. This emerging approach has attracted considerable attention due to the remarkable design freedom it offers, allowing the fabrication of customized devices with virtually unlimited geometries [2]. The possibility of easily and cost-effectively producing extraction accessories of any shape represents a significant technological advancement, particularly in the context of miniaturization and process integration [3]. Such modularity enables the design of microfluidic systems capable of combining multiple pretreatment steps [4], extraction supports with enhanced retention capacities [5], and devices with geometries optimized to maximize the enrichment factor of the extraction technique [6]. However, these advantages come at the cost of introducing new synthetic materials into the analytical workflow. The present work aims to propose a solution that merges the structural adaptability and modularity of 3D-printed architectures with the concept of polymer recycling and reuse. To this end, LEGO® bricks were selected as the basis for developing extraction devices for analytes in complex matrices. As inherently modular and reconfigurable units, LEGO® bricks can be assembled into a wide variety of geometries, limited only by the operator's creativity. This proposal also represents one of the first examples of recycling polymeric blends within sample pretreatment processes, since LEGO® bricks are composed of acrylonitrile–butadiene–styrene (ABS), a copolymer for which large-scale and easy recycling strategies are still lacking [7]. In the following study, various LEGO®-based configurations are explored as supports for a menthol-based sustainable extractant containing carboxylated multi-walled carbon nanotubes. The resulting devices are designed to be self-rotating during adsorption, indefinitely reusable, and to enable near zero-waste pretreatment procedures. The demonstrated analytical applicability, compliance with common analytical performance standards, and structural

reproducibility open the way for a broader use of LEGO®-based platforms across various areas of analytical chemistry, from sensing and separation sciences to microfluidics.

References

[1] Li, F., Ceballos, M. R., Balavandy, S. K., Fan, J., Khataei, M. M., Yamini, Y., & Maya, F. (2020). 3D Printing in analytical sample preparation. *Journal of Separation Science*, *43*(9-10), 1854-1866. https://doi.org/10.1002/jssc.202000035

[2] Monteiro, S. A., Scheid, C., Deon, M., & Merib, J. (2023). Fundamentals, recent applications, and perspectives of 3D printing in sample preparation approaches. *Microchemical Journal*, *195*, 109385. https://doi.org/10.1016/j.microc.2023.109385

[3] Soares da Silva Burato, J., Vargas Medina, D. A., de Toffoli, A. L., Vasconcelos Soares Maciel, E., & Mauro Lanças, F. (2020). Recent advances and trends in miniaturized sample preparation techniques. *Journal of separation science*, *43*(1), 202-225. https://doi.org/10.1002/jssc.201900776

[4] Wang, L., & Pumera, M. (2021). Recent advances of 3D printing in analytical chemistry: Focus on microfluidic, separation, and extraction devices. *TrAC Trends in Analytical Chemistry*, *135*, 116151. https://doi.org/10.1016/j.trac.2020.116151

[5] Kołodziej, D., Sobczak, Ł., & Goryński, K. (2022). Polyamide noncoated device for adsorption-based microextraction and novel 3D printed thin-film microextraction supports. *Analytical Chemistry*, *94*(6), 2764-2771. https://doi.org/10.1021/acs.analchem.1c03672

[6] Carrasco-Correa, E. J., Herrero-Martínez, J. M., Simó-Alfonso, E. F., Knopp, D., & Miró, M. (2022). 3D printed spinning cup-shaped device for immunoaffinity solid-phase extraction of diclofenac in wastewaters. *Microchimica Acta*, *189*(5), 173. https://doi.org/10.1007/s00604-022-05267-9

[7] Deshmukh, D., Kulkarni, H., Srivats, D. S., Bhanushali, S., & More, A. P. (2024). Recycling of acrylonitrile butadiene styrene (ABS): A review. Polymer Bulletin, 81(13), 1-38. https://doi.org/10.1007/s00289-024-05269-y

Paper V: LEGO® Bricks as Modular Platforms for Circular Sample Preparation

L. Antonelli, M. Bartocci, N. Felli, M. G. De Cesaris, A. Gentili (2026). **LEGO® brick supporting a thermo-responsive sorptive phase: a modular platform for circular sample preparation.** *Under submission*

Graphical abstract

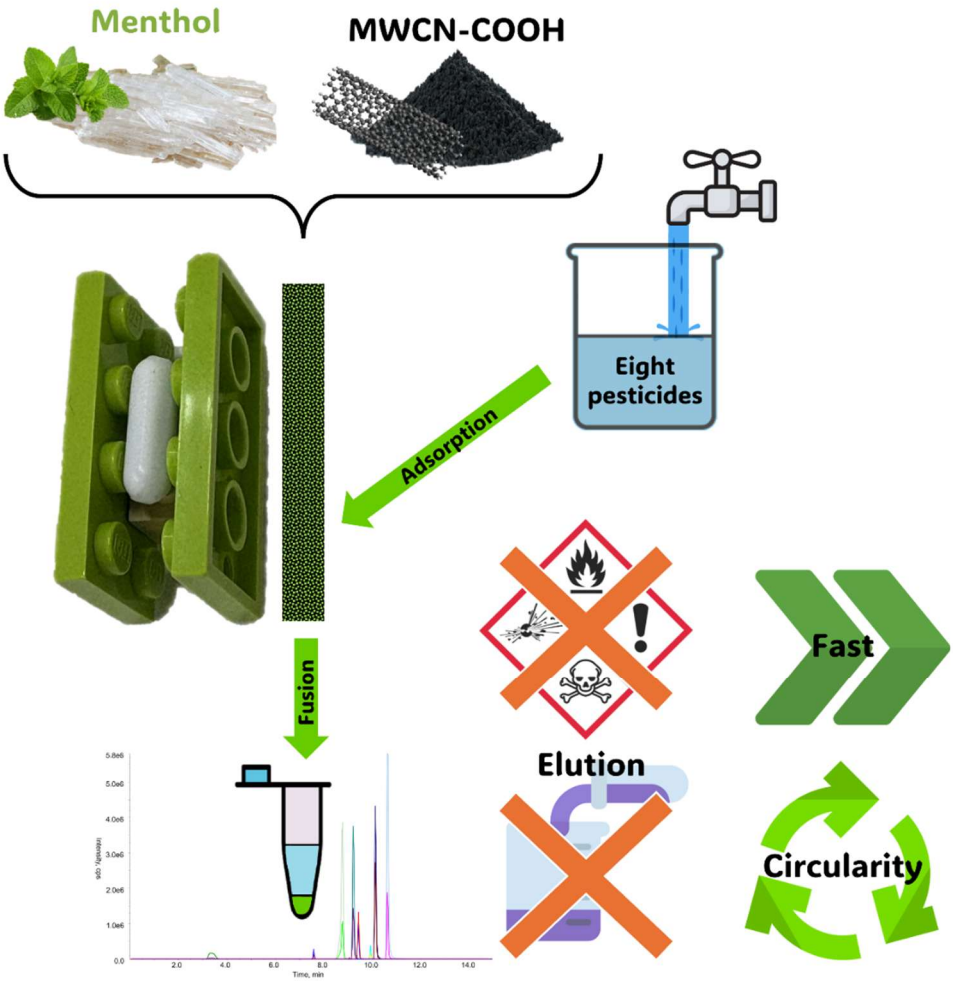

Abstract

This work is framed within the paradigm of Circular Analytical Chemistry (CAC), which promotes the integration of waste-derived materials, minimization of resource consumption, and development of near closed-loop analytical procedures. In line with this prevailing trend, we present a proof-of-concept extraction device constructed entirely from recycled LEGO® bricks, serving as supports for a thin coating composed of carboxylated multi-walled carbon nanotubes dispersed in L-menthol (1.3 % w/w). The proposed tool combines a modular and indefinitely reusable Acrylonitrile Butadiene Styrene plastic support, with a sorptive phase derived from renewable and low-impact components. The extraction procedure was applied to the extraction of eight common pesticides from tap water samples thanks to the adsorption properties of the coating layer, solid at room temperature; the analyte desorption step was realized placing the brick in a becker and heating at 59°C to melt menthol. The workflow is nearly zero-waste, requiring only 200 μL of isopropanol to wash the brick and avoid solidification of the menthol extract, which can be directly injected for the chromatographic analysis after centrifugation. Besides its sustainable design, the method demonstrates good analytical performance, with average recoveries ranging from 86.6 to 113 %, precision between 2.7 and 15 %, and limits of quantification ≤ 0.15 μg L^{-1}, comparable or even better than conventional extraction techniques. Besides analytical performance, this approach embraces the concepts of recycling, moving beyond the traditional approaches of Green Analytical Chemistry toward strategies that valorize waste materials and pursue the broader goals of CAC.

Keywords:

Circular Analytical Chemistry, Green Sample Preparation, Recycled Plastic, Menthol, Carbon nanotubes

1. Introduction

The exponential growth in the consumption of polymeric materials has led to the generation of vast quantities of plastic waste, raising major concerns regarding environmental sustainability and resource efficiency [1, 2]. Among these plastics, Acrylonitrile Butadiene Styrene (ABS) is particularly widespread [3]. ABS is an engineering thermoplastic composed of particulate rubber, typically polybutadiene, uniformly dispersed in a styrene–acrylonitrile matrix [3-6]. The excellent impact resistance, dimensional stability, chemical resistance, and ease of processing have led to its extensive application in industries ranging from automotive and electronics to household appliances and toys [7]. In particular, ABS is the material used in the production of LEGO® bricks, making it one of the most consumed and recognizable polymers worldwide [8]. Despite its versatility, ABS waste represents a significant challenge due to its persistence in the environment, limited biodegradability, and the need for effective recycling strategies [9, 10]. In this context, the emerging paradigm of Circular Analytical Chemistry (CAC) provides a comprehensive framework for rethinking how materials, methods, and workflows are conceived and implemented in analytical science [11]. CAC seeks to decouple analytical performance from resource consumption and to promote the transition toward a closed-loop, waste-free sector. Beyond the principles of Green Analytical Chemistry (GAC) [12], CAC emphasizes waste collection and reuse, optimization of resource and energy efficiency, minimization of hazards, and the integration of post-consumer waste into new analytical applications. A particularly dynamic field where these principles are being realized is sample preparation, where the valorisation of waste-derived materials is increasingly recognized as a sustainable innovation driver [13]. A growing body of literature demonstrates how recycling strategies can be effectively incorporated into analytical procedures, with numerous examples of solid-phase extraction (SPE) [14-16], dispersive solid-phase extraction (d-SPE) [17], and microextraction methods [18, 19] relying on sorbents obtained from end-of-life plastics [20, 21], biopolymer residues [22-24], or industrial by-products [14, 25]. These recycled adsorbents, part of

the broader class of green sorbents [26-28], not only reduce the environmental footprint of analytical workflows but also offer efficient and cost-effective alternatives to conventional synthetic materials.

One recent technological trend in sample preparation is the three-dimensional (3D) printing [29, 30] to fabricate cost-effective customizable solid-phase extraction (SPE) cartridges [31], liquid–liquid extraction chambers, and membrane-based separators [32]. These devices can be further improved by surface functionalization [33], incorporation of micro- or nanostructured sorbents [34], or post-printing chemical modifications [35] to enhance their analytical performance. The strength of 3D printing lies in its ability to rapidly produce modular and adaptable platforms, which can be tailored to specific extraction workflows.

Building on this concept, we introduce an alternative strategy that combines the recycling of ABS plastic waste with the development of modular analytical devices. Specifically, we present the first proof-of-concept of a sample preparation device constructed entirely from recycled LEGO® bricks. LEGO® units provide distinct advantages: they are standardized, mechanically robust, and can be readily assembled into customizable three-dimensional configurations. This approach resembles the flexibility of 3D printing, yet it requires no specialized fabrication infrastructure and, importantly, introduces no additional polymeric material into the analytical workflow. Such modularity offers a versatile and sustainable platform that can be reshaped and adapted to a wide range of analytical applications.

The specific aim of this study is to develop and evaluate, for the first time, a LEGO®-based extraction device coated with a thin sorptive phase composed of carboxylated-Multi-Walled Carbon Nanotubes (COOH-MWCNTs) dispersed in L-menthol. The device was tested for the extraction of some common pesticides - acetamiprid, acibenzolar-S-methyl, pyraflufen-ethyl, clofentezine, diflufenican, oxyfluorfen, propaquizafop, and pendimethalin - from tap water. Taking advantage of the low melting point of L-menthol (42-44 °C), the extraction steps are obtained playing on its different physical state: solid for the analyte adsorption carried at room temperature and liquid for the analyte release

conducted through a mild heating to melt menthol. Beyond the high analytical standards, this application highlights the potential of LEGO® bricks as highly available and reproducible building units, whose intrinsic versatility and modularity can lead to the design of many other modular extraction devices.

2. Experimental section

2.1. Materials and reagents

A wide assortment of LEGO® bricks was gathered from the authors' personal collections. Various brick typologies were selected to define the optimal structural configuration of the device, all of which are illustrated in **Fig. E1** of the Appendix E. All reagents were of analytical grade or better. UPLC grade methanol was obtained by VWR International, Radnor, USA and used as the B component of the mobile phase and dilution solvent for stock solutions preparation. Isopropanol hypergrade for LC-MS was from Supelco (Merck Life Science S.r.l., Milan, Italy). Formic acid (HCOOH, ≥ 98 %) was from Acros Organics B.V.B.A. (Waltham, USA). Milli-Q water was generated by the "Direct-Q® 3 UV System", Merck KGaA (Darmstadt, Germany) and used as the A component of the mobile phase. Acetamiprid (≥ 99.0 %) was purchased from Dr. Ehrenstorfer (LGC standards, Milan, Italy). Acibenzolar-S-methyl (≥ 98.0 %), pyraflufen-ethyl (≥ 98.0 %), clofentezine (≥ 98.0 %), diflufenican (≥ 95.0 %), oxyfluorfen (≥ 98.0 %), propaquizafop (≥ 98.0 %), pendimethalin (≥ 98.0 %), L-menthol (≥ 98.5 %) and COOH-MWCNTs (> 8 % carboxylic acid functionalized) were supplied by Sigma Aldrich (Merck Life Science S.r.l., Milan, Italy).

The chemical classification, logP, pKa, molecular formula, CAS number, vapor pressure, boiling point, exact mass and structure of each analyte is reported in **Table E1** of the Appendix E. The individual standards were weighed using a precision analytical balance (Ohaus DV215CD Discovery semi-micro and analytical balance, 81/210 g capacity, 0.01/0.1 mg readability) and diluted in 2 mL of methanol to prepare stock solutions (1 mg mL^{-1} for all the analytes except for clofentezine at 0.2

mg mL^{-1}). A composite standard solution of the eight analytes was prepared at 1 mg L^{-1}. Other working solutions and calibrators at different concentrations were prepared by diluting the stock composite standard solution with methanol. All solutions were stored at 4 °C.

2.2. Tap water samples

Tap water was collected directly from three different households located in Rome and its surrounding areas. Samples were taken weekly from Monteverde Vecchio, Appio Alessandrino, and Guidonia-Montecelio, respectively. The water samples were transferred to the laboratory in sterile glass containers, pooled, and stored at 4 °C for no longer than one week prior to use. The pooled water was confirmed to be free of pesticides through preliminary analysis and employed as a blank matrix for the preparation of fortified samples.

2.3. Thermogravimetric analysis of the polymeric support

TGA analysis was conducted to follow the thermal behaviour of ABS from LEGO® bricks, to define a temperature range of stability before degradation. The analysis was realized with a Thermal Analysis System TGA 2 from Mettler-Toledo (Milan, Italy) and obtained under the following conditions: 25–800 °C, heating rate of 10 °C min^{-1}, in air.

2.4. Preparation of the extraction device

The extraction device developed for pesticide recovery from aqueous matrices was assembled from interlocking LEGO® bricks. Specifically, each extraction unit consists of two LEGO® PLATE 2×4 units (ID: 3020) and two LEGO® TECHNIC BRICK 1×1 units (ID: 6541).

The two PLATE components were coated with a pre-prepared menthol/COOH-MWCNT mixture, in which COOH-MWCNTs were incorporated at 1.3 % w/w relative to L-menthol. The mixture was obtained by weighing the components in the appropriate ratio into a 20 mL vial, stirring at ~50 °C for 10 min on a magnetic stirrer plate and sonicating in a water bath at 50°C for the following 2 min to prevent COOH-MWCNT aggregation and obtain and homogeneous dispersion. Aliquots of 200 µL

were pipetted onto the concave side of each PLATE unit and uniformly spread to cover the entire surface, yielding a coating with an average thickness of ~ 1 mm. The procedure was repeated for both PLATE components, which were then left to dry at room temperature until the menthol coating had completely solidified.

Once coated, the device was assembled by anchoring the PLATE unit to the TECHNIC BRICK unit, exploiting the interlocking fit between the central studs of the PLATE and the central holes of the TECHNIC BRICK. The cavity formed above the TECHNIC BRICK was suitable for accommodating a magnetic stir bar (5 x 15 mm). The final configuration is illustrated in **Fig. 1a**. The device, once assembled, can be immersed in the sample and agitated using a conventional magnetic stirrer to promote extraction of the analytes mediated by menthol/COOH-MWCNTs.

2.5. The extraction procedure

Aliquots of 40 mL of tap water were transferred into twelve 100-mL beakers containing the extraction units. The beakers were placed on a 12-position magnetic stirrer for 30 min, setting the agitation at low speed (130 rpm) to maintain a small, steady vortex. After the adsorption step, each device was removed from the solution using tweezers and left to dry for 5 min. The PLATE units were then transferred into 5-mL vials and heated at 60 °C to melt the menthol-based sorptive phase. The menthol/COOH-MWCNT suspension was collected at the bottom of the vial. To ensure complete recovery, 200 µL of isopropanol was used as a dissolving agent, allowing the full amount of menthol coating to detach from the PLATE surface. Extracts from both PLATE units were combined in a single Eppendorf tube and brought to a final volume of 1 mL with isopropanol. The addition of this solvent prevented re-solidification of the extractant by lowering the melting point of the mixture. Finally, the tube was centrifuged to sediment the COOH-MWCNTs, and the supernatant was transferred into vials for direct UPLC-DAD or UPLC-MS/MS analysis (3 µL injection volume). The whole procedure is illustrated in **Fig. 1b**.

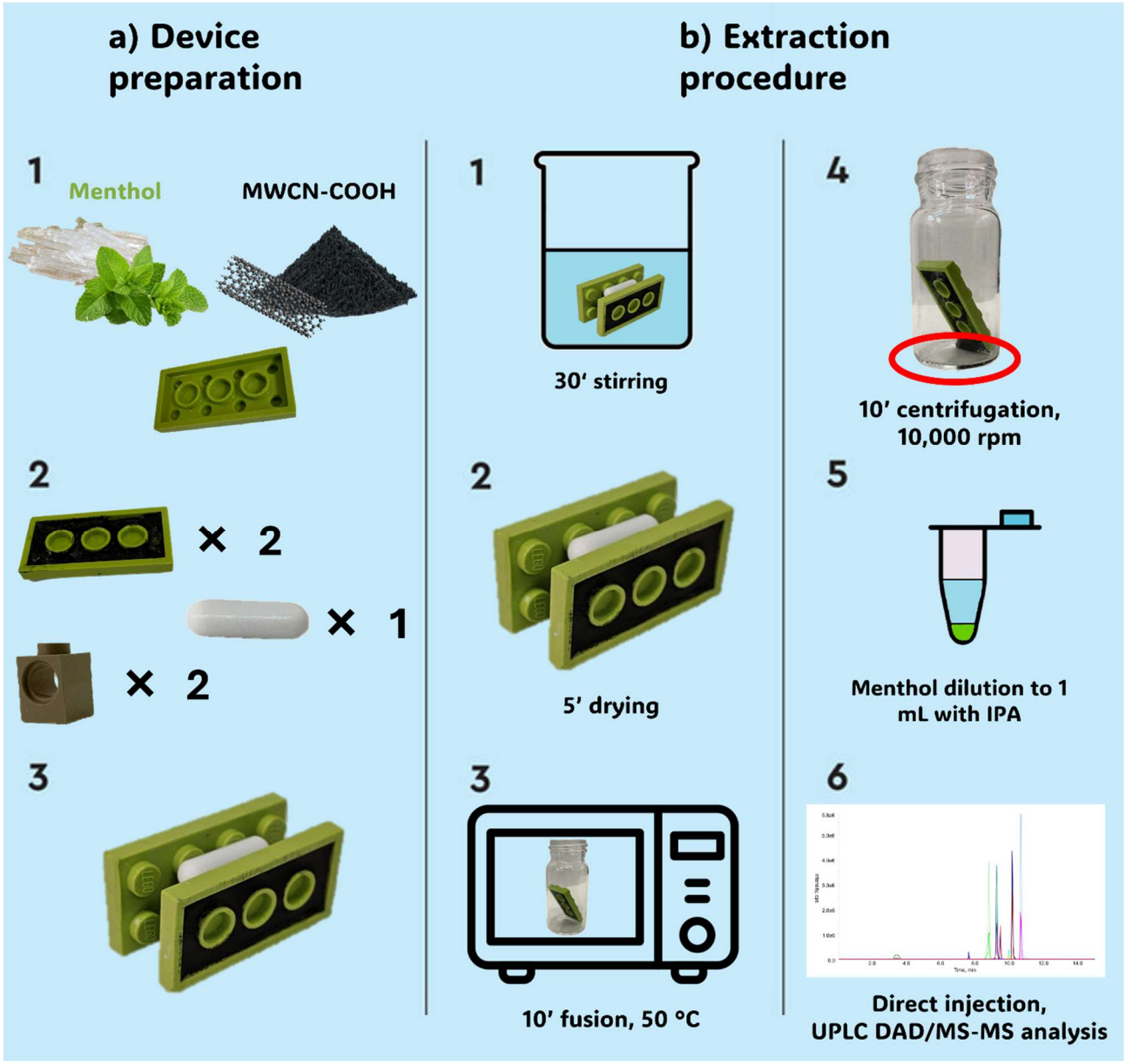

Fig. 1 Device composition (**a**) and extraction procedure (**b**) of the method.

2.6. UPLC-DAD conditions

Chromatographic analyses for the optimization study were carried out on a Shimadzu ultra-performance liquid chromatography system (UPLC-DAD, Shimadzu Corporation, Kyoto, Japan) consisting of a system controller (CBM-40), a degassing unit (DGU-405), a binary solvent delivery module (LC-40D xR), an autosampler (SIL-40C xR), a column oven (CTO-40C), and a diode array detector (SPD-M40). The instrumentation was equipped with an HSS T3 column (2.1 × 100 mm, 1.8 µm, C18 chemistry; Waters Corporation), protected by a VanGuard Pre-Column® with the same stationary phase (2.1 × 5 mm). The mobile phases consisted of Milli-Q water with 0.1 % formic acid

(A) and methanol with 0.1 % formic acid (B). Separation was performed at a flow rate of 0.3 mL min^{-1} with the following gradient program: 0–3 min, isocratic at 50 % B; 3–16 min, linear gradient from 50 % to 100 % B; 16–18 min, isocratic at 100 % B; 18–18.1 min, linear gradient from 100 % to 50 % B to restore initial conditions.

System control, data acquisition, and processing were performed using LabSolutions software (Shimadzu). Chromatograms were acquired for each analyte at the wavelength of the maximum absorption (acetamiprid: 246 nm; acibenzolar-S-methyl: 255 nm; pyraflufen-ethyl: 250 nm; clofentezine: 272; diflufenican: 277 nm; oxyfluorfen: 276 nm; propaquizafop: 246 nm; pendimethalin: 245 nm).

2.7. UPLC-MS/MS conditions

The chromatographic separation for the validation study was carried out on an ACQUITY UPLC H-Class PLUS® system (Waters Corporation, Milford, MA, USA); the instrument was equipped with the same column of the UPLC-DAD instrumentation, and the analyses were carried out at the same eluent conditions.

The effluent from the chromatographic column was directed to a Turbo V electrospray ionization (ESI) source coupled to a triple quadrupole mass spectrometer (API 4000 QTrap, AB SCIEX, Foster City, CA, USA). Data acquisition was performed in dual polarity mode, with capillary voltages of +5000 V (positive ionization) and −4500 V (negative ionization). The chromatograms were acquired in Multiple reaction monitoring (MRM), selecting two MRM transitions for each analyte. Nitrogen, generated by a Parker-Balston 75A74 generator (Haverhill, MA, USA), was used as collision gas (4 mTorr) and curtain gas (5 L min^{-1}). Nebulizer gas (air, 2 L min^{-1}) and drying gas (air, 20 L min^{-1} at 450 °C) were supplied by a Jun-Air 4000-40M compressor (Bromsgrove, UK).

Mass resolution was maintained at unit resolution by setting the full width at half maximum (FWHM) to 0.7 ± 0.1 m/z in each quadrupole. LC-MS parameters optimized for the eight target analytes are

summarized in **Table 1**. A representative UPLC-MRM chromatogram of the composite working solution (0.3 ng injected) is shown in **Fig. E2** of the Appendix E.

Data acquisition and processing were performed using Analyst software version 1.5.1.

Table 1 UPLC-MS/MS parameters for the identification of the eight analytes in real samples.

Elution order	**Compound**	**Retention time** (min)	**1st Transition** quantifier (m/z)[a]	**2nd Transition** qualifier (m/z)[a]	**Detection polarity** (+)/(-)
1	**Acetamiprid**	3.30	223.1/126.2	223.1/90.1	+
2	**Acibenzolar-S-methyl**	7.58	211.3/136.0	211.3/139.9	+
3	**Pyraflufen-ethyl**	8.75	413.2/339.3	413.2/289.1	+
4	**Clofentezine**	9.20	303.1/138.1	303.1/102.1	+
5	**Diflufenican**	9.44	393.1/329.0	393.1/272.0	-
6	**Oxyfluorfen**	9.91	362.1/316.0	362.1/237.0	+
7	**Propaquizafop**	10.11	444.4/100.1	444.4/371.1	+
8	**Pendimethalin**	10.61	282.3/212.1	282.3/194.1	+

2.8. The method validation

The analytical method was validated in matrix following the ICH harmonised tripartite guidelines for the validation of analytical procedures (ICH Q2(R1)) [36]. The validation parameters evaluated included recovery, repeatability and intermediate precision, accuracy, limit of detection (LOD), limit of quantification (LOQ), sensitivity, and linearity. Data processing and all related calculations were performed using Microsoft Excel 2010 (Microsoft Corporation, Redmond, WA, USA).

3. Results and discussion

3.1. LEGO® bricks stability studies and device composition optimization

To define the most suitable procedure for coating the surface of the LEGO® bricks, a series of chemical and physical stability tests were carried out. Specifically, to define the range of treatments tolerated by the polymer, the material was subjected to both thermal and solvent-based stress tests. For the thermal test, four PLATE units were exposed for 30 min at −18 °C, 50 °C, 80 °C, and 150

°C. These experiments were complemented by thermogravimetric analysis (TGA) in the 50–800 °C range to monitor potential degradation phenomena. The thermal screening revealed that the polymer preserved its mechanical integrity up to 80 °C, showing no macroscopic changes in rigidity. In contrast, exposure to 150 °C for 30 min resulted in the collapse of the polymeric structure, with evident melting and complete loss of rigidity. TGA analysis confirmed that no degradation process is occurring to the copolymer under 200 °C (for detailed information about TGA analysis, see **Fig. E3** of the Appendix E).

To investigate chemical stability, the solubility behaviour of ABS was evaluated in silico using Hansen Solubility Parameters (HSP) [37, 38]. Literature values for toy-grade ABS were adopted [39]: dispersion = 16.8 $(MPa)^{1/2}$, polarity = 11.9 $(MPa)^{1/2}$, and hydrogen bonding = 5.4 $(MPa)^{1/2}$, with a solubility sphere radius of 6.8. In Hansen space, solvents predicted to dissolve ABS fall within this sphere, while non-solvents are located outside. Using the Green Solvent Selection Tool [40], five common laboratory solvents were mapped: acetone, acetonitrile, methanol, ethanol, and isopropanol. The predictions indicated acetone as a strong solvent for ABS, while methanol, ethanol, and isopropanol were expected to be inert. Acetonitrile was located exactly at the edge of the solubility sphere, suggesting borderline solvent behaviour. The in-silico data, in terms of Hansen parameters and mapping in the Hansen space, are reported in **Fig. 2**.

Experimental validation confirmed these predictions. For solvent contact stress evaluation, 5 different PLATE units have been immersed in 14 mL of methanol, ethanol, isopropanol, acetone and acetonitrile, in a 20 mL vial. After 10 min of contact, the polymeric surface remained unchanged in the presence of methanol, ethanol, and isopropanol, whereas acetone and acetonitrile significantly compromised the surface, reducing mechanical strength and resistance to stress (see **Fig. 2**).

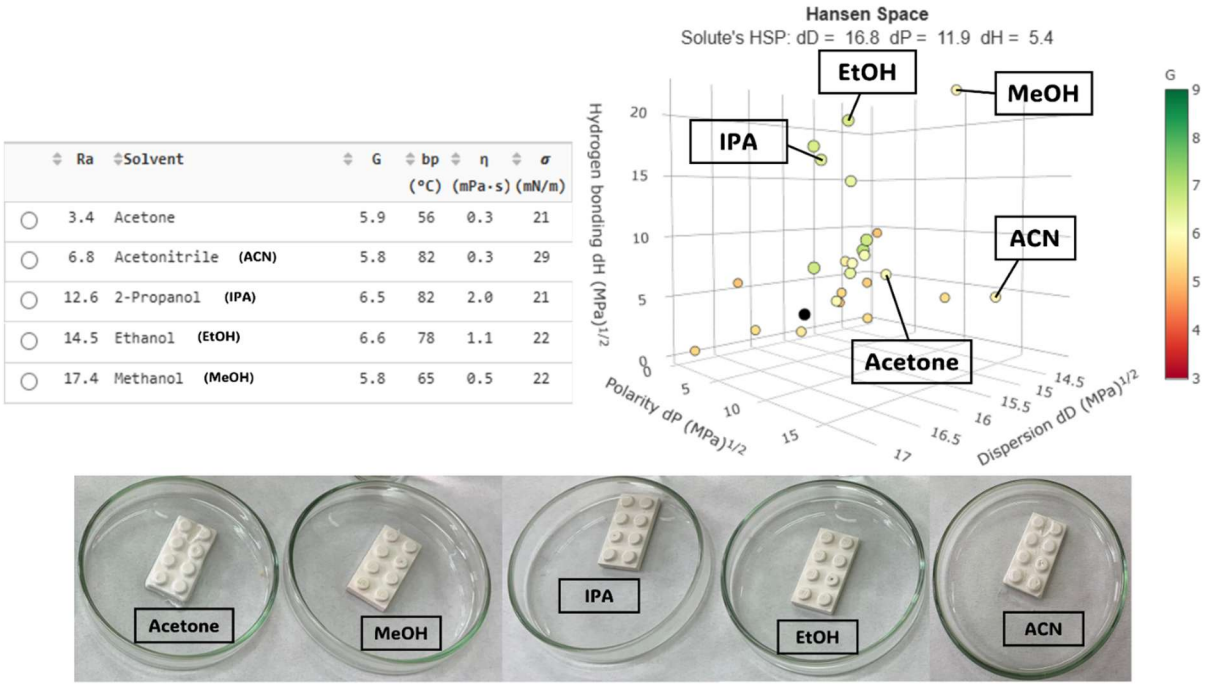

Fig. 2 Prediction of ABS solubility in common organic solvents based on Hansen Solubility Parameters (HSP) theory [37], validated through experimental tests on LEGO® bricks treated with the selected solvents. The Hansen space was represented using the Green Solvent Selection Tool [40].

Based on the data collected on chemical and physical stability, some common strategies to coat or functionalize the surface of the LEGO® polymer were excluded. Consequently, in this work, an alternative coating strategy was devised to ensure preservation of the support, facile removal of the extractant, reproducibility of the process, and reuse of the plastic device. To this end, L-Menthol was selected as coating medium since it does not alter the ABS support and offers the practical advantage of preparing a thermo-responsive composite sorptive phase. In fact, L-menthol is solid at room temperature, while it melts at relatively low temperatures (above 44 °C) making it useful for the analyte adsorption when it is in its solid-state and for the analyte release when it is in its liquid state, simply applying mild heating. L-menthol is also a suitable medium for incorporating and dispersing COOH-MWCNTs so to obtain a composite phase with enhanced sorptive capacity, particularly for moderately polar analytes. COOH-MWCNTs are especially effective toward analytes with aromatic or heterocyclic structures, hydrogen-bond donor or acceptor groups (–OH, –NH_2, –COOH, –$CONH_2$, etc.), and amphiphilic or hydrophobic behaviour, exploiting the balanced hydrophilic/hydrophobic nature of the modified nanotube surface. Recent studies additionally indicate that COOH-MWCNTs

display a more homogeneous dispersion, and reduced tendency to form entanglements compared to pristine MWCNTs, further supporting their suitability for this application [41, 42].

In parallel, different LEGO® BRICK configurations were tested to assess their adsorption performance. **Table 2** summarizes the specifications and sorptive capacities of three distinct devices. Devices 1 and 2 were built by anchoring four LEGO® ROUND BRICK 1×1 units onto the concave side of a LEGO® PLATE 4×4 ROUND W. SNAP, arranged either individually at equidistant positions or stacked in pairs. A central LEGO® TECHNIC BRICK 1×1 was included to provide a housing for a 5×15 mm magnetic stir bar. Coating with menthol/COOH-MWCNTs was applied exclusively to the external surface of the ROUND BRICK modules, achieved by dip-coating in the molten extractant mixture. These two devices were compared with Device 3 (the optimized configuration) in terms of menthol loading, effective sorbent surface area, and adsorption efficiency. Adsorption efficiency was evaluated by comparing chromatographic peak areas before and after extraction of spiked tap water (40 mL, 100 µg L^{-1}, 1 h adsorption time, 2 % w/w COOH-MWCNTs relative to menthol) using HPLC-DAD analysis. The results highlighted the superior performance of Device 3: despite offering a smaller surface area, its higher adsorption capacity can be attributed to more effective contact between the sorptive phase and the analytes during the adsorption step, driven by the intrinsic geometry of the device. This configuration was therefore selected for subsequent optimization studies.

Table 2 Comparison of device parameters to identify the optimal configuration for extraction applications.

	DEVICE 1	**DEVICE 2**	**DEVICE 3**
			
Device composition	1 × LEGO® PLATE 4 × 4 ROUND W. SNAP 4 × LEGO® ROUND BRICK 1 × 1 1 × LEGO® TECHNIC BRICK 1 × 1 1 × magnetic stir bar (5 × 15 mm)	1 × LEGO® PLATE 4 × 4 ROUND W. SNAP 4 × LEGO® ROUND BRICK 1 × 1 1 × LEGO® TECHNIC BRICK 1 × 1 1 × magnetic stir bar (5 × 15 mm)	2 × LEGO® PLATE 2 × 4 2 × LEGO® TECHNIC BRICK 1 × 1 1 x magnetic stir bar (5 × 15 mm)
Deposition modality	Dip coating	Dip coating	Micropipette transfer (300 µL)
Functionalization section	Outer surface of 4 LEGO® ROUND BRICK 1×1 units	Outer surface of 4 LEGO® ROUND BRICK 1×1 units	Concave side of 2 LEGO® PLATE 2 × 4 units
Amount of menthol/COOH-MWCNT deposited (n=5)	0.077 g × 4 = 0.310 g (RSD = 17.3 %)	0.096 g × 2 = 0.192 g (RSD = 22.7 %)	0.323 g × 2 = 0.646 g (RSD = 3.1 %)
Functionalized surface area	2.26 cm^2 × 4 = 9.04 cm^2	2.26 cm^2 × 4 = 9.04 cm^2	3.48 cm^2 × 2 = 6.96 cm^2
Total adsorbance efficiency (n=5)	32 µg g^{-1} (RSD = 21.2 %)	29 µg g^{-1} (RSD = 25.9 %)	34 µg g^{-1} (RSD = 5.5 %)
Technical observations	Low reproducibility of the coating. Inhomogeneity of the coating phase. Stable rotation rate.	Low reproducibility of the coating. Inhomogeneity of the coating phase. Stable rotation rate.	Highly reproducible deposition procedure. Less stable rotation rate.

3.2. Optimization of extraction methodology

The optimization of the extraction procedure was carried out by systematically evaluating the main process variables, namely adsorption time, volume of menthol, COOH-MWCNT loading, pH and ionic strength of samples. A Box–Behnken experimental design was first applied to explore the effects and correlations between variables related to the adsorption process (adsorption time, menthol volume, COOH-MWCNT loading). Subsequent one-variable-at-a-time analysis (OVAT) were performed to refine the procedure with respect to pH and ionic strength of the sample solution,

parameters known to influence adsorbent charge and interaction with analytes. This combined approach provided a robust basis for defining the final working conditions of the extraction procedure.

As far as Box–Behnken design is concerned, all experiments were carried out using Milli-Q water fortified at a concentration of 100 μg L^{-1}, under natural pH and ionic strength conditions (pH ≈ 6, ionic conductivity = 13 × 10^{-5} mS cm^{-1}). Absolute recoveries for all eight analytes were determined based on the chromatographic peak areas obtained in each trial using UPLC-DAD instrumentation, and their mean values were employed as the desirability factor. The main effects plot of the individual variables (see **Fig. 3a**), with respect to the average absolute recovery of the eight analytes, highlights that the amount of COOH-MWCNTs is a key parameter significantly influencing extraction performance within the studied range. Maximum recovery was achieved at COOH-MWCNT loadings of approximately 1.3 % w/w relative to the total menthol content. At lower loadings, the sorbent fails to provide sufficient binding capacity for analyte retention, resulting in decreased absolute recoveries. At loadings higher than 1.3 % w/w, self-aggregation of nanotubes occurs, markedly reducing the available surface area of the carbonaceous sorbent. Subsequently, Response Surface Methodology (RSM) was applied to evaluate the correlation between the two remaining variables and to determine the optimal extraction conditions. The surface response plots, generated at a fixed COOH-MWCNT amount, show that the best recoveries are obtained at longer adsorption times, while the menthol volume exerts only a minor influence. **Fig. 3b** reports the surface response averaged across all analytes. Notably, minimal menthol volumes yield recoveries comparable to those obtained with larger amounts of menthol used as extractant. Furthermore, at reduced menthol volumes, adsorption time exerts a weaker effect on mean absolute recovery, likely due to faster kinetics and efficient equilibration within shorter times for a larger fraction of the extractant. For this reason, and as a compromise between performance, time, and resource optimization, 200 μL of menthol and 30 minutes of adsorption time were selected as the final optimized parameters.

Once the optimal conditions for the adsorption step were established, the extraction procedure was further refined by evaluating the influence of pH and ionic strength on extraction yields from aqueous standards. The pH was adjusted using formic acid or ammonia and measured with a digital microprocessor-based pH meter (Amel Instruments, Milan, Italy). The solution pH directly affects the charge state of the composite sorbent, thereby modulating its interaction with the analytes. Extraction performance was assessed at five pH values (3.0, 5.3, 7.0, 9.0, and 11.0), with each condition tested in triplicate. As shown in **Fig. 3c**, the highest extraction efficiency was obtained at pH 3, a value below the point of zero charge (PZC) of the carbon nanomaterial. Although reliable estimates are scarce since the degree of carboxylation can vary significantly depending on preparation methods, the PZC of COOH-MWCNTs is generally reported within the range of pH 4.5-6.0 [43]. Accordingly, at pH 3 the carboxyl groups are fully protonated, and the surface is not ionized, thus improving the adsorption of neutral and lipophilic compounds (such as the selected pesticides); moreover, more effective π–π interactions can be established between the anaytes and the graphitic structure of the COOH-MWCNTs. Finally, the effect of ionic strength was investigated by analysing spiked water samples (100 μg L^{-1}) at the optimized pH of 3, but with varying conductivities. Incremental amounts of NaCl (0, 0.1, 0.25, 0.5, and 1 % w/v) were added to the spiked samples, yielding measured conductivities of 0.00013, 1.95, 4.59, 8.92, and 16.51 mS cm^{-1}, respectively. Each condition was tested in triplicate. As shown in **Fig. 3d**, extraction efficiency decreased progressively with increasing conductivity. Therefore, no salts were added to adjust ionic strength prior to extraction.

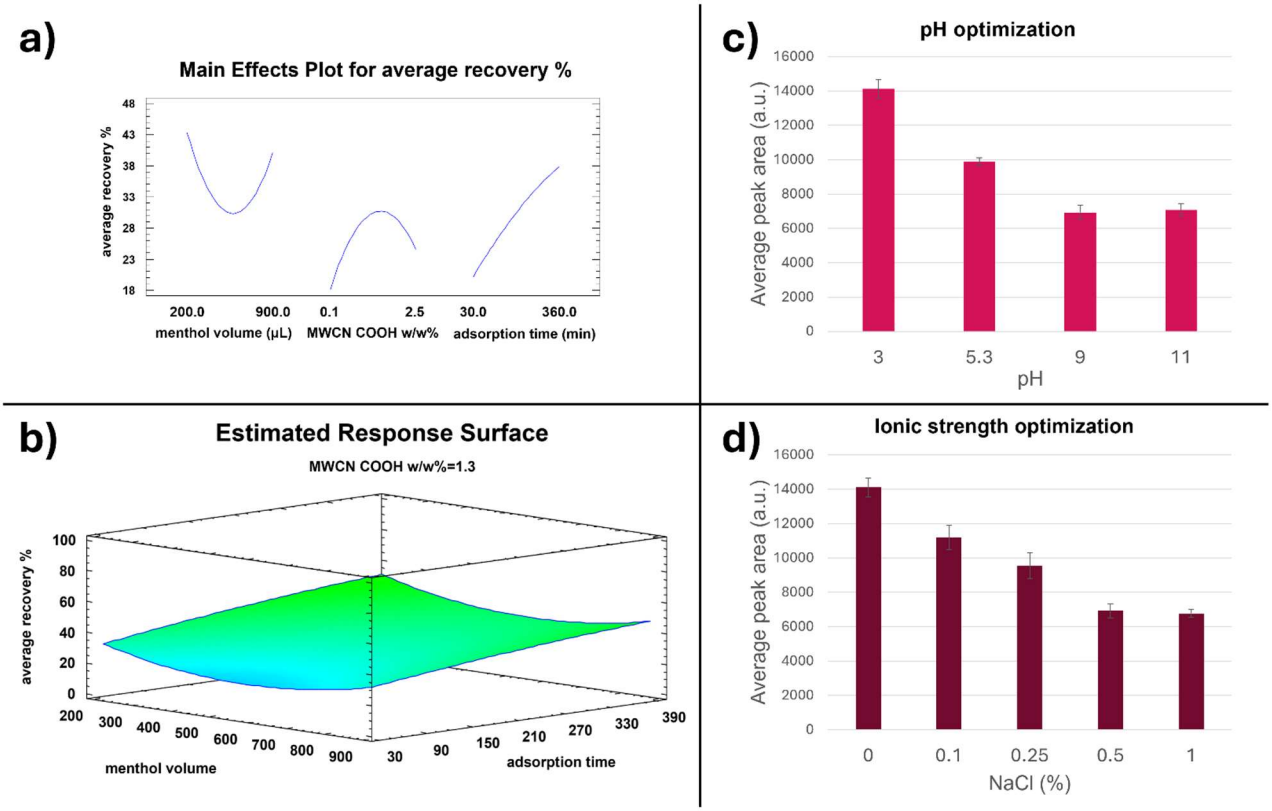

Fig. 3 Optimization of the extraction procedure using a Box–Behnken experimental design to evaluate the effects of menthol volume, COOH-MWCNT amount, and adsorption time (**a**, **b**). Additional OVAT studies were carried out to optimize the pH (**c**) and ionic strength (**d**) of the water samples.

Elution was not included in the developed analytical procedure. By omitting this step, the workflow was streamlined, leading to significant savings in both time and resources. In the final stage of the process, menthol was returned to the liquid state by gently heating the PLATE and subsequently stabilized at room temperature through the addition of isopropanol. Both 50 °C and 60 °C were tested as melting temperatures. Although 50 °C was sufficient to induce melting, complete liquefaction required approximately 10 minutes. Therefore, 60 °C was selected as the optimal compromise between efficiency and practicality (4 min for complete melting). The choice of solvent was guided by considerations of menthol solubility, compatibility with the polymeric support, and the overall sustainability of the method. The solubility results showed in **Section 3.1** identify alcohols as suitable candidates for use in the removal and dilution step of the menthol/MWCNT extractant without damaging the ABS support. Among them, isopropanol was selected as the optimal solvent, owing to its superior solubility for menthol (as confirmed both experimentally and by HSP theory [37]), its green credentials, user-friendly handling, and the possibility of synthesis from renewable sources.

3.3. Figures of merit of the validated method

The analytical performance of the method was evaluated through validation experiments conducted in accordance with the ICH harmonised tripartite guidelines (ICH Q2(R1)). The principal figures of merit are reported in **Table 3**. Calibration curves in matrix were prepared for all analytes using tap water collected from three independent sampling sites (see **Section 2.2**). Pooled blank samples were spiked at eight to ten concentration levels (depending on analyte-specific quantification limits) prior to extraction and processed through the complete analytical workflow. Calibration functions were obtained by plotting the mean chromatographic peak areas from triplicate injections against the corresponding concentrations. All analytes showed excellent linearity, with coefficients of determination (R^2) greater than 0.98, across a dynamic range extending from the limit of quantification (LOQ) to 200 µg L^{-1}. This wide working range supports robust quantification over environmentally relevant concentration intervals. Calibration models for the eight analytes in tap water are shown in **Fig. E4** of the Appendix E.

LODs were defined as the concentrations providing a signal-to-noise ratio of 3 (S/N = 3), while LOQs were established as the lowest concentrations meeting accuracy and precision criteria within 20 %. The resulting LODs ranged between 0.003 µg L^{-1} and 0.04 µg L^{-1}, while LOQs were between 0.005 µg L^{-1} and 0.15 µg L^{-1} (**see Table 3**).

Precision and accuracy were determined in line with ICH recommendations. For these experiments, a separate pool of tap water samples free of target analytes was used, and spiking was performed at three fortification levels: low QC (L-QC, approximately 2-3 x LOQ), medium QC (M-QC, ~30-50 % of the calibration range), and high QC (H-QC, ≥ 75 % of the upper calibration level). Precision was expressed as relative standard deviation (RSD, %), while accuracy was expressed as relative recovery, calculated according to:

$$Relative\ recovery\ (\%) = \frac{C_{measured}}{C_{spiked}}\ x\ 100$$

where $C_{measured}$ represents the analyte concentration obtained by interpolating the mean chromatographic peak area at each fortification level using the corresponding calibration curve in matrix, and C_{spiked} is the nominal spiking concentration. Both repeatability (or intra-assay precision, i.e. precision under the same operating conditions over a short interval of time) and intermediate precision (representative of within-laboratories variations: different days, different analysts, different equipments) were evaluated. Intra-assay precision and accuracy were assessed from five replicates within a single batch, while intermediate precision was determined using three independent batches, each comprising five replicates, performed on three separate days. As summarized in **Table 3**, relative standard deviations (RSDs) were consistently below 15 % for all analytes across all concentration levels, with the sole exception of the intra-assay precision at the H-QC level for acibenzolar-S-methyl. Relative recovery values ranged from 86.6 % to 113 %, confirming that the method provides acceptable accuracy and precision throughout the tested range.

Table 3 Figures of merit of the 8 pesticides analyzed in spiked samples of tap water. Precision and accuracy are reported at all tested concentration levels.

Analyte	**LOD ± st. dv. (µg L^{-1})**	**LOQ ± st. dv. (µg L^{-1})**	**Intra-assay precision (RSD %, n=5)**			**Intermediate precision (RSD %, n=11)**			**Accuracy (Relative recovery %, n=11)**		
			L-QC	M-QC	H-QC	L-QC	M-QC	H-QC	L-QC	M-QC	H-QC
Acetamiprid	0.04 ± 0.01	0.15 ± 0.04	4.3	8.8	4.6	4.2	8.4	8.4	109	104	102
Acibenzolar-methyl	0.04 ± 0.01	0.10 ± 0.03	5.4	8.0	15	5.5	7.6	15	95.2	112	103
Pyraflufen-ethyl	0.006 ± 0.002	0.015 ± 0.004	8.2	9.1	7.8	7.8	11	8.3	101	96.0	108
Clofentezine	0.006 ± 0.001	0.015 ± 0.003	7.0	12	6.4	8.4	12	7.4	113	92.7	95.2
Diflufenican	0.023 ± 0.008	0.07 ± 0.02	5.7	6.2	5.6	6.1	8.5	6.3	104	94.3	93.5
Oxyfluorfen	0.036 ± 0.005	0.10 ± 0.02	7.9	8.3	7.1	7.4	8.7	8.1	103	97.5	108
Propaquizafop	0.005 ± 0.001	0.014 ± 0.004	10	8.6	11	9.9	9.4	10	105	92.3	106
Pendimethalin	0.003 ± 0.001	0.013 ± 0.004	3.4	2.8	5.7	3.5	2.7	5.5	91.7	86.6	108

3.4. Compliance with GAC and CAC goals

The methodological framework presented in this work is situated within the emerging paradigm of CAC [11], a novel frontier in the development of analytical workflows that are closed-loop, sustainable, and resource-efficient. In line with this programmatic vision, this section aims to highlight the aspects of the developed method that align with CAC principles, positioning the approach not merely as a green analytical method but as one that explicitly embraces circularity. It is important to note that it is not feasible to apply every single principle of CAC to an individual analytical protocol. CAC represents a broad conceptual framework that encompasses diverse dimensions of analytical practice, from resource management to waste minimization, instrument efficiency, and material reuse. For this reason, we have combined reflections on circularity compliance with more conventional assessments of method greenness.

From this perspective, the Sample Preparation Metric of Sustainability (SPMS) [44] was applied as a quantitative tool to assess the sustainability of the sample preparation step. The procedure obtained a score of 7.05, confirming its green profile but also revealing certain limitations. SPMS, in fact, accounts only for consumables and waste generation, without considering analytical performance or the specific requirements of the sample matrix. In our case, the use of a relatively large sample volume (40 mL) was essential to maximize the enrichment factor (indispensable consideration for environmental samples, where contaminant levels are typically very low). This choice inevitably lowered the SPMS score, yet it was necessary to ensure sensitivity and applicability. Moreover, the metric does not capture key features of the method, such as the recyclability of the support, the nearly zero-waste workflow, and the minimal environmental impact of the employed materials. Consequently, while SPMS offers useful indications, its scope remains inherently limited when applied to methods deliberately designed around application requirements and principles of circularity. The score plot of the SPMS applied to the current method is presented in **Fig. E5** of the Appendix E.

From the standpoint of circularity, however, the method exhibits several technical advantages that place it in close alignment with the goals of CAC. The extraction support can be fabricated from recycled materials, reshaped as needed, and reused indefinitely, since it is not chemically degraded by the reagents it encounters. This feature directly supports Goal 1 (Closed-loop materials), Goal 3 (Resource minimization), and Goal 12 (Sustainable reuse) of CAC. Moreover, the careful experimental design and optimization of the workflow minimized both reagent consumption and waste, effectively merging pretreatment steps into a streamlined, low-waste procedure (Goals 2 and 3). The use of menthol as the extractant further strengthens sustainability credentials, as it ensures operator safety, relies on renewable sources, and carries negligible environmental impact (Goals 5 and 8).

In addition, reliance on low-energy instrumentation throughout the optimization process reduces energy waste, consistent with Goal 4 (Energy efficiency). At a broader level, the deliberate investment of time and resources to maximize sustainability and design a nearly zero-waste workflow reflects a strong programmatic commitment to CAC principles, aligning with Goal 7 (Embedding sustainability in analytical practice). A graphical assessment and explanation of the compliance of the method with the CAC goals is reported in **Fig. 4**.

Taken together, these considerations position the developed and validated method as more than a conventional green analytical technique: it constitutes a deliberate evolution toward CAC, embedding principles of sustainability, resource efficiency, and circularity into its very design.

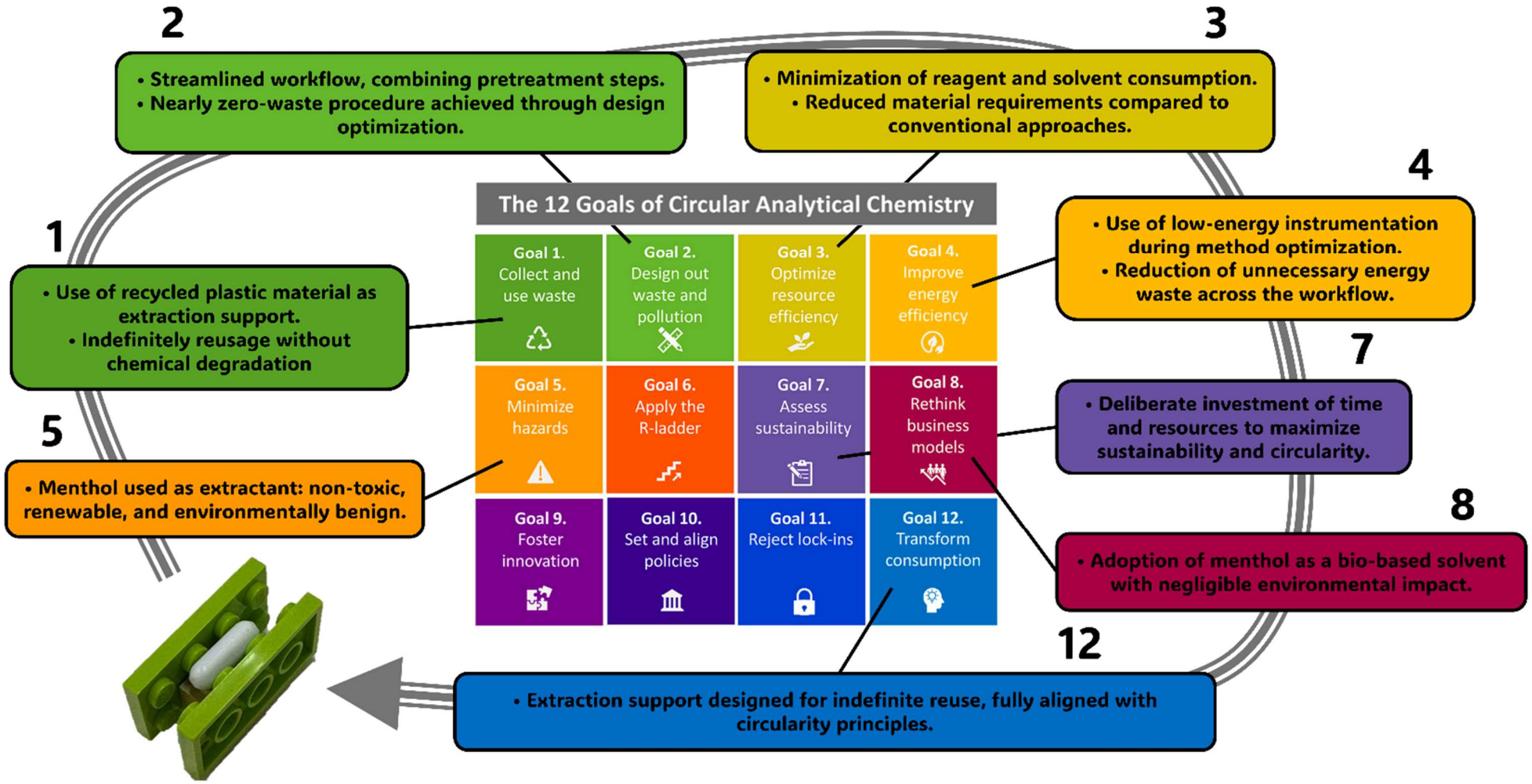

Fig. 4 Assessment of the compliance of the method with the single CAC Goals [11].

4. Conclusion

This study presented a proof-of-concept analytical device built from recycled LEGO® bricks and coated with a sorptive phase composed of menthol and COOH-MWCNTs for the extraction of pesticides from water. Beyond the demonstration of reliable analytical performance, the work introduces a conceptual and methodological innovation that directly intersects with the principles of CAC. The device exemplifies how widely available waste-derived materials can be reconfigured into robust, modular, and reproducible analytical platforms without the need for additional polymeric inputs or specialized manufacturing. The low melting and solidification point of menthol enables the development of a thermo-responsive sorptive phase, thereby minimizing the need for organic solvents. From a methodological perspective, the system achieves recoveries, and quantification limits comparable to conventional extraction methods. Critically, the study highlights the unique strengths of LEGO®-based devices: reusability, adaptability, and scalability. These attributes make the approach attractive not only as a sustainable alternative to traditional sample preparation but also as a pedagogical and practical tool for broadening the accessibility of analytical innovation. At the same time, challenges remain, including the coating standardization, the potential variability in waste-derived polymers, and the scalability of the workflow for routine or high-throughput analysis. Taken together, this work advances the vision of CAC by providing a tangible example of how post-consumer waste can be valorised in analytical science. It demonstrates that circularity and performance can coexist and even reinforce one another, setting the stage for further integration of recycled materials, modular design, and green extractants in the development of next-generation analytical technologies.

References

[1] Evode, N., Qamar, S. A., Bilal, M., Barceló, D., & Iqbal, H. M. (2021). Plastic waste and its management strategies for environmental sustainability. *Case studies in chemical and environmental engineering*, *4*, 100142. https://doi.org/10.1016/j.cscee.2021.100142

[2] Gautam, B. P. S., Qureshi, A., Gwasikoti, A., Kumar, V., & Gondwal, M. (2024). Global scenario of plastic production, consumption, and waste generation and their impacts on environment and human health. In *Advanced strategies for biodegradation of plastic polymers* (pp. 1-34). Cham: Springer Nature Switzerland. https://doi.org/10.1007/978-3-031-55661-6_1

[3] Chang, M. C. O., David, B., Ray-Chaudhuri, T., Sun, L. L., & Wong, R. P. (1997). Acrylonitrile-butadiene-styrene (ABS) polymers. *Handbook of thermoplastics*, 135-159. https://doi.org/10.1002/0471238961.01021911211209.a01.pub2

[4] Olivera, S., Muralidhara, H. B., Venkatesh, K., Gopalakrishna, K., & Vivek, C. S. (2016). Plating on acrylonitrile–butadiene–styrene (ABS) plastic: a review. *Journal of materials science*, *51*(8), 3657-3674. https://doi.org/10.1007/s10853-015-9668-7

[5] Deshmukh, D., Kulkarni, H., Srivats, D. S., Bhanushali, S., & More, A. P. (2024). Recycling of acrylonitrile butadiene styrene (ABS): A review. *Polymer Bulletin*, *81*(13), 1-38. https://doi.org/10.1007/s00289-024-05269-y

[6] Jakubowicz, I., & Yarahmadi, N. (2024). Review and assessment of existing and future techniques for traceability with particular focus on applicability to ABS plastics. *Polymers*, *16*(10), 1343. https://doi.org/10.3390/polym16101343

[7] Letcher, T., Rankouhi, B., & Javadpour, S. (2015, November). Experimental study of mechanical properties of additively manufactured ABS plastic as a function of layer parameters. In *ASME international mechanical engineering congress and exposition* (Vol. 57359, p. V02AT02A018). American Society of Mechanical Engineers. https://doi.org/10.1115/IMECE2015-52634

[8] What LEGO® bricks are made of, https://www.lego.com/en-us/service/help-topics/article/what-lego-bricks-are-made-of

[9] Jung, S. M. (2025). Recent Progress in Sustainable Recycling of Waste Acrylonitrile–Butadiene–Styrene (ABS) Plastics. *Sustainability*, *17*(19), 8742. https://doi.org/10.3390/su17198742

[10] Nevzorova, T., & Carlsson, R. (2024, September). Traceability Options for Products Containing ABS Plastic: A Systematic Literature Review. In *International Conference on Sustainable Design and Manufacturing* (pp. 171-181). Singapore: Springer Nature Singapore. https://doi.org/10.1007/978-981-96-4459-9_16

[11] Psillakis, E., & Pena-Pereira, F. (2024). The twelve goals of circular analytical chemistry. *TrAC Trends in Analytical Chemistry*, *175*, 117686. https://doi.org/10.1016/j.trac.2024.117686

[12] Armenta, S., Garrigues, S., & de la Guardia, M. (2008). Green analytical chemistry. *TrAC Trends in Analytical Chemistry*, *27*(6), 497-511. https://doi.org/10.1016/j.trac.2008.05.003

[13] Arancon, R. A. D., Lin, C. S. K., Chan, K. M., Kwan, T. H., & Luque, R. (2013). Advances on waste valorization: new horizons for a more sustainable society. *Energy Science & Engineering*, *1*(2), 53-71. https://doi.org/10.1002/ese3.9

[14] Celeiro, M., Vazquez, L., Sergazina, M., Docampo, S., Dagnac, T., Vilar, V. J., & Llompart, M. (2020). Turning cork by-products into smart and green materials for solid-phase extraction-gas chromatography tandem mass spectrometry analysis of fungicides in water. *Journal of Chromatography A*, *1628*, 461437. https://doi.org/10.1016/j.chroma.2020.461437

[15] Lopez-Tellez, J., Ibarra, I. S., Cruz-Borbolla, J., Vega, M., & Rodriguez, J. A. (2023). Retention and Determination of Polycyclic Aromatic Hydrocarbons from Urban Air Based on Recycled Polyurethane Foam Modified with Expanded Polystyrene. *Polycyclic Aromatic Compounds*, *43*(10), 9347-9359. https://doi.org/10.1080/10406638.2022.2162931

[16] Lopez-Tellez, J., Rodriguez, J. A., Miranda, J. M., Mondragon, A. C., & Ibarra, I. S. (2024). Determination of polycyclic aromatic hydrocarbons in aqueous samples using recycled polystyrene for pipette tip-solid phase extraction followed by HPLC-FLD. *International Journal of Environmental Analytical Chemistry*, *104*(15), 3486-3495. https://doi.org/10.1080/03067319.2022.2086051

[17] Antonelli, L., Frondaroli, M. C., De Cesaris, M. G., Felli, N., Dal Bosco, C., Lucci, E., & Gentili, A. (2024). Nanocomposite microbeads made of recycled polylactic acid for the magnetic solid phase extraction of xenobiotics from human urine. *Microchimica Acta*, *191*(5), 251. https://doi.org/10.1007/s00604-024-06335-y

[18] Ghambari, H., Reyes-Gallardo, E. M., Lucena, R., Saraji, M., & Cárdenas, S. (2017). Recycling polymer residues to synthesize magnetic nanocomposites for dispersive micro-solid phase extraction. *Talanta*, *170*, 451-456. https://doi.org/10.1016/j.talanta.2017.04.026

[19] Antonelli, L., López-Lorente, Á. I., Gentili, A., Lucena, R., & Cárdenas, S. (2025). Microbeads from recycled polystyrene yogurt cups for the in-syringe micro solid-phase extraction of four opioids from environmental and biological samples. *Sustainable Chemistry and Pharmacy*, *45*, 102036. https://doi.org/10.1016/j.scp.2025.102036

[20] Mehmandost, N., Soriano, M. L., Lucena, R., Goudarzi, N., Chamjangali, M. A., & Cardenas, S. (2019). Recycled polystyrene-cotton composites, giving a second life to plastic residues for environmental remediation. *Journal of Environmental Chemical Engineering*, *7*(5), 103424. https://doi.org/10.1016/j.jece.2019.103424

[21] Saleem, J., Moghal, Z. K. B., & McKay, G. (2023). Up-cycling plastic waste into swellable super-sorbents. *Journal of Hazardous Materials*, *453*, 131356. https://doi.org/10.1016/j.jhazmat.2023.131356

[22] Wang, J., Liu, S., Chen, C., Zou, Y., Hu, H., Cai, Q., & Yao, S. (2014). Natural cotton fibers as adsorbent for solid-phase extraction of polycyclic aromatic hydrocarbons in water samples. *Analyst*, *139*(14), 3593-3599. https://doi.org/10.1039/c4an00195h

[23] Lebre, D. T., Thipe, V. C., Cotrim, M. E., & Bustillos, J. O. V. (2022). Use of sugar cane bagasse as solid extraction phase sorbent to analyze hormones from industrial effluent. *ACS omega*, *7*(12), 10069-10076. https://doi.org/10.1021/acsomega.1c06064

[24] Adenuga, A. A., Ayinuola, O., Adejuyigbe, E. A., & Ogunfowokan, A. O. (2020). Biomonitoring of phthalate esters in breast-milk and urine samples as biomarkers for neonates' exposure, using modified quechers method with agricultural biochar as dispersive solid-phase extraction absorbent. *Microchemical Journal*, *152*, 104277. https://doi.org/10.1016/j.microc.2019.104277

[25] Reinert, N. P., Vieira, C. M., Da Silveira, C. B., Budziak, D., & Carasek, E. (2018). A low-cost approach using diatomaceous earth biosorbent as alternative SPME coating for the determination of

PAHs in water samples by GC-MS. *Separations*, *5*(4), 55. https://doi.org/10.3390/separations5040055

[26] Godage, N. H., & Gionfriddo, E. (2020). Use of natural sorbents as alternative and green extractive materials: A critical review. *Analytica Chimica Acta*, *1125*, 187-200. https://doi.org/10.1016/j.aca.2020.05.045

[27] Jagirani, M. S., & Soylak, M. (2024). Green sorbents for the solid phase extraction of trace species. *Current Opinion in Green and Sustainable Chemistry*, *47*, 100899. https://doi.org/10.1016/j.cogsc.2024.100899

[28] Hashemi, B., Zohrabi, P., & Dehdashtian, S. (2018). Application of green solvents as sorbent modifiers in sorptive-based extraction techniques for extraction of environmental pollutants. *TrAC Trends in Analytical Chemistry*, *109*, 50-61. https://doi.org/10.1016/j.trac.2018.09.026

[29] Li, F., Ceballos, M. R., Balavandy, S. K., Fan, J., Khataei, M. M., Yamini, Y., & Maya, F. (2020). 3D Printing in analytical sample preparation. *Journal of Separation Science*, *43*(9-10), 1854-1866. https://doi.org/10.1002/jssc.202000035

[30] Monteiro, S. A., Scheid, C., Deon, M., & Merib, J. (2023). Fundamentals, recent applications, and perspectives of 3D printing in sample preparation approaches. *Microchemical Journal*, *195*, 109385. https://doi.org/10.1016/j.microc.2023.109385

[31] Ren, X., Balavandy, S. K., Li, F., Breadmore, M. C., & Maya, F. (2022). Miniaturized 3D printed solid-phase extraction cartridges with integrated porous frits. *Analytica Chimica Acta*, *1208*, 339790. https://doi.org/10.1016/j.aca.2022.339790

[32] Clark, M. J., Garg, T., Rankin, K. E., Bradshaw, D., & Nightingale, A. M. (2024). 3D printed filtration and separation devices with integrated membranes and no post-printing assembly. *Reaction Chemistry & Engineering*, *9*(2), 251-259. https://doi.org/10.1039/D3RE00245D

[33] Jiang, P., Ji, Z., Wang, X., & Zhou, F. (2020). Surface functionalization–a new functional dimension added to 3D printing. *Journal of Materials Chemistry C*, *8*(36), 12380-12411. https://doi.org/10.1039/D0TC02850A

[34] Majooni, Y., Abioye, S. O., Fayazbakhsh, K., & Yousefi, N. (2024). Nano-enabled 3D-printed structures for water treatment. *ACS ES&T Water*, *4*(5), 1952-1965. https://doi.org/10.1021/acsestwater.3c00770

[35] Mattio, E., Ollivier, N., Robert-Peillard, F., Di Rocco, R., Branger, C., Margaillan, A., Brach-Papa, C., Knoery, J., Bonne, D., Boudenne, J., & Coulomb, B. (2019). Modified 3D-printed device for mercury determination in waters. *Analytica Chimica Acta*, *1082*, 78-85. https://doi.org/10.1016/j.aca.2019.06.062

[36] Guideline, I. H. (2022). Bioanalytical method validation and study sample analysis M10. ICH Harmonised Guideline: Geneva, Switzerland.

[37] Hansen, C., Poulsen, T. (2007). Hansen Solubility Parameters A User's Handbook (2nd ed.). https://doi.org/10.1201/9781420006834

[38] Diorazio, L. J., Hose, D. R., & Adlington, N. K. (2016). Toward a more holistic framework for solvent selection. *Organic Process Research & Development*, *20*(4), 760-773. https://doi.org/10.1021/acs.oprd.6b00015

[39] Lu, T., & Chen, W. T. (2023). Material recycling of Acrylonitrile Butadiene Styrene (ABS) from toy waste using density separation and safer solvents. *Resources, Conservation and Recycling*, *197*, 107090. https://doi.org/10.1016/j.resconrec.2023.107090

[40] Larsen, C., Lundberg, P., Tang, S., Ràfols-Ribé, J., Sandström, A., Mattias Lindh, E., Wang, J., & Edman, L. (2021). A tool for identifying green solvents for printed electronics. *Nature Communications*, *12*(1), 4510. https://doi.org/10.1038/s41467-021-24761-x

[41] Liu, C. X., & Choi, J. W. (2012). Improved dispersion of carbon nanotubes in polymers at high concentrations. *Nanomaterials*, *2*(4), 329-347. https://doi.org/10.3390/nano2040329

[42] Kumar, P., Park, J. S., Randhawa, P., Sharma, S., Shin, M. S., & Sekhon, S. S. (2011). A study on the effect of different chemical routes on functionalization of MWCNTs by various groups (-COOH, -SO_3H, -PO_3H_2). Nanoscale research letters, 6(1), 583. https://doi.org/10.1186/1556-276X-6-583

[43] Kuśmierek, K., Dąbek, L., & Świątkowski, A. (2023). The use of modified multi-walled carbon nanotubes for the removal of selected pharmaceuticals from the aqueous environment. *Desalination and Water Treatment*, *288*, 60-71. https://doi.org/10.5004/dwt.2023.29140

[44] González-Martín, R., Gutiérrez-Serpa, A., Pino, V., & Sajid, M. (2023). A tool to assess analytical sample preparation procedures: sample preparation metric of sustainability. *Journal of Chromatography A*, *1707*, 464291. https://doi.org/10.1016/j.chroma.2023.464291

Conclusion

This research demonstrates that the reuse and recycling of materials for sample preparation constitute a viable, sustainable, and analytically robust alternative to conventional approaches. The studies presented collectively show that circular strategies can effectively merge environmental responsibility, economic feasibility, and analytical performance. Natural and waste-derived materials proved to be efficient sorbents for the extraction of a wide range of organic and inorganic contaminants. Their use reduces preparation time, solvent consumption, and energy demand, leading to a smaller environmental footprint. When necessary, mild modification processes such as activation or carbonization further improved adsorption performance, confirming the adaptability of these materials to diverse analytical contexts. Recycled polymers, including polylactic acid (PLA), polystyrene, and cellulose acetate, were successfully transformed into functional adsorbents and devices. PLA-based nanocomposites exhibited strong magnetic responsiveness and analytical performances, while recycled polystyrene materials achieved high recoveries, precision, and selectivity in extracting pollutants from complex matrices. Micro-spherical materials prepared with recycled cellulose acetate proved to be effective in the removal of a wide range of contaminants, highlighting the effectiveness of merging polymer recycling and water remediation. These results confirm that post-consumer plastics can be upcycled into effective, low-cost analytical materials without compromising analytical reliability.

The introduction of extraction systems built from recycled LEGO® bricks further extended the concept of circularity to the design of analytical devices. Their modular and reusable structures exemplify how sustainability can be practically implemented in analytical workflows offering interesting scenarios to the materials development and evolution.

Overall, the outcomes of this thesis confirm that sustainability and analytical excellence are not mutually exclusive. Instead, they can be mutually reinforcing when guided by the principles of

circular economy and green chemistry. The findings lay the foundation for the future large-scale implementation of recycling strategies in analytical laboratories, where material recovery, modularity, and cost efficiency will play central roles. These advances pave the way toward a new generation of analytical tools that are technically sound, economically viable, and environmentally responsible.

Appendix A

Table A1 The table reports some of the newly proposed microextraction techniques, from 2020 to 2024.

Web searching keywords	Research paper name	Year	Method	Adsorbent material	Analytes of interest	Matrix	Ref.
nanocomposite microbeads microextraction	Using Fe_3O_4-graphene oxide-modified chitosan with melamine magnetic nanocomposite in the removal and magnetic dispersive solid-phase microextraction of Cr (VI) ion in aquatic samples	2024	Magnetic dispersive solid-phase microextraction	Magnetic melamine-functionalized chitosan-modified graphene oxide (MCMGO) nanocomposite	Cr (VI) ion	Water	[1]
nanocomposite microbeads microextraction	Magnetic Luffa@metal-organic frameworks (MOF-199) nanocomposite for the solid phase microextraction of some metal ions at trace levels from food and water samples	2023	Solid phase microextraction	Magnetic Luffa@MOF-199 nanocomposite	Ni(II), Pb(II), Cr(III) and Cd(II)	Water	[2]
nanocomposite microbeads microextraction	Determination of selected pesticides by GC-FID after CNO/MOF nanocomposites-based dispersive solid phase extraction coupled with liquid microextraction	2023	Dispersive solid phase extraction (DSPE)	CNO-ZIF67 nanocomposite	Pesticides	Vegetables	[3]
nanocomposite microbeads microextraction	Covalent organic framework in situ grown on Fe_3O_4 hollow microspheres for stir bar sorptive-dispersive microextraction of triazole pesticides	2023	Stir bar sorptive-dispersive microextraction	TFPB-BD/Fe_3O_4 nanocomposite	Triazole pesticides	Fruit, vegetables	[4]
nanocomposite microbeads microextraction	Application of ZnS/S/S-RGO three-component nanocomposites in dispersive solid-phase microextraction coupled with ion mobility spectrometry for ultra-trace determination of multiclass pesticides	2022	Dispersive solid-phase microextraction	ZnS/S/S-RGO nanocomposite	Multiclass pesticides	Well water, agricultural wastewater, soil, and rice	[5]
nanocomposite microbeads microextraction	Application of Fe_3O_4@TbBd nanobeads in microextraction by packed sorbent (MEPS) for determination of BTEXs biomarkers by HPLC–UV in urine samples	2022	Microextraction packed sorbent (MEPS)	Fe_3O_4@TbBd nanobeads	BTEXs biomarkers	Urine	[6]

nanocomposite microbeads microextraction	Novel polyphenol/graphene nanocomposite for solid-phase microextraction of bisphenol A and bisphenol B leached from plastic containers	2021	Solid-phase microextraction	Polyphenol (PPh) and graphene oxide nanosheets (GONSs) nanocomposite	Bisphenol A and bisphenol B	Plastic	[7]
nanocomposite microbeads microextraction	Polyaniline-coated core-shell silica microspheres-based dispersive-solid phase extraction for detection of benzophenone-type UV filters in environmental water samples	2021	Dispersive-solid phase extraction (DSPE)	CSMS@PANI nanocomposite microspheres	Benzophenone-type UV filters	Water	[8]
nanocomposite microbeads microextraction	Core-shell structured $Fe_2O_3/CeO_2@MnO_2$ microspheres with abundant surface oxygen for sensitive solid-phase microextraction of polycyclic aromatic hydrocarbons from water	2021	Solid-phase microextraction	$Fe_2O_3/CeO_2@MnO_2$ microspheres	Polycyclic aromatic hydrocarbons	Water	[9]
nanocomposite microbeads microextraction	Sono-synthesized Fe_3O_4–GO–NH_2 nanocomposite for highly efficient ultrasound-assisted magnetic dispersive solid-phase microextraction of hazardous dye Congo red from water samples	2021	Ultrasound-assisted magnetic dispersive solid-phase microextraction (UA-MDSPME)	Fe_3O_4–GO– NH_2 nanocomposite	Congo red dye	Water	[10]
nanocomposite microbeads microextraction	An $Ag_2S@ZnS$-coated fiber for efficient, long-life solid-phase microextraction of polycyclic aromatic hydrocarbons in water	2020	Solid-phase microextraction	$Ag_2S@ZnS$-coated fiber	Polycyclic aromatic hydrocarbons	Water	[11]
nanocomposite microbeads microextraction	Decoration of $Fe_3O_4@SiO_2@ZnO$ as a high performance nanosorbent on a stir bar microextraction device for preconcentration and determination of cadmium in real water samples	2020	Stir bar microextraction	$Fe_3O_4@SiO_2@ZnO$ core–shell nanosorbent	Cadmium	Water	[12]
nanocomposite microbeads microextraction	Optimization by response surface methodology of a dispersive magnetic solid phase extraction exploiting magnetic graphene nanocomposite coupled with UHPLC-PDA for simultaneous determination of new oral anticoagulants (NAOs) in human plasma	2020	Dispersive magnetic solid phase extraction	Reduced graphene@ Fe_3O_4 nanocomposite	Novel oral anticoagulants (NOAs)	Human plasma	[13]
nanocomposite microbeads microextraction	Magnetic solid-phase extraction of sulfonamide antibiotics in water and animal-derived food samples using core-shell magnetite and molybdenum disulfide nanocomposite adsorbent	2020	Magnetic solid-phase extraction	$Fe_3O_4@MoS_2$ nanocomposite	Sulfonamide antibiotics	Water, food	[14]

nanocomposite microbeads microextraction	Graphene oxide-Fe_3O_4 nanocomposite magnetic solid phase extraction followed by UHPLC-MS/MS for highly sensitive determination of eight psychoactive drugs in urine samples	2020	Magnetic solid phase extraction	GO- Fe_3O_4 nanocomposite	Eight psychoactive drugs	Urine	[15]

References

[1] Bagheri V, Naseri A, Sajedi-Amin S, Soylak M, Zhang Z (2024) Using Fe3O4-graphene oxide-modified chitosan with melamine magnetic nanocomposite in the removal and magnetic dispersive solid-phase microextraction of Cr (VI) ion in aquatic samples. Chem. Pap. 78:381–396. https://doi.org/10.1007/s11696-023-03096-5

[2] Ahmed HEH, Soylak M (2023). Magnetic Luffa@metal-organic frameworks (MOF-199) nanocomposite for the solid phase microextraction of some metal ions at trace levels from food and water samples. J. Food Compos. Anal. 121:105396-105407. https://doi.org/10.1016/j.jfca.2023.105396

[3] Abbasalizadeh A, Ghalkhani M, Marzi Khosrowshahi E, Mazani A, Hosseini A, Sohouli E, Ahmadi F (2023) Determination of selected pesticides by GC-FID after CNO/MOF nanocomposites-based dispersive solid phase extraction coupled with liquid microextraction. Diam. Relat. Mater. 137:110087-110097. https://doi.org/10.1016/j.diamond.2023.110087

[4] Wang YX, Shen XF, Feng YW, Pang YH (2023) Covalent organic framework in situ grown on Fe3O4 hollow microspheres for stir bar sorptive-dispersive microextraction of triazole pesticides. Microchim. Acta. 190:34-42. https://doi.org/10.1007/s00604-022-05613-x

[5] Rahmani S, Aibaghi B (2022) Application of ZnS/S/S-RGO three-component nanocomposites in dispersive solid-phase microextraction coupled with ion mobility spectrometry for ultra-trace determination of multiclass pesticides. Microchim. Acta. 189:9-18. https://doi.org/10.1007/s00604-021-05116-1

[6] Kurd N, Bahrami A, Afkhami A, Shahna FG, Assari MJ, Farhadian M (2022) Application of Fe3O4@TbBd nanobeads in microextraction by packed sorbent (MEPS) for determination of BTEXs biomarkers by HPLC–UV in urine samples. J Chromatogr. B 1197:123197-12406. https://doi.org/10.1016/j.jchromb.2022.123197

[7] Behzadi M (2021) Novel polyphenol/graphene nanocomposite for solid-phase microextraction of bisphenol A and bisphenol B leached from plastic containers. Sens. Actuators A: Phys. 321:112599-112606. https://doi.org/10.1016/j.sna.2021.112599. https://doi.org/10.1016/j.sna.2021.112599

[8] Wang A, Hu L, Liu J, Tian M, Yang L (2021) Polyaniline-coated core-shell silica microspheres-based dispersive-solid phase extraction for detection of benzophenone-type UV filters in environmental water samples. Environ. Adv. 3:100037-100045. https://doi.org/10.1016/j.envadv.2021.100037

[9] Xu S, Dong P, Qin M, Liu H, Long A, Chen C, Feng S, Wu H (2021) Core-shell structured Fe2O3/CeO2@MnO2 microspheres with abundant surface oxygen for sensitive solid-phase microextraction of polycyclic aromatic hydrocarbons from water. Microchim. Acta 188:337-346. https://doi.org/10.1007/s00604-021-05004-8

[10] Sricharoen P, Chanthai S, Lamaiphan N, Sakaew C, Limchoowong N, Nuengmatcha P, Oh WC (2021) Sono-synthesized Fe3O4–GO–NH2 nanocomposite for highly efficient ultrasound-assisted magnetic dispersive solid-phase microextraction of hazardous dye Congo red from water samples. J. Korean Ceram. Soc. 58(2):201–211. https://doi.org/10.1007/s43207-020-00089-y

[11] Liu H, Fan H, Wang X, Dang S, Gu A (2020) An Ag2S@ZnS-coated fiber for efficient, long-life solid-phase microextraction of polycyclic aromatic hydrocarbons in water. J Sep. Sci. 43:3646–3654. https://doi.org/10.1002/jssc.202000282

[12] Banihashemi M, Dalali N, Sehati N, Farajmand B (2020) Decoration of Fe3O4@SiO2@ZnO as a high performance nanosorbent on a stir bar microextraction device for preconcentration and determination of cadmium in real water samples. Microchem. J. 154:104599-104607. https://doi.org/10.1016/j.microc.2020.104599

[13] Ferrone V, Todaro S, Carlucci M, Fontana A, Ventrella A, Carlucci G, Milanetti E (2020) Optimization by response surface methodology of a dispersive magnetic solid phase extraction exploiting magnetic graphene nanocomposite coupled with UHPLC-PDA for simultaneous determination of new oral anticoagulants (NAOs) in human plasma. J. Pharm. Biomed. Anal. 179:112992-113001. https://doi.org/10.1016/j.jpba.2019.112992

[14] Zhao Y, Wu R, Yu H, Li J, Liu L, Wang S, Chen X, Chan D (2020) Magnetic solid-phase extraction of sulfonamide antibiotics in water and animal-derived food samples using core-shell magnetite and molybdenum disulfide nanocomposite adsorbent. J. Chromatogr. A 1610:460543-460550. https://doi.org/10.1016/j.chroma.2019.460543

[15] Lu Q, Guo H, Zhang Y, Tang X, Lei W, Qi R, Chu J, Li D, Zhao Q (2020) Graphene oxide-Fe3O4 nanocomposite magnetic solid phase extraction followed by UHPLC-MS/MS for highly sensitive determination of eight psychoactive drugs in urine samples. Talanta 206:120202-120210. https://doi.org/10.1016/j.talanta.2019.120212

Table A2 The table shows the chemical structure of each pesticide, and lists: the exact mass, IUPAC name, chemical classification, and agrochemical/pharmaceutical action.

Common name	Structure	Exact mass	IUPAC name	Common name	Structure	Exact mass
Diuron	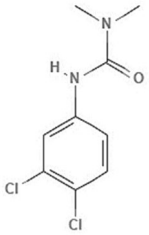	232.0170	3-(3,4-dichlorophenyl)-1,1-dimethylurea	Phenylurea derivatives	Herbicides	[1]
Bensulfuron-Me	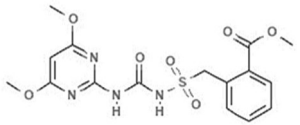	410.0896	methyl 2-[(4,6-dimethoxypyrimidin-2-yl)carbamoylsulfamoylmethyl] benzoate	Sulfonylurea derivatives	Herbicides	[2]
Me-Testosterone	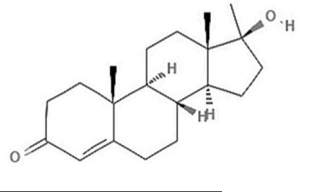	302.2245	(8R,9S,10R,13S,14S,17S)-17-hydroxy-10,13,17-trimethyl-2,6,7,8,9,11,12,14,15,16-decahydro-1H-cyclopenta[a]phenanthren-3-one	Hydroxy steroids	Hormone	[3]
Flamprop	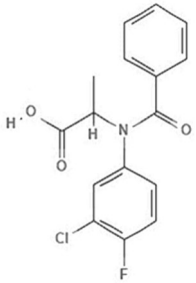	321.0568	2-(N-benzoyl-3-chloro-4-fluoroanilino)propanoic acid	Benzamides	Herbicides	[4]

4-chloro-2-methylphenol	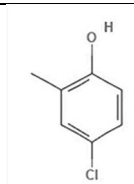	142.0185	4-chloro-2-methylphenol	Chlorophenols	Herbicides metabolite	[5]
Mecoprop	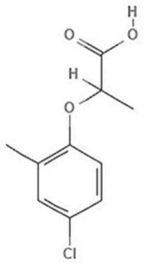	214.0397	2-(4-chloro-2-methylphenoxy)propanoic acid	Phenoxyacetates	Herbicide	[6]
Linuron	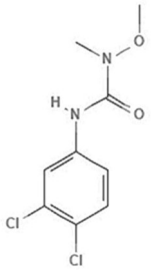	248.0119	3-(3,4-dichlorophenyl)-1-methoxy-1-methylurea	Phenylurea Compounds	Herbicides	[7]
Nimesulide	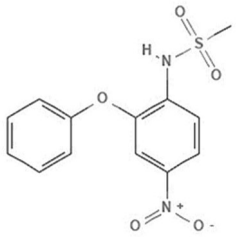	308.0467	N-(4-nitro-2-phenoxyphenyl)methanesulfonamide	Sulfonamides	Nonsteroidal Anti-inflammatory Drug	[8]

MCPB	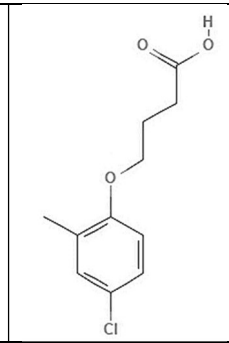	228.0553	4-(4-chloro-2-methylphenoxy)butanoic acid	Phenoxybutirrates	Herbicide	[9]
Carprofen	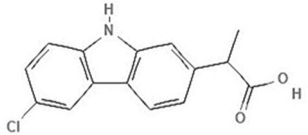	273.0557	2-(6-chloro-9H-carbazol-2-yl)propanoic acid	Carbazoles	Nonsteroidal Anti-inflammatory Drug	[10]
Diclofenac	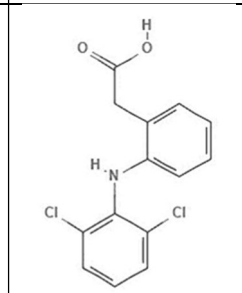	295.0167	2-[2-(2,6-dichloroanilino)phenyl]acetic acid	Phenylacetates	Enzyme Inhibitor	[11]
Ibuprofen	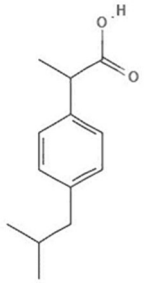	206.1307	2-[4-(2-methylpropyl) phenyl]propanoic acid	Phenylpropionates	Nonsteroidal Anti-inflammatory Drug	[12]

Malathion	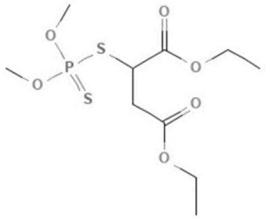	375.0485	diethyl 2-dimethoxy phosphinothioyl sulfanylbutanedioate	Aryloxyphenoxypropionic esters	Herbicide	[13]
Progesterone	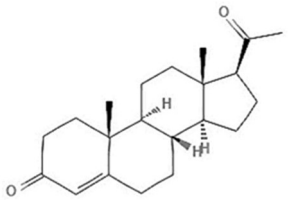	314.2246	(8S,9S,10R,13S,14S,17S)-17-acetyl-10,13-dimethyl-1,2,6,7,8,9,11,12,14,15,16,17-dodecahydrocyclopenta[a]phenanthren-3-one	C21-Steroids	Hormone	[14]

References

[1] PubChem [Internet]. Bethesda (MD): National Library of Medicine (US), National Center for Biotechnology Information; 2004-. PubChem Compound Summary for CID 3120, Diuron; [cited 2023 Dec. 1]. Available from: https://pubchem.ncbi.nlm.nih.gov/compound/Diuron

[2] PubChem [Internet]. Bethesda (MD): National Library of Medicine (US), National Center for Biotechnology Information; 2004-. PubChem Substance Record for SID 318040044, 2-[[[[[(4,6-dimethoxy-2-pyrimidinyl)amino]carbonyl]amino]sulfonyl]methyl]benzoic acid methyl ester, Source: iChemical Technology USA Inc; [cited 2023 Dec. 1]. Available from: https://pubchem.ncbi.nlm.nih.gov/substance/318040044

[3] PubChem [Internet]. Bethesda (MD): National Library of Medicine (US), National Center for Biotechnology Information; 2004-. PubChem Compound Summary for CID 6010, Methyltestosterone; [cited 2023 Dec. 1]. Available from: https://pubchem.ncbi.nlm.nih.gov/compound/Methyltestosterone

[4] PubChem [Internet]. Bethesda (MD): National Library of Medicine (US), National Center for Biotechnology Information; 2004-. PubChem Compound Summary for CID 42807, Flamprop; [cited 2023 Dec. 1]. Available from: https://pubchem.ncbi.nlm.nih.gov/compound/Flamprop

[5] PubChem [Internet]. Bethesda (MD): National Library of Medicine (US), National Center for Biotechnology Information; 2004-. PubChem Compound Summary for CID 14855, 4-Chloro-2-methylphenol; [cited 2023 Dec. 1]. Available from: https://pubchem.ncbi.nlm.nih.gov/compound/4-Chloro-2-methylphenol

[6] PubChem [Internet]. Bethesda (MD): National Library of Medicine (US), National Center for Biotechnology Information; 2004-. PubChem Compound Summary for CID 7153, Mecoprop; [cited 2023 Dec. 1]. Available from: https://pubchem.ncbi.nlm.nih.gov/compound/Mecoprop

[7] PubChem [Internet]. Bethesda (MD): National Library of Medicine (US), National Center for Biotechnology Information; 2004-. PubChem Compound Summary for CID 9502, Linuron; [cited 2023 Dec. 1]. Available from: https://pubchem.ncbi.nlm.nih.gov/compound/Linuron

[8] PubChem [Internet]. Bethesda (MD): National Library of Medicine (US), National Center for Biotechnology Information; 2004-. PubChem Compound Summary for CID 4495, Nimesulide; [cited 2023 Dec. 1]. Available from: https://pubchem.ncbi.nlm.nih.gov/compound/Nimesulide

[9] PubChem [Internet]. Bethesda (MD): National Library of Medicine (US), National Center for Biotechnology Information; 2004-. PubChem Compound Summary for CID 7207, 4-(4-Chloro-2-methylphenoxy)butanoic acid; [cited 2023 Dec. 1]. Available from: https://pubchem.ncbi.nlm.nih.gov/compound/4-_4-Chloro-2-methylphenoxy_butanoic-acid

[10] PubChem [Internet]. Bethesda (MD): National Library of Medicine (US), National Center for Biotechnology Information; 2004-. PubChem Compound Summary for CID 2581, Carprofen; [cited 2023 Dec. 1]. Available from: https://pubchem.ncbi.nlm.nih.gov/compound/Carprofen

[11] PubChem [Internet]. Bethesda (MD): National Library of Medicine (US), National Center for Biotechnology Information; 2004-. PubChem Compound Summary for CID 3033, Diclofenac; [cited 2023 Dec. 1]. Available from: https://pubchem.ncbi.nlm.nih.gov/compound/Diclofenac

[12] PubChem [Internet]. Bethesda (MD): National Library of Medicine (US), National Center for Biotechnology Information; 2004-. PubChem Compound Summary for CID 3672, Ibuprofen; [cited 2023 Dec. 1]. Available from: https://pubchem.ncbi.nlm.nih.gov/compound/Ibuprofen

[13] PubChem [Internet]. Bethesda (MD): National Library of Medicine (US), National Center for Biotechnology Information; 2004-. PubChem Compound Summary for CID 4004, Malathion; [cited 2023 Dec. 1]. Available from: https://pubchem.ncbi.nlm.nih.gov/compound/Malathion

[14] PubChem [Internet]. Bethesda (MD): National Library of Medicine (US), National Center for Biotechnology Information; 2004-. PubChem Compound Summary for CID 5994, Progesterone; [cited 2023 Dec. 1]. Available from: https://pubchem.ncbi.nlm.nih.gov/compound/Progesterone

Section A1: Synthesis of magnetic nanoparticles

To prepare MNPs, 1.352 g of $FeCl_3 \cdot 6H_2O$ and 0.695 g of $FeSO_4 \cdot 7H_2O$ (molar ratio 2:1) were dissolved in 200 mL of a 0.5 M HCl solution. After the drop-by-drop addition of a 1.25 M NaOH solution, a black precipitate of MNPs was immediately formed. The addition was stopped when a neutral pH was reached. The solid residue was then washed five times with 10 mL of Milli-Q water, every time by centrifuging and removing the washing water. After this procedure, the same cleaning step was realized with ethanol (10 mL). The dried solid residue was pounded in a glass mortar and the resulting powder stored in a weighing bottle.

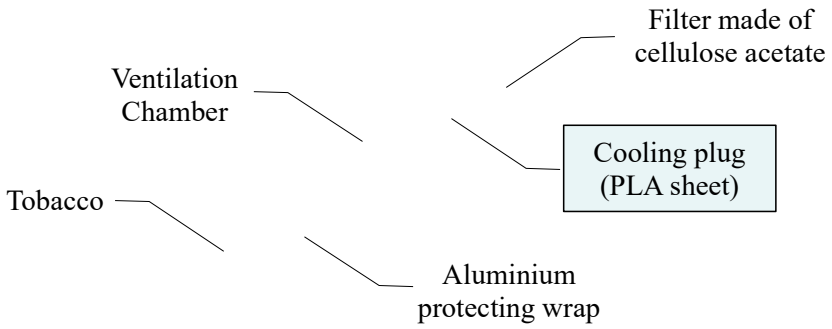

Fig. A1 Representation of the cross-section of a HEETS® filter.

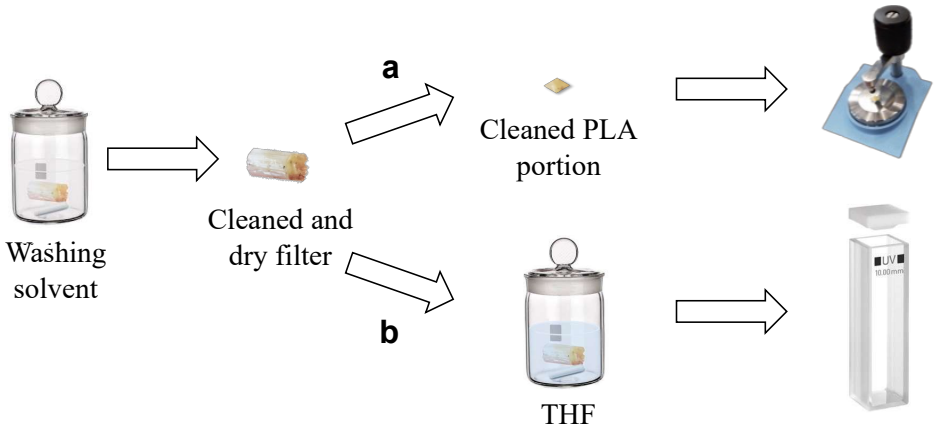

Fig. A2 Procedure for preparing the used-PLA filter to the ATR-FTIR (**a**) and UV-Vis (**b**) spectroscopic analysis.

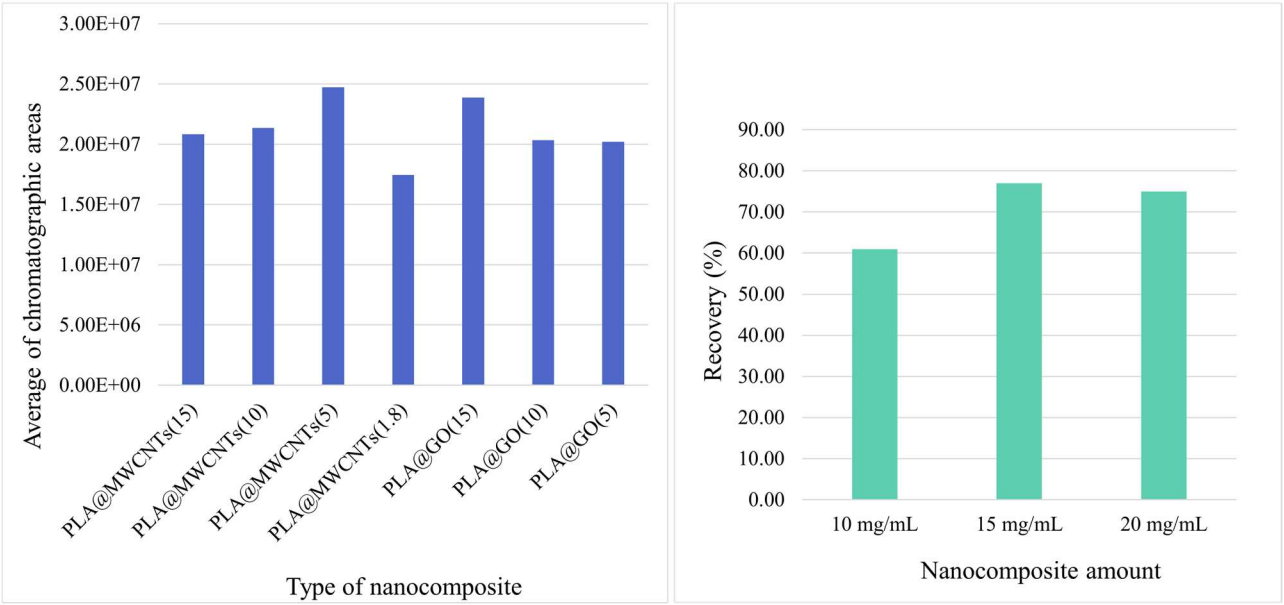

Fig. A3 In **a**, the performance of the six types of microbeads was evaluated comparing the average chromatographic areas of all the analytes in the final extracts, achieved with the different materials. PLA@MWCNTs(5) and PLA@GO(15) registered the best efficiency in analytes recovery. In **b**, nanocomposite amount of PLA@MWCNTs(5) in 1 mL of spiked matrix solution is tested. By comparison among three reasonable conditions, the 15 mg/mL batch proves to be the best solution.

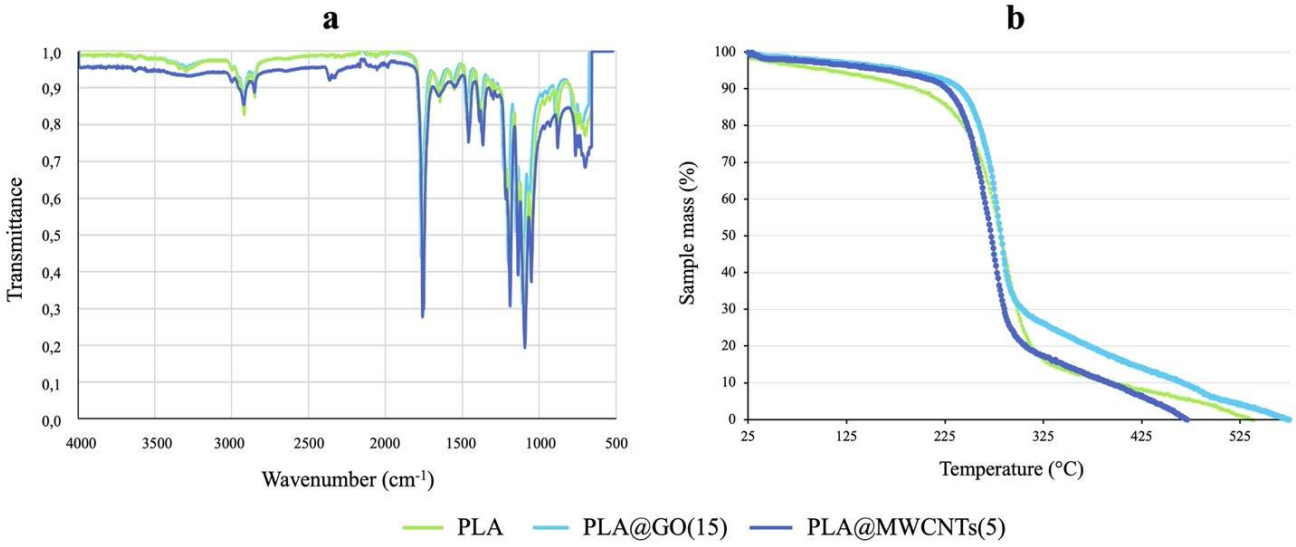

Fig. A4 ATR-FTIR (**a**) and Thermogravimetric (**b**) analysis of pure PLA, PLA@GO(15) and PLA@MWCNTs(5) nanocomposites.

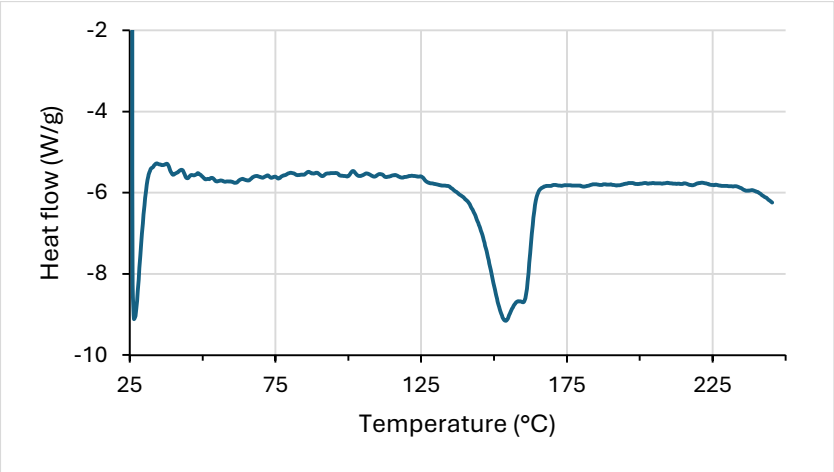

Fig. A5 Thermogram DSC of the composite device in which the double endothermic peak of PLA is visible associated with the melting of the polymer.

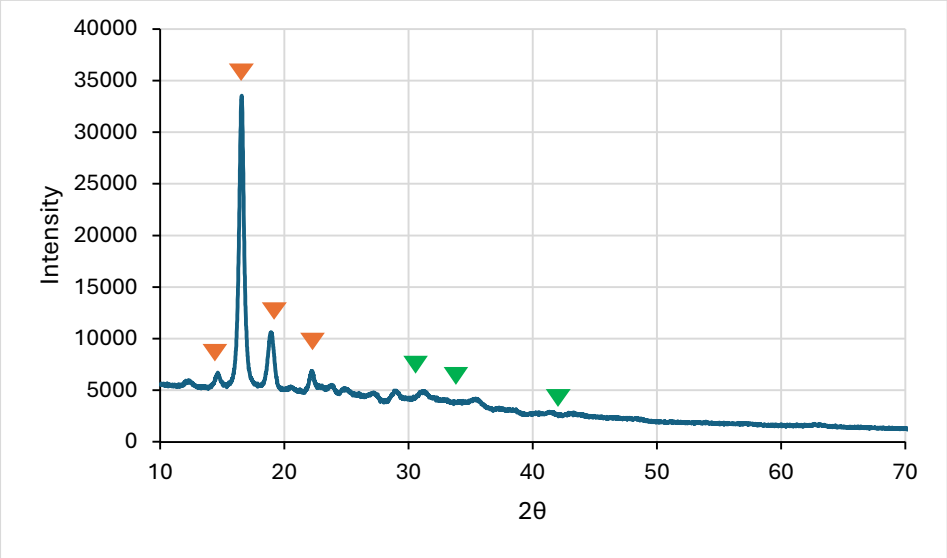

Fig. A6 Diffractogram of the composite device in with are visible the scattering pattern of PLA (orange triangles) and iron oxide (green triangles).

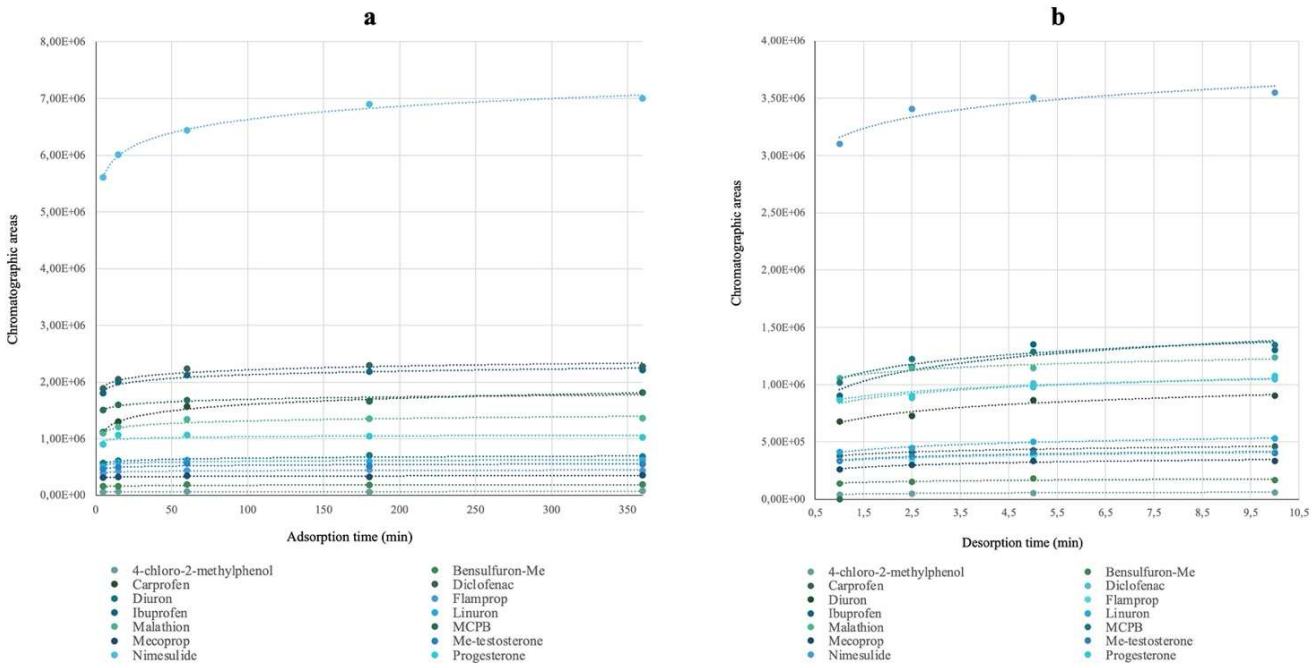

Fig. A7 Kinetic experiments elucidate the time needed for the equilibrium to be reached in both adsorption (**a**) and desorption (**b**) steps. The adsorption equilibrium is reached in less than 5 minutes for most of the analytes. Otherwise, 1 minute is enough to conclude the desorption step for each involved analyte.

Table A3 Recovery, precision and accuracy of the 14 analytes analyzed with the m-SPE-UPLC-MRM method proposed in this work for the middle (6 μg L^{-1}) and the highest spike levels (15 μg L^{-1}).

Compound	Spike level = 6 μg L^{-1}					Spike level = 15 μg L^{-1}				
	Recovery (%)	Precision (%)		Accuracy (%)		Recovery (%)	Precision (%)		Accuracy (%)	
		Within-run	Between-run	Within-run	Between-run		Within-run	Between-run	Within-run	Between-run
Diuron	70	3.0	5.2	13.0	13.4	74	2.0	5.0	12.8	13.0
Bensulfuron-methyl	80	6.8	8.8	8.0	8.9	80	6.5	8.0	8.0	8.6
Methyl-testosterone	70	6.6	7.0	10.0	10.2	72	6.6	7.2	9.8	10.0
Flamprop	75	6.2	6.4	10.0	10.4	76	6.0	6.4	9.8	10.0
4-Chloro-2-methylphenol	64	3.6	5.2	5.1	5.5	65	3.0	5.0	5.0	5.4
Mecoprop	89	7.5	9.9	9.8	10.2	91	7.0	10.0	9.5	9.8
Linuron	80	3.8	5.0	5.0	5.5	80	3.5	4.6	5.0	5.2
Nimesulide	72	7.9	9.8	5.4	5.8	71	7.9	9.6	5.5	5.8
MCPB	77	3.7	4.2	5.0	5.5	78	2.9	4.0	5.0	5.4
Carprofen	93	5.6	5.9	9.0	9.4	93	5.0	5.2	8.7	9.0
Diclofenac	100	4.1	5.2	5.2	6.0	100	4.0	5.2	5.0	5.8
Ibuprofen	76	3.5	4.8	5.0	5.6	78	3.5	4.6	5.0	5.6
Malathion	95	4.7	6.8	5.0	5.4	95	4.6	6.6	4.8	5.2
Progesterone	82	3.7	3.7	13.0	13.5	84	2.7	3.2	12.5	12.9

Table A4 Linear regression parameters for the calibration curves built spiking the urine aliquots pre-extraction with the analytes (mean of six independent analyses).

Compound	$b \pm S_b t_{(0.05;6)}$ (x 10^2)	$a \pm S_a t_{(0.05;6)}$ (x 10^2)	R^2
Diuron	274.9 ± 6.9	35.4 ± 0.7	0.9904
Bensulfuron-methyl	92.2 ± 2.4	3.6 ± 0.2	0.9955
Methyl-testosterone	312.0 ± 9.4	48.2 ± 1.7	0.9902
Flamprop	98.1 ± 2.8	4.4 ± 0.3	0.9925
4-Chloro-2-methylphenol	20.20 ± 0.46	2.30 ± 0.57	0.9938
Mecoprop	133.2 ± 4.0	21.3 ± 0.9	0.9903
Linuron	257.3 ± 7.5	5.60 ± 0.15	0.9930
Nimesulide	977 ± 20	144.8 ± 2.9	0.9927
MCPB	156.6 ± 3.9	30.4 ± 1.1	0.9904
Carprofen	199.7 ± 6.4	49.0 ± 1.3	0.9937
Diclofenac	563.8 ± 13.5	34.7 ± 0.66	0.9958
Ibuprofen	192.9 ± 6.4	40.7 ± 1.3	0.9938
Malathion	825 ± 19	26.48 ± 0.79	0.9907
Progesterone	500 ± 14	34.60 ± 0.69	0.9910

Table A5 Linear regression parameters for the calibration curves built spiking the urine aliquots post-extraction with the analytes (mean of six independent analyses).

Compound	$b \pm S_b t_{(0.05;6)}$ (x 10^{-2})	$a \pm S_a t_{(0.05;6)}$ (x 10^{-2})	R^2
Diuron	432.1 ± 8.7	1.66 ± 0.03	0.9907
Bensulfuron-methyl	121.5 ± 3.5	12.91 ± 0.39	0.9902
Methyl-testosterone	456 ± 10	93.20 ± 0.28	0.9960
Flamprop	136.2 ± 4.1	23.95 ± 0.72	0.9910
4-Chloro-2-methylphenol	37.36 ± 0.93	11.55 ± 0.35	0.9903
Mecoprop	154.6 ± 3.9	15.04 ± 0.48	0.9950
Linuron	345.5 ± 9.0	1.301 ± 0.033	0.9977
Nimesulide	2103 ± 50	343 ± 10	0.9908
MCPB	436 ± 14	90.3 ± 2.9	0.9982
Carprofen	550 ± 15	79.0 ± 2.5	0.9905
Diclofenac	560 ± 18	119.4 ± 3.6	0.9943
Ibuprofen	276.2 ± 8.8	142.5 ± 4.7	0.9938
Malathion	875 ± 26	256.1 ±7.7	0.9799
Progesterone	632 ± 14	35.13 ± 0.70	0.9905

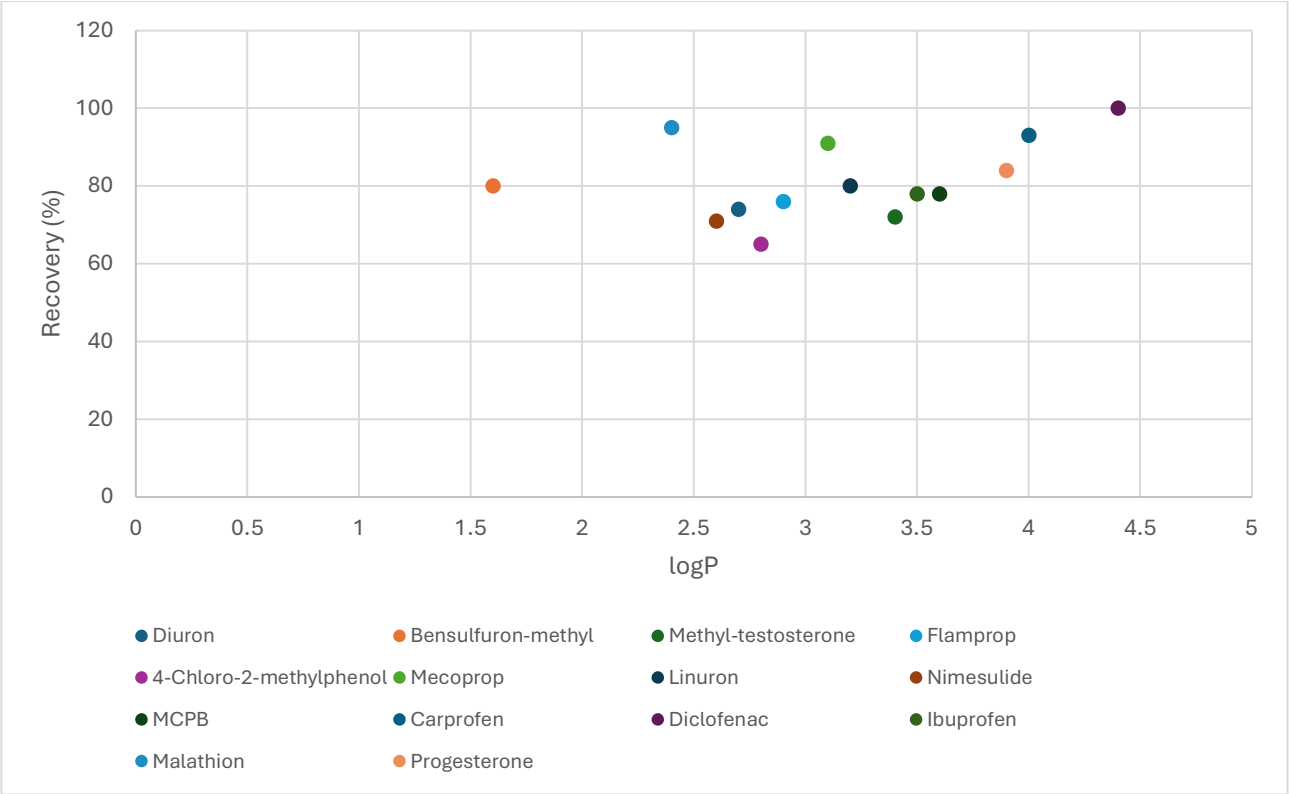

Fig. A8 In the presented graph logP of analytes is plotted against the recoveries obtained with the presented analytical procedure. A general linear trend is shown by the data, displaying the occurrence of a linear dependence between the considered variables.

Table A6 Comparison with other methods aimed at determining the analytes selected in this study in urine samples.

Common name	Method	Recovery (%) (spike levels)	Precision (RSD %) (spike levels)	Enrichment factor	Method limits	Common name	Method
Diuron, Diclofenac	DLLME[a]- HPLC-DAD	75-120 (25-250 µg L^{-1})	8-21 (25-250 µg L^{-1})	~ 13-16	10.0 (LOQ)	~ 10	[1]
Mecoprop, MCPB	SPE-Capillary LC–UV	66-100 (25-150 µg L^{-1})	1-5 (25-150 µg L^{-1})	-	18-19 (LOQ)	~ 30	[2]
Linuron	QuEChERS-UHPLC-MS	94-101 (10-50 µg L^{-1})	4-9 (10-50 µg L^{-1})	~ 0.5 (extract dilution)	13.1 (LOQ)	> 30	[3]
Nimesulide	CPE[b]-HPLC–MS	95.6-107.3 (67-5000 µg L^{-1})	0.04-13 (67-5000 µg L^{-1})	~ 55	67 (LOQ)	~ 10	[4]
Ibuprofen	SBSE[c]-GC-MS	97.2-100.6 (0.5-5 µg L^{-1})	4.37-4.57 (0.5-5 µg L^{-1})	~ 245	0.53 (LOQ)	~ 40	[5]
Malathion	DPE-GC-MS	71-87 (10-70 µg L^{-1})	4.7-6.8 (10-70 µg L^{-1})	~ 4	5.0 (LOQ)	5	[6]
Progesterone	LLE-UHPLC-MS	94 (20-2000 µg L^{-1})	7 (20-2000 µg L^{-1})	~ 5	0.98 (LOQ)	60	[7]
Diuron, Diclofenac, Mecoprop, MCPB, Linuron, Nimesulide, Ibuprofen, Malathion, Progesterone	m-SPE-UHPLC-MS	64-100 (1-15 µg L^{-1})	2.0-10.7 (1-15 µg L^{-1})	~ 6	0.3-2.2 (LLOQ)	15	This work

[a] DLLME = dispersive liquid–liquid microextraction; [b] CPE = Cloud point extraction; [c] SBSE = Stir bar sorptive extraction; [d] DPE = Disposable pipette extraction

References

[1] C. Will, E. Omena, G. Corazza, G. Bernardi, J. Merib, E. Carasek (2020). Expanding the applicability of magnetic ionic liquids for multiclass determination in biological matrices based on dispersive liquid–liquid microextraction and HPLC with diode array detector analysis. J. Sep. Sci., 43(13), 2657-2665. https://doi.org/10.1002/jssc.202000143

[2] N. Rosales-Conrado, M. E. León-González, L. V. Pérez-Arribas, L. M. Polo-Díez (2008). Multiresidue determination of chlorophenoxy acid herbicides in human urine samples by use of solid-phase extraction and capillary LC–UV detection. Anal. Bioanal. Chem., 390, 759-768. https://doi.org/10.1007/s00216-007-1701-5

[3] C. Sweeney, Y. Park, J. S. Kim (2019). Comparison of sample preparation approaches and validation of an extraction method for nitrosatable pesticides and metabolites in human serum and urine analyzed by liquid chromatography-Orbital ion trap mass spectrometry, J. Chromatogr. A 1603 83–91. https://doi.org/10.1016/j.chroma.2019.06.065

[4] O. G. Makukha, L. A. Ivashchenko, O. A. Zaporozhets, Volodymyr O. Doroschuk (2019). Cloud point extraction combined with HPLC-MS for the determination of nimesulide in biological samples, Chem. Zvesti. 73, 693–699. https://doi.org/10.1007/s11696-018-0618-0

[5] P. Mohammadi, M. Masrournia, Z. Es'haghi, M. Pordel (2021). Hollow fiber coated Fe3O4@Maleamic acid-functionalized graphene oxide as a sorbent for stir bar sorptive extraction of ibuprofen, aspirin, and venlafaxine in human urine samples before determining by gas chromatography-mass spectrometry, J. Iran. Chem. Soc. 18 2249–2259. https://doi.org/10.1007/s13738-021-02185-0

[6] A. Luiz Oenning, J. Merib, E. Carasek (2018). An effective and high-throughput analytical methodology for pesticide screening in human urine by disposable pipette extraction and gas chromatography-mass spectrometry. J. Chromatogr. B, 1092, 459-465. https://doi.org/10.1016/j.jchromb.2018.06.047

[7] Y. Zhou, Z. Cai (2020). Determination of hormones in human urine by ultra-high-performance liquid chromatography/triple-quadrupole mass spectrometry, Rapid Communications in Mass Spectrom. 34 e8583. https://doi.org/10.1002/RCM.8583

Appendix B

Optimization of the synthesis of the polymeric microbeads

For the optimization of the emulsion solidification parameters, a reasonable range and some representative values for each involved variable were selected, i.e., volume of the polymeric phase (mL), concentration of the PS in the organic phase (w/v %), ratio of the organic and aqueous phase (o:w) and ratio of the saturated NaCl and sodium dodecyl sulphate solutions in the aqueous phase (NaCl:SDS). A 3 x 4 factorial design, comprising 3 levels and 4 factors (3^4) was employed, leading to the 81 syntheses procedures of PS microspheres, to which a qualitative score was attributed. The final procedure was selected being the one that returns the most satisfactory microbeads, from a morphological point of view, with the lowest consumption of solvents. **Table B1** depicts the studied variables and the selected values for each of them.

Table B1 Selected parameters and explored relative values for the optimization study of the synthetic procedure. Underlined values are the selected ones.

Parameter	Lower value	Intermediate value	Higher value
Volume of the organic polymeric phase (mL)	<u>0.25</u>	1	2
Concentration of the organic polymeric phase (w/v %)	1	<u>2.5</u>	5
Ratio of the organic and aqueous phase (o:w)	1:1	1:4	<u>1:7</u>
Ratio of NaCl saturated solution and Na-dodecyl sulphate 1 % solution in the aqueous phase (NaCl:SDS)	5:2	1:1	<u>2:5</u>

Optimization of the extraction procedure

Variables related to the extraction process were optimized with one experimental design and different one-variable-at–a–time analysis (OVAT) studies, grouping variables on the basis of their possible correlations. Firstly, a three-factor three level Box–Behnken design (BBD) methodology was performed, selecting loading volume (X_1), concentration of the loaded spiked solution (X_2) and PS microbeads amount (X_3) as potentially critical variables affecting the extraction of analytes. X_1 ranged between 1 to 5 mL, being the higher limit imposed by the volume of the syringe itself, while the lower limit considers the necessity to maximise the pre-concentration factor. For the X_2 variable, a range of values between 50 to 250 μg L^{-1} was selected. The choice for high concentration values is explained by the aim of defining load quantities limit for the analytes in competitive conditions, determining saturation limits and breakthrough quantities for each of them. For X_3, since the scalability of the synthetic procedure was not studied, the number of synthetic products loaded in the same syringe was chosen as the quantitative parameter, related to the sorbent amount. X_3 was ranged between 1 and 3 loaded synthetic products. The conditions for the other variables were pH 9 and elution with 300 μL of methanol. pH values around 9 were selected, since this value is higher or quite similar to the pKa of each considered analyte (**Table B2**), promoting interactions between analytes and PS under ionic suppression conditions.

The analytical responses (Y_i) included in the design were the average recovery values. The simultaneous monitoring of X_1 and X_2 allows to control the dependence of the extraction efficiency against the loaded quantity of analytes ($X_1 \cdot X_2$). A similar study permits to define ideal and maximum load quantity for each analyte, being this parameter of essential importance to establish the volume of loaded sample and the dilution level for a selected real sample. Finally, an optimum value for X_3 was established with the experimental model, while simultaneously monitoring the load quantity of the analyte and the saturation limit.

The number of tests of the BBD was calculated using the following equation:

$$N = 2k(k-1) + Cp$$

where N is the number of experiments, k is the number of factors, and Cp is the number of the central points. A total of 30 experiments were performed, carrying out the design by duplicate and including 3 replicates of the central point for the assessment of the test error. The design was built after selecting the range of factors (high and low). Additionally, the multiple linear regression for each response, including linear, quadratic, and interacting terms of independent variables were evaluated following the quadratic polynomial equation:

$$Y = \beta_0 + \sum \beta_i \chi_i + \sum \beta_{ii} \chi_i^2 + \sum \beta_{ij} \chi_i \chi_j + \varepsilon$$

where Y refers to the analytical response; β_0 is the constant coefficient; β_i, β_{ii} and β_{ij} are the regression coefficients of the model; χ_i and χ_j represent the independent variables; and ε is the residual error associated to the experiments.

A desirability function approach was used to find the optimal extraction conditions to maximize the extraction efficiency of the analytes. The global desirability of the experiment (D) is defined by the following equation:

$$D = (d_1(Y_1) d_2(Y_2) \cdots d_n(Y_n))^{1/n}$$

where n is the number of responses studied in each experiment and $d_i(Y_i)$ is the individual desirability of each response in the experiment, calculated as follows:

$$(d_i) = \frac{Y_i - Y_{min}}{Y_{max} - Y_{min}}$$

For each response, $Y_i(x)$, a desirability function $d_i(Y_i) = 1$ represents a completely desirable value obtained by the response surface methodology. The statistical analysis was performed using the StatGraphics Centurion XVI (Stat Point Inc., Herndon, VA, USA) software.

In addition, pH was optimized by performing extractions in the range between 3 and 10 at a concentration of 50 μg L^{-1}, loading 1 PS synthesis and passing through 5 mL of aqueous sample. In the same way, dependence of extraction recoveries was studied against the ionic strength, with solutions with conductance ranging from 16.2 μMHO to 0.32 MHO. Electrolyte concentration was controlled by dissolving different amounts of sodium chloride in MilliQ water spiked samples.

Parameters related to the desorption step of the extraction procedure were optimized with OVAT studies. The composition of the eluent phase was optimized by choosing the most effective option from either bare methanol or with acidic or basic organic modifiers (i.e., formic acid and ammonia), at a 1% v/v concentration. Lastly, the volume of the desorption methanolic phase was evaluated, performing the whole extraction with different elution volumes (ranging from 200 to 500 μL) and working in triplicates.

Table B2 Structure and relevant chemical parameters of the selected opioids. Multiple reaction monitoring (MRM) transitions of the analytes.

Common name	Structure	Exact mass (u)	logP	pKa	1st transition (m/z)[a]	2nd transition (m/z)[a]
Morphine	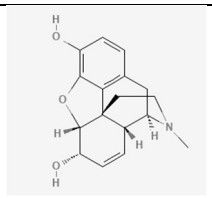	285.1365	0.8	8.21	286.1/201.1	286.1/157
Codeine	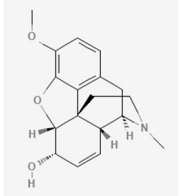	299.1521	1.1	8.20	300.1/199	-
Tramadol	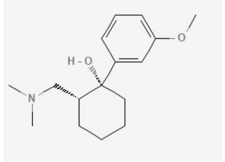	263.1885	2.6	9.23	264.2/58.2	264.2/246.1

Methadone	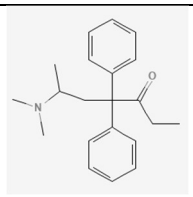	309.2093	3.9	8.95	310.2/265.1	310.2/105.1

[a] The first MRM transition is the most intense one (quantifier), while the other is the second most intense (qualifier). Data obtained from PubChem [Internet]. Bethesda (MD): National Library of Medicine (US), National Center for Biotechnology Information; 2004. PubChem Compound Summary for CID 5288826, Morphine; [cited 2024 Mar. 4]. Available from: https://pubchem.ncbi.nlm.nih.gov/compound/Morphine; PubChem Compound Summary for CID 5284371, Codeine; [cited 2024 Mar. 4]. Available from: https://pubchem.ncbi.nlm.nih.gov/compound/Codeine; PubChem Compound Summary for CID 33741, Tramadol; [cited 2024 Mar. 4]. Available from: https://pubchem.ncbi.nlm.nih.gov/compound/Tramadol; PubChem Compound Summary for CID 4095, Methadone; [cited 2024 Mar. 4]. Available from: https://pubchem.ncbi.nlm.nih.gov/compound/Methadone.

TGA characterization of the synthetic PS microspheres

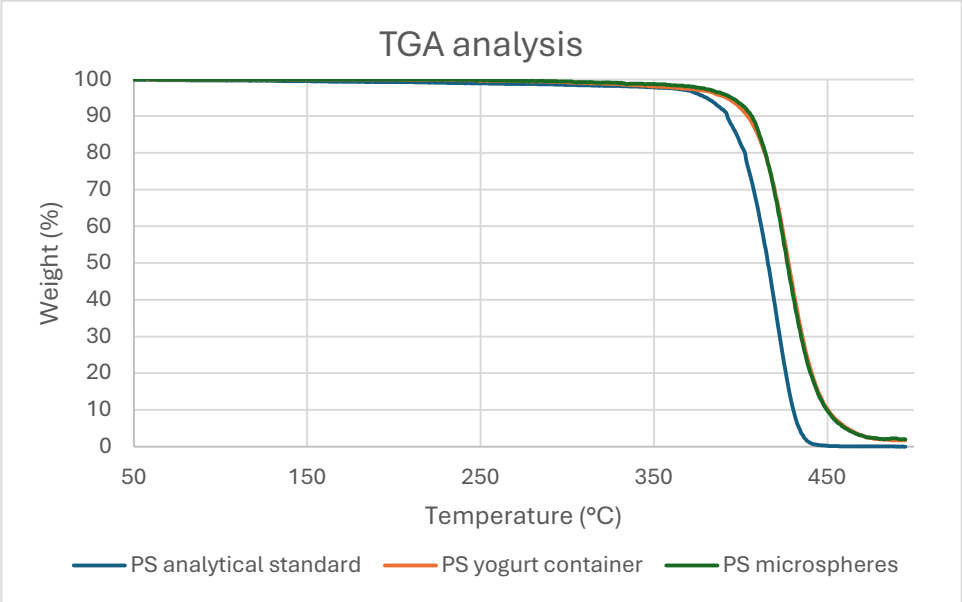

Fig. B1 Thermogravimetric analysis (TGA) curves for polystyrene (PS) analytical standard, commercial PS (recovered from a yogurt container), and synthesized microspheres. All samples exhibit the characteristic thermal degradation profile of polystyrene. Experimental conditions: nitrogen atmosphere (20 mL min^{-1}), temperature range 50–500 °C, heating rate 10 °C min^{-1}.

ATR-IR characterization of the modified paper

The FTIR spectrum of polystyrene exhibits a characteristic absorption band in the range at around 3020 cm^{-1} attributed to =C–H stretching vibrations associated with the aromatic ring. Peaks observed at 2918 cm^{-1} and 2843 cm^{-1} correspond to the symmetric and asymmetric stretching vibrations of CH_2 groups. Additionally, absorption bands at 1604 cm^{-1}, 1490 cm^{-1}, and 1445 cm^{-1} are indicative of the C=C stretching vibrations within the benzene ring. A band at 1024 cm^{-1} is associated with C–O

stretching, while the bands between 680 and 800 are attributed to the rocking of C–H of the benzene ring.

On the other hand, the FTIR spectrum of cellulose displays an absorption band at 3345 cm^{-1}, attributed to the stretching vibrations of hydroxyl groups. Bands observed at 2910 cm^{-1} and 1340 cm^{-1} correspond to the stretching and deformation vibrations of the C–H group within the glucose units, respectively. The signal at 1040 cm^{-1} is assigned to the -C–O- group associated with secondary alcohol and ether functionalities present in the cellulose backbone.

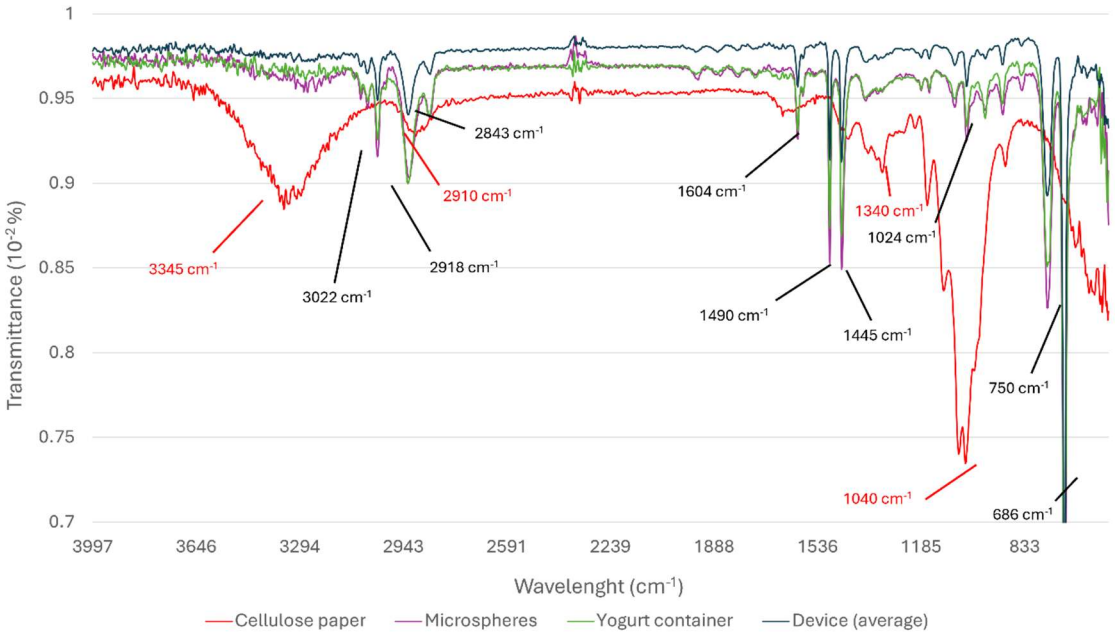

Fig. B2 ATR-FTIR spectra of cellulose paper, with and without functionalization, PS microspheres and the original waste polymeric material.

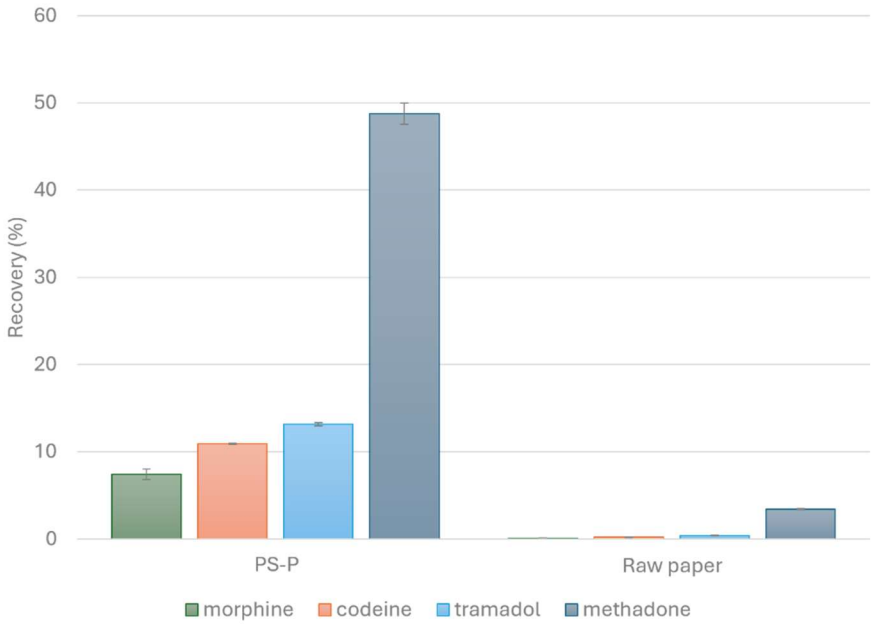

Fig. B3 Comparison between pristine paper and PS-P in terms of extraction performances (average recoveries on three replicates) at the same experimental conditions (5 mL of a 500 µg L^{-1} loading solution at pH 9, 300 µL of MeOH as the elution solvent).

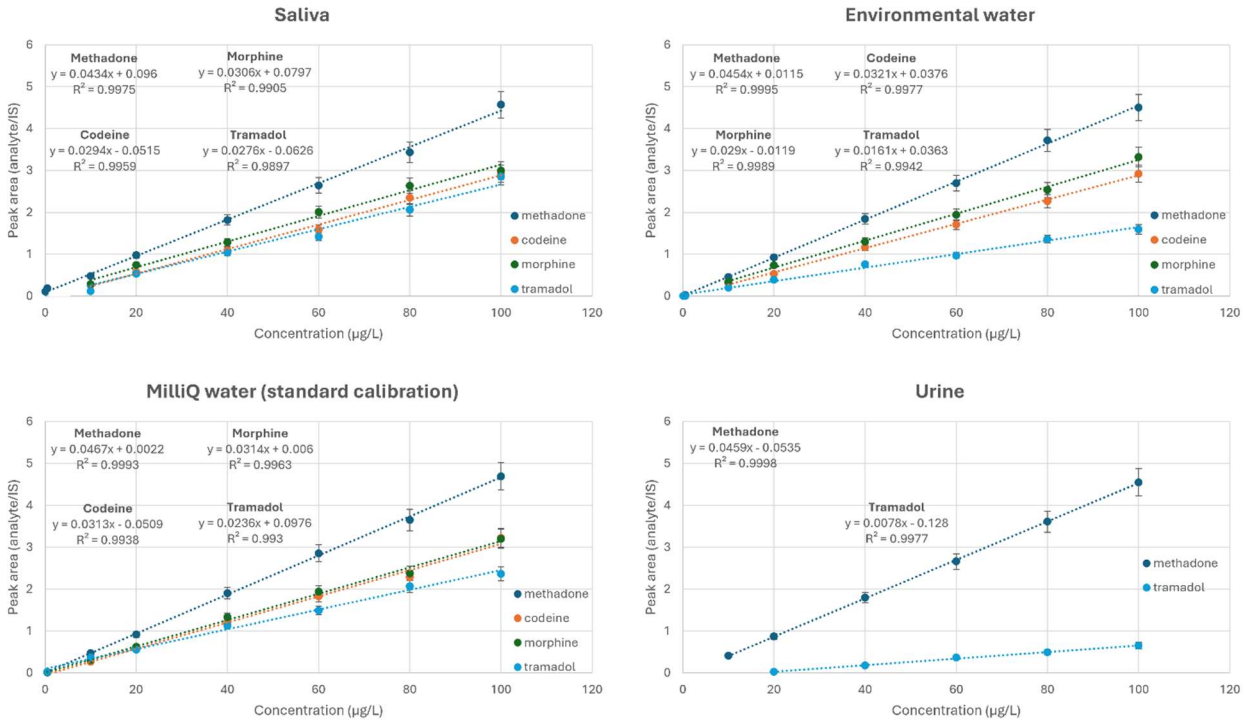

Fig. B4 Matrix matched calibration curves for the analytes in solvent (MilliQ water) and in three different complex matrices are reported in the graphs. The concentration range is included between 0.1 and 100 µg mL^{-1}, taking as the lowest point the LOQ of the analyte in the specific extraction medium. R^2 and linear model equations, extrapolated by the experimental data, are also displayed.

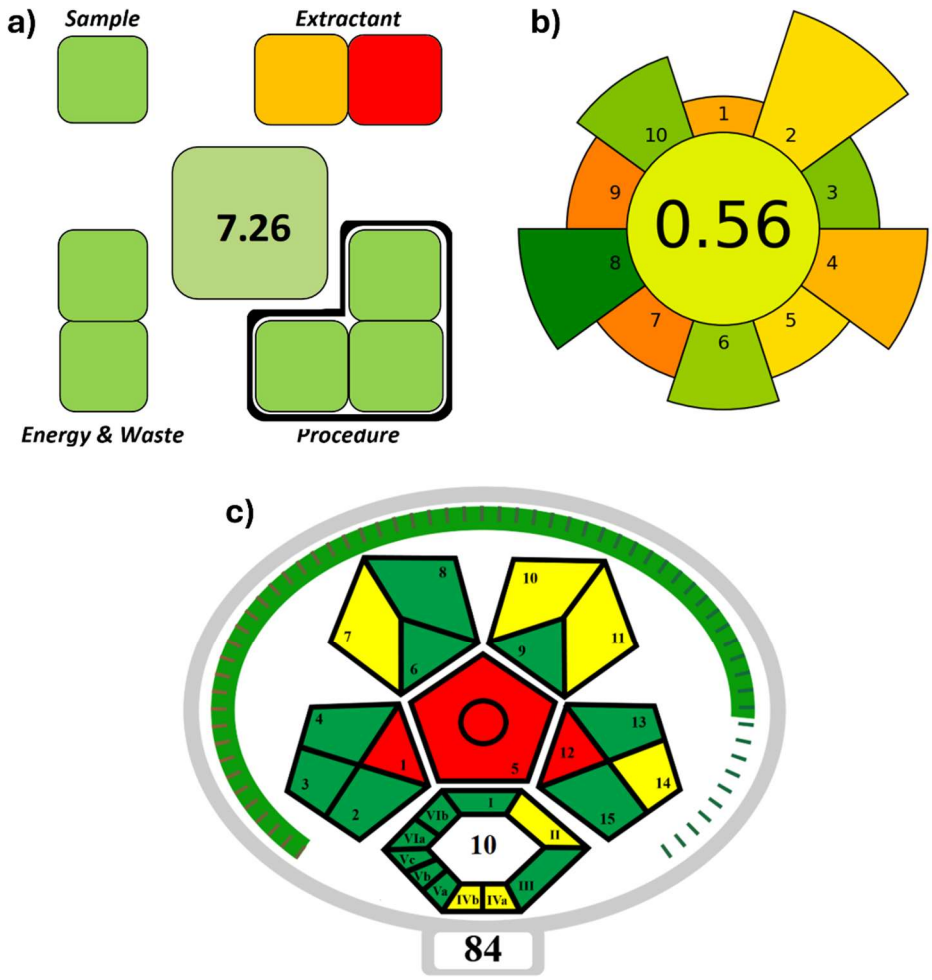

Fig. B5 Evaluation of the sustainability of the proposed method using **A)** Sample preparation metric of sustainability (SPMS), **B)** Analytical greenness metric for sample preparation (AGREEprep) software and C**)** ComplexMoGAPI total scoring system and software.

Table B3 Comparison of the proposed analytical method with other articles reporting the determination of methadone, codeine, morphine and/or tramadol in biological fluids.

Instrumental technique	Extraction Technique	LOQ (μg L^{-1})				Extraction Time (min)	Chromat. Separation	Matrix	Recycling Material	Ref.
		ME	CO	MO	TRA					
HPLC-UV	DES-LPME	-	1.5	1.5	-	< 2	yes	blood	no	(Binjawhar et al., 2024)
GC-MS	MSPE-DLLME	0.10	-	-	0.11	12	yes	urine	no	(Isazad et al., 2022)
CD-IMS	EME-SFME	2.5	-	-	2.5	17.5	no	urine	no	(Behpour et al., 2022)
DI-MS/MS	TFME	5	5	5	5	> 90	no	saliva	no	(Pedraza-Soto et al., 2024)
HPLC-UV	DMSPE	-	0.3	-	0.15	> 20	yes	saliva	no	(Soltani et al., 2023)
HPLC-UV	IT-G-EME	-	10	-	15	5	yes	plasma	no	(Rahbarian et al., 2023)
GC-MS/MS	MEPS	-	1	1	1	NS	yes	urine	no	(Simão et al., 2022)
DI-MS/MS	TFME	10	-	-	10	> 180	no	saliva	no	(Calero-Cañuelo et al., 2023)
DI-MS/MS	ISμSPE	0.02-2.4	5.9-6.5	5.6-9.1	0.1-14.5	< 5	no	urine, saliva, water	yes	This work

LOQ, limit of quantification. Pre-treatment: DES-LPME, deep eutectic solvent based liquid phase microextraction; MSPE-DLLME, magnetic-dispersive solid-phase extraction coupled with dispersive liquid–liquid micro-extraction; EME-SFME, electromembrane extraction and slug flow microextraction; TFME, thin film-microextraction; DMSPE, dispersive micro-solid phase extraction; IT-G-EME, in-tube gel electromembrane extraction; MEPS, microextraction by packed sorbent; ISμSPE, in-syringe micro solid-phase extraction. Instrumental technique: HPLC-UV, high-performance liquid chromatography ultra-violet detection; GC-MS, gas chromatography-mass spectrometry; CD-IMS, corona discharge-ion mobility spectrometry; DI-MS/MS, direct infusion-tandem mass spectrometry; GC-MS/MS, gas chromatography-tandem mass spectrometry

References

Behpour, M., Maghsoudi, M., Nojavan, S., 2022. Analysis of methamphetamine, methadone, tramadol, and buprenorphine in biological samples by ion mobility spectrometry after electromembrane extraction in tandem with slug flow microextraction. J. Chromatogr. A, 1678, 463355. https://doi.org/10.1016/j.chroma.2022.463355

Binjawhar, D. N., Mohammedsaeed, W., 2024. pH-switchable hydrophobic deep eutectic solvent-based liquid phase microextraction for detecting morphine and codeine in whole blood samples followed by HPLC-UV. J. King Saud Univ. Sci., 103303. https://doi.org/10.1016/j.jksus.2024.103303

Calero-Cañuelo, C., Casado-Carmona, F. A., Lucena, R., Cárdenas, S., 2023. Mixed-mode cationic exchange sorptive tapes combined with direct infusion mass spectrometry for determining opioids in saliva samples. J. Chromatogr. A, 1702, 464097. https://doi.org/10.1016/j.chroma.2023.464097

Isazad, M., Amirzehni, M., Akhgari, M., 2022. Highly efficient dispersive liquid-liquid microextraction assisted by magnetic porous carbon composite-based dispersive micro solid-phase extraction for determination of tramadol and methadone in urine samples by gas chromatography-mass spectrometry. J. Chromatogr. A, 1670, 462989. https://doi.org/10.1016/j.chroma.2022.462989

Pedraza-Soto, A. M., Lucena, R., Cárdenas, S., 2024. Mixed-mode cationic exchange paper combined with direct infusion mass spectrometry, a sustainable approach to determine opioids in biosamples. Sustin. Chem. Pharm., 41, 101723. https://doi.org/10.1016/j.scp.2024.101723

Rahbarian, H., Nojavan, S., Maghsoudi, M., Tabani, H., 2023. In-tube gel electromembrane extraction: A green strategy for the extraction of narcotic drugs from biological samples. J. Chromatogr. A, 1688, 463714. https://doi.org/10.1016/j.chroma.2022.463714

Simão, A. Y., Monteiro, C., Marques, H., Rosado, T., Margalho, C., Barroso, M., Gallardo, E., 2022. Analysis of opiates in urine using microextraction by packed sorbent and gas chromatography-tandem mass spectrometry. J. Chromatogr. B, 1207, 123361. https://doi.org/10.1016/j.jchromb.2022.123361

Soltani, N., Habibollahi, S., Salamat, A., 2023. Application of oxidized multi-walled carbon nanotubes and zeolite nanoparticles for simultaneous preconcentration of codeine and tramadol in saliva prior to HPLC determination. J. Chromatogr. B, 1222, 123693. https://doi.org/10.1016/j.jchromb.2023.123693

Appendix C

Table C1 Physicochemical properties, retention times, and mass spectrometric transitions of selected sulfonamides.

Common name	Structure	Exact mass (u)	logP	pKa	Retention time (min)	1st transition (m/z)	2nd transition (m/z)
Sulfamerazine	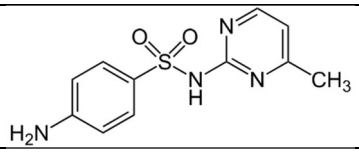	264.0681	0.14	7.06	2.6	265/156	265/92.2
Sulfadiazine	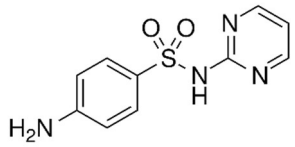	250.0524	-0.09	6.36	2.9	251/92.2	251/65.3
Sulfaguanidine	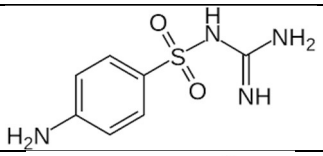	214.0524	-0.7	11.25	5.1	215/92.2	215/65.2
Sulfanilamide	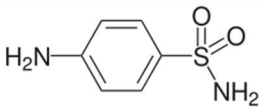	172.0306	-0.62	10.6	5.5	173/56	173/92

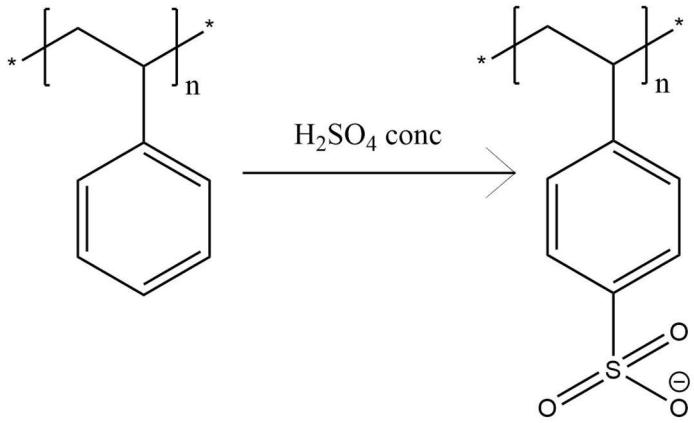

Fig. C1 Sulfonation process of polystyrene.

ATR-FTIR characterization of the materials

The FTIR spectrum of polystyrene displays a distinctive absorption band around 3020 cm^{-1}, corresponding to =C–H stretching vibrations of the aromatic ring. The bands at 2918 cm^{-1} and 2846 cm^{-1} are assigned to the asymmetric and symmetric stretching modes of CH_2 groups, respectively. Furthermore, prominent peaks at 1602 cm^{-1}, 1490 cm^{-1}, and 1450 cm^{-1} reflect the C=C stretching vibrations within the benzene ring. An absorption band near 1025 cm^{-1} is attributed to C–O stretching, while bands in the 680–800 cm^{-1} range are associated with the out-of-plane rocking vibrations of C–H bonds in the aromatic ring.

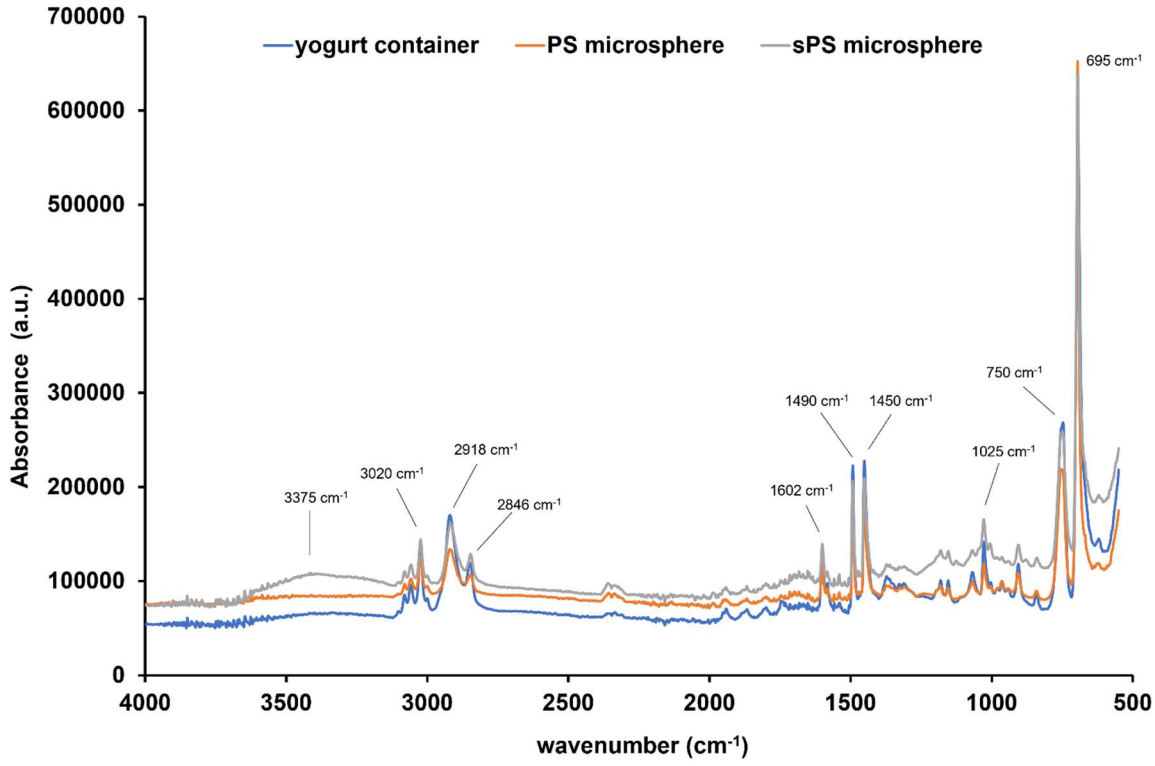

Fig. C2 ATR-FTIR spectra of polystyrene waste, pristine polystyrene microbeads, and sulfonated microbeads after the sulfonation process.

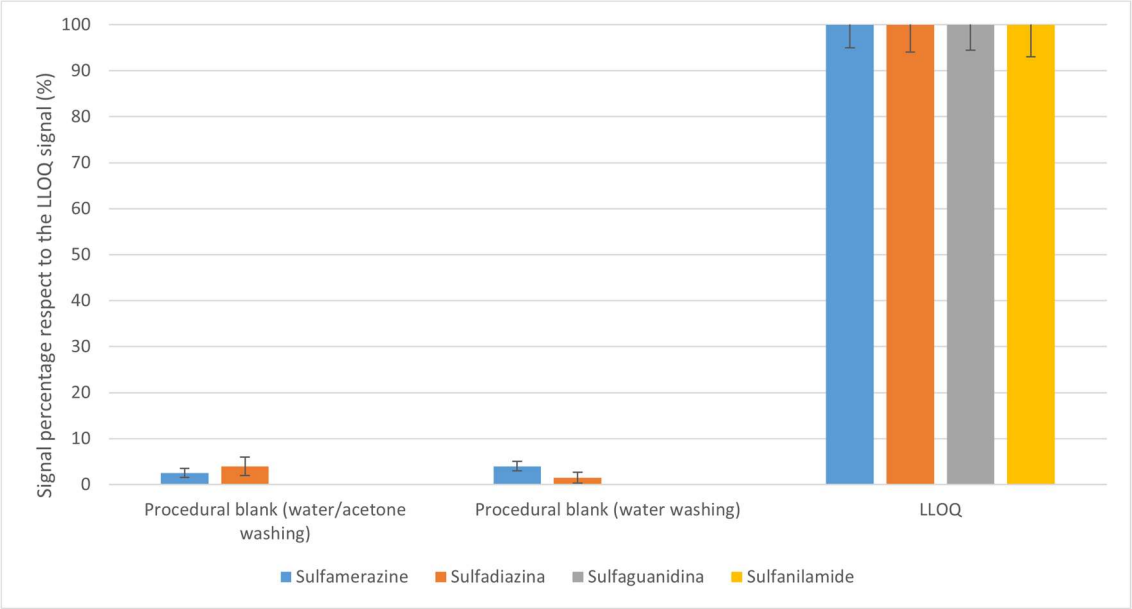

Fig. C3 Effectiveness of the washing protocol procedure, resulting in a negligible memory effect of the reused materials.

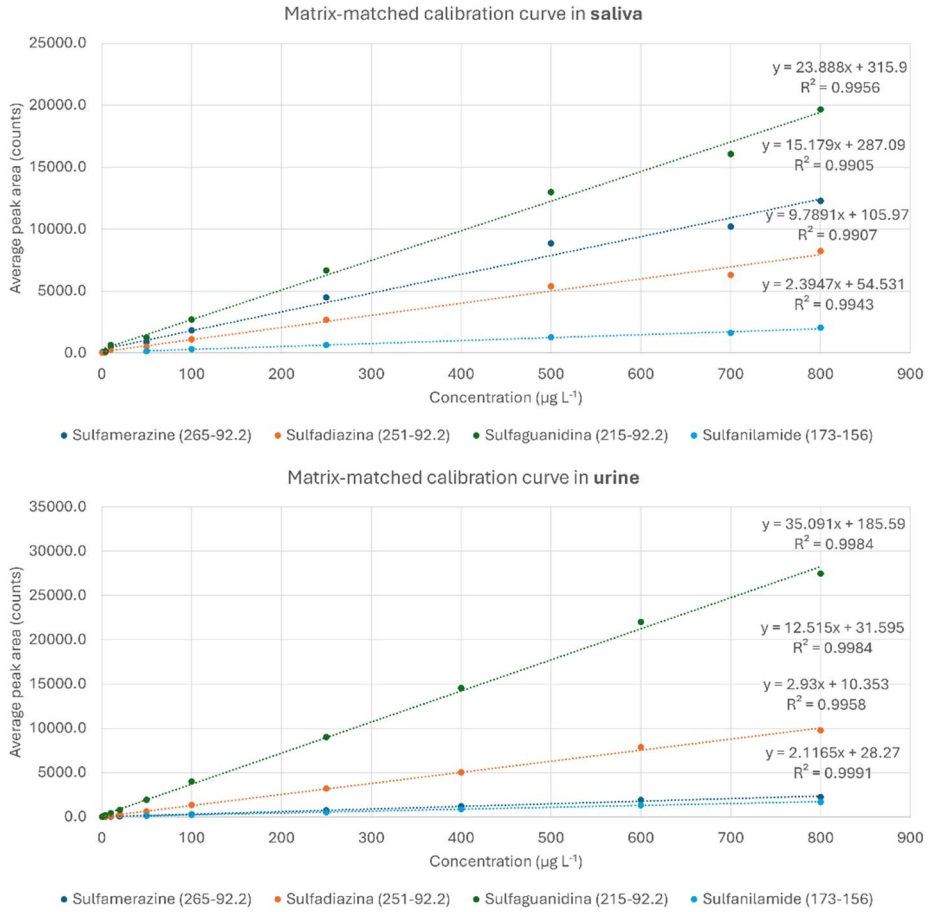

Fig. C4 Matrix-matched calibration curves of the selected sulfonamides in real biological samples.

Table C2 Comparison of the proposed analytical method with other articles reporting the determination of sulfadiazine (SD), sulfamerazine (SM), sulfanilamide (SA) and sulfaguanidine (SG) in biological fluids.

Instrumental technique	**Extraction Technique**	**LOQ (µg L^{-1})**				**Extraction time (min)**	**Matrix**	**Recycling Material**	**Ref.**
		SD	**SM**	**SA**	**SG**				
Spectrophotometric	Disk-SPME	6.26	4.49	11.19	-	> 20	River water	no	[1]
Spectrophotometric	SPE	130	100	60	-	> 30	Seawater	no	[2]
Smartphone-based fluorimetry	Pipette-tip SPME	-	9.1	-	-	n.a.	Environmental water	no	[3]
HPLC-DAD	SPE with 3D-printed device	20	3	-	-	40	Environmental water	no	[4]
HPLC-MS/MS	LLLME	-	-	0.22	-	~ 60	Wastewater	no	[5]
HPTLC	MISPE	10	-	-	10	~ 60	Environmental water	no	[6]
LC-MS/MS	QuEChERS	5-12 (ng g^{-1})	5-13 (ng g^{-1})	3-10 (ng g^{-1})	3-10 (ng g^{-1})	~ 70	Animal tissues and products	no	[7]
HILIC-QTOF-MS	dSPE	5 (ng g^{-1})	5 (ng g^{-1})	-	-	> 3 h	Food product	no	[8]
HPLC-MS/MS	IS-dSPME	4-5	4-5	50	2-4.8	~ 35	Biological matrices	yes	This work

HPLC-DAD: High-Performance Liquid Chromatography with Diode Array Detection; MS: Mass spectrometry; HPTLC: High Performance Thin-Layer Chromatography; HILIC-QTOF-MS: Hydrophilic Interaction Liquid Chromatography - Quadrupole Time-of-Flight Mass Spectrometry; SPME: solid-phase microextraction; SPE: solid-phase extraction; LLLME: liquid–liquid–liquid microextraction; MISPE: Molecularly Imprinted Polymer Solid-Phase Extraction; dSPE: dispersive solid phase extraction; IS-dSPME: in-syringe dispersive solid-phase microextraction.

References

[1] Peixoto, P. S., Tóth, I. V., Machado, S., Barreiros, L., Machado, A., Bordalo, A. A., Lima, J. L. F. C., Segundo, M. A. (2018). Screening of sulfonamides in waters based on miniaturized solid phase extraction and microplate spectrophotometric detection. Anal. Methods., 10(7), 690-696. https://doi.org/10.1039/C7AY02624B

[2] Ait Errayess, S., Ait Lahcen, A., Idrissi, L., Marcoaldi, C., Chiavarini, S., Amine, A. (2017). A sensitive method for the determination of Sulfonamides in seawater samples by Solid Phase Extraction and UV–Visible spectrophotometry. Spectrochim. Acta A Mol. Biomol. Spectrosc., 181, 276-285. https://doi.org/10.1016/j.saa.2017.03.061

[3] Barzallo, D., Ferrer, L., Palacio, E. (2024). Eco-friendly screening method for sulfonamides using a 3D handheld smartphone-based fluorescence detection device and graphene nanoplatelet-packed pipette tip microextraction. J. Environ. Chem. Eng., 12(2), 111888. https://doi.org/10.1016/j.jece.2024.111888

[4] Barzallo, D., Palacio, E., March, J., Ferrer, L. (2023). 3D printed device coated with solid-phase extraction resin for the on-site extraction of seven sulfonamides from environmental water samples preceding HPLC-DAD analysis. Microchem. J., 190, 108609. https://doi.org/10.1016/j.microc.2023.108609

[5] Schlüsener, M. P., Bester, K. (2005). Determination of steroid hormones, hormone conjugates and macrolide antibiotics in influents and effluents of sewage treatment plants utilising high-performance liquid chromatography/tandem mass spectrometry with electrospray and atmospheric pressure chemical ionisation. Rapid Commun. Mass Spectrom., 19(22), 3269-3278. https://doi.org/10.1002/rcm.2189

[6] Pavlović, D. M., Nikšić, K., Livazović, S., Brnardić, I., Anžlovar, A. (2015). Preparation and application of sulfaguanidine-imprinted polymer on solid-phase extraction of pharmaceuticals from water. Talanta, 131, 99-107. https://doi.org/10.1016/j.talanta.2014.06.065

[7] Kim, Y. R., Park, S., Kim, J. Y., Choi, J. D., Moon, G. I. (2024). Simultaneous determination of 31 Sulfonamide residues in various livestock matrices using liquid chromatography-tandem mass spectrometry. Appl. Biol. Chem., 67(1), 13. https://doi.org/10.1186/s13765-024-00864-z

[8] Petrarca, M. H., de Campos Braga, P. A., Reyes, F. G. R., Bragotto, A. P. A. (2022). Exploring miniaturized sample preparation approaches combined with LC-QToF-MS for the analysis of sulfonamide antibiotic residues in meat-and/or egg-based baby foods. Food Chem., 366, 130587. https://doi.org/10.1016/j.foodchem.2021.130587

Appendix D

Table D1 Physicochemical properties, structure and classification of the studied analytes.

Chemical class	Analyte	logP	pKa	CAS number	M.W. (g mol^{-1})	Structure
Insecticide	**Acephate**	-0.85	8.35	30560-19-1	183.2	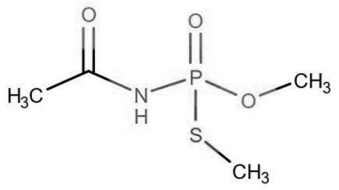
Herbicides	**Butoxycarboxim**	1.1	3.83	34681-23-7	222.26	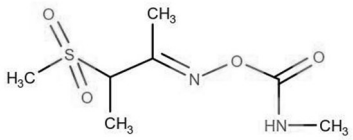
Insecticide	**Methomyl**	0.60	13.27	16752-77-5	162.21	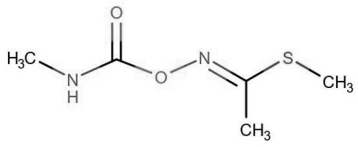
Antibiotic	**Sulfaguanidine**	-1.2	2.37	57-67-0	214.0524	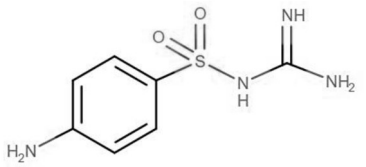
Antibiotic	**Sulfamerazine**	0.89	7.4	127-79-7	264.305	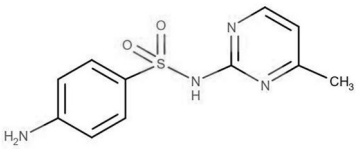
Insecticide	**Pirimicarb**	1.7	4.34	66246-88-6	238.29	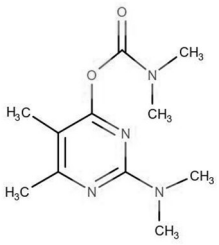
Antibiotic	**Sulfamonomethoxine**	1.7	6.0	1220-83-3	264.5	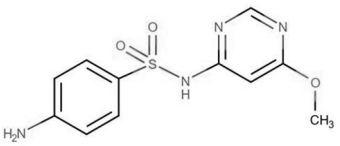
Antibiotic	**Sulfachloropyridazine**	1.54	6.5	80-32-0	28472	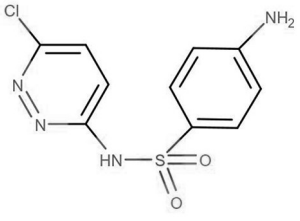

Herbicide	**Dimethoate**	0.78	14.40	60-51-5	229.26	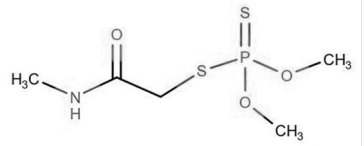
Herbicide	**Picloram**	2.81	4.1	1918-02-1	239.92	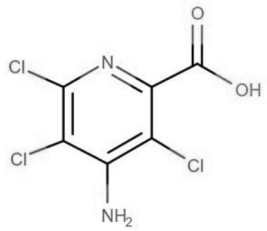
Antibiotic	**Sulfathiazole**	0.17	7.2	72-14-0	255.319	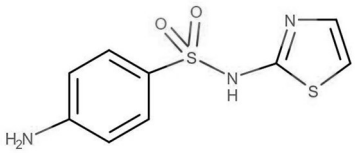
Antibiotic	**Sulfamethoxazole**	1.58	5.6	723-46-6	253.27	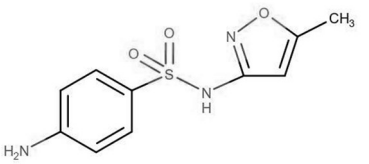
Herbicide	**Butocarboxim**	1.46	13.83	34681-10-2	190.26	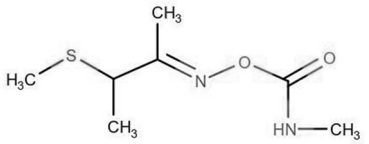
Hormone	**Prednisolone**	1.62	12.46	50-24-8	360.44	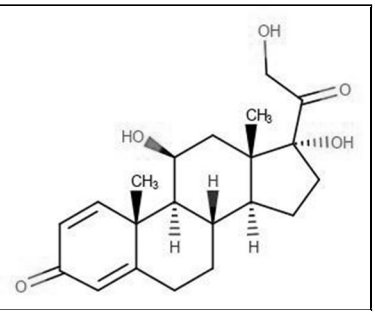
Herbicide	**Thifensulfuron-Me**	2.5	2.2	79277-27-3	387.4	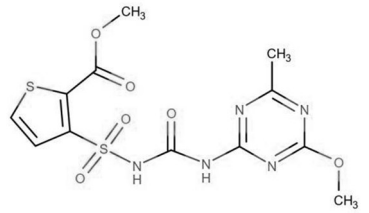
Insecticide	**Propoxur**	1.52	12.28	114-26-1	209.24	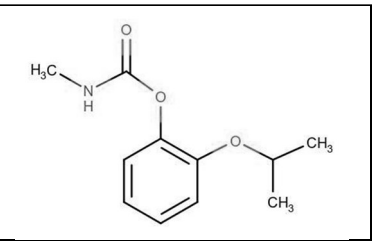

Hormone	**Dexamethasone**	1.83	12	50-02-2	392.46	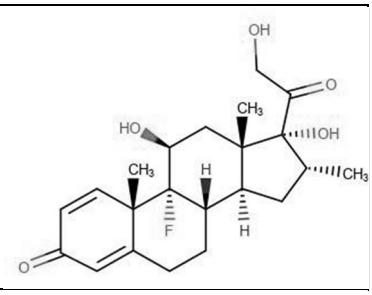
Herbicide	**Cinosulfuron**	1.4	2.4	94593-91-6	413.41	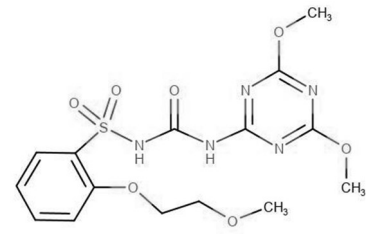
Herbicide	**Metsulfuron-Me**	1.54	2.9	74223-64-6	381.36	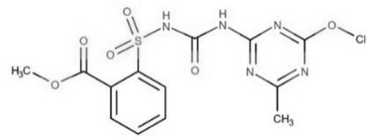
Herbicide	**Chlorsulfuron**	1.4	2.4	64902-72-3	413.41	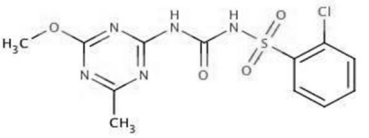
Insecticide	**Carbaryl**	2.36	10.4	63-25-2	201.22	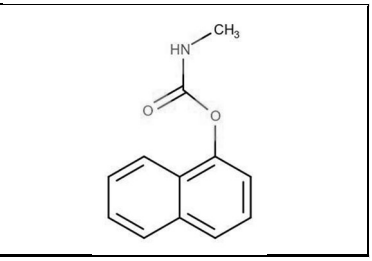
Herbicide	**Atrazine**	2.6	1.7	1912-24-9	215.68	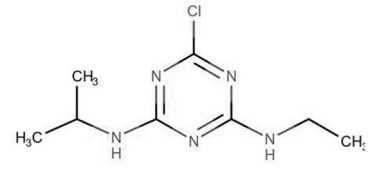
Herbicide	**Isoproturon**	2.87	25.6	34123-59-6	206.3	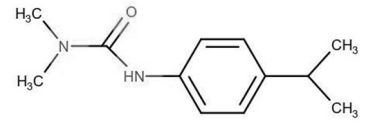
Herbicide	**Metobromuron**	-0.19	2.2	3060-89-7	228.67	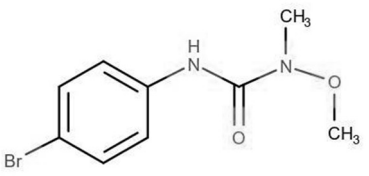

Herbicide	**2,4-Dichlorophenol**	3.09	7.85	120-83-2	163.9	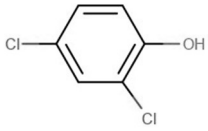
Herbicide	**2,4-Dichlorophenoxyacid**	2.43	2.64	94-75-7	221.03	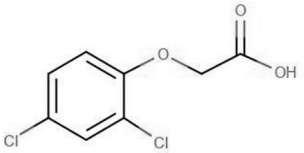
Drug	**Naproxen**	3.18	4.28	22204-53-1	230.26	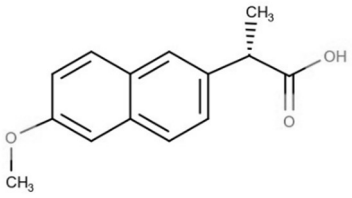
Hormone	**Testosterone**	3.32	-0.88	58-22-0	288.42	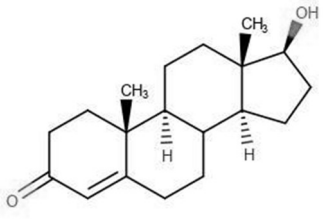
Herbicide	**Flamprop**	3.09	3.6	57973-67-8	321.73	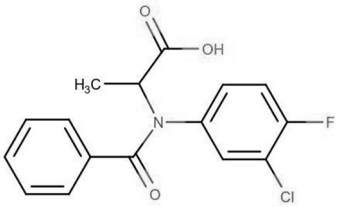
Hormone	**Me-Testosterone**	3.4	10.4	58-18-4	302.45	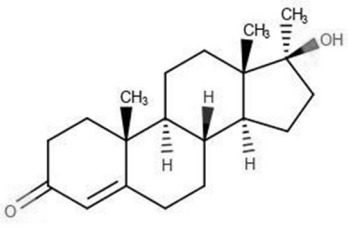
Herbicide	**Linuron**	3.2	4.1	330-55-2	249.09	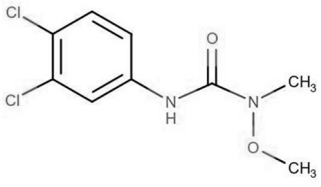
Herbicide	**Desmedipham**	3.53	12.96	13684-56-5	300.31	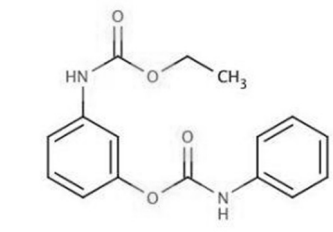

Herbicide	**Phenmedipham**	3.59	13.03	13684-63-4	300.31	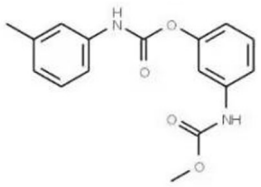
Drug	**Nimesulide**	2.6	6.56	51803-78-2	308.31	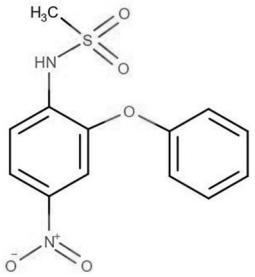
Drug	**Ibuprofen**	3.5	4.45	15687-27-1	206.28	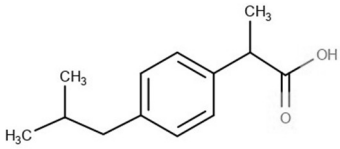
Fungicide	**Procymidone**	3.8	2.1	32809-16-8	284.14	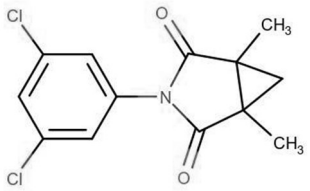
Insecticide	**Malathion**	2.4	10.6	121-75-5	330.36	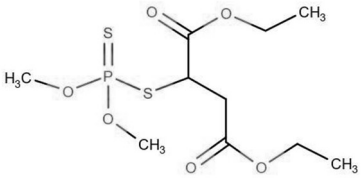
Drug	**Phenylbutazone**	3.16	4.5	50-33-9	308.37	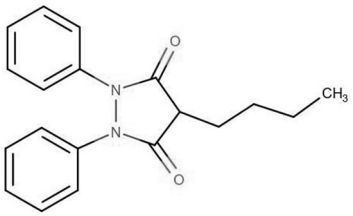
Hormone	**Progesterone**	3.9	-	57-83-0-	314.46	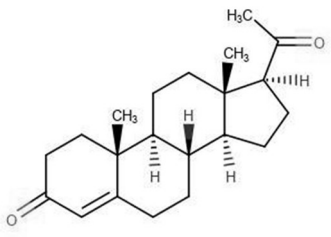

Fungicide	**Iprodion**	3.1	9.19	36734-19-7	330.17	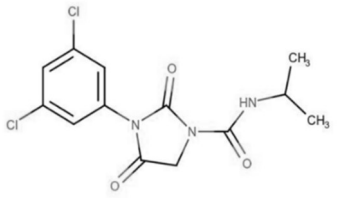

Section D1: Characterization of the recovered material

Uv-VIS, FTIR and thermogravimetric analysis is performed on the recovered material, in order to confirm the composition of it and to certify the effectiveness of the washing procedure in removing combustion by-products and restoring a material as close as possible to the virgin polymer. The physicochemical and spectral properties of the recovered polymer were compared with those of virgin filters and filters before the washing steps.

D1.1. UV-VIS analysis

The characterization of cellulose acetate (CA) was conducted using UV–Vis spectrophotometry (model 760, PG Instruments Ltd., Leicester, UK) over the 190–450 nm spectral range, employing a 1 cm pathlength quartz cuvette. CA solutions (0.5% w/v in acetone) were prepared from pristine CA, clean cigarette filters (CFs), and unwashed CFs. The resulting spectra (**Fig. D1**) displayed a characteristic absorption band between 330 and 350 nm. The spectral profiles of pristine CA and clean recovered CA were nearly identical, indicating minimal alteration to the polymer structure during the cleaning process. In contrast, the spectrum of the unwashed CA exhibited significantly higher absorption and a visible yellow-orange coloration, likely attributable to the presence of conjugated species such as polycyclic aromatic hydrocarbons and aromatic amines formed during cigarette combustion.

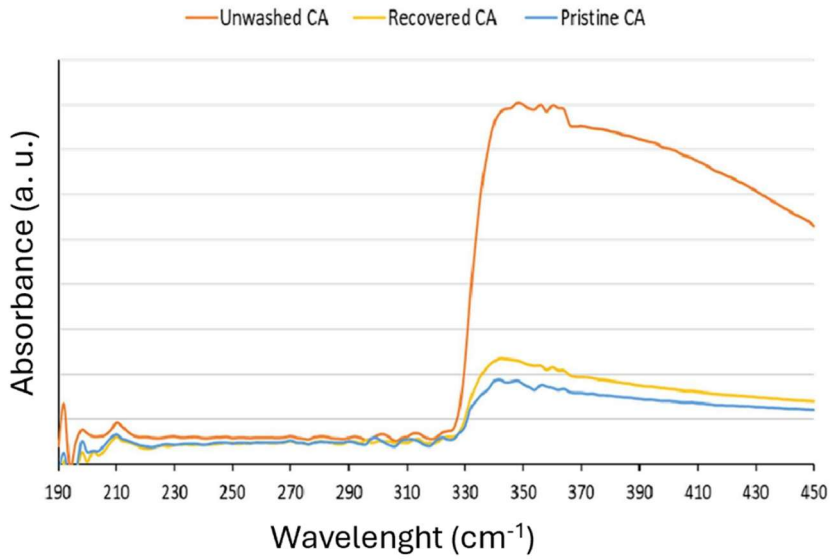

Fig. D1 UV spectra of the virgin material and CFs before and after the washing protocol.

D1.2. FTIR spectroscopy evidence

Attenuated Total Reflectance Fourier Transform Infrared (ATR-FTIR) spectroscopy was employed to analyse small fragments of virgin CA, regenerated CA, and unwashed CFs, using a Nicolet 6700 instrument (Thermo Fisher Scientific, Waltham, MA, USA). Spectra were recorded over the 400–4000 cm^{-1} range and are reported in **Fig. D2**. The following characteristic absorption bands were observed:

- **3500–3000 cm^{-1}**: O–H stretching vibrations,
- **3000–2750 cm^{-1}**: C–H stretching vibrations,
- **1750–1730 cm^{-1}**: C=O stretching of carbonyl groups,
- **1210–1163 cm^{-1}**: C–O stretching of ester linkages,
- **1120–1090 cm^{-1}**: C–O stretching of secondary alcohols,
- **<900 cm^{-1}**: fingerprint region, associated with C–H bending modes.

The spectrum of the unwashed CA displays the typical bands of cellulose acetate but also exhibits additional signals, particularly in the 1700–1500 cm^{-1} region, likely due to the presence of functional groups from combustion-derived contaminants. Following the washing procedure, the spectral

profiles of the regenerated CA and the pristine material were nearly superimposable, indicating effective removal of impurities and preservation of the polymer's structural integrity.

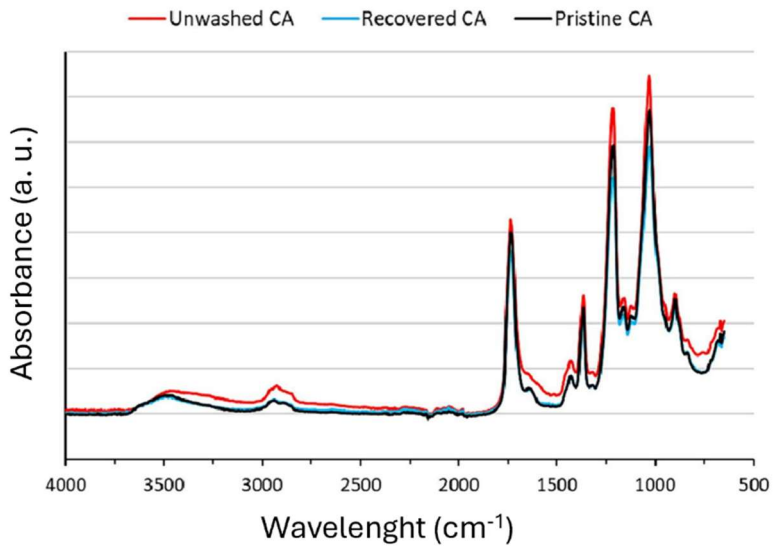

Fig. D2 FT-IR spectra of the virgin material and CFs before and after the washing protocol.

D1.3. TGA analysis

Thermogravimetric analyses were performed on a Mettler TG 50 thermobalance (Mettler Toledo, Columbus, OH, USA) with a temperature ramp from 25 to 650 °C at a heating rate of 10 °C min^{-1} under an N_2 flow. The physicochemical and thermal properties of the recovered polymer were compared with those of virgin filters and CFs before the washing protocol. In all spectra (**Fig. D3**), a 3% weight loss was observed between 27°C and 127°C, attributed to water evaporation. For the virgin polymer and for CF before the washing procedure, an additional 10% weight loss occurred between 127°C and 338°C, hypothesized to result from the degradation of plasticizing chemical additives. This weight loss was not observed in the regenerated polymer, suggesting that the washing procedure effectively removed most of the plasticizers. This hypothesis was confirmed by subjecting the virgin material to the washing protocol, after which TGA analysis revealed the complete absence of weight loss in the 127°C to 338°C range (data not shown). The decomposition observed in all reported thermograms, characterized by a ~60% weight loss occurring between 360 °C and 390 °C, can be

attributed to the thermal degradation of CA. Finally, a 13–15% weight loss was attributed to the decomposition of ash and residues at high decomposition temperatures (>400°C). Also in this case, the analysis profile of the regenerated material is significantly over imposable with the one of the pristine polymers, except for plasticisers, whose removal offers clear practical advantages.

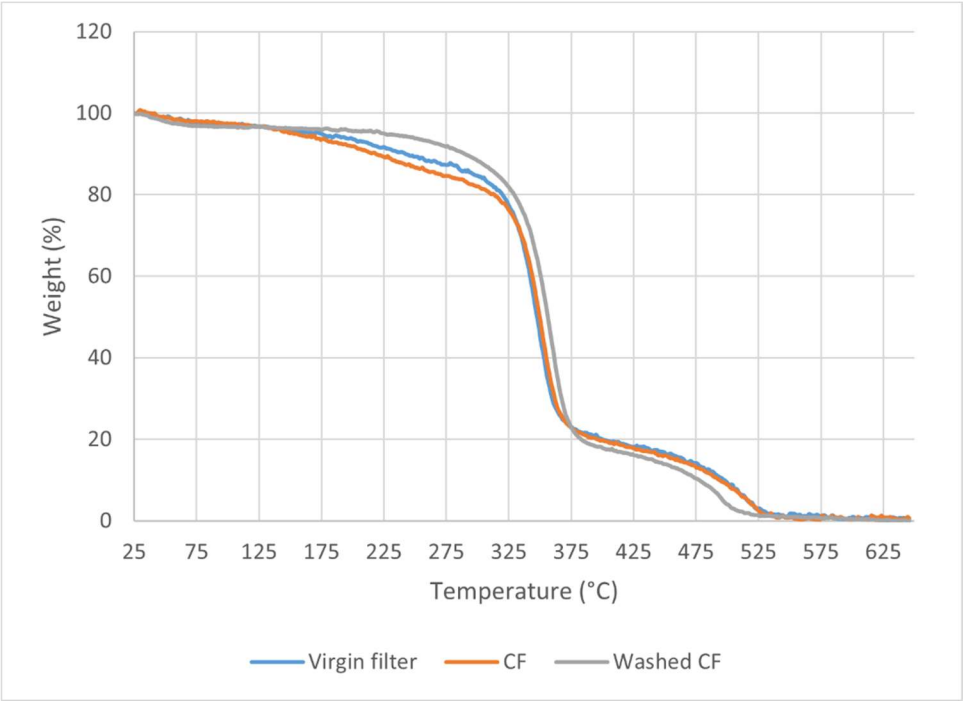

Fig. D3 Thermograms of the virgin material and the CFs before and after the washing protocol.

Table D2 LC-MS parameters for the identification of the thirty analytes under optimized conditions.

Compound	Retention time (min)	Q1 (m/z)	Q3 (m/z)	Detection polarity (+/-)	DP (V)	EP (V)	CE (V)	CXP (V)
Acephate	2.82	184.0	143.0	+	41.0	10.0	20.0	6.0
			95.0		41.0	12.0	32.0	6.0
Butoxycarboxim	3.16	223.1	106.0	+	93.0	10.0	15.0	4.0
			166.0		84.0	8.0	15.0	8.0
Methomyl	4.03	163.0	88.0	+	15.0	4.0	13.0	3.0
			106.0		15.0	4.0	13.0	3.0
Sulfaguanidine	4.1	215.0	108.0	+	60.0	10.0	20.0	9.0
			122.0		60.0	10.0	25.0	9.0
8.0Sulfamerazine	4.23	265.0	156.0	+	41.0	8.0	25.0	8.0
			108.0		41.0	8.0	35.0	11.0
Pirimicarb	4.78	239.1	182.2	+	61.0	10.0	39.0	4.0
			72.1		53.0	34.0	39.0	4.0
Sulfamonomethoxine	6.01	281.1	92.0	+	135.0	14.0	30.0	9.0
			107.9		135.0	14.0	30.0	9.0
Sulfachloropyridazine	6.57	285.0	156.0	+	35.0	9.0	20.0	11.0
			92.0		35.0	13.0	40.0	11.0
Dimethoate	6.80	230.1	125.0	+	70.0	9.0	10.0	10.0
			171.0		76.0	12.0	15.0	8.0
Picloram	7.06	242.9	224.9	+	20.0	10.0	20.0	11.0
			196.9		20.0	10.0	31.0	15.0

Sulfathiazole	7.28	254.0	155.9	+	38.0	4.0	25.0	15.0
			92.0		66.0	10.0	37.0	6.0
Sulfamethoxazole	7.28	254.0	156.0	+	41.0	10.0	25.0	9.0
			107.9		41.0	13.0	35.0	4.0
Butocarboxim	8.07	213.0	75.0	+	60.0	7.7	41.3	9.8
			156.0		93.1	10.4	14.8	4.2
Prednisolone	9.02	361.2	147.1	+	40.0	10.0	30.0	11.0
			343.3		40.0	10.0	32.0	11.0
Thifensulfuron-Me	10.5	388.0	167.0	+	70.0	10.0	23.0	7.0
			205.0		70.0	10.0	34.0	7.0
Propoxur	10.8	210.1	111.0	+	35.0	10.0	19.0	3.0
			168.0		40.0	10.0	20.0	5.0
Dexametasone	10.9	393.4	355.3	+	50.0	10.0	18.0	11.0
			373.3		50.0	10.0	18.0	11.0
Cinosulfuron	11.0	414.2	183.0	+	50.0	10.0	20.0	11.0
			215.3		50.0	10.0	20.0	11.0
Metsulfuron-Me	11.1	382.1	167.0	+	60.0	10.0	20.0	6.0
			141.1		60.0	10.0	20.0	7.0
Chlorsulfuron	11.8	358.0	141.1	+	93.0	10.0	25.0	11.0
			167.1		93.0	10.0	25.0	11.0
Carbaryl	12.1	202.1	145.1	+	56.0	6.0	25.0	6.0
			127.1		60.0	6.0	38.0	6.0
Atrazine	12.4	216.1	104.0	+	40.6	10.0	38.3	7.1

			174.0		40.6	10.0	19.9	6.9
Isoproturon	12.7	206.7	72.1	+	25.0	10.0	15.0	11.0
			46.1		25.0	10.0	20.0	11.0
Metobromuron	13.4	258.5	169.9	+	60.0	10.0	20.0	11.0
			227.0		60.0	10.0	20.0	11.0
2,4-Dichlorophenol	13.6	160.9	125.0	-	-48.0	-8.0	-22.0	-7.0
			88.9		-42.0	-4.0	-37.0	-5.0
2,4-Dichlorophenoxyacetic Acid	13.6	218.9	160.9	-	-46.0	-5.0	-16.0	-11.0
			124.8		-30.0	-8.0	-17.0	-7.0
Naproxen	13.8	229.1	170.0	-	-35.0	-8.0	-22.0	-5.0
			185.5		-35.0	-8.0	-21.0	-7.0
Testosterone	14.1	289.3	97.0	+	120.0	10.0	20.0	11.0
			109.1		120.0	10.0	20.0	11.0
Flamprop	14.2	321.9	105.1	-	26.0	10.0	5.0	4.0
			129.0		40.0	10.0	10.0	4.0
Me-Testosterone	15.0	303.2	97.1	+	120.0	10.0	20.0	11.0
			109.1		120.0	10.0	20.0	11.0
Linuron	15.1	249.0	182.1	+	120.0	10.0	20.0	11.0
			161.0		30.0	30.0	25.0	4.0
Desmedipham	15.3	301.1	182.1	+	56.0	10.0	20.0	11.0
			136.0		46.0	11.0	20.0	7.0
Phenmedipham	15.3	301.1	168.1	+	51.0	10.0	10.0	7.0
			136.1		81.0	10.0	12.0	10.0

Nimesulide	17.0	307.0	228.9	-	-47.0	-2.0	-17.0	-2.0
			79.1		-70.0	-6.0	-22.0	-6.0
Ibuprofen	17.0	205.2	161.0	-	-55.0	-10.0	-13.0	-15.0
			189.0		-55.0	-10.0	-13.0	-15.0
Procymidone	17.1	284.1	256.1	+	94.0	9.0	24.0	13.0
			133.0		90.0	10.0	21.0	10.0
Malathion	17.4	331.0	99.0	+	21.0	10.0	35.0	3.0
			127.0		26.0	10.0	35.0	3.0
Phenylbutazone	17.7	307.0	92.0	-	-40.0	-10.0	-20.0	-15.0
			131.0		-40.0	-10.0	-20.0	-15.0
Progesterone	18.8	315.2	97.1	+	45.0	10.0	20.0	11.0
			109.1		45.0	10.0	20.0	11.0
Iprodion	22.6	328.0	288.0	+	21.0	19.0	10.0	8.0
			245.2		46.0	21.0	10.0	42.0

Table D3 Selected parameters and explored relative values for the optimization study of the synthetic procedure. Underlined values are the selected ones, ensuring the best final result and highest throughput.

Parameter	Lower value	Intermediate value	Higher value
Concentration of the organic polymeric phase (w/v %)	1.2	**5.6**	10
Amount of active carbon in the polymeric phase (% w/w)	5	10	**20**
Magnetic stirring speed (rpm)	100	**200**	300
Volume of the emulsion breaking solution (MilliQ water, mL)	7	9	**11**

Table D4 Features and performances of the developed analytical method (UPLC-ESI-MS/MS) for each of the involved analytes.

Analyte	LOD (µg/L)	LOQ (µg/L)	Precision (RSD %) (n=5, 50 µg/L)	Linear range (µg/L)
Acephate	1.4	4.6	8.3	5-1000
Butoxycarboxim	5.9	19.8	9.8	20-1000
Methomyl	1.2	4.1	5.0	5-1000
Sulfaguanidine	0.6	2.1	6.7	5-1000
Sulfamerazine	1.0	3.2	8.6	5-1000
Pirimicarb	2.5	8.4	2.3	10-1000
Sulfamonomethoxine	3.2	10.5	6.1	20-1000
Sulfachloropyridazine	0.5	1.7	7.0	5-1000
Dimethoate	2.1	6.8	5.8	10-1000
Picloram	8.6	28.7	4.3	50-1000
Sulfathiazole	1.2	4.0	11.6	5-1000
Sulfamethoxazole	0.9	3.0	10.1	5-1000
Butocarboxim	5.9	19.8	5.4	20-1000
Prednisolone	9.3	30.9	4.1	50-1000
Thifensulfuron-Me	0.2	0.8	11.6	5-1000
Propoxur	3.6	11.9	8.1	20-1000
Dexametasone	2.2	7.3	11.4	10-1000
Cinosulfuron	1.9	6.2	4.8	10-1000
Metsulfuron-Me	0.3	1.1	7.5	5-1000
Chlorsulfuron	14.2	47.2	6.8	50-1000

Carbaryl	0.7	2.4	1.8	5-1000
Atrazine	10.0	33.3	8.8	50-1000
Isoproturon	0.6	1.9	10.5	5-1000
Metobromuron	3.4	11.2	7.2	20-1000
2,4-Dichlorophenol	4.0	13.4	4.8	20-1000
2,4-Dichlorophenoxyacetic Acid	2.0	6.7	3.5	10-1000
Naproxen	1.6	5.4	7.3	5-1000
Testosterone	1.0	3.3	10.8	5-1000
Flamprop	0.9	3.1	8.8	5-1000
Me-Testosterone	1.7	5.6	5.8	5-1000
Linuron	1.1	3.8	8.6	5-1000
Desmedipham	1.5	4.9	3.8	5-1000
Phenmedipham	1.2	4.0	4.4	5-1000
Nimesulide	0.9	3.0	3.5	5-1000
Ibuprofen	3.4	11.4	5.4	20-1000
Procimidone	5.7	19.0	2.2	20-1000
Malathion	6.3	20.9	2.0	20-1000
Phenylbutazone	1.0	3.3	9.7	5-1000
Progesterone	1.1	3.7	8.8	5-1000
Iprodion	1.4	4.8	10.0	5-1000

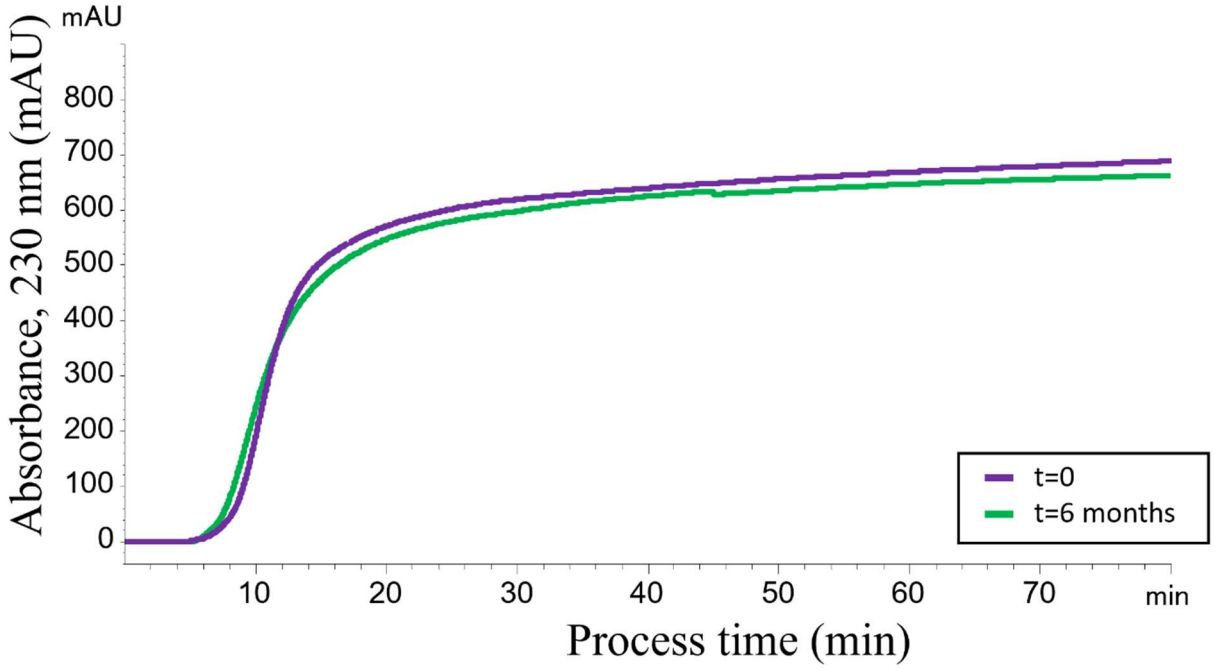

Fig. D4 Integrated breakthrough curve comparison obtained respectively with a freshly prepared material and with material prepared six months before. Each curve is the average of triplicate trials. The final results are almost over imposable, with a statistical deviation of the results lower than 15%.

Appendix E

Table E1 Structure and relevant chemical-physical parameters of the selected pesticides.

Chemical class	Analyte	logP	pKa	Formula	CAS number	Vapor pressure (mmHg)	Boiling point (°C)	Exact mass (uma)	Structure
Insecticide	**Acetamiprid**	0.80	0.7	$C_{10}H_{11}ClN_4$	160430-64-8	$4.4 \cdot 10^{-5}$	Decomposes before boiling	222.07	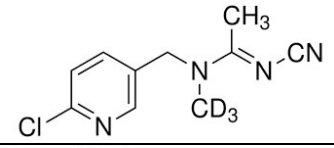
Profungicide	**Acibenzolar-methyl**	3.1	n. r.	$C_8H_6N_2OS_2$	135158-54-2	$3.30 \cdot 10^{-6}$	267	209.99	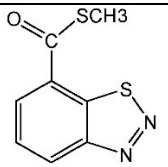
Herbicide	**Pyraflufen-ethyl**	3.49	n. r.	$C_{15}H_{13}Cl_2F_3N_2O_4$	129630-19-9	$1.2 \cdot 10^{-10}$	Decomposes before boiling	412.02	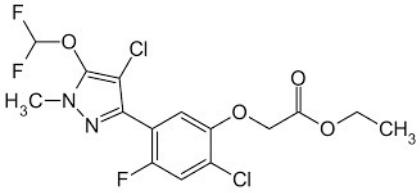
Acaricide	**Clofentezine**	4.09	unstable	$C_{14}H_8Cl_2N_4$	74115-24-5	$6.0 \cdot 10^{-4}$	Decomposes before boiling	303.15	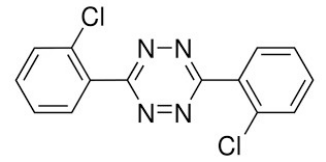

Herbicides	**Diflufenican**	-	n. r.	$C_{19}H_{11}F_5N_2O_2$	83164-33-4	$4.25 \cdot 10^{-3}$	Decomposes before boiling	394.07	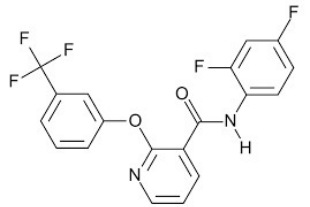
Herbicide	**Oxyfluorfen**	4.73	n. r.	$C_{15}H_{11}ClF_3NO_4$	42874-03-3	$2 \cdot 10^{-7}$	358.2	361.03	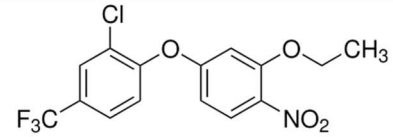
Herbicide	**Propaquizafop**	4.6	n. r.	$C_{22}H_{22}ClN_3O_5$	111479-05-1	negligible	Decomposes before boiling	443.12	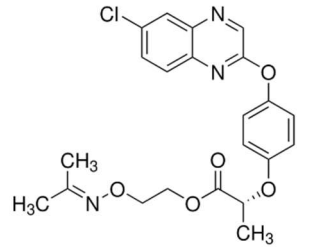
Herbicide	**Pendimethalin**	5.20	2.8	$C_{13}H_{19}N_3O_4$	40487-42-1	$9.4 \cdot 10^{-6}$	Decomposes on distillation	281.31	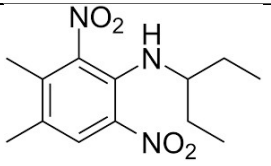

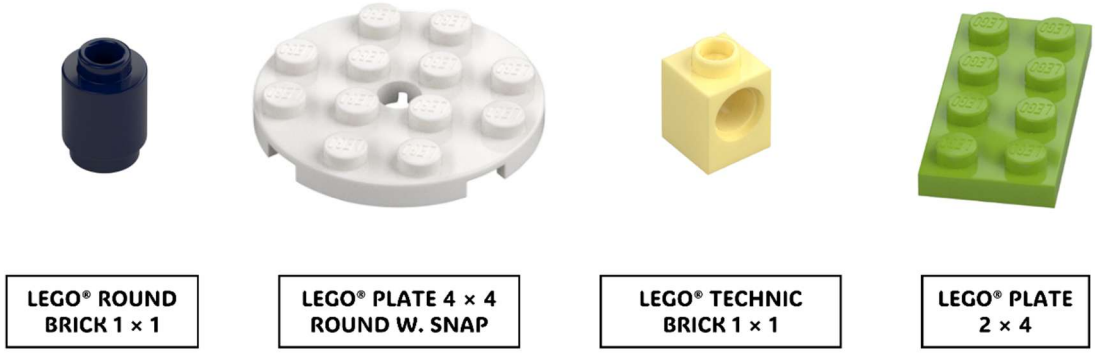

Fig. E1 LEGO® bricks typologies involved in the current study.

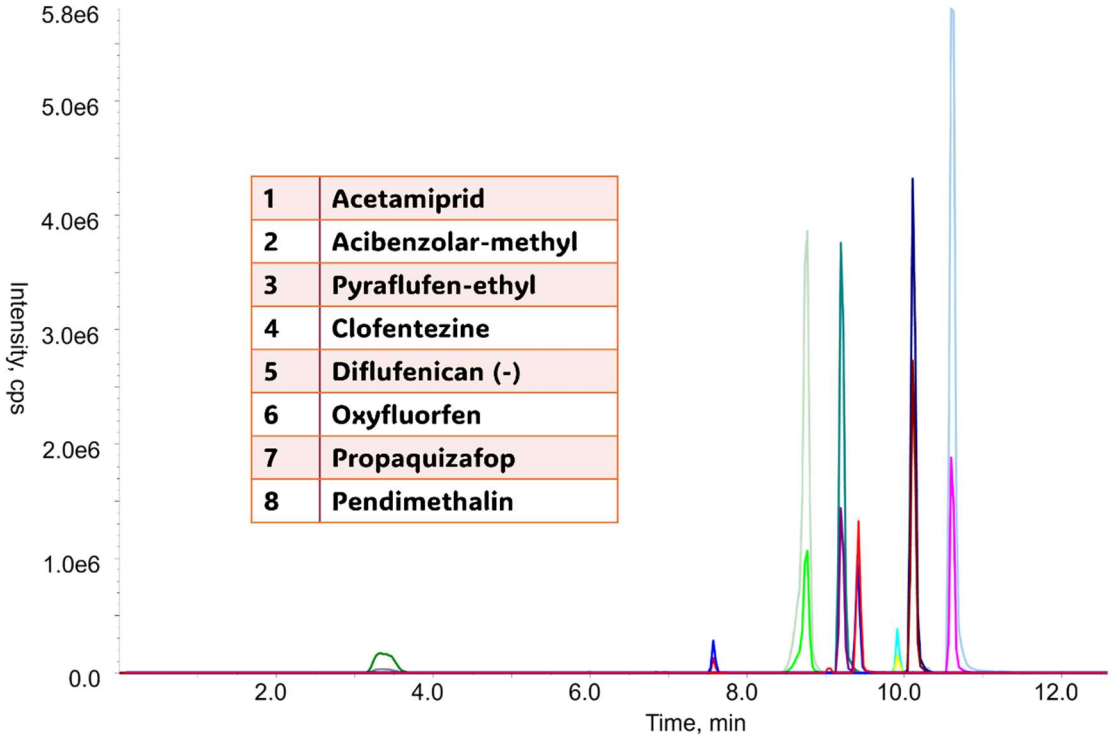

Fig. E2 UPLC-MRM chromatogram from a 3 µL injection of the composite working solution (0.3 ng injected).

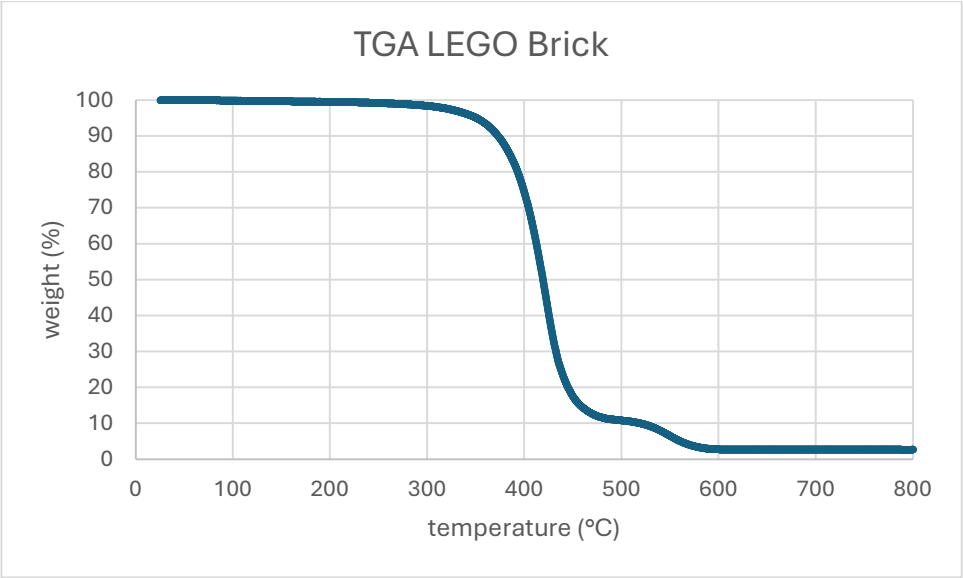

Fig. E3 TGA curve of a LEGO® brick fragment (~5 mg) obtained under the following conditions: 25–800 °C, heating rate of 10 °C min^{-1}, in air. It was realized with a SEIKO TG/DTA 7200 from Seiko Instrument Inc. (Neu-Isenburg, Germany). The copolymer degradation occurs in two main steps, at approximately 430 and 545 °C [Alonso, A., Lazaro, M., Lazaro, D., & Alvear, D. (2023). Thermal characterization of acrylonitrile butadiene styrene-ABS obtained with different manufacturing processes. *Journal of Thermal Analysis & Calorimetry*, *148*(20)]. Specifically, butadiene degradation starts around 340 °C, styrene around 350 °C, and acrylonitrile near 400 °C. The highlighted events correspond to the overlap of these three processes, which occur over similar temperature ranges.

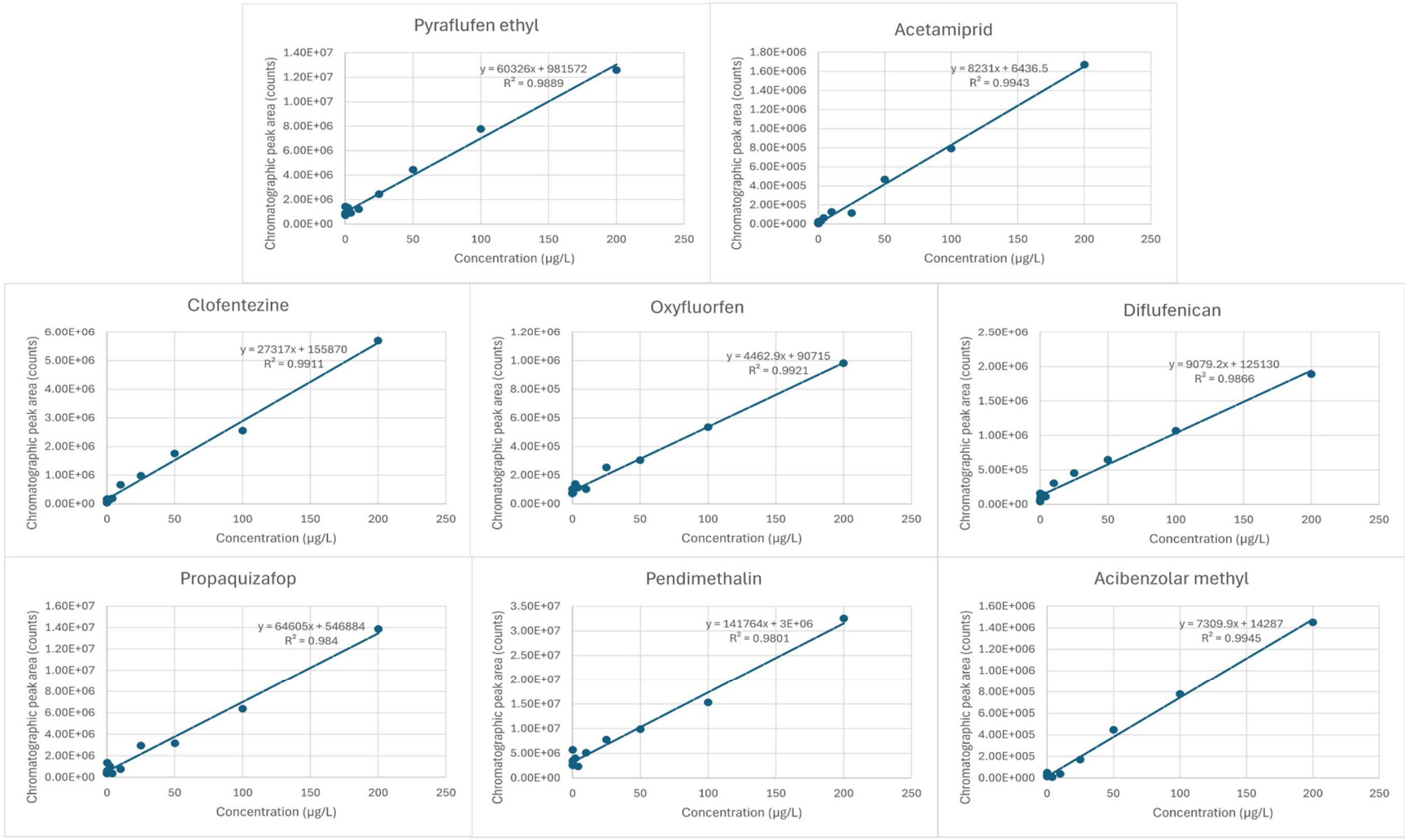

Fig. E4 Linear quantification models for the analysis of the eight pesticides in spiked tap water.

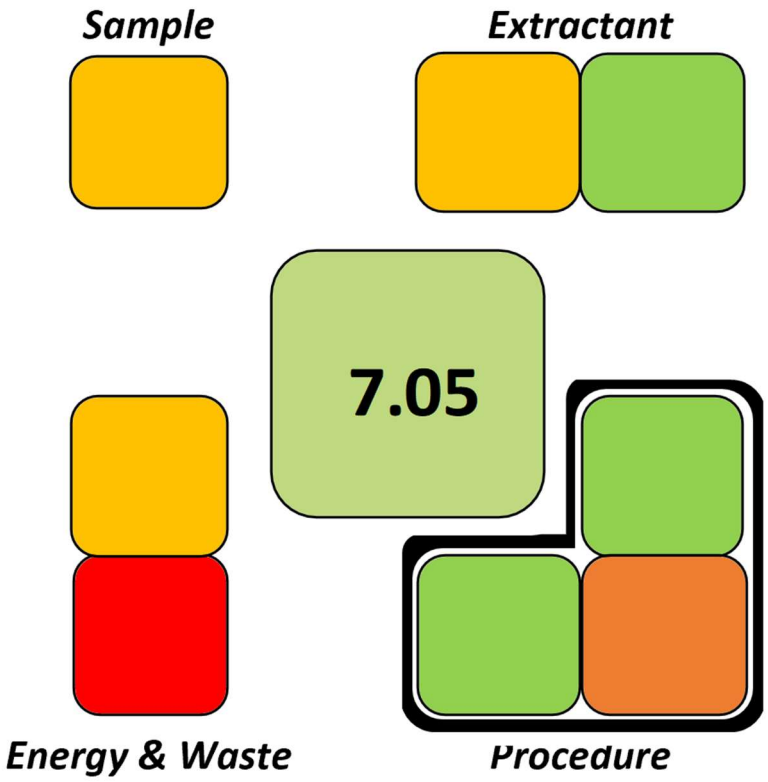

Fig. E5 Score plot of the SPMS applied to the optimized workflow of the extraction method